1226

TRANSPORTATION RESEARCH RECORD

International Symposium on Recent Developments in Concrete Fiber Composites

TRANSPORTATION RESEARCH BOARD
NATIONAL RESEARCH COUNCIL
WASHINGTON, D.C. 1989

Transportation Research Record 1226
Price: $15.50

modes
1 highway transportation
2 public transit
3 rail transportation
4 air transportation
5 other

subject area
32 cement and concrete

Library of Congress Cataloging-in-Publication Data
National Research Council. Transportation Research Board.

International Symposium on Recent Developments in Concrete Fiber Composites (1989 : Washington, D.C.)
International Symposium on Recent Developments in Concrete Fiber Composites.
p. cm.—(Transportation research record, ISSN 0361-1981 ; 1226)
ISBN 0-309-04953-9
1. Fibrous composites—Congresses. 2. Reinforced concrete, Fiber—Congresses. I. National Research Council (U.S.). Transportation Research Board. II. Title. III. Series.
TE7.H5 no. 1226
[TA418.9.C6]
388 s—dc20
[624.1'834] 90-33602
CIP

Transportation Research Record 1226

Contents

Foreword v

Current Research and Applications of Fiber Reinforced Concrete Composites in India 1
V. S. Parameswaran, T. S. Krishnamoorthy, and K. Balasubramanian

Fiber Reinforced Concrete and Shotcrete for Repair and Restoration of Highway Bridges in Alberta 7
Colin D. Johnston and Paul D. Carter

Flexural Fatigue Strength, Endurance Limit, and Impact Strength of Fiber Reinforced Concretes 17
V. Ramakrishnan, George Y. Wu, and G. Hosalli

Optimum Use of Pozzolanic Materials in Steel Fiber Reinforced Concrete 25
Ziad Bayasi and Parviz Soroushian

Chemical Treatments of Polypropylene Fiber Surfaces Used in Fiber Reinforced Concretes 31
M. F. Fahmy and Norbert L. Lovata

Fatigue Strength of Fibrillated Polypropylene Fiber Reinforced Concretes 36
M. Nagabhushanam, V. Ramakrishnan, and Gary Vondran

Field Evaluation of Steel Fiber Reinforced Concrete Overlay With Various Bonding Mechanisms 48
G. Chanvillard, P.-C. Aïtcin, and C. Lupien

Natural Fiber Reinforced Concrete 57
R. Sethunarayanan, S. Chockalingam, and R. Ramanathan

Properties and Design of Fiber Reinforced Roller Compacted Concrete 61
Antonio Nanni

Flexural Behavior and Toughness of Fiber Reinforced Concretes 69
V. Ramakrishnan, George Y. Wu, and Girish Hosalli

A Comparative Evaluation of Plain, Polypropylene Fiber, Steel Fiber, and Wire Mesh Reinforced Shotcretes 78
D. R. Morgan, N. McAskill, B. W. Richardson, and R. C. Zellers

An Investigation of the Toughness and Compressive Toughness Index of Steel Fiber Reinforced Concrete 88
Jinghai Zhao, Peng Xu, and Chengmou Fan

Analysis of Fiber Reinforced Concrete Beams Under Combined Loadings 94
A. K. Sharma

Study of the Mix Proportion of the No Slump Concrete Melt-Extracted Carbon Steel Fiber 98
Chengmou Fan and Liying Zhu

Foreword

To date little use of fiber-reinforced composites has been made in transportation in the United States. This international symposium should serve to stimulate the consideration of these materials for use in transportation systems. This Record covers applications of natural and manufactured fibers in various types of concretes. Parameswaran et al. highlight current research efforts and the application of FRC to precast and cast-in-place structural components in India. Johnston and Carter cover laboratory studies and field applications of fiber-reinforced concrete in bridge beams, deck overlays, and shotcrete repairs to beams, piers, and abutments in Alberta. Ramakrishnan et al. present the results of an extensive experimental investigation of the behavior and performance characteristics of the most commonly used fiber reinforced composites subjected to fatigue loading. Bayasi and Soroushian studied the effects on fresh and hardened material properties of substituting fly ash and silica fume for cement in steel fiber reinforced concrete. Fahmy et al. discuss the results of an experimental investigation of the results of the chemical treatment of polypropylene fibers used in reinforced concretes. Nagabhushanam et al. present the results of an experimental investigation of the flexural-fatigue strength of concretes reinforced with different concentrations of fibrillated polypropylene fibers. Chanvillard et al. report on an experimental steel-fiber-reinforced, thin concrete overlay on the Transcanadian Highway. Sethunarayanan et al. present a critical review of the factors which affect the properties and behavior of natural fiber reinforced concrete. The paper by Nanni contains compression and split tension strength results of laboratory cylinders and field cores of roller-compacted concrete containing different types and various percentages of steel fibers. In their second paper, Ramakrishnan et al. discuss the results of an extensive investigation of the behavior and performance characteristics of commonly used fiber reinforced composites for potential applications in airfield pavements and overlays. Morgan et al. present the results of studies comparing the performance of certain common wire-mesh reinforced shotcretes to shotcretes reinforced with high-volume concentrations of a collated, fibrillated polypropylene fiber. Zhao et al. compare various methods for determining toughness of steel-fiber-reinforced concretes. Sharma derives a model for the analysis of fiber reinforced concrete beams under axial compression, bending, and torsion. Fan and Zhu report on an investigation of the mix proportions of melt-extracted, carbon-steel-fiber-reinforced no-slump concrete.

Current Research and Applications of Fiber Reinforced Concrete Composites in India

V. S. PARAMESWARAN, T. S. KRISHNAMOORTHY, AND K. BALASUBRAMANIAN

Cement and concrete matrices reinforced with randomly oriented short fibers are finding increasing applications in both precast and in situ concrete construction. Fibers made of steel, polypropylene, and glass are already being used in load-bearing structural members; attention is turning now to using organic and natural fibers as macroreinforcement in cement and concrete matrices. Research and developmental work in fiber reinforced concrete composites began in India in the early 1970s. Fiber concrete technology is no longer confined to laboratory experiments—it is used in the production of precast concrete components and for in situ strengthening and repairs of concrete structures. Current applications are for flooring and roofing components, pipes, manhole covers and frames, precast thin-wall elements, construction of blast-resistant structures, and currency vaults.

The behavior of fiber reinforced concrete (FRC) composites subjected to combined static loads and to impact, dynamic, and blast loads has been studied by researchers in India for quite some time. Work is under way too on the development of polymer-impregnated fiber reinforced concrete and fibrous ferroconcrete, with which precast concrete components can be produced to meet specific functional and strength requirements. A great deal of work has also been carried out in developing precast roofing units, particularly for housing, using natural fibers. This paper describes some of these current research efforts and applications for FRC composites in India.

BACKGROUND

Combining two or more materials to obtain a composite is not new to the civil engineer. Natural fibers such as straw have long been used in brickmaking to modify and improve the properties of the brittle matrix. The concept behind FRC is that the deformation of the matrix under stress will transfer the load to the fibers. (Asbestos cement roofing sheets, used for more than six decades, are one example of a cement composite in which fibers play an important role in improving the strength and deformation properties of the cement matrix.) But to realize substantial improvements in the composites' static, dynamic, and impact strength properties, the added fibers must be strong and possess good bonding properties.

Fibers have been produced in various shapes and sizes from steel, carbon, glass, polypropylene, nylon, rayon, polyethylene, and asbestos, as well as from cotton, coir, sisal, and other natural fibers. Low-modulus fibers such as nylon and polypropylene may not lead to significant improvement in composite strength, but they do help absorb huge amounts of energy and resist impact and shock loading. For structural applications using concrete, however, steel and glass fibers are usually used since they possess a high modulus of elasticity and lead to strong, stiff composites.

How much high-modulus steel and other fibers can strengthen composites depends on the strength characteristics of the fibers themselves, the bond in the matrix-fiber interface, the ductility of fibers, the volume of fiber reinforcement and its spacing, the dispersion of orientation of fibers, and their shapes and aspect ratios. High-strength fibers, a large volume of fibers, longer fibers, and small-diameter fibers each improve the strength of the composites.

Research and developmental work on FRC composites started in India in the early 1970s. The analytical and experimental investigations carried out during that time were confined mostly to the use of steel fibers (*1–5*). Interest in fibers such as polypropylene and polymer-impregnated glass fibers and natural fibers such as coir or cotton arose later; investigations covering their use for specific applications have been detailed in several publications.

Steel fibers are not yet produced on a commercial scale in India, although plans for their manufacture, in collaboration with U.S. fiber manufacturers, are under way. Fibers must therefore be obtained from wire coils. The usual procedure is to straighten the coil and chop it into small lengths, producing plain, smooth, round fibers with diameters from 0.4 to 1.5 mm. (Some investigators, however, have used black annealed steel binding wires to produce fibers with diameters ranging from 0.5 to 2.0 mm.) Most investigations of steel fiber reinforced concrete (SFRC) in India therefore address only such plain steel fibers or wires.

Natural fibers, such as coir and bamboo, and synthetic fibers, such as nylon and polypropylene, have also been used in India for the production of roofing sheets and other housing structural components. Alkali-resistant glass fibers are not now being produced in India, so the use of glass fibers in concrete is precluded. Nevertheless, the properties of glass fiber reinforced resin composites, both with and without polymer impregnation, have been investigated; the experimental test results are promising (*6,7*).

Structural Engineering Research Centre, Madras 600 113, India.

STUDIES ON STEEL FIBER REINFORCED CONCRETE STRUCTURAL ELEMENTS

Several studies have addressed the flexural behavior of steel fiber reinforced concrete (SRFC) beams, focusing particularly on improvements in cracking resistance, stiffness, and ductility. Other improvements attributable to the addition of steel fibers, for instance, in shear capacity, impact resistance, resistance to abrasion, and energy absorption, have also been noted by investigators. Early investigations carried out at the Structural Engineering Research Centre, Madras (hereafter SERC), studied improvements in the properties of concrete when plain steel wires were randomly distributed with an aspect ratio of about 100 (*1*,*2*). More recently investigations were conducted on the behavior of SFRC beams provided with equal tension and compression reinforcement (*8*).

The SERC investigation employed test beams 200 by 100 mm, with an effective span of 2060 mm, which were designed to avoid shear failure. Steel fibers 40-mm long and 0.4 mm in diameter were used, with the percentage of fiber in the composite varying from 0.5 to 1.0, by volume. The concrete used was M-20 grade (cube compressive strength of 20 N/mm^2). Details of the test beams are presented in Table 1.

SERC experiments on the beams revealed that SFRC beams have much better load distribution characteristics than do normal reinforced concrete beams. Experimental data led to empirical expressions for determining the static rigidity of beams subjected to differing levels of bending moments. The SFRC beams were found to fail by the rupture of tensile steel preceded by large rotation and deflection similar to laced reinforced concrete beams, thereby establishing their potential for use in the design of blast-resistant structural elements.

SERC also examined the dynamic behavior of SFRC beams by varying the percentages of steel fibers and the main reinforcing steel (*9*). Test beams with cross sections measuring 100 by 200 mm were cast with equal tension and compression reinforcement. They were subjected successively to steady-state forced vibration tests after they were loaded to particular static loads that simulated different levels of cracking. A schematic diagram of the dynamic test set-up is shown in Figure 1. Dynamic flexural rigidity (EI_d) and damping (ξ) were determined from the data collected from the tests.

Tests showed that the dynamic stiffness of SFRC beams in the uncracked state was only marginally higher (about 15 percent for a fiber-volume content of 1 percent) than for reinforced concrete beams. However, the increase in stiffness in the post-cracking stage was larger; it was nearly the same for all the fiber volumes studied (0.5 to 1.0 percent). In addition, the damping values exhibited by SFRC beams showed significant scatter.

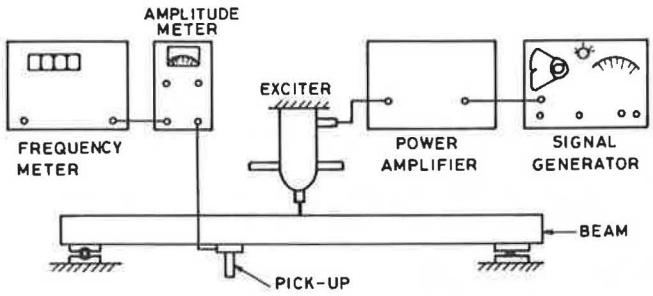

FIGURE 1 Schematic diagram of dynamic test set-up.

Researchers concluded that the average value, in the uncracked state, applicable to the design of machine foundations is 1-percent critical. Equations were formulated from the tests results to estimate the dynamic stiffness of SFRC beams in the post-cracking stage for use in designs involving SFRC elements in blast- and earthquake-resistant structures. Further tests to quantify the variation of stiffness with fiber content and to evaluate the impact resistance of SFRC beams are in progress.

Rao et al. (*10*) studied the influence of fiber reinforcement on the ultimate strength of reinforced concrete columns subjected to axial compression and uniaxial bending. The main variable in their study was applied compression, which varied from 0 to 150 mm for test columns that were 100 by 150 by 1200 mm. The tests indicated that adding fibers to columns reinforced with main continuous steel bars produced only minor improvement in ultimate carrying capacity. However, for plain concrete columns, the addition of fibers significantly improved the columns' ultimate strength. Substantial improvement was also reported in reduction of tranverse tensile stress and deformations.

Dwarakanath and Nagaraj (*11*) investigated whether beams incorporating steel fibers over the entire beam depth performed better than beams with fibers over only half the depth, on the tension side. They found that, for under-reinforced beams, including the fibers over half the depth proved as beneficial as full-depth inclusion in controlling cracking and deflection and in increasing the stiffness of the beams. For over-reinforced beams, however, the fiber addition was not found to be effective in bringing about any appreciable modification in the deformational behavior of the beams.

Studies on the influence of concrete strength, aspect ratio, volume of steel fiber, and quantity of tensile reinforcement on the cracking characteristics of SFRC beams have been reported by the Indian Institute of Technology, Madras. Smooth, round, galvanized iron binding wires of 0.56-mm diameter were cut into small lengths to produce the fibers for

TABLE 1 DETAILS OF TEST BEAMS

Serial Number	Designation	Main Reinforcement (at top and bottom)		Volume (%) of Fibers	Transverse Steel
1	B1	2 nos.	10#	0.50	2 legged 8# at 150 mm centers
2	B2	2 nos.	10#	0.75	2 legged 8# at 150 mm centers
3	B3	2 nos.	10#	1.00	2 legged 8# at 150 mm centers
4	B4	2 nos.	12#	1.00	2 legged 8# at 150 mm centers
5	B5	2 nos.	16#	1.00	2 legged 8# at 150 mm centers
6	B6	2 nos.	10#	0.00	2 legged 8# at 150 mm centers

the experiments. The concrete mix proportion was 1:1.25:1.25, with a water/cement ratio of 0.48. Findings were that inclusion of the steel fibers over the whole section of the SFRC beam produced an increase of 50 to 128 percent in the load at first visible crack. The increase dropped to about 30 percent when fibers were provided only around the tension steel. Inclusion of fibers also substantially reduced both crack width and crack height. Similar observations were reported by several other investigators in India who used fiber contents varying from 0.5 to 1 percent by volume and aspect ratios from 80 to 100. Besides finding significant improvement in crack control and crack propagation, the investigators reported attainment of concrete compressive strain at ultimate load ranging from 330 to 700 $\times$ 10^{-5}.

Moment distribution characteristics of two-span SFRC continuous beams have been studied at the College of Engineering, Madras (*12*). The test beams, 100 by 200 mm in cross section, were supported at three points with two equal spans of 2900 mm. Beam reinforcement was sufficient to prevent premature shear failure. Fibers (1 percent by volume) were added only to the midspan and support portions of the continuous beams. The inclusion of steel fibers in the hinging zones resulted in a 25-percent increase in stiffness at service load, a 15-percent increase in ultimate load, a 20-percent reduction in crack widths, a 10-percent increase in ductility, and 25 percent less stiffness degradation, compared to conventional reinforced concrete beams. Monotonic and reverse cycle loading carried out on prestressed FRC and on conventional prestressed concrete beams showed FRC to be superior with respect to load carrying capacity, stiffness, ductility, and energy absorption characteristics. (In the reverse cycle loading tests, however, the improvement was noted only before the yield level.)

Corrosion of fibers in SFRC is one important factor affecting the durability of the composite matrix under prolonged exposure to adverse environmental conditions. Some investigators in India have reported, however, that the damage due to corrosion in SFRC beams is generally not very extensive (*13*). Experiments conducted by these investigators employed a fiber content of 1.5 percent by volume, with an aspect ratio of 60 to 80. The fiber was obtained from 0.46-mm diameter mild steel annealed wires. The mix proportion was 1:2.07:2.4, with a water/cement ratio of 0.62.

Using steel fibers as web reinforcement in reinforced concrete beams is being studied by many researchers in the country. Findings suggest that conventional vertical stirrups could effectively be replaced by steel fibers and that the shear strength could be predicted using the equation proposed by Muhudin (*14*). The studies concluded so far have shown that inclusion of fibers up to 1.5 percent by volume (with an aspect ratio of 100) increases the ultimate nominal shear stress by about 67 percent. In addition, the ultimate concrete compressive strain has proved to be around 0.007, compared to 0.0035 for reinforced concrete beams.

The use of fibers in ferrocement structural components has been investigated at SERC. Preliminary experiments indicate that the fibers contribute to the flexural stiffness and fracture toughness of the composite. Further investigations are in progress. SERC is also looking into the effects of using a very large percentage volume of fibers (as much as 8 to 12 percent) to improve the impact and abrasion resistance properties of cement mortar. The role of "fiber casements" in confining concrete in compression members is being studied as well.

Other research and academic institutions in India are studying several other aspects of the behavior of SFRC elements subjected to combined static loading, including torsion, and to dynamic, impact, and reversal of loads. The drift of all the investigations, at SERC and elsewhere, is that SFRC structural components present advantages over conventional components, particularly in crack control, improvement in ductility and resistance to impact, abrasion, blast, and other kinds of impulse loads.

INVESTIGATIONS USING NATURAL FIBERS

Most of the natural fibers used for investigations in India are of vegetable origin. Of these, sisal, coir, jute, and bamboo fibers have commonly been used in experiments and in field applications. Besides the work carried out by many universities in the country, research laboratories such as the Regional Research Laboratories at Jorhat, Bhopal, and Trivandrum have carried out a number of experiments using vegetable fibers in the production of precast structural elements. Tests conducted on concrete cubes and flexural beams containing bamboo and coir fibers have shown that the addition of fibers effectively arrests the growth and propagation of cracks, although it does not improve compressive strength. Coconut fibers (coir) have been used in the production of roofing sheets and tiles; reportedly, the durability of these products is good (*15*).

Some research has been carried out on the use of asbestos fibers in its macrofine form in lightweight, reinforced, aerated precast concrete components. Because asbestos fibers may pose some health hazard, however, further investigations are required before their use in aerated and other types of concrete can be advocated.

INVESTIGATIONS USING GLASS AND SYNTHETIC MANMADE FIBERS

Not much work has been done in India yet on the use of glass fibers in FRC because the available fibers are not alkali-resistant. Experiments were conducted at SERC on polymer-impregnated glass fiber reinforced concrete and cement composites in an effort to find a way to protect the glass fibers from the alkalinity in concrete. Polymer impregnation, besides making the glass fibers durable, makes the composites resistant to chemicals. The abrasion resistance of polymer-impregnated glass fiber reinforced mortar composites was found to be more than those without fibers (*6*). E-glass fibers 6- and 12-mm long were used to reinforce the mortar. Methyl methacrylate monomer with benzoyl peroxide as a catalyst was used for impregnation of the glass reinforced mortar specimens. A cement mortar ratio of 1:2, with a 0.5 water/cement ratio, was used to prepare the test specimens, which essentially consisted of cylinder, direct tension specimens, and flexural prisms. Investigations are now under way on the behavior of polyester resin composites reinforced with E-glass fibers.

Investigators have studied nylon and polypropylene fibers, too, with the aim of developing precast concrete components.

DEVELOPMENT OF ULTRAHIGH-STRENGTH STEEL FIBERS

Recent research by a steel manufacturing concern in the country has suggested the possible application of ultrahigh-strength steel fibers, which reportedly possess a superior combination of strength and durability. The ultimate tensile strength typically varies from 165 kg/mm^2 to 200 kg/mm^2, compared to 120 kg/mm^2 for the low carbon steel fibers presently available in India. These high-strength, high-ductility steel fibers are produced with a ferritic-martensitic steel formula in diameters ranging from 0.4 to 1 mm. The fibers have a corrugated profile which improves their bonding characteristics with concrete. Preliminary investigations carried out by the firm on fibers with an 80 aspect ratio have shown considerable improvement in both flexural strength and toughness, compared to conventional plain fibers. These new fibers will likely be commercially available in the country soon.

NEW SHAPES OF FIBERS

At present, only straight steel fibers are used in SFRC. However, some experimental work carried out at SERC on helical and twisted fibers indicates their superiority over plain fibers in pull-out strength and also in the elimination of balling when they are mixed with concrete (*3*). The shapes of the fibers are shown in Figure 2.

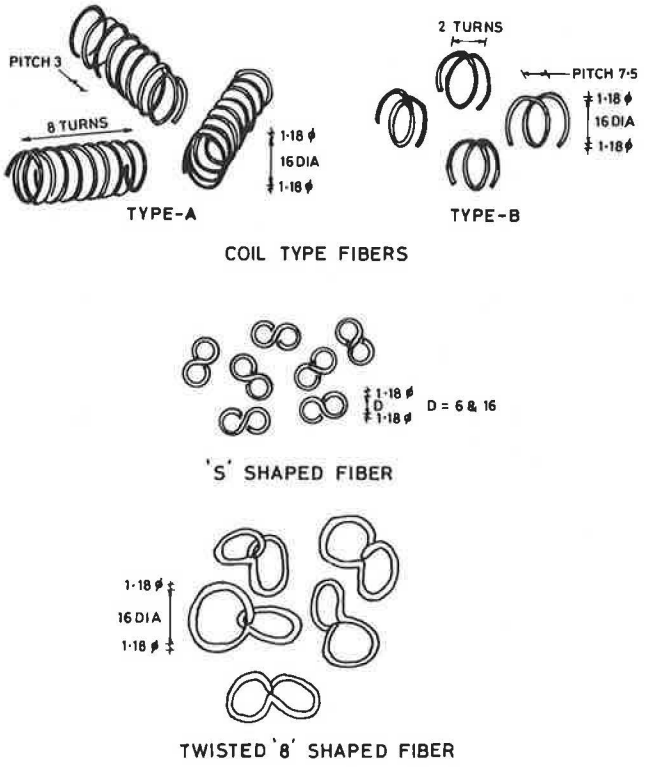

FIGURE 2 Different shapes of steel fibers (in mm) developed at SERC, Madras.

PRODUCTION OF FRC IN INDIA

Conventional techniques are now used only in mixing, placing, and compaction of fiber reinforced concrete. Both pan and tilt-up drum mixers are used for mixing concrete with fibers. Normally, the fibers are dispersed by sieves or by hand after all other ingredients have been placed inside the mixer drum, although special fiber-dispensing devices sometimes are used. The fiber volume content generally ranges from 0.5 to 2 percent, depending on the application. Sand content is usually more in concrete mix proportions, and coarse aggregates sized greater than 10 mm are not usually used. Superplasticizers, which are now available in India, are used only in certain applications. In most of the investigations carried out in the laboratories and in many applications in the field, the FRC mix is so designed that it is workable without the addition of superplasticizers. The compaction of the wet mix inside the molds or over the forms is achieved by means of a table or shutter vibrator. The slump cone test is used to measure workability, even though this test is not unfailingly reliable. The cement content in a typical fiber concrete mix used in laboratory and field applications varies from 350 kg/m^3 to 400 kg/m^3.

When the percentage of fibers added is more than 1.5 percent, superplasticizers are generally used, and sometimes fly ash is also added to improve workability and to reduce cement consumption. For very high-volume FRC mortars containing 6 to 12 percent of fibers, the fibers are first spread on the molds/forms and compacted thoroughly by rolling or other means before the cement slurry is added. Superplasticizers are invariably used in such situations to make the slurry flow freely.

While straight fibers are generally chopped from coils with a shear cutting machine, the Cement Research Institute at New Delhi (now the National Council for Cement and Building Materials) has developed a fiber-forming machine that can produce fibers in various shapes at the rate of about 600 gm/hr. The machine can handle steel wires 0.32 to 0.50 mm in diameter and produce fibers from 25-mm to 45-mm long. The Institute also developed a steel fiber dispenser which ensures that the fibers are de-nested and fed uniformly into the concrete mixing drum, thereby avoiding the balling effect. The dispenser's capacity to feed fibers is 20 kg/min and can be increased by suitable scaling up.

APPLICATIONS OF FRC COMPOSITES IN INDIA

One of the largest applications of FRC has been in the production of precast manhole covers and frames, which make use of both steel and polypropylene fibers. SERC developed the design and production technology for light-, medium-, and heavy-duty manhole covers and frames using SFRC (see Figure 3), and this technology has already been transferred to 17 parties in the country for commercial exploitation. Covers and frames are also being produced using polypropylene fibers, the technology for which was developed by an entrepreneur in New Delhi. The FRC manhole covers and frames possess high ductility and impact resistance and cost less than companion cast iron manhole covers and frames.

FIGURE 3 Fiber reinforced concrete manhole cover and frame developed at SERC, Madras.

FIGURE 4 FRC corrugated roofing sheets used in Orissa, India.

Applications of SFRC in the construction of blast-resistant structures and currency safe vaults is also being investigated by SERC. Preliminary tests carried out on prototype wall elements indicate that the addition of fibers improves the rotation at failure of the structural element, thereby enabling it to absorb the high energy released due to blast, impact, and other types of high velocity impulse loads. Use of steel fibers in machine foundations is being investigated, as it is in ferrocement construction to improve impact resistance. Permanent stay-in-place forms made out of SFRC are being developed at SERC for use in the construction of floor slabs, beams, columns, etc. Moreover, polymer-impregnated precast FRC components and in-situ overlays are expected to find field application soon, based on SERC research and development.

Both steel and vegetable fibers have been used in the development and production of several FRC building components by the Central Building Research Institute, Roorkee. Some of the components developed by the Institute are as follows:

Precast doubly curved roofing tile:
1000-mm long, 1000-mm wide, and 20-mm thick
Precast doubly curved roofing tile:
700-mm long, 700-mm wide, and 20-mm thick
Precast lintel:
1200-mm long, 230-mm wide, and 75-mm thick
Precast plank:
1200-mm long, 400-mm wide, and 25- or 50-mm thick

Corrugated roofing sheets made out of coconut-fiber reinforced concrete or enriched mortar were used at a leprosy settlement in a village near Titilagarh in Orissa, under the technical guidance of the Swiss Centre for Appropriate Technology (SKAT), Switzerland (see Figure 4). Production of the sheets began in 1982, and the roofs have already withstood five monsoon seasons. Such roofing is also being used in several villages in Andhra Pradesh.

Producing coir-reinforced FRC sheets is simple and does not call for special skills; only a metal frame, a working bench, molds, plastic sheets, and traditional masonry tools are needed for their production. First, the plastic sheet is laid on the table top. The metal frame, with a 10-mm thickness, is then placed on the sheet. The mortar is mixed manually with coir fibers, and then the mixture is cast on the table. It is spread by trowels and leveled according to the thickness of the metal frame. After lifting off the metal frame, the wet mortar laid on the plastic sheet is slid, with the support of the plastic sheet, over a corrugated asbestos cement sheet which forms the mold. The sheet is demolded 24 hours after production, and the normal curing procedure begins. The production cost of these FRC sheets is around $2–3 (U.S.) per square meter. FRC tiles with coir fibers have also been produced using molds. The 6-mm-thick tiles are made using 1:2 or 1:3 cement mortar. By vibrating the wet mix in the mold, the consumption of cement content in the mix can be reduced. A hand-operated or electric power vibrating table is used for this purpose. The economic benefits of the coir FRC sheets are obvious: the simplicity of the production procedure leads to an affordable product, yet the producers still get income.

SFRC made with straight fibers has also been used by the International Airport Authority of India in the construction of airfield pavement at New Delhi (*15*). The thickness of the pavement was 300 mm, compared to the 400-mm thickness of its companion plain concrete slab. The reduction in thickness was made possible by the flexural strength of SFRC, which was found to be 80 to 100 kg/cm^2 for the pertinent FRC mix. Conventional methods of handling and laying were adopted, with a slight modification to the conventional concrete mixer. Salient features of the SFRC mix are presented in Table 2.

A simulated dynamic aircraft loading was carried out on the slabs when they were vibrated with a dynamic force of ± 3.6 tons, coupled with the static load of equipment weighing 8.2 tons. The SFRC slab showed more resistance to fatigue and failure during the tests than the companion plain concrete slab of greater thickness. The frequency of the load in the test was kept equal to the natural frequency of the slabs (which was measured earlier with the same dynamic equipment). The pavement has now been in service for nearly 6 years and is used for parking B-747s, DC-10s, and similar classes of aircraft. No cracking, spalling, pitting, or damage of any other kind has appeared in the SFRC slabs.

SFRC in the form of precast interlocking blocks is proposed

TABLE 2 SALIENT FEATURES OF MIX DESIGN FOR SFRC

Cement Content	410 kg./m^3
Water/Cement Ratio	0.6
Sand	730 kg./m^3
Coarse Aggregate:	
10 to 20 mm	399 kg./m^3
4.75 to 10 mm	339 kg./m^3
2.36 to 4.75 mm	151 kg./m^3
Steel Fibres	106 kg./m^3
Shape	Trough type
Length	36 mm
Diameter	0.45 mm

for haul roads used by heavy-duty dumpers in an iron ore project site in Central India. The blocks are now undergoing trials at SERC. The possibility of using SFRC overlays on roads traversed by army tanks is also being explored. The percentage of added fibers will have to be very high to resist the high impact and abrasion loads caused by sudden braking and maneuvering of the tanks on the roads.

CONCLUSIONS

FRC's potential is now well known in the country, but its application has not yet caught up with its repute. Fiber reinforced concrete has many potential areas of applications, such as mass concrete structures, pavements, bridge decks, airport runways, tunnel linings, defense installations, and precast products. The technology of FRC is well understood in India, but the problem remains that metal fibers are not being manufactured in India on a commercial scale. Commercial production of steel fibers is expected to begin within the next couple of years, which may boost the use of FRC composites for a variety of structures. Natural fibers have also proved effective and useful in making low-cost roofing sheets and tiles; their use in housing construction projects is increasing.

Several applications of FRC using either steel or natural fibers have been reported, and the performance of structures and products built with FRC has been laudable. Several institutions and research laboratories in the country are now conducting research and development work aimed at utilizing the full potential of FRC either alone or in combination with ferrocement and polymer impregnation.

ACKNOWLEDGMENT

This paper is being published with the permission of the Director, Structural Engineering Research Centre, Madras, India.

REFERENCES

1. K. Rajagopalan and V. S. Parameswaran. A Study on the Mechanics of Fiber Debonding in Concrete with Micro-reinforcement. *RILEM Materiaux et Constructions*, Vol. 8, No. 46, July–Aug., 1975, pp. 305–314.
2. V. S. Parameswaran and K. Rajagopalan. Strength of Concrete Beams with Aligned or Random Steel Fiber Micro-reinforcement. *Proc. RILEM Symposium on Fiber Reinforced Cement and Concrete*, London, Vol. 1, 1975, pp. 95–103.
3. V. S. Parameswaran and T. S. Krishnamoorthy. Experimental Investigations on the Use of Specially Shaped Steel Fibers in Cement Concrete. Presented at the 1st NCB International Seminar on Pragmatic Strategies for Productivity and Modernisation, New Delhi, India, Jan. 6–9, 1987.
4. V. S. Parameswaran. Fiber Reinforced Concrete—A Versatile Construction Material. Presented at the CIB-IYSH International Seminar on Low Cost Housing and Alternate Building Materials, New Delhi, India, Feb. 10–11, 1988.
5. C. B. Kukreja, S. K. Kaushik, M. B. Kanchi, and O. P. Jain. Economics and Applications of Steel Fiber Reinforced Concrete. *Indian Concrete Journal*, Aug. 1984, pp. 202–206.
6. M. Neelamegam and B. Venkateswarlu. Properties of Glass Fiber Reinforced Cement Composites with and without Polymer Impregnation. *Proc., International Symposium on Fiber Reinforced Concrete*, Madras, India, Vol. I, Dec. 16–19, 1987, pp. 3.67–3.81.
7. A. K. Sachan, D. K. Sharma, and C. V. S. Kameswara Rao. Fiber Reinforced Concrete Machine Foundations. *Proc., International Symposium on Fiber Reinforced Concrete*, Madras, India. Vol. I, Dec. 16–19, 1987, pp. 3.33–3.40.
8. V. S. Parameswaran, T. S. Krishnamoorthy, K. Balasubramanian, and N. Lakshmanan. Behavior of Fiber Reinforced Concrete Beams with Equal Tension and Compression Reinforcement. *Proc., International Symposium on Fiber Reinforced Concrete*, Madras, India, Vol. I, Dec. 16–19, 1987, pp. 1.57–1.67.
9. P. Srinivasulu, N. Lakshmanan, K. Muthumani, and B. Sivarama Sarma. Dynamic Behavior of Fiber Reinforced Concrete Beams. *Proc., International Symposium on Fiber Reinforced Concrete*, Madras, India, Vol. I, Dec. 16–19, 1987, pp. 2.85–2.94.
10. D. L. N. Rao, S. V. Rao, and R. Ramachandra Rao. Steel Fiber Reinforced Concrete Columns with and without Conventional Bar Reinforcement under Uniaxial Bending. *Proc., International Symposium on Fiber Reinforced Concrete*, Madras, India, Vol. I, Dec. 16–19, 1987, pp. 1.91–1.100.
11. H. V. Dwarakanath and T. S. Nagaraj. Flexural Behavior of Reinforced Fiber Concrete Beams. *Proc., International Symposium on Fiber Reinforced Concrete*, Madras, India, Vol. I, Dec. 16–19, 1987, pp. 2.49–2.58.
12. M. Lakshmipathy. *Ductility of Reinforced Fibrous Concrete Structural Members*. Ph.D. thesis presented to the University of Madras, India, April 1983.
13. R. M. Vasan, V. K. Tiwari, S. K. Kaushik, and P. N. Godbole. Corrosion of Steel Fibers in Steel Fiber Reinforced Concrete. *Proc., International Symposium on Fiber Reinforced Concrete*, Madras, India, Vol. II, Dec. 16–19, 1987, pp. 5.39–5.47.
14. N. A. Muhudin. *Design Criteria for Fiber Reinforced Concrete*. Ph.D. thesis. Polytechnic of Central London, 1977.
15. Hans Eric Gram, J. P. M. Parry, K. Rhyner, Beat Schaffner, R. Stulz, K. Wehrle, and H. Wehrli. *FRC-Fiber Concrete Roofing*. SKAT (Switzerland); IT Publication Ltd. (UK), 1987, pp. 138–150.
16. N. Raghavendra, H. K. Kulshrestha, and Rattan Lal. Fiber Reinforced Concrete for Airfield Pavements. *Indian Concrete Journal*, March 1985, pp. 64–67.

Fiber Reinforced Concrete and Shotcrete for Repair and Restoration of Highway Bridges in Alberta

COLIN D. JOHNSTON AND PAUL D. CARTER

Under contract with the Research and Development Branch of the Alberta Transportation Department, the University of Calgary began work to assess the first-crack strength and toughness parameters of concrete and shotcrete to which steel and polypropylene fibers had been added. Laboratory tests employed concrete typical of that normally specified for bridge deck overlays and shotcrete typical of that used for repairing deteriorated portions of supporting bridge structures. To these mixtures were added various types and sizes of steel and polypropylene fibers; silica fume was also included in a few fiber-matrix combinations. Laboratory results showed first-crack strengths from 5.0 to 6.4 MPa for matrixes without silica fume and from 7.9 to 8.6 MPa for those with silica fume. Longer high-aspect-ratio fibers suitable for conventionally mixed overlays produced material with elastic-plastic performance and toughness index (I_{10}) about 10, residual strength factor ($R_{5,10}$) about 100. Combinations with other high-aspect-ratio fibers yielded lower levels of performance, as did those with the shorter low-aspect-ratio fibers needed for shotcrete. Based on these laboratory findings, 26 bridge decks were restored with steel fiber reinforced concrete overlays and structural repairs were made to the beams, piers, or abutments of 19 bridges using steel fiber reinforced, dry-process shotcrete.

In December 1984, the Research and Development Branch of Alberta Transportation expressed interest in the possibility of using steel or polypropylene fibers in several types of concrete repair to existing bridges. Following discussions with the Bridge Branch, a laboratory testing program was finalized and a contract agreement was reached with The University of Calgary to complete the work by April 1985. This paper presents details of the types of mixtures used, experience gained with their use, and data on their in-place performance.

LABORATORY EVALUATION OF FIBER PERFORMANCE

The performance of different fibers was initially assessed in a laboratory study involving flexural testing of beams to determine first-crack strength and toughness parameters in accordance with ASTM C1018. To represent bridge deck overlay applications, five types of steel fiber up to 60-mm long and two types of polypropylene fiber up to 38-mm long were evaluated in a 30-MPa matrix typical of concrete normally specified for this purpose. A silica fume additive was evaluated in one of these fiber-matrix combinations. To represent shotcreting applications, nine types of steel fiber up to 30-mm long were evaluated in a matrix proportioned to represent as closely as possible the mortar normally specified for dry-process shotcrete. A silica fume additive and 7 percent dry silica fume by weight of cement were separately evaluated in one fiber-matrix combination.

C.D. Johnston, Civil Engineering Department, The University of Calgary, Alberta, Canada, P.D. Carter, Alberta Transportation and Utilities, Edmonton, Alberta, Canada.

Concretes for Bridge Deck Overlays

Alberta Transportation's Class D concrete for bridge deck overlays that are up to 75-mm thick employs 13-mm coarse aggregate with Type I cement to achieve a specified strength of 30 MPa with air-entrainment. The concrete matrix for the laboratory work employed 13-mm gravel with 345 kg/m^3 of Type I cement, at a water-to-cement ratio of 0.52; its average strength was 38 MPa at 28 days. The initial slump of 50 to 70 mm was increased to about 175 mm by a constant dose of 2285 ml/m^3 of high-range, water-reducing admixture (about 0.8 percent by weight of cement) before fibers were added. Five types of steel and two types of polypropylene fiber were evaluated in this matrix, and a silica fume slurry admixture was included in the matrix with one type of steel fiber (see Table 1). Air-entrainment was omitted so that the performance of different fibers could be compared without superimposing the effect of between-batch differences in air content on the results.

Workability

The workability of each mixture after addition of fibers was evaluated in terms of time of flow through an inverted slump cone in accordance with the newest revision to ASTM C995, which requires a clearance of 100 mm below the cone instead of the 75 mm previously specified. This test assesses the mixture's ability to flow under internal vibration; flow times from 8 to 15 seconds indicate that concretes are readily placeable using vibration. Since vibration would obviously be employed to overlay work, this test—or an alternative one that employs vibration, such as the V-B test—is a more relevant measure of workability than slump. Johnson (*1*) has discussed comparative measures of the workability of fiber reinforced concrete in terms of inverted cone time, V-B time, and slump.

In general, mixtures with 0.8 percent by volume of any of the five types of steel fiber had inverted cone times in the

range of 8 to 13 seconds (see Table 1), indicating satisfactory workability. The mixture with 0.8 percent of 13-mm monofilament polypropylene had a time of 19 seconds, a test result consistent with its visibly greater stiffness and cohesion. The mixture with 0.8 percent of 38-mm fibrillated polypropylene was quite unworkable, so a mixture with fiber content reduced to 0.35 percent was tested as well. It was quite workable in that it could be consolidated into molds with vibration, but flow slowed in the inverted cone test at 20 seconds and ceased at 27 seconds, leaving about a 75-mm depth of material in the cone that was cohesive enough to support itself with a hole in the center left by the vibrator. This and subsequent experience has suggested that the test may not be appropriate for polypropylene fiber reinforced concrete with long fibers because, even when the mixtures can be fairly easily consolidated into molds with vibration, the test results may not be meaningfully measurable since the fibers induce high cohesion and tend to wrap around the internal vibrator. Recent experience shows that the V-B test can more effectively distinguish the effects of increasing fiber content and fiber length on the workability of fibrillated polypropylene fiber reinforced concretes.

First-Crack Strength

First-crack strengths were determined from load-deflection curves obtained in accordance with ASTM C1018 based on deflection measurements at the midspan. Flexural strengths corresponding to the maximum load reached were also recorded. Both standard 350-by-100-by-100-mm beams and 350-by-150-by-75-mm specimens, more representative of the thickness of a typical overlay, were tested over a 300-mm span; span-depth ratios were 3.0 and 4.0, respectively. The mean values of first-crack and flexural strength for the sets of four specimens representing nine fibrous mixtures are shown in Table 2.

With the exception of the mixture with silica fume, OCS4S, first-crack strengths of the concretes with steel and polypropylene fibers are within 10 percent (about two standard deviations) of the flexural strength of the concrete without fibers, so none of the fibers has significant increased first-crack strength at the 0.8-percent volume concentration employed.

For most of the mixtures, fiber addition did not lead to an appreciable increase in flexural strength over first-crack strength—the values are nearly equal. For two of the fiber

TABLE 1 PROPERTIES OF FIBER REINFORCED CONCRETES FOR BRIDGE DECK OVERLAY APPLICATIONS

Fiber Characteristics			Fiber Content		ICT	Mixture
Type	Description	Size-mm	-%vol	kg/m^3	-s	Symbol[a]
N/A	N/A	N/A	NIL	NIL	--	OC
Steel	Crimped crescent	60x0.8 to 1.3Ø	0.81	60	11	OCS1
Steel	Crimped wire	60x0.9Ø	0.81	60	13	OCS2
Steel	Crimped wire	60x1.0Ø	0.81	60	8	OCS3
Steel	Hooked-end wire	50x0.5Ø	0.81	60	13	OCS4
Steel	Hooked-end wire[b]	50x0.5Ø	0.81	60	13[b]	OCS4S
Steel	Deformed wire	30x0.5Ø	0.81	60	9	OCS5
Polypropylene	Monofilament	13 long	0.78	7.1	19	OCP1
Polypropylene	Fibrillated	38 long	0.78	7.1	ND[c]	OCP2
Polypropylene	Fibrillated	38 long	0.36	3.3	27	OCP3

a - Symbols used in tables 2 and 3.
b - Silica fume slurry additive equivalent to 2.9% fume by weight of cement
c -Not determinable

TABLE 2 FLEXURAL AND FIRST-CRACK STRENGTHS OF OVERLAY CONCRETES IN MPa FOR TWO SIZES OF SPECIMEN

Mixture	350x100x100 mm size		350x150x75 mm size	
Symbol	Flexural	First-Crack	Flexural	First-Crack
OC	5.85	--	5.31	--
OCS1	5.45	5.18	5.24	5.19
OCS2	5.95	5.79	5.83	5.69
OCS3	5.68	5.64	5.74	5.66
OCS4	6.78	5.65	7.02	5.99
OCS4S	8.26	8.13	7.79	7.70
OCS5	5.91	5.79	5.46	5.41
OCP1	5.30	5.20	5.33	5.16
OCP2	5.22	5.16	5.47	5.40
OCP3	5.03	4.95	5.37	5.29

types, however, the flexural strength calculated from the maximum load is higher than the first-crack value for some specimens because the maximum occurs at a deflection much higher than the first-crack deflection. The resulting type of load-deflection curve is the exception rather than the rule, but it does occur consistently with relatively high concentrations of certain types of steel fiber that are highly resistant to pullout from the matrix. As a consequence, the concept of flexural strength becomes meaningless because it can correspond to a highly deflected cracked condition in some cases (curves 2 and 3 in Figure 1 and curves 2, 3, and 4 in Figure 2), and in other cases to a much lower deflection and degree of cracking (curves 1 and 4 in Figure 1 and curve 1 in Figure 2) that is sometimes equivalent to the first-crack condition (curves 1 and 4 in Figure 1). This applies to specimens from the same batch when the post-crack portion of the load-deflection curves approximates perfectly plastic material behavior, even though the within-batch variability of the data is well within the norms for such data, because some specimens slightly exceed this level of behavior while others fall slightly below it. (Coefficients of variation for toughness index I_5 are 5.9 and 6.2 percent in Figures 1 and 2, respectively, and for index I_{10} they are 10.3 and 8.2 percent, respectively.) Consequently, flexural strength is of little significance in defining the performance of fiber reinforced concrete.

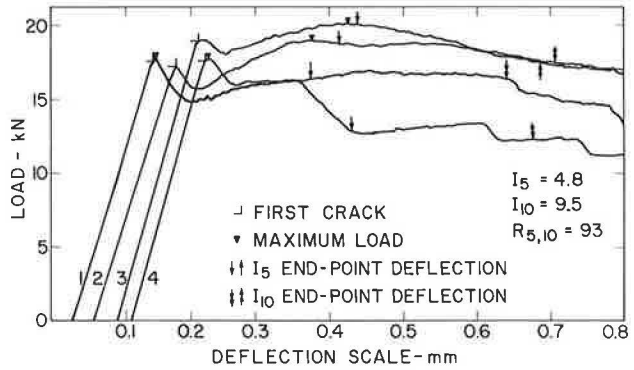

FIGURE 1 Load-deflection curves for overlay concrete OCS1 with 60 kg/m³ of 60-mm crimped crescent-shaped steel fibers.

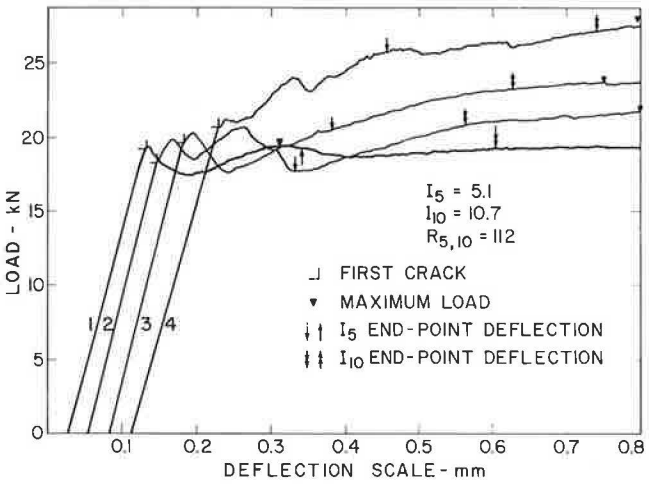

FIGURE 2 Load-deflection curves for overlay concrete OCS4 with 60 kg/m³ of 50-mm hooked-end circular steel fibers.

A more rational approach advocated by Johnston (*2*) is to make a clear distinction between strengthening prior to first crack and toughening thereafter. ASTM C1018 carefully distinguishes between the effect of fiber and matrix parameters on strength in terms of first-crack strength and their effect on toughness in terms of toughness indexes I_5 and I_{10} and other optional toughness indexes with larger endpoint deflections (for example, I_{20} based on 10.5 times the first-crack deflection of I_{30} based on 15.5 times the first-crack deflection). The importance of the distinction between strengthening and toughening becomes particularly obvious when the results for mixture OCS4S with silica fume in the matrix are compared with the equivalent mixture without silica fume, OCS4. The first-crack strength is increased about 30 to 40 percent by the silica fume, which is recorded as a strengthening effect; yet the later effect of silica fume on toughness indexes will be far different from its effect on first-crack strength.

In summary, these results support the concept that first-crack strength is primarily a matrix-dependent property rather than a fiber-dependent property. Unlike flexural strength, it is associated with a particular degree of cracking and deflection, namely the onset of cracking in the matrix and a deflection corresponding to the transition from essentially elastic material behavior to distinctly inelastic or plastic behavior. In contrast, flexural strength based only on the maximum load has no definite and consistent meaning for fiber reinforced concrete in terms of the degree of cracking and deflection associated with it.

Toughness Parameters

Toughness indexes I_5 and I_{10} were determined from load-deflection curves in accordance with ASTM C1018, again using two sizes of specimen; the mean values for the sets of four specimens representing nine mixtures are shown in Table 3. In addition, a parameter termed the residual strength factor, $R_{5,10}$, was calculated from the equation $R_{5,10}$ equals 20 $(I_{10} - I_5)$. This represents the average level of strength retained between the I_5 and I_{10} endpoint deflections as a percentage of the first-crack strength, and by definition is 0 for plain concrete and 100 for a material exhibiting perfectly plastic behavior after first crack, e.g., mild steel after the yield point.

Clearly, the effect of changing the type of fiber is much greater for toughness parameters than for first-crack strength (Table 3). For the standard 350-by-100-by-100-mm specimens,

TABLE 3 TOUGHNESS PARAMETERS OF OVERLAY CONCRETES FOR TWO SIZES OF SPECIMEN

Mixture	350x100x100 mm size			350x150x75 mm size		
Symbol	I_5	I_{10}	$R_{5,10}$	I_5	I_{10}	$R_{5,10}$
OC	1.0	1.0	0	1.0	1.0	0
OCS1	4.80	9.45	93	4.02	7.34	66
OCS2	4.49	8.65	83	3.79	6.87	62
OCS3	4.20	8.28	82	3.80	6.79	60
OCS4	5.12	10.70	112	5.08	10.62	111
OCS4S	4.49	8.54	81	3.96	7.57	72
OCS5	4.43	8.41	80	3.50	5.93	49
OCP1	3.51	4.68	23	3.33	4.69	27
OCP2	3.57	6.03	49	3.41	5.85	49
OCP3	3.64	4.70	21	3.05	4.60	31

I_5 and I_{10} values that approach or exceed 5.0 and 10.0 (elastic-plastic and yield-like material behavior respectively), coupled with residual strength factors close to 100, characterize the two steel fiber mixtures (OCS1 and OCS4) at the top of the performance spectrum for the normal-strength 30-MPa concrete matrix. At the bottom of the performance spectrum are polypropylene fibers with I_5 and I_{10} values of about 3.6 and 4.7 for mixtures of acceptable workability (OCP1 and OCP3). They exhibit a level of material behavior well below elastic-plastic, with residual strength factors of 20 to 30 (Figure 3 and Table 3).

Although the toughness parameters in Table 3 are clearly fiber-dependent, silica fume in the matrix (OCS4S) has much less effect on those parameters than it does on first-crack strength. This supports the view that toughness parameters, unlike first-crack strength, are primarily fiber-dependent rather than matrix-dependent.

Mortars for Shotcrete Repair Work

Alberta Transportation shotcretes for repair work typically have a sand-to-cement ratio of about 3.4, giving a cement content of about 490 kg/m³ with 5-mm nominal maximum-size aggregate. To avoid the high cost and often high variability encountered in shotcrete test panels, the mortar was prepared at a slump of 0 to 5 mm, a constant dose of 2160 ml/m³ of high-range, water-reducing admixture (about 0.5 percent by weight of cement) was added, and the fibers were then incorporated. The idea was to closely simulate the proportions of sand, cement, and water in an equivalent dry-process shotcrete while producing a mixture that could still be consolidated in normal molds by vibration. The final slump was 20 to 50 mm, depending on fiber type, and the water-to-cement ratio was 0.47.

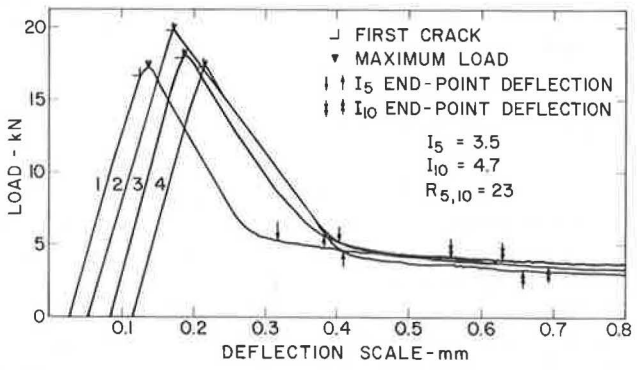

FIGURE 3 Load-deflection curves for overlay concrete OCP1 with 7 kg/m³ of 13-mm monofilament polypropylene fibers.

First-Crack Strength

First-crack and flexural strengths for standard 350-by-100-by-100-mm specimens, and in some cases for comparable 350-by-100-by-50-mm specimens more representative of actual shotcrete thicknesses, are shown in Table 4 for sets of four specimens representing ten mixtures with eight types of steel fiber. Generally, first-crack strengths are in the narrow range of 5.8 to 6.4 MPa regardless of fiber type, except where silica fume is present and the strength is significantly increased. This is entirely consistent with the results for overlay concretes in Table 2, demonstrating again that first-crack strength is primarily matrix-dependent.

Since the fibers employed are considerably shorter than their equivalents used in the overlay concretes because of the practical requirements of the shotcreting process, the load-deflection curves (Figures 4, 5, and 6) do not approach the elastic-plastic level of material performance seen in Figures 1 and 2. Consequently, flexural strengths are without exception only slightly greater than first-crack strengths because the maximum load is reached very soon after first crack.

Toughness Parameters

Toughness indexes I_5 and I_{10} and the derived residual strength factor $R_{5,10}$ are shown for the sets of specimens in Table 5.

TABLE 4 FLEXURAL AND FIRST-CRACK STRENGTHS OF SHOTCRETE MIXTURES IN MPA FOR TWO SIZES OF SPECIMEN

Fiber Characteristics[a]		350x100x100 mm size		350x100x50 mm size		Mixture
Description	Size-mm	Flexural	First-Crack	Flexural	First-Crack	Symbol[b]
Crimped crescent	25x0.8 to 1.3Ø	5.81	5.77	6.03	5.66	SC1
Crimped wire	25x0.9Ø	6.20	6.14	--	--	SC2
Crimped wire	30x1.0Ø	5.99	5.94	6.70	6.21	SC3
Hooked-end wire	25x0.5Ø	6.32	6.27	--	--	SC4
Slit sheet	19x0.3x0.6	6.56	6.41	6.75	6.47	SC5
Smooth wire	25x0.5Ø	6.08	5.96	--	--	SC6
Deformed wire	30x0.5Ø	6.49	6.41	--	--	SC7
Enlarged-end slit sheet	18x0.3x0.6	6.38	6.30	--	--	SC8
Hooked-end wire[c]	25x0.5Ø	8.69	8.63	--	--	SC4S1
Hooked-end wire[d]	25x0.5Ø	7.91	7.87	--	--	SC4S2

a - Steel at 0.8% volume, 60 kg/m³
b - Symbols used in Table 5
c - Silica fume slurry additive equivalent to 3.2% fume by weight of cement
d - Dry silica fume, 7% by weight of cement

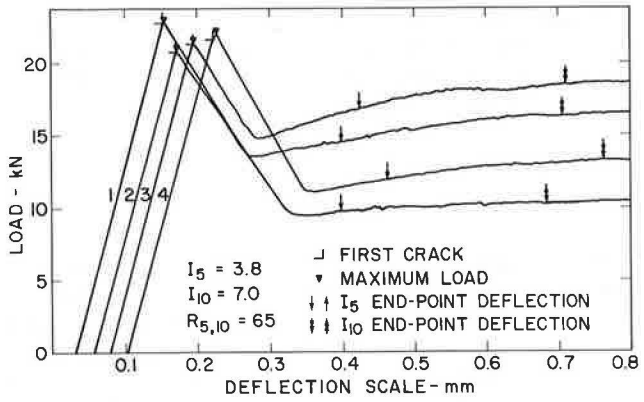

FIGURE 4 Load-deflection curves for shotcrete mixture SC4 with 60 kg/m³ of 25-mm hooked-end circular steel fibers.

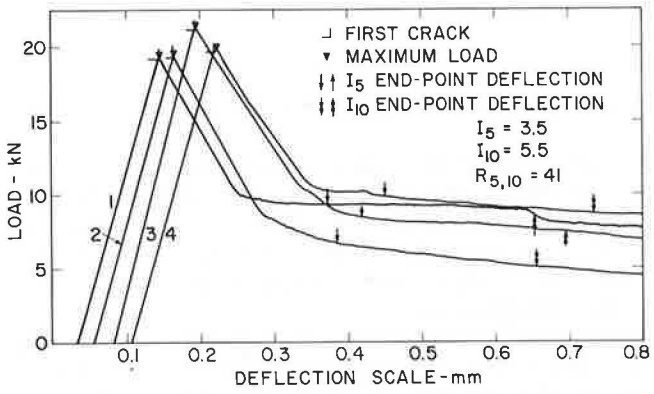

FIGURE 5 Load-deflection curves for shotcrete mixture SC1 with 60 kg/m³ of 25-mm crimped crescent-shaped steel fibers.

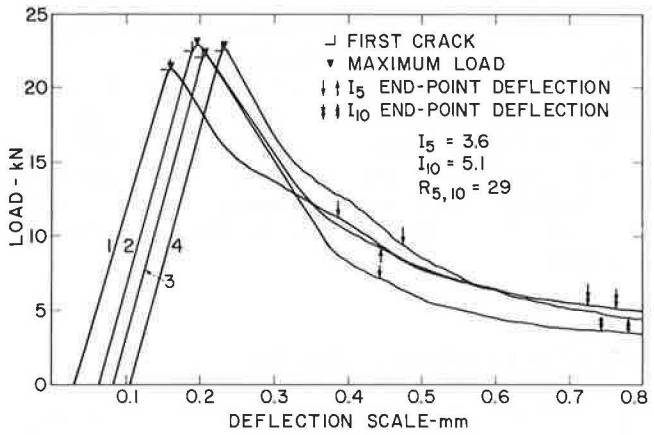

FIGURE 6 Load-deflection curves for shotcrete mixture SC5 with 60 kg/m³ of 19-mm rectangular-shaped steel fibers.

Again, changing the type of fiber has more effect on toughness parameters than on first-crack strength. For the normal-strength matrix without silica fume, the SC4 mixture is at the top of the performance spectrum (Figure 4), the SC1 mixture almost in the middle of it (Figure 5), and the SC5 mixture at the bottom (Figure 6).

Once again, the presence of silica fume has a small effect on toughness parameters compared with its effect on first-crack strength.

TABLE 5 TOUGHNESS PARAMETERS OF SHOTCRETE MIXTURES FOR TWO SIZES OF SPECIMEN

Mixture Symbol	350x100x100 mm size			350x150x75 mm size		
	I_5	I_{10}	$R_{5,10}$	I_5	I_{10}	$R_{5,10}$
SC1	3.47	5.50	41	2.88	4.37	30
SC2	3.53	5.39	37	-	-	-
SC3	3.50	5.32	36	2.78	4.25	29
SC4	3.78	7.02	65	-	-	-
SC5	3.59	5.05	29	3.11	4.50	28
SC6	3.61	5.34	35	-	-	-
SC7	3.83	6.73	58	-	-	-
SC8	3.89	6.26	47	-	-	-
SC4S1	3.66	6.32	53	-	-	-
SC4S2	3.78	7.44	73	-	-	-

Consistent Trends in Overlay and Shotcrete Data

The following trends are among the most important and consistent for both sets of data for standard 350-by-100-by-100-mm specimens:

- A wide range of levels of material performance in terms of toughness parameters is possible, with residual strength factors from about 20 to over 110 (Figures 1 through 6). The differences in performance reflect differences primarily in fiber type and geometry, since fiber concentration is constant at about 0.8 percent by volume.
- Long high-aspect-ratio steel fibers with hooked ends or substantial crimping that are amenable to conventional mixing and placement procedures offer essentially elastic-plastic material performance with a residual strength factor approaching or exceeding 100 (Figures 1 and 2). Steel fibers for shotcrete similar in shape to these types but necessarily shorter and therefore with a lower aspect-ratio offer intermediate performance, with $R_{5,10}$ from 40 to 65 (Figures 4 and 5).
- Other types of steel fiber with less effective resistance to pullout from the matrix as a consequence of their geometry show a lower level of performance. The longer varieties suitable for conventional mixing have $R_{5,10}$ from 70 to 90 (Table 3). The shorter varieties suitable for shotcreting have $R_{5,10}$ from 30 to 40 (Figure 6 and Table 5).
- Although the very limited data for polypropylene fibers obtained in this program indicates $R_{5,10}$ in the 20- to 30-range for workable mixtures (Figure 3 and Table 3), subsequent data confirm that values up to 50 are possible with reasonably workable mixtures using high-range, water-reducing admixtures.
- Silica fume added to the matrix consistently and significantly increases the first-crack strength in both overlay and shotcrete mixtures by 30 to 40 percent. Its effect on toughness parameters is less clear: toughness was considerably decreased in the case of the slurry additive (Tables 3 and 5) yet was slightly increased for the dry silica fume alone. One possible explanation is that, for the slurry additive, the silica fume may have settled, causing the amount of silica fume actually added to be less than intended. Other data (*3*) show that dry silica fume in excess of 5 percent by weight of cement improved toughness parameters when using a uniform straight fiber instead of the hooked-end type employed in this comparison.
- A system comprising a properly proportioned concrete or mortar matrix with silica fume and an appropriate amount of a high-performance fiber probably offers optimum

strengthening and toughening for either overlay or shotcrete applications.

Effect of Specimen Size

In both overlay and shotcrete mixtures, thin sections representative of the application thickness can be compared with standard 350-by-100-by-100-mm specimens on the basis of differences in the volume of the zone of probable material failure, V′ (product of the length of the midspan plus one-eighth of the shear span, the width, and one-eighth of the depth) a concept developed elsewhere (*4*) to explain the effects of specimen span, depth, crossection, and mode of loading on flexural strength. Accordingly, the flexural strength of the 350-by-150-by-75-mm specimens should be 98.8 percent of the strength of the standard specimens; the actual average based on 10 comparisons is 98.8 percent, although the range is 91 to 107 percent. The strength of the 350-by-100-by-50-mm specimens should be 107.2 percent of the strength of the standard specimens; the actual average based on only three comparisons is 106.2 percent. The effects of specimen geometry on strength in this study are therefore consistent with previous work (*4*).

There is no substantive database against which to assess the effects of specimen geometry on toughness indexes. Preferential fiber alignment by the mold surfaces in the thin specimens to a greater degree than in the standard specimens should, if anything, increase toughness indexes. Instead, the thinner sections give toughness indexes I_5 and I_{10} consistently lower than for the standard specimens by 11 to 17 percent in both overlay and shotcrete mixtures. The increased span/depth ratio of the thinner specimens may be partly responsible insofar as the ratio influences the role of shear, but differences in the softness of the testing system probably also play a role. Studies conducted subsequent to this testing program have shown (*3*) that toughness indexes based on nominal midspan deflection are less than those based on true midspan deflection (nominal midspan deflection, minus the average deflection at the two supports). There were simply not enough data in this study to isolate the cause of the differences between the thin-section and standard specimens. The point is that toughness indexes are by definition (*2,5*) independent of specimen geometry, provided that shear does not unduly influence the flexural behavior and that the measurement of deflection reflects the true value of deflection, exclusive of deformation of the supports; comparisons of different types of specimen can be valid only if deflection is properly measured and the influence of shear is negligible, or at least constant. Shear is certainly not negligible when the span/depth ratio is 3.0, the minimum stipulated in ASTM C1018 and the value most frequently employed by users of the standard. Also, ASTM C1018 does not require that measurement of deflection include allowance for deformation at the supports in calculating the midspan deflection, a feature that is likely important when tests involve the effects of specimen geometry on toughness indexes.

Precision

The levels of precision achieved in various facets of this laboratory program are tabulated in Table 6; they are expressed as averages for the within-batch coefficient of variation, that is, the 1S% term defined in ASTM C670. The results represent sets of four specimens for the various fiber types and specimen sizes identified in Tables 1 and 4. Except for the 350-by-100-by-50-mm shotcrete mixtures, where the loads were very small relative to the load capacity of the testing equipment, all averages are well within the limits recommended in ASTM C1018.

Concluding Comments on Laboratory Evaluation

Comparative evaluations allow various fiber types to be ranked by performance at a given volume concentration. A larger concentration of a cheaper fiber may give equivalent performance, however, thus proving cost-competitive. If this possibility arises, fiber content should be included as a variable in the testing program.

While the benefits of strengthening concrete are readily understood, field experience is not yet sufficient to enable the benefits of toughening it to be fully appreciated, and it is not yet possible to specify the minimum toughness criteria that can predict satisfactory performance in particular applications, such as overlays. There is only what may perhaps be described as an intuitive perception that a fiber reinforced concrete which approaches the elastic-plastic or yield-like behavior of mild steel should perform better than a plain concrete with brittle, elastic characteristics under the impactive and repeated dynamic loading of traffic producing relatively high deflection on bridge decks or bridge girders. This laboratory evaluation clearly indicates that using silica fume to strengthen the matrix and steel fibers to toughen it probably offers the best possible material performance for these loading conditions.

BRIDGE DECK OVERLAY REPAIRS

Since 1984, Alberta Transportation has placed 26 steel fiber reinforced overlays on bridge decks and approximately 12 more are scheduled for 1989.

TABLE 6 AVERAGES FOR WITHIN-BATCH COEFFICIENTS OF VARIATION FOR SETS OF FOUR SPECIMENS IN VARIOUS SPECIMEN SIZES

	Overlay Concretes		Shotcrete Mixtures		ASTM C1018
	350x100x100 mm Specimens	350x150x75 mm Specimens	350x100x100 mm Specimens	350x100x50 mm Specimens	Maximum limits
Flexural Strength	5.9%	4.6%	3.4%	5.2%	5 to 8%
First-Crack Strength	4.8%	4.8%	3.5%	5.9%	5%
Toughness Index I_5	5.6%	5.1%	4.3%	8.5%	12%
Toughness Index I_{10}	8.9%	6.7%	9.6%	16.4%	14%

Form of Deterioration

Most of the bridges are constructed of precast channel-shaped girders bolted together laterally, which, in the absence of adequate lateral connections, have developed longitudinal cracks in the asphalt or high-density concrete wearing surfaces. The resulting leakage of salt or water has caused corrosion of rebar in the girder legs. Approximately 300 such bridges in the primary highway system in Alberta are regularly subjected to deicing and a further 3,300 are located on secondary and local roads where deicers are not normally used.

Nature of Repair

The purpose of the repairs is restoration of the lateral connections to eliminate or reduce the movements that cause longitudinal cracking, thereby stopping flow of water or salt to the deck support structure. Grouting and placement of epoxy-coated bar to augment the existing lateral connections precedes overlay placement. Fiber reinforced concrete is supposedly better able to withstand whatever movements remain without cracking, and it is considered to be structurally adequate at a lesser thickness than its plain concrete equivalent when additional dead loads by repair must be minimized. The bridges so far selected for repair are expected to remain in service for at least another 20 years; hence, that fatigue performance may be important also favors the use of fiber reinforced concrete.

Initial Trials and Specifications

Initially, the work involved private contractors, government highway crews, various finishing machines and texturing methods, and mixtures with fly ash, silica fume, and high-range water-reducing admixtures. Some of the problems encountered were difficulty in emptying prebagged material due to set during transport, fiber balling during mixing, surface tearing during texturing or finishing, shrinkage cracking probably caused by excessive slump or a poorly wetted porous subsurface, poor freeze-thaw durability caused by an inadequate air void system, and excessive fibers on the surface prior to their disappearance by corrosion (Table 7). Materials and practices have subsequently been refined to address these problems.

Current Practice and 1988 Specifications

The work is now done mostly by private contractors. Surface preparation following final sandblasting of existing concrete and reinforcement consists of prewetting the entire deck for a minimum of 3 hours, removal of free surface water by compressed air, and application of a 1:1 sand-cement grout followed immediately by placement of concrete. The minimum thickness of new concrete on the prepared surface is normally 70 mm. Placement is permitted only by approved Gomaco LS300 and Bidwell OF400 and OF500 machines having at least one internal vibrator per 1.5 m of screed length.

The specification calls for a prebagged concrete with 20-mm aggregate, 5-percent silica fume by weight of cement, and 60 kg/m^3 of 63-mm crimped, crescent-shaped fibers. High-range water-reducers or fly ash are not permitted. Water and an air-entraining agent are added at the site to a rotating drum transit mixer operating at about 75 percent capacity. Slump must not exceed 50 mm. The air void content is 7, plus or minus 1 percent. Specified compressive strength at 28 days is 35 MPa. Strengths between 27.5 and 35 MPa are subject

TABLE 7 BRIDGE DECK OVERLAY REPAIRS, 1984–88

Bridge Name	Year of Repair	Deck Area (m^2)	Present Condition
Rourke Creek	1984	281	surface scaling
Oldman Creek	1984	326	surface scaling
Strawberry Creek	1984	347	surface scaling
Lonepine Creek	1985	186	good
Rosebud River	1985	280	good
Athabasca River	1985	1600	good
Wolf Creek	1985	981	good
Gardner Gr.Sep.	1986	776	shrinkage cracks
Morley Trail Underpass	1986	725	shrinkage cracks
Paintearth Creek	1986	334	good
Iron Creek	1986	209	good
Blackmud Creek	1986	186	good
Sawridge Creek	1986	281	good
Wolf Creek	1987	407	good
Lesser Slave River	1987	776	good
Tawatinaw River	1987	210	good
Baptiste River	1987	667	good
Grade Separation	1987	326	good
Berry Creek	1987	343	good
Brown Creek	1987	258	good
Driedmeat Creek	1988	373	*
Grade Separation	1988	429	*
Pine Creek	1988	317	*
Meeting Creek I	1988	333	*
Meeting Creek II	1988	242	*
Willow Creek	1988	209	*
	TOTAL	11,402	

* Too soon to comment on condition

to an incremental penalty schedule, and material weaker than 27.5 MPa is rejected.

Following passage of a vibratory screed, the surface is magnesium-floated to a tolerance of 3 mm on a 3-m straightedge and grooved to a depth of 3 to 5 mm with a curved rake that slides over the surface without snagging any fibers. When slump is about 50 mm, the surface fibers settle horizontally into the paste and permit texturing without tearing.

Moist-curing with wet burlap commences normally within 30 minutes, and is maintained for 72 hours or longer at the discretion of the engineer. An automatic sprinkling system is required for the first 24 hours, with the option of covering the burlap with polyethylene film thereafter. Careful attention to curing and placement in the morning hours when temperatures are relatively low helps to eliminate shrinkage cracking, as do prewetting the subsurface and maintaining an overlay thickness of at least 70 mm. A surface sealant is applied at least 4 days after the completion of the moist-curing regime.

Fibers left on the surface subsequently corrode, causing stains that may be unsightly, but such corrosion is confined to the surface, tends to disappear under the action of traffic, and is not a structural problem.

Conclusions on Bridge Deck Overlay Repairs

Despite some early problems which have been largely eliminated by refinements incorporated into the 1988 specification, the program of bridge deck overlay repairs commenced in 1984 has been technically and economically successful. While restoring the lateral connections between the underlying bridge girders is essential for the success of any repair technique, fiber reinforcement improves resistance to cracking caused by whatever potential remains for movement between girders and likely improves long-term performance with respect to the fatigue and impact conditions produced by traffic. Elimination of cracking prevents access of water and the debonding caused by it that in turn leads to spalling of pieces of concrete in high density or other nonfibrous overlays. Even if cracking does occur in fibrous overlays, the spalling tendency is reduced by the ability of the fibers to bridge cracks and maintain continuity. Silica fume improves strength and durability with respect to chloride penetration, although a proper air void system remains essential for freeze-thaw resistance. The combination permits the use of thinner overlays than would otherwise be possible, and alleviates the tendency for bridges to become overloaded by the additional dead loads associated with the repair. Although the performance of decks repaired to date is promising (Table 7), a few more years of satisfactory performance are needed to confirm the longevity of the repair technique. Nevertheless, 15 of the 20 overlays that have been in place for at least one winter are rated good in Table 7, which means cracking is negligible or nonexistent.

SHOTCRETE REPAIRS TO BRIDGES

Since 1984, Alberta Transportation has repaired 19 bridges using prebagged, steel fiber reinforced shotcrete. Before then, site-mixed latex-modified shotcrete was used. The advantages of prebagged, steel fiber reinforced shotcrete are less surface cracking, easier finishing, better quality control, elimination of about 90 percent of meshing and anchoring, and improved mechanical properties; moreover, many perceive that using the steel fiber reinforced concrete leads to easier, quicker, and more economic repairs that can be carried out by a greater number of qualified contractors. Experts consider the main disadvantages of the new mix to be weaker bond strength and increased permeability to water and deicing salts. An acrylic surface sealant was specified to address the latter concern.

Forms of Deterioration

Some bridges consisted of a precast deck bound by precast, prestressed channel-shaped girders bolted together laterally to facilitate load sharing and overlaid with a 50-mm asphalt concrete wearing surface. With the passage of time and exposure to heavy truck traffic, the lateral connections had loosened and destroyed the load-sharing between girders, resulting in greater deflections, cracking of the asphalt, ingress of water and deicing salts, and eventual spalling over the main reinforcing bars in the girders.

Other bridges having steel superstructures had suffered concrete deterioration due to freezing and thawing of portions of abutments or piers kept highly saturated by leakage from open deck joints above. Another problem was cracking near anchor bolts caused by corrosion and seizing of expansion bearings, aided by temperatures ranging from 40°C to −45°C. Two bridges constructed in the 1920s contained concrete of relatively low quality made with rounded aggregate up to 300 mm in size.

Trial Mixtures and Specifications

The 1984 specification required a prebagged, dry-process shotcrete mixture using 8-mm aggregate to produce a 28-day cube compressive strength of 45 MPa. Six trial mixtures with an aggregate-to-cement ratio by weight of about 3.4 (4.0 by volume), varying amounts of two types of fiber, and an accelerator were evaluated using cubes and beams prepared by qualified nozzlemen (Table 8). The mixture finally selected contained 60 kg/m^3 of 25-mm crimped, crescent-shaped fibers and no accelerator. It was applied to surfaces prewetted for a minimum of 2 hours and it was kept moist overnight following application. The final layer of shotcrete contained no fibers (to avoid fiber rusting) and, following light sandblasting, it was coated with one of seven approved acrylic sealants.

Nature and Performance of 1984 Repairs

Repairs were made in 1984 to seven bridges (Table 9). Generally, the shotcrete was used simply to replace deteriorated structurally suspect concrete and to restore the original shape of the concrete elements. However, drainage was sometimes improved since it was possible to reshape contours and round edges or corners, which is not usually the case with formed repairs.

Subsequent inspections revealed few major problems. The repairs were generally crack-free and well bonded. The few cracks that were visible seemed to be either shrinkage cracks caused by insufficient prewetting when shooting thin patches

TABLE 8 PREQUALIFICATION OF PREBAGGED SHOTCRETE MIXTURES

Fiber Characteristics			Accelerator	Strengths[a] (MPa)			Density
Description	Size (mm)	Amount kg/m^3	-% by wt. of cement	Compressive 7-d	Compressive 28-d	Flexural 7-d	kg/m^3
Crimped crescent	25×0.8 to 1.3Ø	59	1	45.7	54.7	5.7	2369
" "	"	35	1	58.3	74.8	8.2	2404
" "	"	59	0	50.9	64.7	8.8	2379
Deformed wire	30×0.5Ø	59	0	64.0	74.4	8.1	2394
" "	"	47	0	66.4	75.2	8.3	2397
" "	"	47	2	41.1	54.7	6.3	2371

a - Cubes and beams sawed from 600×600×100 mm slabs

TABLE 9 NATURE AND PERFORMANCE OF 1984 SHOTCRETE REPAIRS

Bridge Name (Date Constructed)	Elements Repaired	Volume of repair-m^3	Average depth-mm	Area sealed-m^2	Strength-MPa 7-d	Strength-MPa 28-d	Density -kg/m^3	Present Condition
N.Sask.River (1957)	2 piers	5.5	118	94	56	64	2372	Good, some shrinkage cracks
Pembina River (1922)	1 pier and 1 abutment	3.3	150	106	48	62	2363	Good
McLeod River (1953)	1 pier	8.3	50	151	56	73	2363	Good when removed (1987)
Redwater River (1955)	1 pier and 1 abutment	0.4	100	6	54	71	2384	Good
L. Smoky River (1925)	1 pier	3.6	100	88	72	81	2382	Good
Strawberry Creek (1963)	precast girders	9.4	65	144	54	66	2364	Good, some cracks
Rourke Creek (1962)	precast girders	4.9	63	77	47	59	2325	Good, some cracks
TOTALS (AVERAGES)		35		666	(55)	(68)	(2362)	

on large porous members or by inadequate curing in hot, windy weather, or reflective cracks possibly caused by a lack of construction joints in long continuous layers.

Current Practice and 1987 Specifications

Effective April 1987, the specification limits nominal aggregate maximum size to 6 mm for fiber reinforced mixtures and 3 mm for the no-fiber finishing coat. Fiber content is 60 kg/m^3 of 25-mm, crimped, crescent-shaped fibers or an approved equivalent. The specified cube compressive strength from 75-mm-thick test panels is 40 MPa at 7 days (previously 45 MPa at 28 days), with up to 1 percent non-chloride accelerator permitted. Use of approved and tested prebagged material is stipulated to reduce the number of variables that could create problems. Silica fume is permitted if the contractor so requests. Foremen and nozzlemen must have at least 5 years' experience in shotcreting. Strengths between 28 and 40 MPa are subject to an incremental penalty schedule which awards 50 percent of the unit price for strengths of 25 to 28 MPa and no payment for strengths under 25 MPa. Cast-in-place construction may be required for depths greater than 150 mm, and is priced at 85 percent of the shotcrete bid. Sealed construction joints are permitted. Inspection by Alberta Transportation engineers who have sufficient experience to deal with contractors is virtually full-time.

Between 1985 and 1987, 12 more projects were completed, totaling 166 m^3. Of the 19 projects completed since 1984, 10, including the 6 most recent, are rated good in 1988, 4 have some cracks attributed to insufficient curing of silica fume mixtures, and the remainder have some minor cracking due to other causes (Table 10). Over the years, prewetting has been increased for porous surfaces. Continuous wetting for 4 to 24 hours is required, depending on the porosity of the underlying concrete, with final decisions made by the engineer. The prewetted concrete is allowed to surface dry and must not be wetted again prior to shotcreting.

TABLE 10 NATURE AND PERFORMANCE OF 1985–87 SHOTCRETE REPAIRS

Bridge Name	Elements Repaired	Volume of Repair-m^3	Year Repaired	Present Condition
Sheep River	curb parapets	8.2	1985	some cracks *
Shunda Creek	underside precast	10.2	1985	some cracks *
Carvel Corner	1 pier	4.4	1985	some cracks
N.Saskatchewan River	2 piers	22.4	1985	cracks *
Grade Separation	precast girders	10.2	1985	cracks *
Oldman Creek	curb, precast girders	15.3	1986	some cracks
Vermilion River	precast girders	2.9	1986	good
N.Saskatchewan River	6 piers	30.6	1986	good
Little Smoky River	? piers	30.4	1986	good
Gardner Grade Sep.	precast girders	20.7	1986	good
CPR Overpass	2 piers, 1 abutment	5.8	1987	good
Sawridge Creek	precast girders	4.8	1987	good
	TOTAL	166		

* shrinkage cracks resulted from insufficient curing of silica fume mixtures

The period of moist-curing required has been extended when a sealant is not applied or when silica fume is used. Moist-curing must commence within 4 hours of placement and continue for 24 hours when a sealant is to be applied. When no sealant is used, or when silica fume is present, moist-curing is extended to 48 hours. The benefits of higher strength and less rebound in overhead work associated with using silica fume are substantial.

Various categories of finish are specified. For areas not visible to the public, an as-shot fibrous layer with fibers exposed is permitted, with an 8-mm tolerance over 2 m. For highly visible areas, the requirement is a smooth, hand-finished, no-fiber layer with no fibers protruding from the underlying layer, with a tolerance of 4 mm over 2 m.

Conclusions on Shotcrete Repairs

Overall, the program of shotcrete repairs undertaken since 1984 has been technically and economically successful. There have been no durability problems, partly because of a policy of eliminating potential sources, such as leakage or poor drainage, before shotcreting. The technique is judged cost-effective (60 to 70 percent of the cost of the latex-modified concrete previously employed), less mesh is needed, finishing is easier, and bid prices are more competitive because there are more qualified contractors.

ACKNOWLEDGMENT

Financial support for the laboratory work was provided by the Research and Development Branch of Alberta Transportation; testing was performed by Paul R. Houle, a research assistant at the University of Calgary. Data for field projects were supplied by the Bridge Services Branch of Alberta Transportation.

REFERENCES

1. C. D. Johnston. Measures of the Workability of Steel Fiber-Reinforced Concrete and Their Precision. *Cement, Concrete and Aggregates*, Vol. 6, No. 2, Winter 1984, pp. 74–83.
2. C. D. Johnston. "Toughness of Steel Fiber-Reinforced Concrete," Proceedings of a U.S.–Sweden Joint Seminar on Steel Fiber Concrete, Swedish Cement and Concrete Institute, Stockholm, 1985, and Elsevier Applied Science Publishers Ltd., 1986, pp. 333–360.
3. C. D. Johnston and R. J. Gray. Flexural Toughness and First-Crack Strength of Fibre-Reinforced Concrete using ASTM Standard C1018. *Proc., Third International Symposium on Developments in Fibre Reinforced Cement and Concrete*, Sheffield, RILEM, July 1986.
4. C. D. Johnston, Steel Fiber-Reinforced and Plain Concrete: Factors Affecting Flexural Strength Measurements. *Journal of the American Concrete Institute*, Vol. 79, March–April 1982, pp. 131–138.
5. C. D. Johnston, Definition and Measurement of Flexural Toughness Parameters for Fiber-Reinforced Concrete. *Cement, Concrete and Aggregates*, Vol. 4, No. 2, Winter 1982, pp. 53–60.

Flexural Fatigue Strength, Endurance Limit, and Impact Strength of Fiber Reinforced Concretes

V. RAMAKRISHNAN, GEORGE Y. WU, AND G. HOSALLI

In many applications, particularly in pavements, bridge deck overlays, and offshore structures, the flexural fatigue strength and endurance limit are important design parameters because these structures are designed on the basis of fatigue load cycles. This paper presents the results of an extensive experimental investigation to determine the behavior and performance characteristics of the most commonly used fiber reinforced concretes (FRC) subjected to fatigue loading. A comparative evaluation of fatigue properties is presented for concretes with and without four types of fibers (hooked-end steel, straight steel, corrugated steel, and polypropylene) at two different quantities (0.5 and 1.0 percent by volume), using the same basic mix proportions for all concretes. The test program involved the determination of fresh concrete properties, including slump, vebe time, inverted cone time, air content, unit weight, and concrete temperature; and the determination of hardened concrete properties, including flexural fatigue strength, endurance limit, and impact strength. The addition of the four types of fibers caused a considerable increase in the flexural fatigue strength and the endurance limit for 4 million cycles, with the hooked-end steel fiber providing the highest improvement (143 percent) and the straight steel and polypropylene fibers providing the least. The impact strength was increased substantially by the addition of all four types of fibers, with straight steel fiber producing the lowest increase.

The recent interest in reinforcing portland cement based materials with randomly distributed fibers was spurred by pioneering research on fiber reinforced concrete (FRC) conducted in the United States in the 1960s. Earlier work (*1–19*) has established that the addition of steel fibers improves the static flexural strength, flexural fatigue strength, impact strength, shock resistance, ductility, and failure toughness in concrete.

In many applications, particularly in pavements and bridge deck overlays, the flexural fatigue strength and endurance limit are important design parameters because these structures are designed on the basis of fatigue load cycles. The greatest advantage of adding fibers to concrete is the improvement in fatigue resistance. Plain concrete has a fatigue endurance limit of 50 to 55 percent of its static flexural strength (*15–17*). A properly designed FRC can achieve a 90 to 95 percent endurance limit. Theoretically, with a higher endurance limit, the concrete cross sections could be reduced. Alternatively, using the same cross section could result in a longer life span or higher load carrying capacity or both.

However, the research cited above involved small-scale, independent pilot projects for various types of fibers. A need remained for an extensive scientific investigation to determine the fatigue performance characteristics of the most commonly used types of fibers and mix proportions. There was a further need to evaluate the comparative fatigue behavior of various types and quantities of fibers. Particularly, little information is available about the flexural fatigue behavior of concretes with different types and quantities of fibers.

The primary objective of this research was to determine the behavior and performance characteristics of FRC subjected to fatigue loading. The other major objectives were

- To determine the fresh concrete properties including workability, balling characteristics, and finishability of concretes reinforced with four types of fibers (hooked-end steel, straight steel, corrugated steel, and polypropylene) and to compare their properties with those of corresponding plain concrete;
- To study the effect on the fresh and hardened concrete properties due to the addition of the four types of fibers at 0.5 and 1.0 percent by volume of fibers to a plain concrete mix; and
- To conduct a detailed investigation of the flexural fatigue strength including the endurance limit for concretes with and without the four types of fibers in two different quantities, using the same basic proportions for all concretes.

MATERIALS, MIXES, AND TEST SPECIMENS

Materials

Fibers

The following four types of fibers were used in this investigation:

1. *Type A*. The 2-in.-long hooked-end fibers used were glued together side by side into bundles with a water-soluble adhesive. During the mixing process, the glue dissolved in water and the fibers separated into individual fibers, creating an aspect ratio of 100.
2. *Type B*. The straight fibers used were made from low carbon steel with a rectangular cross section of 0.009 in. × 0.030 in. and a length of 0.75 in. It has an aspect ratio of approximately 40.
3. *Type C*. The 2-in.-long corrugated fibers used were pro-

V. Ramakrishnan and G. Hosalli, South Dakota School of Mines and Technology, Rapid City, S. Dak. 57701. G. Y. Wu, Naval Civil Engineering Laboratory, Port Hueneme, Calif. 93043-5000.

duced from a mild carbon steel. The diameter of the fiber (or equivalent diameter) was 0.03 to 0.05 in. with an aspect ratio of about 40 to 65.

4. *Type D.* The ¾-in.-long polypropylene fibers used were collated, fibrillated fibers.

Cement

ASTM Type I/II (dual purpose) portland cement was used.

Coarse Aggregate

The aggregates used were blended in two sizes: (a) in a mixture of 60 percent aggregate with a 1-in. maximum size, and (b) 40 percent aggregate with a ⅜-in. maximum size. The mixture satisfied ASTM C33.

Fine Aggregate

The fine aggregate used was natural sand. It had a water absorption coefficient of 1.64 percent and a fineness modulus of 3.02.

Admixtures

A superplasticizer satisfying the requirements of ASTM C494 for chemical admixtures and an air-entraining agent satisfying the requirements of ASTM C260 were used.

Mixes

The same proportions were used for the plain (control) and FRC mixes for the entire investigation. The water-to-cement ratio was maintained at 0.4 for all the concretes. For flexural fatigue testing, two mixes each for plain and Type A, B, C, and D fibers were made with 0.5 percent and 1.0 percent by volume of fibers. The control mix design was as follows:

Cement	658 lb/yd³
Coarse aggregate	1,560 lb/yd³
Fine aggregate	1,560 lb/yd³
Air content	5 ± 1.5 percent

Test Specimens

For the fatigue test, 18 beams of 6 in. × 6 in. × 21 in. (152 mm × 152 mm × 533 mm) were cast in each of plain, 1.0 percent fiber, and 0.5 percent fiber concretes. Cylinders 6 in. × 2.5 in. (152 mm × 64 mm) were made for the impact test.

TESTS FOR FRESH CONCRETE

The freshly mixed concrete was tested for slump (ASTM C143), air content (ASTM C231), fresh concrete unit weight (ASTM C138), temperature, time of flow through an inverted cone (ASTM C995), and vebe time.

TESTS FOR HARDENED CONCRETE

Flexural Fatigue Test

Third point loading was used in the flexural fatigue strength test. The test beams had a span of 18 in. and were subjected to a nonreversed fluctuating load.

The lower load limit was set at 10 percent of the average maximum load obtained from the static flexure test. The upper load limit was set at 90 percent of the average maximum flexural load for the first beam in each mix, and the fatigue test was run between these limits. If the beam failed before completing 2 million cycles, the upper limit was reduced for the next specimen. If the beam survived, another beam was tested at the same upper load as a replicate. Three specimens were tested at each maximum load level.

The frequency of loading used was 20 cycles/sec (Hz) for all tests. The control and monitor system for all tests consisted of a MTS 436 control unit, a Hewlett-Packard oscilloscope, and a digital multimeter working with a MTS load cell.

Impact Test

The impact specimens were tested at 28 days by the drop-weight test method (*7*). Equipment for this test consisted of

- A standard, manually operated, 10 lb (4.54 kg) weight hammer with an 18 in. (457 mm) drop (ASTM D1557);
- A 2.5 in. (63.5 mm) diameter hardened steel ball; and
- A flat steel base plate with a positioning bracket and four positioning lugs.

The specimen was placed on the base plate within the positioning lugs with its rough surface upward. The hardened steel ball was placed on top of the specimen within the positioning bracket, and the compactor was placed with its base on the steel ball. The test was performed on a smooth, rigid floor to minimize the energy losses. The hammer was dropped consecutively, and the number of blows required to cause the first visible crack on the top of the specimen was recorded. The impact resistance of a specimen to ultimate failure was also measured by recording the number of blows required to open the cracks enough that the pieces of the specimen touched three positioning lugs on the base plate.

TEST RESULTS AND DISCUSSION

Fresh Concrete Properties

Room temperature, humidity, and concrete temperature were recorded to ensure that all the mixes were tested under similar conditions. The room temperature and humidity varied in the range of 18° to 27°C and 33 to 58 percent, respectively. The concrete temperature range was 20.4° to 27.2°C.

Workability

Three test were done to determine the workability of the mixes: slump, inverted cone time, and vebe time. The test

results indicated that, in general, satisfactory workability can be maintained even with a relatively high fiber content. This was achieved by adjusting the amount of superplasticizer used; the water-to-cement ratio remained constant (0.4) for all mixes.

Balling tendency for the straight steel fiber mixes was observed at 1.5 percent fiber volumes. To avoid balling, the fibers had to be carefully sprinkled by hand. The concrete had poor workability and more bleeding and segregation with higher quantities of polypropylene fibers. In all other mixes with an appropriate quantity of fibers, there was no balling, bleeding, or segregation. Even though slump values decreased with increasing amounts of fibers, no difficulty was encountered in placing and consolidating the concrete in the laboratory.

It seems that the relationship between vebe time and slump for each fiber type is not affected by fiber contents for the range tested in this investigation. However, the relationship is different for other types of fibers, and markedly different for hooked-end fibers. The rheological properties of fresh concrete with hooked-end steel fibers are different than those for other fibers. This may be due to the higher frictional resistance for movement in hooked-end fibers.

The relationship between vebe time and slump is independent of the air content. Fibrous concrete has less slump than plain concrete. In general, FRC seems to be more workable under vibration than is indicated by the slump. Nevertheless, the energy needed to compact the concrete appears to be proportional to the fiber content in the concrete.

The inverted cone test was specially developed (*12*) to measure the workability of FRC in the field. Since both the inverted cone test and the vebe test are based on the energy requirements for flowability and compaction, there is a linear correlation between the two tests. This facilitates the transfer of laboratory test results to field practice more accurately.

Finishability

Excellent finishability was achieved with the appropriate dosage of superplasticizer.

Hardened Concrete Properties

Flexural Fatigue Behavior

The fatigue properties of FRC were evaluated thoroughly in this study. Beams made with plain concrete and concretes reinforced with 0.5 percent and 1.0 percent by volume of fibers were tested for flexural fatigue. Three specimens were tested at each strength level. Figures 1 through 11 present the various relationships between the number of cycles (N), log N, fatigue strengths, and endurance limits. Based on the data presented in these figures, the following three main properties are discussed:

- Fatigue strength,
- Endurance limit expressed as a percentage of modulus of rupture of plain concrete, and
- Endurance limit expressed as a percentage of its modulus of rupture.

Fatigue Strength Fatigue strength (f_{fmax}) is defined as the maximum flexural fatigue stress at which the beam can withstand 2 million cycles of nonreversed fatigue loading.

The fatigue strength was increased substantially with the addition of fibers to the concrete, as shown in Table 1 and Figure 1. The fatigue strength was 508 psi for plain concrete and 549 psi and 676 psi, respectively, for concrete mixes reinforced with 0.5 percent and 1.0 percent corrugated steel fiber. The increase in fatigue strength was 8 percent and 33 percent, respectively.

Graphs of flexural fatigue stress versus the number of cycles are shown in Figures 2 and 3. The relationship is curvilinear until the fatigue strength of that particular concrete is reached, then the line becomes parallel to the X-axis; the same behavior can be observed for all concretes. Figures 4 and 5 present fatigue flexural stress versus the logarithm of the number of cycles for all the concretes. These figures reveal a linear relationship between fatigue stress and log N. The fatigue strengths of concretes with and without fibers are compared

TABLE 1 FATIGUE PROPERTIES OF CONCRETES WITH DIFFERENT TYPES OF FIBERS

Fiber Type	A		B		C		D		Plain
Fiber Content(%)	0.5	1.0	0.5	1.0	0.5	1.0	0.5	1.0	Conc.
f_{fmax} (in psi)	749	1242	559	594	549	676	478	508	508
EL_1 (%)	95	158	71	76	71	86	61	65	65
EL_2 (%)	76	85	67	59	70	55	70	65	65

f_{fmax} - flexural strength.
EL_1 - Endurance limit expressed as a percentage of modulus of rupture of plain concrete.
EL_2 - Endurance limit expressed as a percentage of its modulus of rupture.

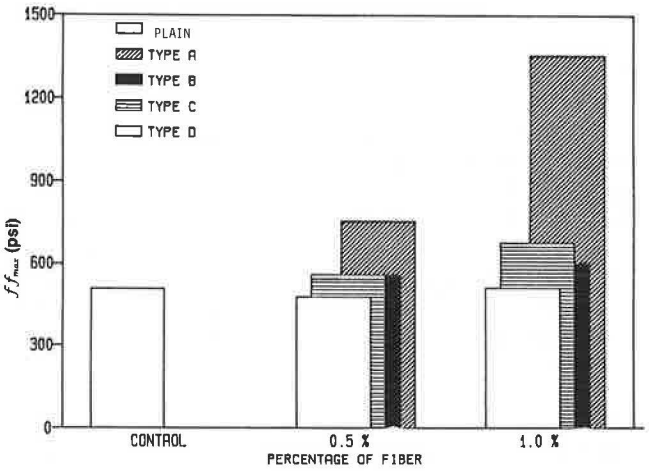

FIGURE 1 Fatigue strength.

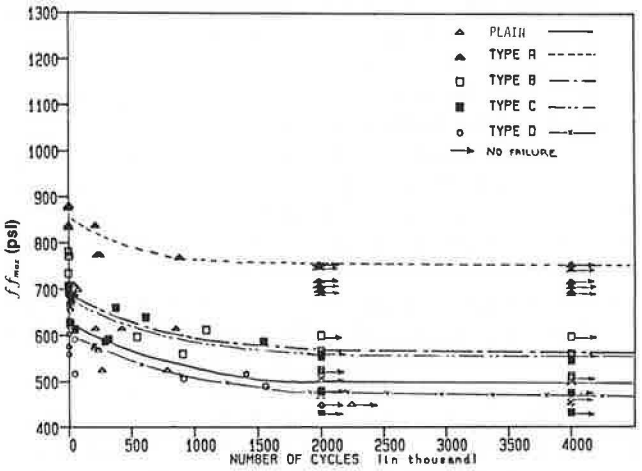

FIGURE 2 Number of cycles versus fatigue stress for 0.5 percent fiber fatigue beams.

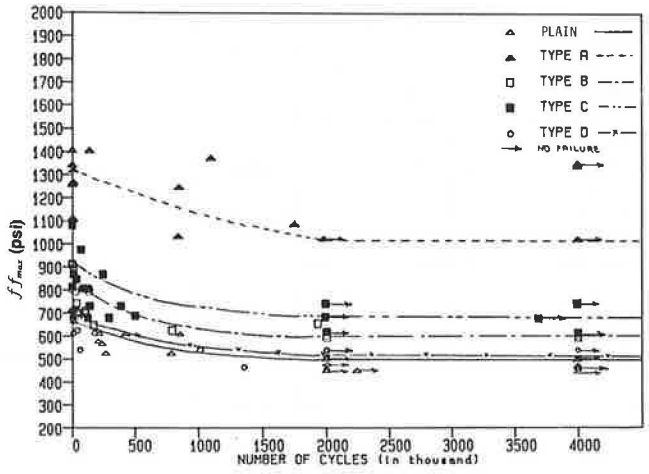

FIGURE 3 Number of cycles versus fatigue stress for 1.0 percent fiber fatigue beams.

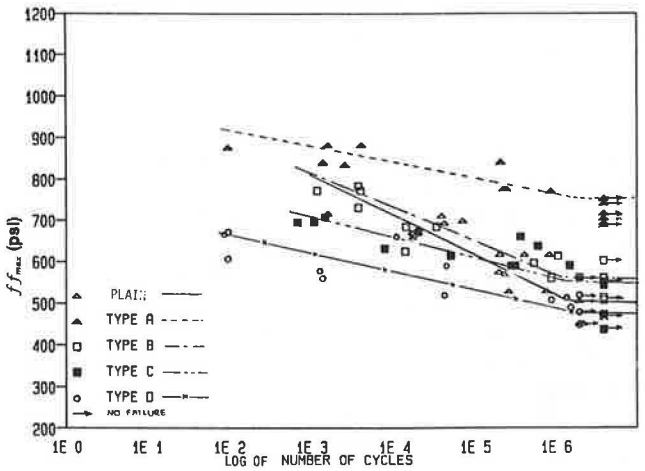

FIGURE 4 Fatigue stress versus log *N* for 0.5 percent fiber fatigue beams.

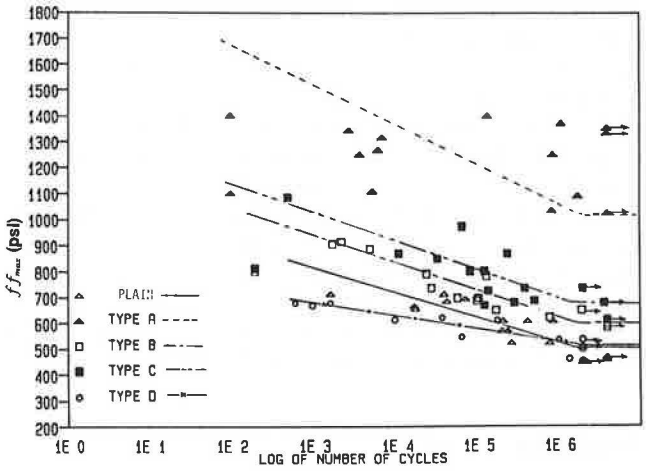

FIGURE 5 Fatigue stress versus log *N* for 1.0 percent fiber fatigue beams.

in Figure 1. As can be seen, the fatigue strength increases with the fiber content for all fiber types. However, there is a larger increase in the fatigue strength with hooked-end fibers (47 percent and 144 percent, respectively, for 0.5 percent and 1.0 percent fiber contents) than with other fibers. The smallest increase in fatigue strength was found with polypropylene and straight steel fibers (see Table 1).

Endurance Limit Expressed as a Percentage of Modulus of Rupture of Plain Concrete The endurance limit (EL_1) is defined as the maximum flexural fatigue stress at which the beam could withstand 2 million cycles of nonreversed fatigue loading, expressed as a percentage of modulus of rupture of plain concrete.

Figure 6 compares the endurance limit values for all fiber concretes and plain concrete. Beams with 0.5 percent and 1.0 percent corrugated steel fiber contents show an appreciable

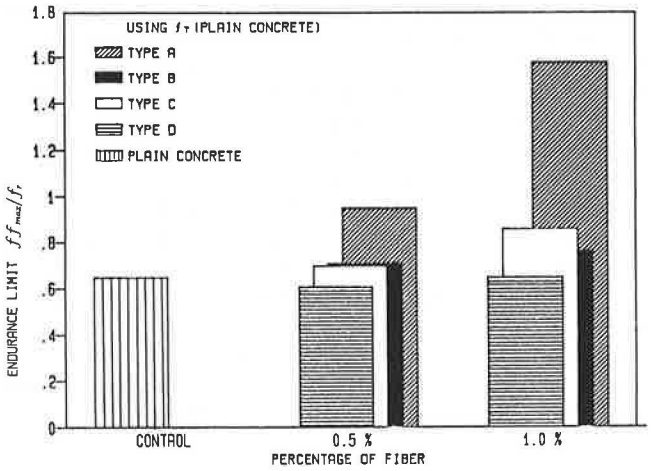

FIGURE 6 Comparison of FRC and plain concrete for endurance limit EL_1.

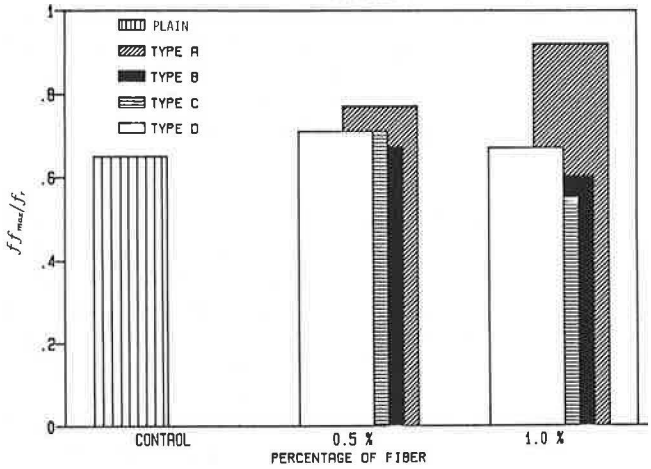

FIGURE 7 Comparison of FRC and plain concrete for endurance limit EL_2.

increase in endurance limit expressed as a percentage of modulus of rupture of plain concrete. The endurance limit was 71 percent for the mix with 0.5 percent fiber content and 86 percent for the mix with 1.0 percent fiber content, whereas the endurance limit for plain concrete was 65 percent. Thus, the endurance limit was increased by 9 percent and 32 percent, respectively, when 0.5 percent and 1.0 percent of fiber contents by volume were added to the concrete. The highest increase was experienced with hooked-end fiber (46 percent and 143 percent for 0.5 percent and 1.0 percent fiber contents, respectively) and the least increase with straight and polypropylene fibers (see Table 1).

Endurance Limit Expressed as a Percentage of Its Modulus of Rupture The endurance limit of concrete (EL_2) can also be defined as the flexural fatigue stress at which the beam could withstand 2 million cycles of nonreversed fatigue loading, expressed as a percentage of its modulus of rupture. Thus defined, endurance limit values are compared for plain concrete and FRC in Figure 7. Unfortunately, this comparison is misleading and shows some fibers unfavorably. For example, corrugated steel fiber concrete with 1.0 percent fiber content by volume had a high fatigue strength compared with plain concrete, although it has a lower endurance limit. This also indicates that the increased benefit due to the increased fiber content is not proportional at higher quantities of fibers.

For Type C fibers, the endurance limit was 70 percent for the mix with 0.5 percent fiber content and 55 percent for the mix with 1.0 percent fiber content (Table 1). The limit for the 1.0 percent mix is low because its modulus of rupture was high compared with that of plain concrete. Hence, the improvement in endurance limit is evident only when the endurance limit is expressed as a percentage of plain concrete modulus of rupture.

With an increase in fiber content, the apparent decrease in endurance limit expressed as a percentage of its modulus of rupture was also true with straight steel fiber and polypropylene fiber. The endurance limits for the straight steel fiber concretes were 67 percent and 60 percent, respectively, for 0.5 percent and 1.0 percent fiber contents. They were 70 percent and 67 percent, respectively, for the concretes with 0.5 percent and 1.0 percent of polypropylene fiber contents (see Table 1). However, the endurance limits for the hooked-end steel fiber concretes were 76 percent and 82 percent, respectively, for 0.5 percent and 1.0 percent fiber contents, which shows an increasing trend with the increase in fiber content. This phenomenon may also be a function of the aspect ratio of the fiber. Further research is necessary to study this aspect more thoroughly.

It was also observed that the variability in fatigue strength of the concrete with 1.0 percent fiber content is high compared with the concrete with 0.5 percent fiber content. Some of the beams that had much lower values than the mean were studied closely; when a fiber count in the fracture zone was performed, it was found that they had a subnormal number. The inconsistency in the distribution of the fibers, particularly in the tension zone, is inherent in fiber concretes with randomly oriented fibers. This is probably the main reason for the high variability in fatigue and static flexural strengths.

Graphs of the ratio of flexural fatigue stress to modulus of rupture (f_{fmax}/f_r) versus the number of cycles are presented in Figures 8 and 9, respectively, for 0.5 percent and 1.0 percent

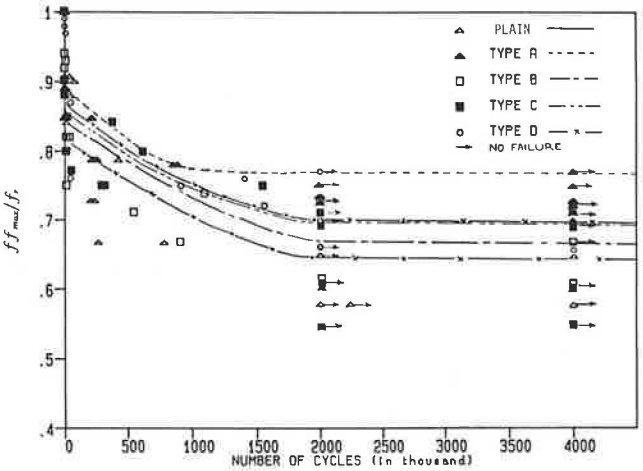

FIGURE 8 Ratio of fatigue stress to flexural stress versus number of cycles for 0.5 percent fiber beams.

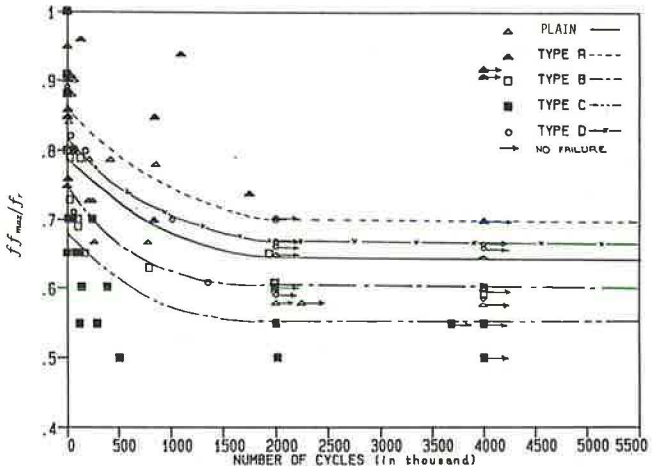

FIGURE 9 Ratio of fatigue stress to flexural stress versus number of cycles for 1.0 percent fiber beams.

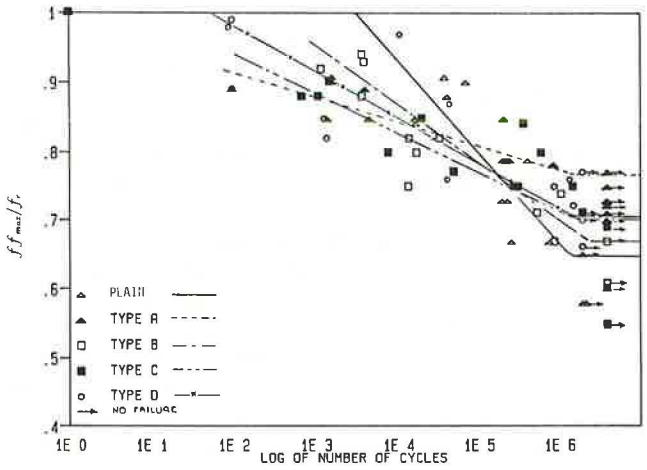

FIGURE 10 Ratio of fatigue stress to flexural stress versus log *N* for 0.5 percent fiber beams.

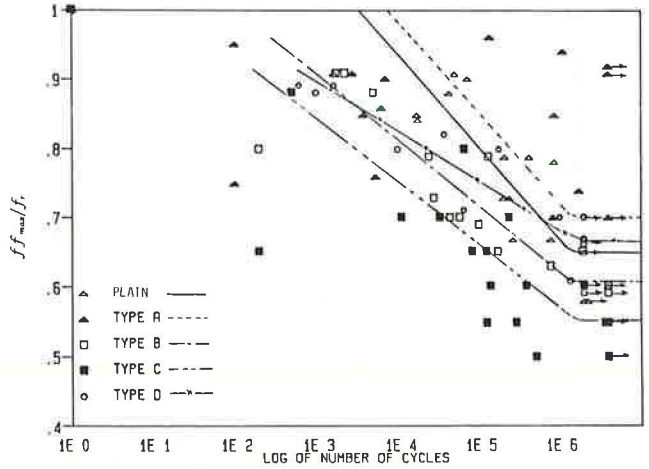

FIGURE 11 Ratio of fatigue stress to flexural stress versus log *N* for 1.0 percent fiber beams.

of fiber contents. The relationship is curvilinear until the fatigue strength of that particular mix is reached, then the line becomes parallel to the X-axis. The same behavior can be observed for all concretes. Graphs were also presented for f_{fmax}/f_r versus the logarithm of the number of cycles for all concretes (Figures 10 and 11). In this case, the relationship between log N and the ratio f_{fmax}/f_r is linear for all concretes.

After a time gap, all beams that had withstood 2 million cycles were further tested for flexural fatigue with an additional 2 million cycles at the same load range. All other beams, except one with 1.0 percent by volume of steel fiber content, withstood 4 million cycles without showing signs of additional distress or cracking. In other words, when a beam is subjected to a stress lower than its fatigue stress (as defined in this paper), then the beam may never fail in fatigue.

Fiber Anchorage and Bond An interesting phenomenon observed in this research was that beams reinforced with hooked-end steel fibers did not fail in fatigue even after extensive cracking. A minor crack was observed in a particular beam with 0.5 percent by volume of hooked-end steel fibers at 426,000 cycles. This crack extended progressively to a height of 5.12 in. in a 6-in.-deep beam and a width of 0.12-in. at 3,850,000 cycles. This shows the excellent anchorage and bond provided by the hooked end of the fibers.

Flexure Test After Fatigue Table 2 compares the results of the flexure test done after fatigue loading for all four types of fibers with 0.5 percent and 1.0 percent by volume. There seems to be an increase in flexural strength for both plain concrete and FRC after they were tested for fatigue. This increase seems to be higher than can be attributed to the increase in age alone and appears to depend on the flexural fatigue stress (f_{fmax}) to which the specimens were subjected earlier. With lower f_{fmax} values, the increase in flexural strength is higher. The same increasing trend is present for all four types of fiber concretes. Thus, it can be said that the increase in flexural strength is inversely proportional to the applied fatigue stress. In general, when fiber concrete is subjected to a fatigue stress below the endurance limit value, there is an increase in the potential flexural strength.

Impact Strength

The drop-weight test (*7*) used in this investigation is not a truly scientific test and was not expected to give accurate values for impact resistance. However, it is a simple, inexpensive test that can be done anywhere, including in the field. If a greater number of specimens can be tested, the mean values are a good qualitative index of the material's impact resistance. For comparison purposes, this is an acceptable test.

Figure 12 shows the number of blows for first crack and full failure. The maximum increase in impact resistance results from the use of Type A fiber; Type C fiber also contributes a higher impact resistance at higher fiber contents. The impact strength at first crack increased considerably with the increase in fiber content. Compared with plain concrete, the increase in impact strengths at full failure were 640 percent, 847 per-

TABLE 2 FLEXURAL STRENGTH AFTER FATIGUE LOADING

Sp. No.	Fiber Type & Percentage	f_{fmax} (psi)	f_{r1} (psi)	f_{r2} (psi)	$(f_{r2}-f_{r1})$ (percentage)
GP3-III13	Plain	455	785	789 *	-
GP3-III16	Concrete	508	"	780 *	-
GP3-I1	"	508	"	633 *	-19%
GP3-III15	"	464	"	1055	+34%
GP3-II9	"	475	"	980	+25%
A4-III6	'A' (0.5%)	689	986	1495	+52%
A4-I6	(Hooked End	697	"	1595	+62%
A4-II4	Fiber)	706	"	1139	+16%
A4-I4	"	719	"	1310	+33%
A4-II5	"	743	"	1118	+13%
A4-III5	"	755	"	688	-30%
A5-II3	'A' (1%)	1028	1473	1559	+6%
A5-I1	"	1342	"	2120	+44%
A5-I2	"	1356	"	2107	+6%
SCC5-III2	'B' (0.5%)	508	834	1015	+22%
SCC5-I3	(Straight	509	"	1120	+34%
SCC5-III3	Steel Fiber)	559	"	1150	+38%
SCC5-II6	"	558	"	965	+16%
SCC5-III5	"	598	"	1225	+47%
SCC60-III1	'B' (1%)	587	1003	1405	+40%
SCC6-III3	"	594	"	1390	+39%
SCC6-I2	"	602	"	1405	+40%
SC6-II1	'C' (0.5%)	433	788	1165	+48%
SC6-III2	(Corrugated	472	"	1210	+54%
SC6-II2	Steel Fiber)	541	"	1010	+28%
SC6-II3	"	546	"	808 *	+3%
SC6-I3	"	560	"	925	+17%
SC5-III6	'C' (1%)	615	1227	1300	+6%
SC5-III2	"	678	1227	1420	+16%
D5-III4	'D' (0.5%)	446	678	940	+39%
D5-III6	(Polypropylene	477	"	901	+33%
D5-II6	Fiber)	478	"	923	+36%
D5-III5	"	520	"	892	+32%
D6-III5	'D' (1%)	453	764	979	+28%
D6-II5	"	454	"	978	+28%
D6-II6	"	503	"	923	+21%
D6-III6	"	509	"	875	+15%
D6-I6	"	512	"	904	+18%
D6-III4	"	535	"	854	+12%

f_{fmax} - max. fatigue flexural stress.
f_{r1} -static flexural strength at the time of fatigue loading
f_{r2} -static flexural strength of the beam after it has been subjected to 4 million cycles of fatigue loading.
+ values of $(f_{r2}-f_{r1})$ indicate increase in flexural strength.
- values of $(f_{r2}-f_{r1})$ indicate decrease in flexural strength
* Beams were tested after 2 million cycles of fatigue loading.

cent, 1,824 percent, and 2,806 percent, respectively, for concretes with 0.5 percent, 1.0 percent, 1.5 percent, and 2.0 percent Type C fiber content. The results prove that fiber concretes incorporating hooked-end and corrugated steel fibers (Types A and C) have excellent impact resistance.

The four fibers used in this investigation are common, commercially available fibers that have substantially different aspect ratios. Type A has an apparent aspect ratio of 100, while Type B has an aspect ratio of only 40. It is well known that the aspect ratio of straight fibers has considerable impact on the performance of fresh and hardened concrete. However, it is not practical to determine the realistic value of the aspect ratio for deformed or modified fibers such as corrugated, hooked, collated, or fibrillated fibers. Therefore, the aspect

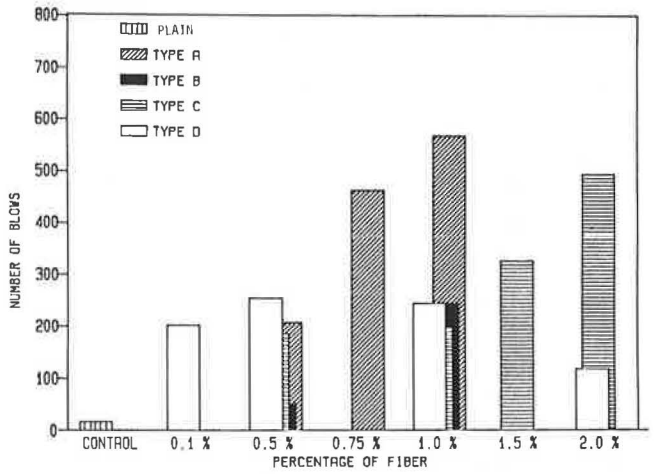

FIGURE 12 Impact results for FRC and control concrete.

ratio was not considered in the analysis. There is also a vast difference in the cost per pound of these fibers: one fiber may cost twice as much as another fiber. Prices were also not taken into account in the comparisons. Hence, the conclusions do not reflect the economy or efficiency of the individual fibers.

CONCLUSIONS

Based on the experimental investigation, the following conclusions can be made:

- The workability of fresh FRC can be improved and maintained with the addition of an appropriate amount of superplasticizer. Generally, there was no difficulty in placing and finishing laboratory-prepared FRC test specimens with less than 1 percent by volume of fibers.
- The fatigue strength of FRC increases with increasing fiber content.
- The endurance limit expressed as a percentage of modulus of rupture of plain concrete increases with increasing fiber content.
- The endurance limit expressed as a percentage of its modulus of rupture increases with increasing fiber content for hooked-end steel fibers. However, the opposite is true for straight steel, corrugated, steel, and polypropylene fibers.
- The static flexural strength of beams that had been subjected to 4 million cycles of fatigue loading was higher than that of corresponding beams that had no previous fatigue loading.

ACKNOWLEDGMENT

The authors gratefully acknowledge the funding support of the Naval Facilities Engineering Command.

REFERENCES

1. V. Ramakrishnan. Superplasticized Fiber Reinforced Concrete for the Rehabilitation of Bridges and Pavements. In *Transportation Research Record 1003*, TRB, National Research Council, Washington, D.C. 1984, pp. 4–12.
2. V. Ramakrishnan and V. Srinivasan. Performance Characteristics of Fiber Reinforced Condensed Silica Fume Concretes. In *Report SP-79*, Vol. 11, American Concrete Institute, Detroit, Mich., 1983, pp. 797–812.
3. E. K. Schrader, J. Paxton, and V. Ramakrishnan. Composite Concrete Pavements with Roller Compacted Concrete. In *Transportation Research Record 1003*, TRB, National Research Council, Washington, D.C., 1984, pp. 50–56.
4. V. Ramakrishnan and W. V. Coyle. *Steel Fiber Reinforced Superplasticized Concrete for Rehabilitation of Bridge Decks and Highway Pavements*. Report DOT/RSPA/DMA-50/84-2. Office of University Research, U.S. Department of Transportation, 1983, p. 410.
5. V. Ramakrishnan, T. Brandshaug, W. V. Coyle, and E. K. Schrader. A Comparative Evaluation of Concrete Reinforced with Straight Steel Fibers and Fibers with Deformed Ends Glued Together into Bundles. *ACI Journal*, Vol. 77, No. 3, May–June 1980, pp. 135–143.
6. ACI Committee 506. State-of-the-Art Report on Fiber Reinforced Concrete. In *Report 544 IR-82: Concrete International. Design and Construction*, American Concrete Institute, May 1982.
7. ACI Committee 544. Measurement of Properties of Fiber Reinforced Concrete. In *Report 544.2R.78: ACI Manual of Concrete Practice*, Part 5, American Concrete Institute, 1982.
8. *Report SP-81: Fiber Reinforced Concrete—International Symposium*. American Concrete Institute, Detroit, Mich., 1984.
9. V. Ramakrishnan. The Role of Superplasticized Fiber Reinforced Concrete and Fiber Shotcrete in the Rehabilitation of Bridges. *Proc., International Symposium on Rehabilitation of Structures*, Bombay, India, Vol. 1, 1981, pp. 111/21–111/28.
10. V. Ramakrishnan and P. N. Balaguru. Freeze-Thaw Durability of Fiber Reinforced Concrete. *ACI Journal*, Vol. 83, No. 3, pp. 374–481.
11. P. Belaguru and V. Ramakrishnan. Mechanical Properties of Superplasticized Fiber Reinforced Concrete Developed for Bridge Decks and Highway Pavements. In *Report SP-93: Concrete in Transportation*, American Concrete Institute, Detroit, Mich., 1986, pp. 563–584.
12. P. Balaguru and V. Ramakrishnan. Comparison of Slump Cone and V-B Tests as Measures of Workability for Fiber Reinforced and Plain Concrete. *Cement, Concrete and Aggregates, CCAGDP*, Vol. 9, No. 1, Summer 1987.
13. V. Ramakrishnan. Materials and Properties of Fiber Reinforced Concrete. *Proc., International Symposium on Fiber Reinforced Concrete*, Madras, India, 1987, pp. 2.3–2.23.
14. V. Ramakrishnan and M. Senthil Kumar. Constitutive Relations and Modelling for Concrete Fiber Composites: A State-of-the-Art Report. *Proc., International Symposium on Fiber Reinforced Concrete*, Madras, India, 1987, pp. 1.21–1.56.
15. V. Ramakrishnan and Charles Josifek. Performance Characteristics and Fatigue Strength of Concrete Steel Fiber Composites. *Proc., International Symposium on Fiber Reinforced Concrete*, Madras, India, 1987, pp. 2.73–2.84.
16. V. Ramakrishnan, S. Gollopudi, and R. Zellers. Performance Characteristics and Fatigue Strength of Polypropylene Fiber Reinforced Concrete. In *Report SP-105: Fiber Reinforced Concrete—Properties and Applications*, American Concrete Institute, Detroit, Mich., 1987, pp. 225–245.
17. V. Ramakrishnan, G. Oberling, and P. C. Tatnall. Flexural Fatigue Strength of Steel Fiber Reinforced Concrete. In *Report SP-105: Fiber Reinforced Concrete—Properties and Applications*, American Concrete Institute, Detroit, Mich., 1987, pp. 225–245.
18. Peter C. Tatnall. Steel Fibrous Concrete Pumped for Burst Protection. *Concrete International Design and Construction*, December 1984, pp. 48–51.
19. P. Balaguru and V. Ramakrishnan. Properties of Fiber Reinforced Concrete: Workability, Behavior Under Long Term and Air-Void Characteristics. *ACI Materials Journal*, Title No. 85-M23, May–June 1988, pp. 189–196.

The views expressed in this paper are those of the authors, who are responsible for its contents. The contents do not necessarily reflect official views or policies of the Naval Facilities Engineering Command.

Optimum Use of Pozzolanic Materials in Steel Fiber Reinforced Concrete

ZIAD BAYASI AND PARVIZ SOROUSHIAN

The effects on fresh and hardened material properties for fly ash caused by substituting cement with fly ash and silica fume in steel fiber reinforced concrete were studied experimentally. The percentage substitution of cement ranged from 0 to 40 percent and from 0 to 20 percent for silica fume. The workability of fresh fibrous mixtures was characterized by measuring the inverted slump cone time. The hardened material was tested at 28 days under compression and flexural loads. The development of compressive strength with time was also assessed in steel fiber reinforced concrete incorporating fly ash. The generated test data were used to decide the optimum ranges of cement substitution with fly ash or silica fume in steel fiber reinforced concrete for achieving desirable fresh mix and hardened material characteristics.

Fly ash and silica fume are commonly used mineral admixtures capable of providing plain and fiber reinforced concrete with distinct performance advantages. Being pozzolanic materials, both silica fume and fly ash react with the calcium hydroxide produced by the hydration of portland cement. This leads to the formation of calcium silicate hydrate, which has desirable effects on the density and microstructure of concrete materials, especially at interfaces between cementitious paste and mix inclusions (e.g., aggregates and fibers), where the concentration of calcium hydroxide is generally high.

Fly ash and silica fume also have their differences. Silica fume is distinguished from fly ash by its fineness, high pozzolanic reactivity, and high silica content. The effects of the two pozzolanic materials on fresh mix workability are also different; while fly ash generally tends to improve workability, the reverse is true for silica fume.

This research was concerned with the partial substitution of cement with fly ash or silica fume in typical steel fiber reinforced concrete mixes. In this paper, the trends in the effects of pozzolan contents on fresh mix workability and hardened material mechanical characteristics are established. In addition, the optimum pozzolan contents for the specific types of fly ash and silica fume used in the mixes of this study are decided.

BACKGROUND

A brief review of the action of fly ash and silica fume in concrete, together with the outcomes of past investigations on pozzolan applications to steel fiber reinforced concrete are given below.

Z. Bayasi, Department of Civil Engineering and Construction, Bradley University, Peoria, Ill. 61625. P. Soroushian, Civil and Environmental Engineering Department, Michigan State University, East Lansing, Mich. 48824.

Fly Ash

Fly ash is the finely divided residue resulting from the combustion of ground or powdered coal (*1*). Probably the most important consideration in the use of fly ash in steel fiber reinforced concrete is its ability to improve the fresh mix workability and fiber dispersability (*2,3*). The round particle shape and fineness of fly ash particles improve the flowability of the mix (*4*). With fly ash, the volume of cementitious paste in the mix increases due to the lower specific gravity of fly ash compared with that of cement (cement is usually replaced with fly ash on an equal mass basis). Thus, a more effective coating of fibers and lubrication of the mix inclusions is achieved (*3*). These effects improve the dispersability of fibers and the workability of the fresh mix. The improvements in fresh mix workability in the presence of fly ash are especially obvious when the fresh material is compacted through vibration (*2,3*). The improvements in fresh mix workability and fiber dispersability lead to enhanced properties of the composite material in the hardened state.

In addition to improving the fresh mix workability and fiber dispersability, the application of fly ash to steel fiber reinforced concrete imparts the following improvements to the material performance:

- Fly ash contributes to the strength of fiber reinforced concrete by reducing the water content without damaging workability, by increasing the volume of paste in the mixture, and by its pozzolanic reaction (*5*).
- The increase in cementitious paste volume in the presence of fly ash leads to a better coating of fibers by the matrix material and improves fiber-matrix interfacial bond characteristics. This may cause significant improvements in the composite material performance (*2,3*).
- All other advantages of using fly ash in plain concrete (enhanced pore system, reduced permeability and improved durability, reduced alkali-aggregate reactivity, economic and echological advantages, etc.) (*1,4,6*) would also apply to steel fiber reinforced concrete.

Certain precautions are needed to take full advantage of fly ash applications in steel fiber reinforced concrete (*1–3,6*):

- The presence of carbon in fly ash reduces the entrained air content in fly ash concrete. Hence, the dosage of the air-entraining agent used in fly ash concrete should be adjusted according to the carbon content of the fly ash.
- Fly ash generally slows down the rates of setting and hardening of concrete, and fly ash concrete is more sensitive

to temperature variations. Thus, it might need more favorable curing conditions than conventional concrete.

- Because fly ash is a byproduct, it has larger variations in chemical and physical properties than portland cement. Therefore, appropriate quality control measures should be taken depending on the specific job requirements.

Silica Fume

Silica fume is a byproduct resulting from the reduction of high-purity quartz with coal in electric arc furnaces during the production of silicon and silicon alloys (*7*). The fineness and high pozzolanic reactivity of silica fume make it highly effective in enhancing the structural density and adhesion capacity in the bulk of the cement paste, especially within the interface zones between the paste and the mix inclusions, including fibers (*8–10*). Enhanced fiber-matrix bond characteristics have important effects on the strength and ductility of fiber reinforced silica fume concrete under different stress systems.

Steel fiber concretes incorporating silica fume also benefit from the improvements imparted to plain concrete by silica fume, including (*7*)

- Increased cohesiveness and reduced segregation tendencies;
- Reduced permeability resulting from the decrease in the number of coarse pores in the cement paste incorporating silica fume, leading to enhanced durability of the material;
- The potential for developing very high strengths; and
- Greater sulfate resistance and reduced alkali-aggregate reactivity.

The optimum application of silica fume in concrete and fiber reinforced concrete would require the following precautions:

- The high surface area of silica fume requires a larger dosage of the air-entraining agent to produce the target entrained air content.
- Silica fume tends to make concrete mixtures rather sticky. Therefore, an increased water content or the use of water-reducing agents, or both, would be necessary to maintain the consistency of the mix.
- Silica fume, mainly due to its high affinity for water, does not leave adequate free water in the mixture and reduces the bleeding of concrete. This reduces the supply of water to the surface and requires the adoption of curing procedures. These procedures prevent early moisture loss from freshly placed concrete, which in turn prevents plastic shrinkage cracking.

EXPERIMENTAL PROGRAM

Different steel fiber reinforced concrete mixes with variable percentages of cement substituted with fly ash or silica fume were manufactured, and their characteristics in the fresh and hardened states were assessed.

The mixes with fly ash had a water-to-binder (cement plus fly ash) ratio of 0.42, and those with silica fume had a water-to-binder (cement plus silica fume) ratio of 0.40. The mixes with fly ash incorporated a 2 percent volume fraction of steel fibers (260 lb/yd^3), while those with silica fume had a fiber volume fraction of 1.5 percent (195 lb/yd^3). The fraction substitutions of cement with fly ash were 0 percent, 20 percent, 30 percent, and 40 percent by weight. In mixes with silica fume, 0 percent, 5 percent, 10 percent, and 20 percent by weight of portland cement were substituted with silica fume.

All the mixes had an aggregate-binder ratio of 4.0 (700–730 lb/yd^3 of binder and 2,800–2,900 lb/yd^3 of aggregates), a sand-gravel ratio of 1.0, a maximum aggregate size of ¾ in. (19 mm), and a superplasticizer-binder ratio of 0.015 by weight.

The steel fibers used in this study were straight and round. They had a length of 2 in. (51 mm), and a diameter of 0.035 in. (0.8 mm), and an aspect ratio of 57.

Type I portland cement was used and the superplasticizer was Daracem 100—a naphtalene-based high-range water reducer capable of maintaining its effectiveness over a relatively long time period. The fly ash was Type F (ASTM C618-85) and was obtained from the Eckert plant of the Lansing Board of Water and Light. Some physical and chemical properties of this fly ash (*11*) are as follows (*13*):

- Chemical composition (loss on ignition = 4.3 percent):

Component	*Percentage by weight*
SiO_2	47.0
Al_2O_3	22.1
Fe_2O_3	23.4
TiO_2	1.1
CaO	2.6
MgO	0.7
K_2O	2.0

- Gradation (lin = 25.4 mm):

Sieve (size)	*Percentage Passing*
#30 (0.6 mm, 600 μ)	100
#200 (0.074 mm, 74 μ)	92
#325 (0.045 mm, 45 μ)	84
(0.020 mm, 20 μ)	63
(0.010 mm, 10 μ)	36
(0.005 mm, 5 μ)	17

- Specific gravity = 2.245.

The silica fume used in this investigation was a product of Elkem Materials, and its chemical and physical properties are:

- Chemical composition:

Component	*Percentage by weight*
SiO_2	96.50
C	1.40
Fe_2O_3	0.15
MgO	0.20
Al_2O_3	0.15
K_2O	0.04
Na_2O	0.20

- Physical properties:

Specific gravity = 2.3
Bulk density = 14 lb/ft^3 = 225 kg/m^3
Specific surface = 200,000 am^3/g = 14 × 10^6 in.^{2}/lb
Average particle size = 0.15 micron = 6 × 10^{-5} in.
Particles smaller than 45 microns (0.018 in.) = 99.5 percent

The aggregates were natural river gravel and sand.

A rotary drum mixer was used to manufacture the steel fiber reinforced concretes with silica fume and fly ash. The fresh mix workability was measured by the inverted slump cone testing procedure (*12*). Note that a shorter inverted slump cone time indicates better workability.

Following the experiments on fresh mix, 6 × 12 in. (150 × 300 mm) cylindrical specimens for the compression test and 6 × 6 × 20 in. (150 × 150 × 500 mm) prismatic specimens for the flexural test were cast and compacted on a vibration table. All specimens were demolded after 24 hr, during which they were kept under a plastic sheet. The fly ash concrete specimens were moist cured at 100 percent relative humidity and 72°F (23°C) for 7 days and were then cured in a regular laboratory environment. A total of 6 compression and 3 flexural test specimens were constructed for each fly ash concrete mix. The three flexural specimens and two of the compression specimens were tested at 28 days. Two of the compression specimens were tested at an age of 1 day and the other two at 7 days. The silica fume concrete specimens (2 compression and 3 flexure) were all moist cured after demolding at 72°F (23°C) and 100 percent relative humidity until the test age of 28 days.

The flexural tests were performed quasi-statically using the four-point loading procedure of ASTM C1018-85 on a span of 18 in. (450 mm), and the load-deflection (at the load point) relationship was monitored throughout the test. Complete stress-strain relationships were obtained in compression tests performed at the age of 28 days.

EXPERIMENTAL RESULTS

The results of tests on the fresh mix and hardened material properties of steel fiber reinforced concretes with different fly ash or silica fume contents are discussed below.

Fresh Mix Workability

The results of the inverted slump cone test on fiber reinforced concretes incorporating fly ash and silica fume are shown in Figures 1 and 2, respectively, as functions of the pozzolan content. As indicated in Figure 1, the substitution of increasing fractions of cement with Type F fly ash reduces the inverted slump cone time of steel fiber reinforced concrete, which indicates improvements in the compactibility of fresh mix under vibration in the presence of fly ash. Except for the mix without fly ash, all steel fiber reinforced concretes (with 20 percent–40 percent fly ash-binder ratios) have inverted slump cone times within the acceptable limit of 10 to 30 sec.

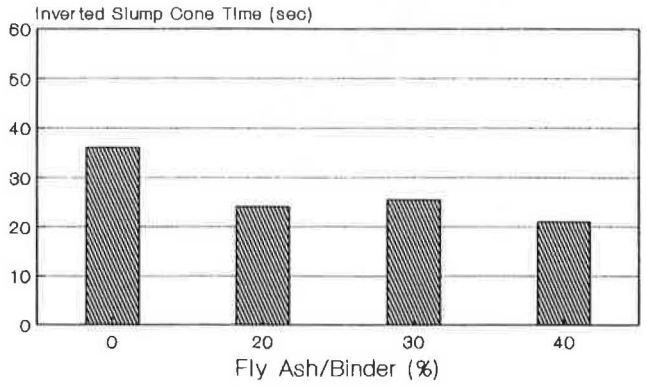

NOTE: Vf = 2 percent.

FIGURE 1 Inverted slump cone test results: fly ash concrete.

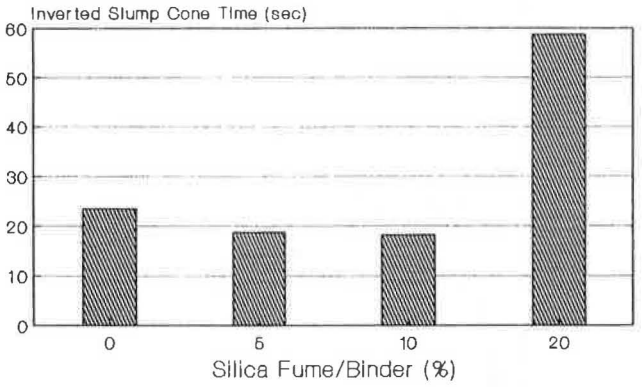

NOTE: Vf = 1.5 percent.

FIGURE 2 Inverted slump cone test results: silica fume concrete.

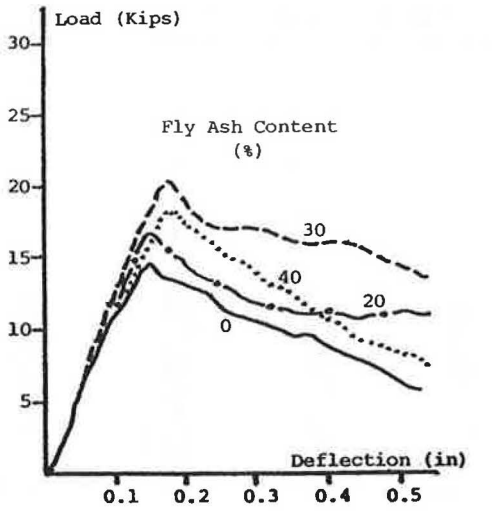

NOTE: 1 kN = 0.22 kip; 1 mm = 0.04 in.; Vf = 2 percent.

FIGURE 3 Flexural load-deflection relationships: fly ash concrete.

Figure 2 shows that the substitution of portland cement with silica fume up to 10 percent by weight has relatively little effect on the fresh mix workability of steel fiber reinforced concrete. Higher silica fume contents, however, tend to damage workability.

Flexural Behavior

Complete flexural load-deflection relationships are shown in Figures 3 and 4 for mixes with fly ash and silica fume, respectively. Each curve represents the average of three test results. Figures 5 and 6 summarize the trends observed in Figures 1

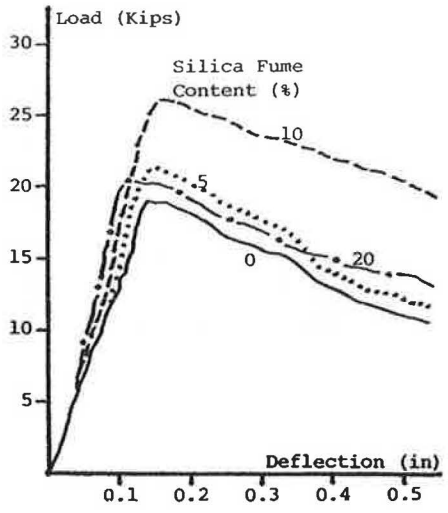

NOTE: 1 kN = 0.22 kip; 1 mm = 0.04 in.; Vf = 1.5 percent.

FIGURE 4 Flexural load-deflection relationships: silica fume concrete.

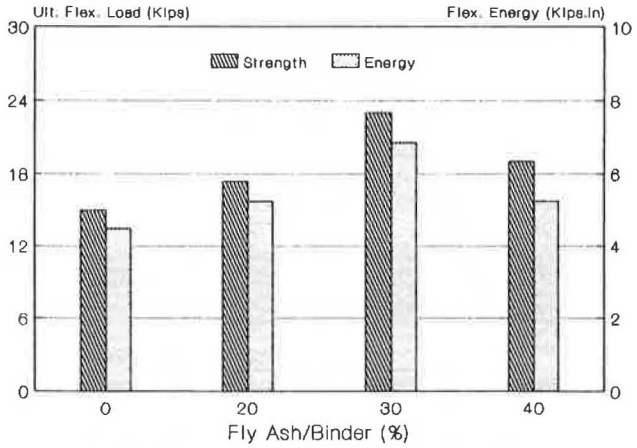

NOTE: 1 kN = 0.22 kip; 1 Nm = 8.7 (lb in.); Vf = 2 percent.

FIGURE 5 Flexural strength and energy absorption test results: fly ash concrete.

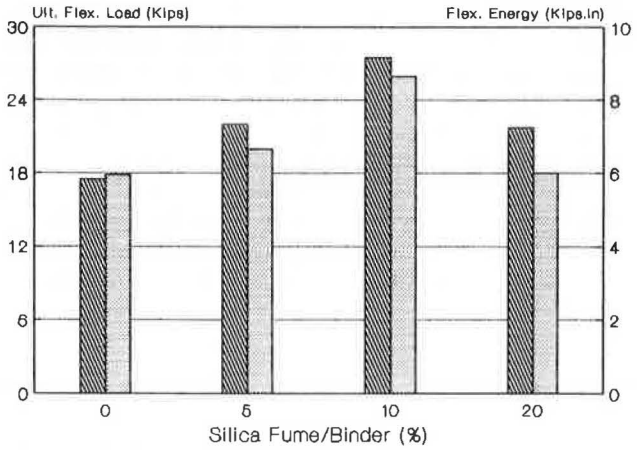

NOTE: 1 kN = 0.22 kip; 1 Nm = 8.7 (lb in.); Vf = 1.5 percent.

FIGURE 6 Flexural strength and energy absorption test results: silica fume concrete.

and 2 regarding the fly ash and silica fume effects, respectively, on flexural strength and flexural energy absorption capacity (the area under the load-deflection diagram up to a deflection 5.5 times the cracking deflection).

The results presented in Figures 3 and 5 indicate that the flexural strength and energy absorption capacity of steel fiber reinforced concrete tend to improve with increasing fly ash content up to a fly ash-binder ratio of 0.3 but drops at higher fly ash contents. From Figures 4 and 6 it can be concluded that the increase in silica fume-binder ratio up to 10 percent improves the flexural strength and energy absorption capacity of steel fiber reinforced concrete. This trend tends to be reversed, however, at higher silica fume contents.

Compressive Behavior

The compressive stress-strain relationships and the compressive strengths and energy absorption capacities derived from test results on steel fiber reinforced fly ash and silica fume concretes are presented in Figures 7 through 10. The compressive energy absorption capacity is defined as the area underneath the compressive stress-strain relationship up to a strain 5.5 times the strain at peak compressive stress.

The test results on steel fiber reinforced fly ash concrete presented in Figures 7 and 9 indicate that an increase in fly ash-binder ratio up to 20 percent improves the compressive strength and energy absorption capacity of steel fiber reinforced concrete. This trend tends to be reversed at higher fly ash contents.

The trends in the effects of silica fume content on the compressive behavior of steel fiber reinforced concrete, shown in Figures 8 and 10, indicate that the increase in silica fume-binder ratio up to 10 percent improves the compressive strength and energy absorption capacity, and the increase in silica fume-binder ratio from 10 percent to 20 percent has a relatively small effect on the compressive behavior.

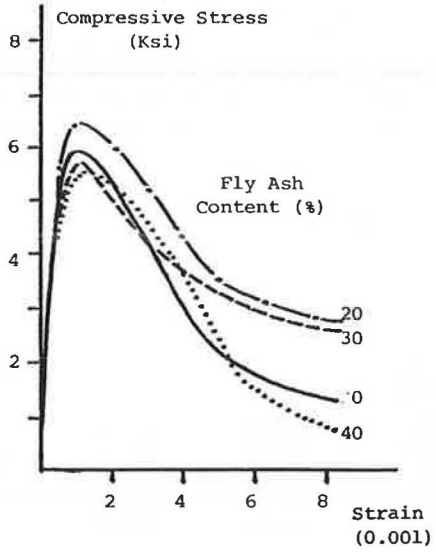

NOTE: 1 MPa = 145 psi; Vf = 2 percent.

FIGURE 7 Compressive stress-strain relationships: fly ash concrete.

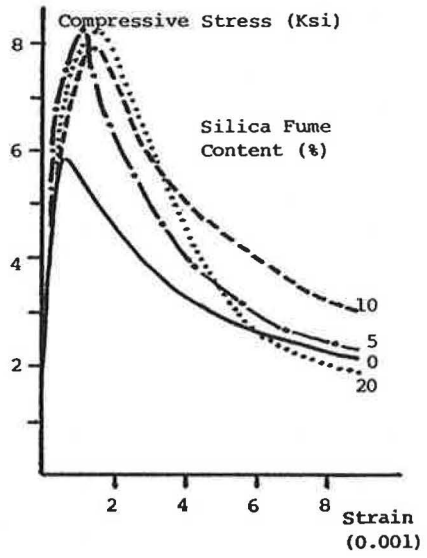

NOTE: 1 MPa = 145 psi; Vf = 1.5 percent.

FIGURE 8 Compressive stress-strain relationships: silica fume concrete.

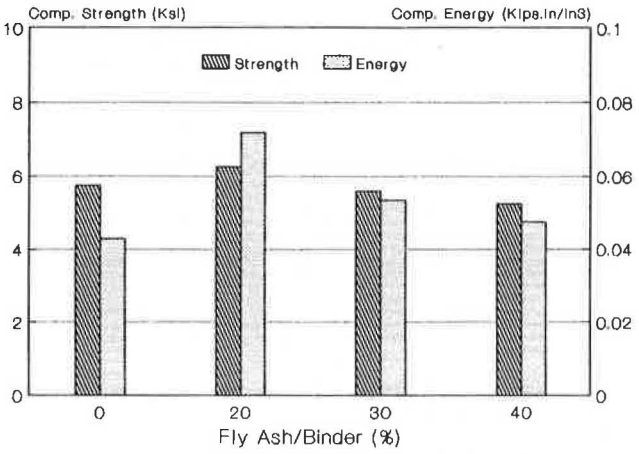

NOTE: 1 MPa = 145 psi; 1Nm/m^3 = 530,000 lb in./in.^{3}; Vf = 2 percent.

FIGURE 9 Compressive and energy absorption strength test results: fly ash concrete.

Development of Strength with Time

For the fly ash concrete mixtures, the effect of fly ash content on the development of compressive strength with time was assessed. The trends in the development of compressive strength with time for steel fiber reinforced concretes incorporating different fly ash contents are shown in Figure 11. Strength at each age has been normalized in this figure with respect to the corresponding strength of the fibrous mix with 0 percent fly ash content. It can be concluded from Figure 11 that the substitution of 20 percent of cement with fly ash increases the compressive strength of steel fiber reinforced concrete even at early ages, when compared with the corresponding mix without fly ash. When 30 percent or 40 percent of cement is substituted by fly ash, however, there seems to be a drop in the rate of strength development with time.

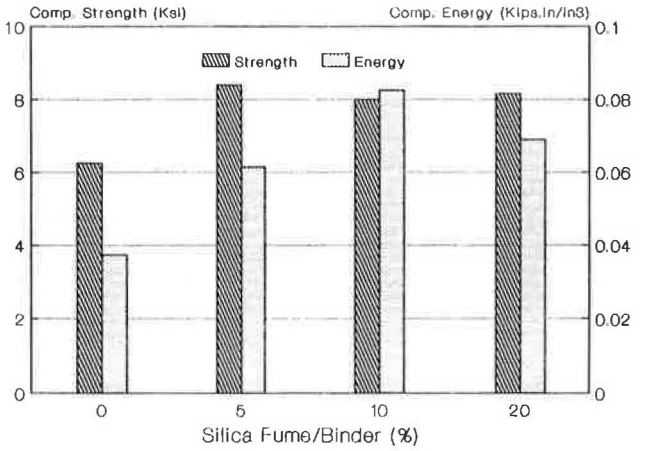

NOTE: 1 MPa = 145 psi; 1Nm/m^3 = 530,000 lb in./in.^{3}; Vf = 1.5 percent.

FIGURE 10 Compressive and energy absorption strength test results: silica fume concrete.

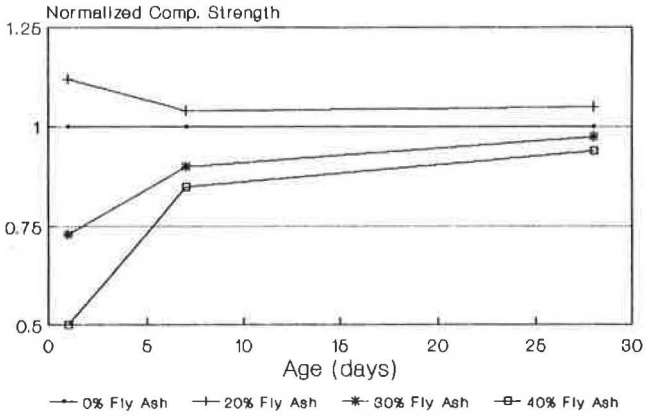

NOTE: Vf = 2 percent.

FIGURE 11 Fly ash effects on development of strength with time in steel fiber reinforced concrete.

SUMMARY AND CONCLUSIONS

The effect of silica fume and Class F fly ash contents on the properties of steel fiber reinforced concrete in fresh and hardened states were investigated experimentally. From the results it was concluded that:

Silica Fume Effects

- The compactibility of steel fiber reinforced concrete, as indicated by the inverted slump cone test results, was not much influenced by the increase in silica fume-binder ratio up to a value of about 0.10. Higher silica fume contents, however, adversely affected the workability of fresh mix.
- The flexural strength and energy absorption capacity of steel fiber reinforced concrete tended to increase with an increasing silica fume-binder ratio up to a value of about 0.10; beyond this value, the effects of silica fume on these aspects of the hardened material behavior were reversed.

- The compressive strength and energy absorption capacity of steel fiber reinforced concrete tended to increase with an increasing silica fume-binder ratio up to a value of 0.10. Further increases in silica fume content had relatively little effect on the compressive behavior of steel fiber reinforced concrete.
- For the steel fiber reinforced concrete mixes used in this study, substitution of 10 percent of cement with silica fume gave the best results with respect to the workability of fresh mix and the strength and energy absorption capacity of the hardened material under the action of flexural and compressive loads.

Fly Ash Effects

- Substitution of cement with Class F fly ash in steel fiber reinforced concrete mixes generally had positive effects on the workability of fresh mix as represented by the inverted slump cone time test results.
- The 28-day flexural strength and energy absorption capacity of steel fiber reinforced concretes tended to rise with an increasing fly ash-binder ratio up to about 0.3. An increase in this ratio from 0.3 to 0.4, however, adversely influenced the flexural performance of steel fiber reinforced concrete.
- The substitution of up to 20 percent of cement with fly ash in steel fiber reinforced concrete mixes resulted in improved 28-day compressive strength and energy absorption capacity of the material. Higher fly ash contents, however, adversely affected the compressive characteristics.
- The substitution of more than 20 percent of cement with fly ash tended to reduce the rate of compressive strength development with time at early ages in steel fiber reinforced concrete.
- The optimum fly ash-binder ratio observed for achieving desirable fresh mix workability and hardened material flexural and compressive properties in steel fiber reinforced concrete mixtures was in the range of 0.20–0.30. The use of fly ash-binder ratios above 20 percent led to a lower rate of strength development at early ages in steel fiber reinforced concrete.

ACKNOWLEDGMENTS

The authors would like to acknowledge to the State of Michigan (Research Excellence Fund), the DEED Research Program of the American Public Power Association, and the Lansing Board of Water and Light for the sponsorship of this research program. Appreciation is also extended to the Composite Materials and Structures Center and the Albert H. Case Center for Computer Aided Engineering at Michigan State University for their technical support.

The steel fibers used in this study were contributed by Ribbon Technology Corporation, the fly ash by the Lansing Board of Water and Light, the silica fume by Elkem Materials, and the superplasticizer by W.R. Grace and Company.

REFERENCES

1. ACI Committee 226. Use of Fly Ash in Concrete. *ACI Materials Journal*, Vol. 84, No. 5, Sept.–Oct. 1987, pp. 381–409.
2. R. Swamy. Steel Fiber Concrete: Fresh Mix Properties and Structural Applications. *Proc., Seminar on Fiber Reinforced Concrete: Design and Applications*, Michigan State University, Feb. 1987, pp. 2-1 to 2-35.
3. R. Swamy, S. Ali, and D. Theodorakopoulas. Engineering Properties of Concrete Composite Materials Incorporating Fly Ash and Steel Fibers. In *Report SP-79: Fly Ash, Silica Fume, Slag and Other Mineral By-Products in Concrete*, American Concrete Institute, 1983, pp. 559–588.
4. J. Virtanen. Freeze-Thaw Resistance of Concrete Containing Blast-Furnace Slag, Fly Ash or Condensed Silica Fume. In *Report SP-79: Fly Ash, Silica Fume, Slag and Other Mineral By-Products in Concrete*, American Concrete Institute, 1983, pp. 923–942.
5. S. Popovics. Strength Relationships for Fly Ash Concrete. *ACI Journal*, Vol. 79, No. 1, Jan.–Feb. 1982, pp. 43–49.
6. G. Bondonado, and J. Nissoux. Road Building Concretes Incorporating Fly Ash or Slag. In *Report SP-79: Fly Ash, Silica Fume, Slag and Other Mineral By Products in Concrete*, American Concrete Institute, 1983, pp. 471–493.
7. ACI Committee 226. Silica Fume in Concrete. *ACI Materials Journal*, Vol. 84, No. 2, March–April 1987, pp. 158–166.
8. P. Mehta. *Concrete Structure, Properties and Materials*. Prentice-Hall, Inc., 1986.
9. P. Robins and S. Austins. Bond of Light-Weight Aggregate Concrete Incorporating Condensed Silica Fume. In *Report SP-91: Fly Ash, Silica Fume, Slag and Natural Pozzolans in Concrete*, American Concrete Institute, 1986, pp. 941–948.
10. V. Ramakrishnan and V. Srinvasan. Silica Fume in Fiber Reinforced Concrete. *The Indian Concrete Journal*, Vol. 56, No. 12, December 1982, pp. 326–334.
11. P. Soroushian and Z. Bayasi. Fly Ash Applications to Concrete. *Symposium Proceedings*, Michigan State University, January 1988.
12. ACI Committee 544. Measurements of the Properties of Fiber Reinforced Concrete. *ACI Journal*, Vol. 75, No. 7, July 1978, pp. 283–289.

Chemical Treatments of Polypropylene Fiber Surfaces Used in Fiber Reinforced Concretes

M. F. FAHMY AND NORBERT L. LOVATA

This paper reports the results of an experimental investigation to determine the effects of chemical treatment of polypropylene fibers (PPF) used in reinforced concretes. The control group concrete was designed at 4,000 psi. The chemical solution used to treat the fiber surfaces was a basic solution of linear alcohol alkoxylates. The investigation included comparison of some static strength as well as the interfacial bond characteristics of unreinforced, plain fiber reinforced, and chemically treated fiber reinforced concretes that were cured for two different periods of 28 and 45 days. Three separate methods of testing were conducted to ascertain the mechanical measures of the concrete samples: compression testing (ASTM 4.02, C-39), flexure strength tests (ASTM 4.02, C-78), and splitting tensile tests (ASTM 4.02, C-496). A random sampling of the failed PPF specimens was prepared and observed using the scanning electron microscopy (SEM) technique. The interfacial features of the fiber surfaces were evaluated to determine the bonding characteristics between the fiber and the concrete matrix. A correlation between the chemical surface treatment of the PPF and the mechanical measures were statistically analyzed.

Since the middle of the 1960s, extensive research has been completed relating to the mechanical bonding of fibers in fiber reinforced concrete composites. Such research brought forth the development and the standards for collated fibrillated polypropylene (CFP) (*1, 2*) which is in wide commercial use today.

Naaman et al. (*3*) cited the characteristics of polypropylene fiber (PPF) as being inert chemically and very stable because of the hydrophobic nature of its surfaces. They also enumerated some of the shortcomings of using such fibers, including its poor bonding with the cementitious matrix, particularly for untreated fibers. A careful review of the literature reveals a paucity of research directly related to the chemical bonding effects of PPF in concrete. Moreover, since the efficiency of fiber reinforcement depends on the interfacial bond strength as well as the mechanical properties of the fiber, studies of the interfacial characteristics of the fiber-matrix interface become very important.

To differentiate between fiber failure and fiber pullout mechanisms, a clearer understanding of the bonding and anchorage of fibers in the concrete matrix is needed. It has been established, however, that such bonding of CFP fibers is far less than that found with steel fibers, which in turn affects the energy absorbed in fiber pullout (*4*). Although there currently are few published reports about the chemical treatment of PPF, some recent studies (*5*) indicate that sulfur infiltrated and polymer impregnated fiber reinforced concretes did indeed exhibit better fibers bonding as well as improvements in the overall strength of the concrete composite.

Regarding techniques used in testing fiber reinforced concretes (FRC), many reports cite the static strength characteristics and properties of such composite systems. Some published studies of compression testing of fiber reinforced concretes, however, indicate conflicting data. Early reports, such as those by Hannat (*1*) found plain concrete to be stronger in compression than polypropylene fiber reinforced concrete (PFRC). It was also reported in the *Concrete Construction Journal* (*6*, p. 468) that PFRC enjoys higher compressive strength after 28 days of cure time than to plain concrete. Several researchers in the FRC field contend that standard compression testing should not be the only procedure used to assess the mechanical properties of such composites. Other mechanical measures should be employed to determine the static strength characteristics of FRC composites.

PPFs, in general, are known as low modulus materials and have the potential strength of between 60 and 100 ksi. Since this strength is generated in tension, it would appear that a more appropriate measure for FRC would be tensile or flexure tests. Empirical evidence has shown, however, that concrete by design is strongest in the compressive mode. It is also well known that, in industrial and commercial applications concrete is designed and subjected to flexure, tension and torque. From this assessment, a determination was made to test the FRC composite samples mechanically in flexure, splitting tensile, and compression modes.

An additional intent of this study was to provide a better understanding of the effects of chemically treating the surface of PPF before mixing it in the concrete matrix. A mild linear alcohol base solution was chosen as the agent for this chemical treatment. The chemical composition of the solution was a 28 percent water solution of the linear nonionic alkoxylate alcohol. This commercially available chemical, known as Basic-H, had revealed promise from a previous investigation (*7*), in which it was tested at only one concentration. In the present study, the chemical was administered at two different concentrations. The manufacturer, Shaklee Corporation, claimed that this chemical would improve the ultimate strength of the concrete composites due to its wettability characteristics, which was a persuasive factor in choosing it for this study.

M. F. Fahmy, Department of Industrial Technology, University of Northern Iowa, Cedar Falls, Iowa. N. L. Lovata, University of Wisconsin, Madison, Wisc.

EXPERIMENTAL DESIGN AND PROCEDURE

A 4,000-psi concrete mix was chosen for this study and also served as the control group (CG) for the modified factorial statistical design. The cementing material used was Type I portland bagged cement, which met ASTM C-150 specifications. The maximum allowable water/cement ratio was 0.47. The coarse aggregate used was a standard ¾-in. top size, AASHTO Size 67 material. The coarse and fine aggregates were obtained from a supplier approved by the Iowa Department of Transportation (DOT). The concrete sand (a natural sand) met fine aggregate requirements for ASTM C-33.

The PPF added to the basic concrete was furnished by a commercial supplier. The fibers were of the D-15 type and met the supplier's requirements for a ¾-in. top size aggregate. The fiber length of the CFP was 2.25 in. The fibers were added to the concrete design mix in the recommended ratio by the manufacturer of 1.6 lb/yd^3 of concrete. This weight ratio was held constant for all the three treatment groups used throughout this study.

As indicated earlier, the chemical chosen for this study was Basic-H, which is furnished by the supplier in full strength as a 28 percent water solution base. The chemical is a nonionic surfactant of linear alcohol alkoxylates. The chemical was diluted by volume fraction with distilled water into two denominations—1:2 and 1:5—for each of the treatment groups. The procedure followed in the chemical treatment of the fiber surfaces and the subsequent soaking and drying of the fibers prior to mixing is described below.

The chemical treatments were prepared first. The PPFs were then weighed and soaked in the chemical bath for 10 min. Next, the fibers were removed from the chemical bath and allowed to air dry. The concrete mix for each treatment group was weighed after drying and then packaged for future use.

The designation of the samples used in this study is as follows:

- CG refers to the control group, which was simply the concrete mix without any fibers added.
- Group A contained plain fibers that had not been treated chemically.
- Group B included fibers that were chemically treated with a diluted solution of 1:2 prior to mixing.
- Group C included fibers that were chemically treated with a diluted solution of 1:5 prior to mixing.

All mixing was done in a drum mixer with a capacity of 5 ft^3. The batching procedure followed ASTM C-92. First, the fine and coarse aggregates were placed in the mixer and rotated dry. Next, three-fourths of the required mixing water was added, and the contents were thoroughly mixed for 1 min. The cement was added next, followed by the remaining water. The fibers were then added, and the concrete was mixed for 3 min. Next followed a 3-min rest period and a final mixing period of 2 min.

There were 12 specimens cast for each test group to meet the required statistical replication factor. The size of the specimens used for both the compression and splitting tensile tests were 6 in. x 12 in. cylinders. The flexure samples were cast as beams with 6 in. × 6 in. × 20 in. dimensions. All the test samples were prepared to conform to ASTM 4.020.

The concrete samples were covered with plastic sheets and cured at room temperature (68°F to 72°F) for 24 hr. The samples were then demolded and placed in a lime-saturated water tank that was maintained at 72°F. Two sets of samples were prepared, with curing periods of 28 and 45 days. After the appropriate time, the samples were removed and tested. The test results were statistically analyzed to determine significant differences among all test groups. A random sampling of fibers was taken from failed specimens for SEM observations. The chunks of concrete containing the designated fibers were mounted and gold coated prior to SEM inspection.

RESULTS

Compressive Strength Tests

The statistical results obtained from the compressive tests were found to be consistent with previously obtained data (*7, 8*). The CG attained the highest compressive strength values among all test groups for both the 28- and 45-day cure periods. The average compressive strength values and their calculated standard deviations are presented in Figure 1.

Splitting Tensile Tests

The data obtained from the splitting tensile tests of the cylindrical samples are shown in Figure 2. As illustrated, the results indicate almost no differences between the CG and the highest values attained by the treatment groups. Curing these specimens for two different cure durations did not result in any observable difference in the split tensile values attained by each group.

Flexure Strength Tests

As shown in Figure 3, the flexure strength tests clearly indicate that the FRC groups assumed part of the applied loads. In two of the three treatment groups, the FRC outperformed the CG with plain concrete.

SEM Observations

A previous study (*7*) reported the morphology of untreated plain fiber surfaces taken from a failed specimen. Small CH crystals with sharp edges were seen to be the major precipitates on these fiber surfaces. The density of these precipitates, however, was not high but appeared to be rather scarce. The same study reported that, when the fibers were presoaked in a full-strength Basic-H solution, more CH crystals with the same morphological features precipitated on the fiber surfaces. The density of these precipitates was still not of high magnitudes. In the study described in this paper, the precipitated crystals retained the same morphological features as reported before when the fibers were soaked in diluted solutions of Basic-H. Figure 4 illustrates this finding for treatment group C, which is representative of both groups B and C. The amount of the precipitated crystals, however, seem to be more dense as a function of the dilution of the solution than that

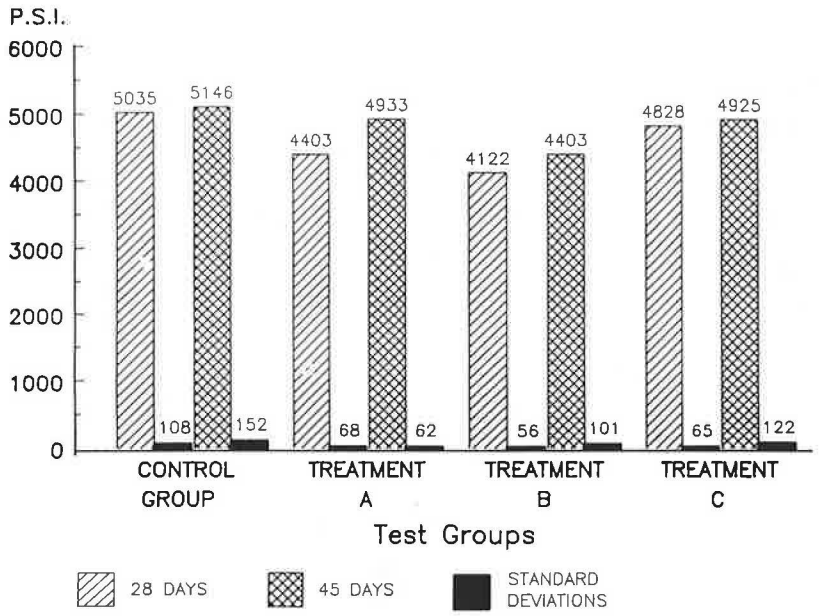

FIGURE 1 Compressive strength test results: comparison between the 28- and 45-day cure time.

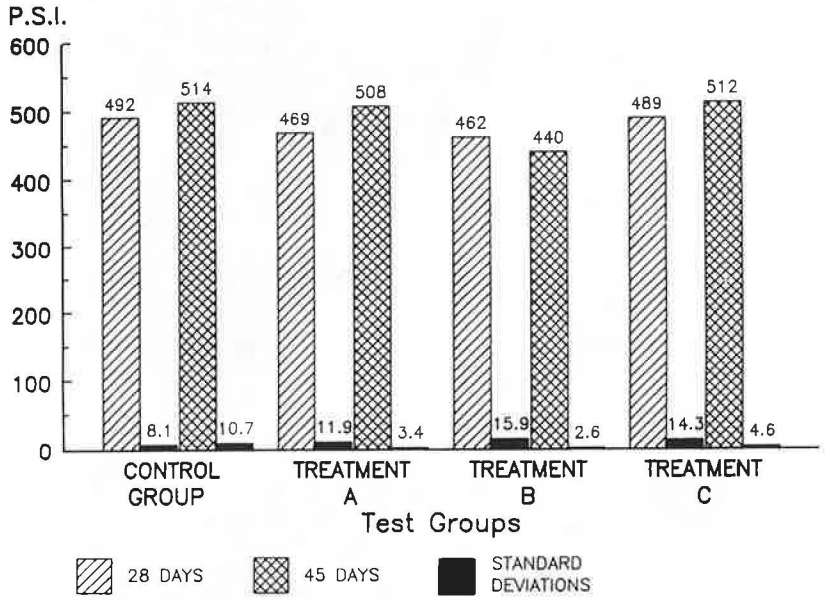

FIGURE 2 Splitting tensile test results: comparison between the 28- and 45-day cure time.

reported earlier. It should be noted that the fibers taken from the split tensile specimens also showed some areas with clear tears. It appears as if the fibers started to fail in shear rather than pullout from the matrix under load.

DISCUSSION

The date obtained from the compressive strength tests indicate that there is almost no change in this property due to fiber reinforcement and chemical treatment. This finding supports what Zollo (*8*) reported a few years ago. In his study, Zollo also concluded that the compressive test does not indicate the fiber contribution in the reinforced concrete samples. One observation that is worth recording is that, during the compression testing of cylinders in the course of this study, one of the cylinders failed and could no longer support further loads even though its surface did not show any major visible cracking. In this case, the specimen obviously failed because of a network of microcracks while the PPFs resisted the propagation of any major cracks to the cylinder surface. Such an observation substantiates the findings of ACI Committee 544

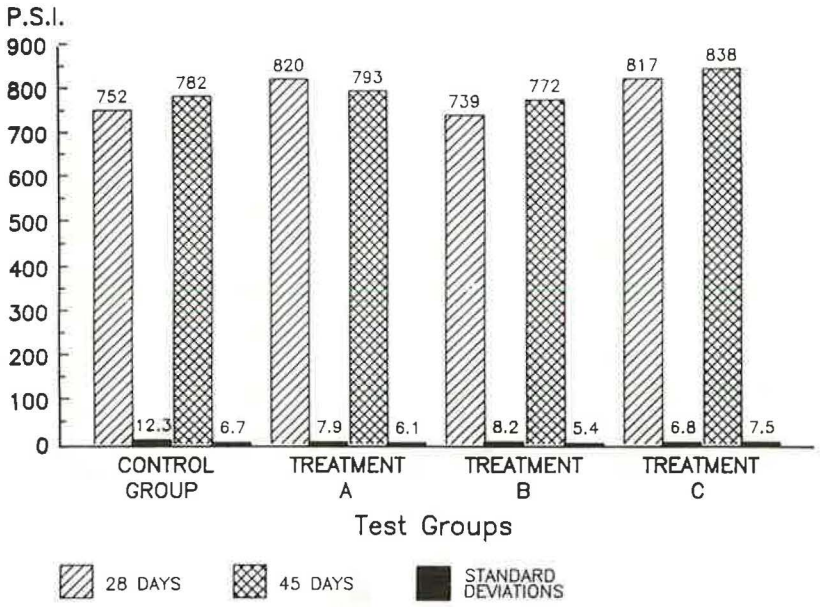

FIGURE 3 Flexural strength test results: comparison between the 28- and 45-day cure time.

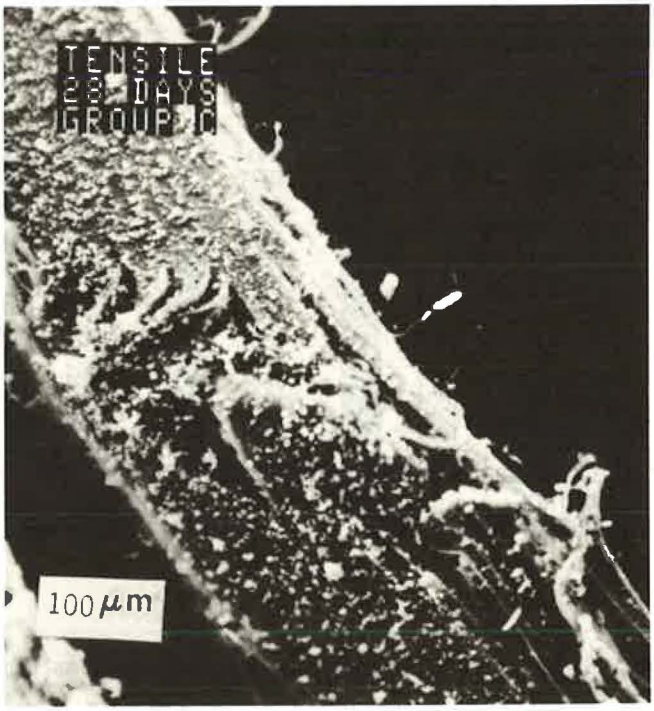

FIGURE 4 Scanning electron micrograph of fiber surface morphology of a failed fiber from the splitting tensile test of treatment group C (28-day cure).

(*5*). This committee concluded that major cracking in concrete beams is usually preceded by slow microcrack growth, which leads to major crack development and the subsequent failure of the beams. This phenomenon also indicates that the PPFs are very efficient in load transfer, especially at peak loading and post loading, where the fibers are believed to have assumed nearly the total applied load.

The post peak load transfer phenomenon was discussed by Ramakrishnan (*9*). During the course of this study, it was noticed that the applied load at failure was sustained for up to 15 sec on the average. This further indicates the ability of fibers to continue being load-bearing members of the composite and to contribute to the post peak load transfer phenomenon. The fibers, in fact, are so efficient in the load transfer that they started to fail themselves (see Figure 4).

The data obtained from the splitting tensile tests revealed

no clear improvement in composite strength, perhaps because this type of testing, as viewed by many researchers, is not in itself a measure of the tensile properties of the composites. Rather, it is another measure indicative of the compression properties of these composites.

The statistical flexure results have the most promising possibilities. Statistical improvement of the FRC becomes apparent when compared to the CG of plain concrete. The almost 10 percent improvement in flexural strength of both group A and the chemically treated group C over the CG is in agreement with Zollo's findings (*8*).

As indicated in the tests and in the figures presented earlier, the 45-day curing resulted in better mechanical static strength properties in almost all cases.

Regarding the bonding between the PPFs and the matrix, the soaking of fibers into the chosen solution prior to mixing improved the wettability of the fiber surfaces. The nonionic linear alcohol alkoxylates present in the solution did indeed promote the formation of CH crystals on the fiber surface. As reported earlier (*7*), the pre-treatment of the fiber surfaces prompted a localized effect on the cement matrix in the fiber vicinity, which resulted in the precipitation of the CH crystals on the otherwise inert fiber surface. The mechanical interaction between the fiber surface asperities and the matrix provided the friction forces necessary for bonding in spite of the absence of direct fiber-matrix bonding. The dilution of the alkali solution up to a 1:5 ratio resulted in more CH crystal density on the fiber surface, hence increasing the mechanical bonding between the fiber and the matrix.

CONCLUSIONS

- The chemical treatment of PPFs with diluted concentrations up to 1:5 by volume of the Basic-H solution improved the flexural strength of the concrete composite up to about a 10 percent increase.
- The surface treatment of fibers with different concentrations of the Basic-H solution improved the precipitation of CH crystals on the fiber surfaces, hence increasing the mechanical friction bonding of the fiber to the cementitious matrix.
- The mechanical bonding of fibers to the matrix increased due to the precipitation of CH crystals to the extent that the fibers started to fail rather than pull out of the matrix under loading.
- Although the addition of PPFs and the chemical treatment used did not significantly improve such static strength characteristics of the composite as the compressive and split tensile strengths, it did prevent massive major crack propagations through the composite.
- The use of chemically treated PPFs is important as secondary reinforcement and crack control.
- The PPFs sustain the load bearing role in post peak loading (for up to 15 sec in compression loading).

ACKNOWLEDGMENT

The authors gratefully acknowledge the support for this project, which was partly funded by a grant from Forta Corporation of Grove City, Pennsylvania.

REFERENCES

1. D. J. Hannat. *Fiber Cements and Fiber Concretes*. John Wiley and Sons, Inc., New York, 1978.
2. R. P. Sheldon. *Composite Polymeric Materials*. Applied Science Publishers, New York, 1982, p. 85.
3. A. E. Naaman, S. P. Shah and J. L. Throne. Some Developments in Polypropylene Fibers for Concrete. In *Report SP 81-18*, American Concrete Institute, Chicago, Ill. 1985, pp. 376–396.
4. R. F. Zollo. Glass, Natural and Synthetic Fiber Uses in Fibrous Concrete. In *Report SCM-10(85): Design with Fiber Reinforced Concrete*, American Concrete Institute, 1985, pp. 1–13.
5. ACI Committee 544. *State-of-the-Art Report on Fiber Reinforced Concrete*. American Concrete Institute, Chicago, Ill., 1985, pp. 411–448.
6. *Concrete Construction Journal*, Vol. 28, No. 6, June 1983.
7. N. L. Lovata and M. F. Fahmy. Interfacial Bond Study of a Chemically Treated Polypropylene Fiber-Reinforced Concrete, *Construction and Building Materials*, Vol. 1, No. 2, June 1987, pp. 83–87.
8. R. F. Zollo. Collated Fibrillated Polypropylene Fibers in FRC. In *Report SP 81-18*, American Concrete Institute, Chicago, Ill., 1985, pp. 397–409.
9. V. Ramakrishnan, S. Gollapudi and R. Zellers. Performance Characteristics and Fatigue Strength of Polypropylene Fiber Reinforced Concrete. In *Report SP-105*, American Concrete Institute, Detroit, Mich., 1987, pp. 159–178.

Fatigue Strength of Fibrillated Polypropylene Fiber Reinforced Concretes

M. NAGABHUSHANAM, V. RAMAKRISHNAN, AND GARY VONDRAN

This paper presents the results of an experimental investigation to determine the flexural fatigue strength of concrete reinforced with three different concentrations of fibrillated polypropylene fibers. The properties and the performance of fresh and hardened concretes with and without fibers are compared. The test program included the evaluation of 1) Flexural fatigue strength and endurance limit; 2) hardened concrete properties, such as compressive strength, static modulus, pulse velocity, modulus of rupture, and toughness indexes; and 3) fresh concrete properties, including slump, vebe time, inverted cone time, air content, and concrete temperature. The test results indicated an appreciable increase in post-crack energy absorption capacity and ductility due to the addition of fibers. When compared with corresponding plain concrete, the flexural fatigue strength and the endurance limit (for 2 million cycles) significantly increased. The static flexural strength increased after being subjected to fatigue loading.

Concrete is one of the most important and widely used construction materials in the world. It has many advantages, including relatively low cost, general availability, and usage of local materials. It is also among the most variable with regard to material properties. The low tensile strength and brittle failure tendency are, however, two major design problems. In an attempt to increase concrete ductility and energy absorption, a relatively new technology of fiber reinforced concrete (FRC) has been introduced. (*1–4*). In FRC, millions of fibers are introduced into the concrete as it is mixed. These fibers are dispersed randomly throughout the concrete and thus improve concrete properties in all directions. Because of their discontinuity and random distribution, they are not intended to replace the function of conventional reinforcement. The random and uniform distribution of fibers throughout the concrete mass also helps to eliminate temperature and shrinkage cracks. Other advantages include the increase in pre-crack tensile strength, fatigue strength, impact strength, and shock resistance.

Fiber has been used in shotcrete for rockfill stabilization and tunnel and canal linings. It is also rapidly gaining acceptance as a suitable material for repair and rehabilitation of concrete structures. In many applications, particularly in pavement and bridge deck overlays, flexural fatigue strength and endurance limit are considered important design parameters, mainly because these structures are subjected to the fatigue load cycles (*1,4,5*).

M. Nagabhushanam and V. Ramakrishnan, South Dakota School of Mines & Technology, Rapid City, S.D. 57701. Gary Vondran, Fibermesh Company, 1550 F Dell Ave, Campbell, Calif. 95008.

Several fiber materials in various sizes and shapes have been developed for use in FRC. Fibrillated polypropylene has been one of the most successful due to some unique properties that make it suitable for reinforcement in concrete. The fibers have very high tensile strength. Further, their high elongation enhances energy absorption and leads to improved ductility, higher fatigue strength, and higher impact resistance of concrete (*1,5*).

OBJECTIVES

The primary objectives of this inverstigation were to determine the behavior of fibrillated polypropylene FRC when subjected to nonreversed fatigue bending and to determine the effect of fiber concentration. Other objectives of this investigation were to

- Determine the behavior of fibrillated polypropylene fibers during and after mixing;
- Determine the properties of the fresh concrete reinforced with three different concentrations of fibrillated polypropylene fibers; and
- Determine the characteristics of hardened concrete, such as compressive strength, static modulus, unit weight, pulse velocity, modulus of rupture, and toughness indexes for concretes with and without fibers but otherwise identical mixes.

MATERIALS, MIXES, AND TEST SPECIMENS

Materials

Type I portland cement satisfying the requirements of ASTM C150 was used for all mixes. The fine aggregate used was natural sand that had a saturated surface dry specific gravity of 2.63 and an absorption of 1.64 percent. The coarse aggregate used was crushed limestone with a maximum size of ¾ in., a saturated surface dry specific gravity of 2.68 and an absorption of 0.54 percent. Both coarse and fine aggregates satisfied grading requirements of ASTM C33.

Tap water from the Rapid City municipal water supply system was used. The air-entraining admixture was a neutralized vinsol resin, satisfying ASTM C260, and the superplasticizers used conformed with Type F ASTM C494 specifications.

The fibrillated polypropylene fibers used in this study were commercially available under the brand name Fibermesh.

During mixing, the small bundles in the mesh separate into individual multifilament fibers. These fibers are rectangular in cross section with fibril links to other main fibers. This geometry, with branching of fibers into spurs or fibrils, enhances bonding and provides excellent mechanical anchoring. Other polypropylene and synthetic fibers may not offer these bonding characteristics. Thus, the results are only applicable to the specific fiber tested. For this investigation, a ¾-in. fiber was used, having a specific gravity of 0.91, a modulus of elasticity of 500 ksi, and a yield tensile strength of 80 to 100 ksi.

Mixes

Twelve mixes were made for the investigation. Three were control mixes without fibers, and the other nine contained varying amounts of fibers. Each mix was made in a batch size of 3.25 ft^3. The mix quantities and designations are given in Table 1. The batching and mixing of all the mixes were performed according to ASTM C192 specifications.

Test Specimens

For the compression and static modulus tests, three to five 6 in. × 12 in. cylinders were cast from each mix. In all mixes, excluding two (NF1 and NF2), two to four 6 in. × 2.5 in. cylinders were made for impact tests. For both the static flexural and flexural fatigue tests, the following specimens were cast:

- Twelve to fifteen 4 in. × 4 in. × 14 in. beams for the NF series, and
- Six to seven beams of 4 in. × 4 in. × 14 in. and six to seven beams of 3.5 in. × 4.5 in. × 16 in. for the G series.

The specimens were cast in steel molds immediately after mixing and then covered with a plastic sheet and cured for 24 hours at room temperature. They were then demolded and immersed in lime-saturated water tanks maintained at 72°F. The specimens for the compression, static flexural, and impact tests remained in the water until they were tested at 7 and 28 days. The specimens for the fatigue test were taken out of the water at 28 days of age and painted with a curing compound.

TESTS FOR FRESH CONCRETE

The freshly mixed concrete was tested for temperature, slump (ASTM C143), air content (ASTM C231), time of flow through an inverted slump cone (ASTM C995), and vebe time (British Standard 1881). The results of these tests are given in Table 2.

TESTS FOR HARDENED CONCRETE

Compressive Strength and Static Modulus

The cylinders were tested for compressive strength and static modulus according to ASTM C39 and C469, respectively.

Static Flexure Test

The beams were tested for static flexural strength by applying third point loading according to ASTM C1018. The load-deflection data recorded for the static flexural strength test was used to calculate the toughness indexes and to investigate the ductility of concrete. A dial gauge accurate to 0.0001 in. was placed under the beam at the centerline to measure the deflection. The rate of deflection was kept in the 0.002 to 0.004 in./min range according to ASTM C1018.

Impact Test

The impact specimens were tested by the drop weight test method (*6*). Equipment for the test consisted of

- A standard, manually operated 10 lb weight with an 128 in. drop (ASTM D1557);

TABLE 1 MIX QUANTITIES AND DESIGNATION

MIX #	FIBER CONTENT (%)	COARSE AGGREGATE (lbs)	FINE AGGREGATE (lbs)	CEMENT (lbs)	W/C RATIO	SPD (cc)	AEA (cc)
NP4	____	187.8	187.8	79.2	0.40	180	25
NF1	0.1	187.8	187.8	79.2	0.40	240	25
NF7	0.1	187.8	187.8	79.2	0.40	240	25
NF3	0.5	187.8	187.8	79.2	0.40	330	25
NF5	0.5	187.8	187.8	79.2	0.40	330	25
NF2	1.0	187.8	187.8	79.2	0.40	380	25
NF6	1.0	187.8	187.8	79.2	0.40	550	30
G1	____	215.8	169.8	65.0	0.50	78	18
G2	0.1	215.8	169.8	65.0	0.50	78	18
G3B	1.0	181.8	142.5	86.9	0.50	208	23
G4	0.5	181.8	142.5	86.9	0.42	156	22
G5	----	181.8	142.5	86.9	0.42	123	22

SPD - Superplasticizer Dosage
AEA - Air Entraining Agent Dosage

TABLE 2 PROPERTIES OF FRESH CONCRETE

MIX #	SLUMP (in) INITIAL SLUMP	SLUMP (in) VEBE SLUMP	CONCRETE TEMP. (°F)	AIR CONTENT (%)	VEBE TIME (sec.)	INVERTED CONE TIME (sec.)
NP4	9.25	6.75	71.4	5.2	0.7	---
NF1	8.25	4.88	70.2	9.0	2.0	---
NF7	6.25	3.50	79.9	4.4	2.0	7.8
NF3	5.25	2.06	70.9	5.4	3.5	23.0
NF5	3.75	2.75	77.7	3.2	3.7	23.7
NF2	0.13	0	70.0	4.4	10.0	90.0
NF6	0.13	0	77.2	3.2	9.5	62.0
G1	3.75	2.25	80.1	5.2	2.2	9.5
G2	1.25	1.06	79.3	3.5	5.5	15.3
G3B	3.13	1.88	80.2	6.9	3.7	56.0
G4	6.50	5.38	80.7	7.6	1.5	6.7
G5	6.25	3.5	81.0	4.3	1.6	6.1

- A 2-½ in. diameter hardened steel ball; and
- A flat steel base plate with a positioning bracket and four positioning lugs.

The specimen was placed on the base plate within the positioning lugs with its rough surface upwards. The hardened steel ball was placed on top of the specimen within the positioning bracket, and the compactor was placed with its base on the steel ball. The test was performed on a smooth, rigid floor to minimize the energy losses. The hammer was dropped consecutively, and the number of blows required to cause the first visible crack on the top of the specimen was recorded. The impact resistance of a specimen to ultimate failure was also recorded. This was accomplished by counting the number of blows required to open the cracks sufficiently so that the pieces of the specimen were touching three positioning lugs on the base plate.

Flexural Fatigue Test

The main thrust of the investigation was to determine the endurance limit in flexural fatigue loading for various concretes. In this test, the endurance limit was defined as the maximum load at which the specimen could withstand 2,000,000 cycles of nonreversed fatigue loading. The 2,000,000-cycle limit was chosen to approximate the life span of a structure that may typically be subjected to fatigue loading, such as a bridge deck or highway pavement. The range of cyclic loading was expressed as a percentage of the average maximum load in static flexure for each mix. The lower limit for all tests was 10 percent of the maximum load. The upper limit varied depending on the particular mix—generally from 55 percent to 80 percent of the maximum load. The fatigue test was then run between these limits. If the beam failed before the 2,000,000-cycle limit, the upper limit was reduced for the next specimen. If the beam survived, the upper limit was raised, and a new beam was tested at the increased upper limit. All beams that survived the 2,000,000-cycle limit were later tested for flexure, and the maximum loads at which they failed were noted.

The frequency of loading used was 20 cycles/sec for all tests. The machine used for these tests was a Material Test System (MTS). The machine could be operated in any of three modes: load control (force applied to the specimen), strain control (strain induced in the specimen), or deflection control (distance traveled by the ram or deflection of the specimen). Since this test was concerned with stress levels, load control was used for fatigue testing.

A choice of three waveforms could be used: sine wave, square wave, and triangular wave. The sine wave was selected because of its similarity to real-world behavior (*2*).

A built-in control unit kept track of the number of cycles to the nearest 100. When the beam failed, this reading was recorded.

TEST RESULTS AND DISCUSSION

Fresh Concrete Properties

The fibrillated polypropylene fibers used in this program performed very well. Although fibers, cement, and aggregates were added to the mixer simultaneously, no fiber balling occurred. The mixing action caused the bundles to open up and expand to fiber mesh form producing individual multifilament fibers uniformly distributed throughout the concrete. The fresh concrete with fibers had no surface bleeding and no segregation.

The results of the tests on fresh concrete are given in Table 2. To ensure that all the mixes were combined under approximately similar conditions, room temperature, humidity, and concrete temperature were recorded for each.

Workability

Three tests were performed to determine the workability of the mixes: slump, inverted cone time, and vebe time. The slump test results indicate that satisfactory workability can be maintained even with a relatively high fiber content. This was achieved by either adjusting the amount of superplasticizer used or adjusting the water and cement content (mix 3GB) to maintain relatively equal strengths and water/cement ratios.

Vebe time was used to measure workability based on the energy needed to compact the concrete. As the slump value decreased, the vebe time increased.

Inverted cone time is a new measurement that tests workability for fibrous concrete only. The inverted cone time

increased with a decrease in slump. Further, as vebe time increased, inverted cone time rose as well.

Finishability

A table vibrator was used to form a layer of mortar on the surface of the member; this made finishing easier. In general, the slump, air content, and concrete temperatures all varied slightly within the allowable variation normally obtained in concrete research. The variations in the fresh concrete properties did not significantly affect the hardened concrete properties.

Fiber Factor

Two higher quantities beyond the fiber manufacturer's recommended amount of 1.5 lb/yd^3 (0.1 percent by volume) were selected: 7.5 lb/yd^3 (0.5 percent by volume) and 15.0 lb/yd^3 (1.0 percent by volume). For the NF series (mixes NF1 to NF7), the water/cement ratio and the mix proportions were maintained at a constant. Fibers in different quantities were added without considering the fiber factor. A higher volume of fibers reduced the slump because of the added surface area of the fibers. The compressive strength and the modulus of rupture values also decreased. Obviously, the same mix proportions could not be used for higher volumes of fibers; fiber factor adjustments are necessary to balance proportions for suitable workability, placeability, appearance, and strength. Optimum mixture proportions should be obtained by trial mixes when using higher fiber volumes.

HARDENED CONCRETE PROPERTIES

Compressive Strength

The results of the tests for compressive strength are given in Table 3. It was observed that compressive strength decreases at high air contents. The coefficient of variation values calculated for all the mixes are below 2, which is the specified value for research work (*7*). The minor differences noticed are expected in experimental work.

An important asset of fiber concrete is the ductile mode of failure, which was demonstrated while testing for compressive strength. The plain concrete cylinder completely failed, shattering into pieces with a loud noise. The fiber concrete cylinders, however, continued to sustain the load and endured large deformations without totally breaking into pieces.

Static Modulus

The static modulus test results are given in Table 3. The average static modulus for all mixes was 4.92×10^6 psi, and its range was between 3.55×10^6 and 5.54×10^6 psi. The addition of fibers had no effect on static modulus.

Pulse Velocity

The pulse velocity test was used for quality control. Test results are given in Table 3. At 28 days, the average pulse velocity was 15,460 ft/sec, with a maximum of 15,920 ft/sec (2.9 percent) and a minimum of 14,600 ft/sec (−5.6 percent). The test results indicate a good degree of consistency and quality control. They also reveal that fiber content has little effect on pulse velocity.

Modulus of Rupture

The results of modulus of rupture are given in Table 3. Neither the fiber reinforcement nor the quantity of fibers had an appreciable effect on flexural strength.

There is always more scatter and sometimes one or two odd results in flexural testing of FRC. This is due to the fiber's

TABLE 3 HARDENED CONCRETE PROPERTIES AT AN AGE OF 28 DAYS

SP.#	f_c' (psi)	E_c (10^6psi)	PULSE VELOCITY (ft/sec)	M.O.R (psi)
NP4	5905	4.94	15590	790
NF1	5940	4.63	15560	660
NF7	6720	5.33	15660	890
NF3	6975	5.29	15810	845
NF5	6780	5.33	15640	810
NF2	6415	5.36	15920	755
NF6	5570	5.07	15690	700
G1	5450	5.54	15380	760
G2	6020	5.33	15750	780
G3B	4970	3.55	14510	660
G4	4870	3.62	14600	670
G5	6450	5.03	15450	775

The values in the above table are the mean values of three to four specimens tested.

f_c' - Compressive Strength

E_c - Static modulus

M.O.R - Modulus of Rupture (Flexural Stress)

random orientation and possible nonuniform distribution of aggregate in small specimens, particularly in the tension zone.

Toughness Index

The results of the calculation for toughness index are given in Table 4. Typical load-deflection comparison curves for plain concrete and the concretes with three different fiber contents (0.1 percent, 0.5 percent, and 1.0 percent by volume) are given in Figures 1 and 2. The figures illustrate the improvement in elastic-plastic behavior of fiber concrete composite that occurs with the increase in fiber content from 0.1 percent to 1.0 percent.

The toughness index is defined as the area under the load-deflection curve up to a specified deflection, divided by the area under the curve up to the point where the concrete first cracks (first-crack toughness). The area under the curve represents the energy in inch-pounds required to cause the deflection of the beam. The toughness index measures the capacity of fracture energy absorption and the ductility of the specimen. Plain concrete fails immediately upon cracking, without further load-carrying capabilities. Since this is a brittle failure, I_5, I_{10}, and I_{30} are always equal to 1.0. Concrete beams reinforced with polypropylene fibers, however, will continue to deflect in a ductile fashion and carry loads well past the point of first crack. In this case, the toughness index will be greater than 1.0. A straight line was used to connect the first crack point and the point immediately after crack.

The calculated values of toughness indexes (I_5, I_{10}, and I_{30}) are given in Table 4. The beams with higher fiber content had higher energy absorption and ductility compared with beams with fewer fibers (see Figure 3).

The values equal to 2 and 3 for I_{10}/I_5 and I_{30}/I_{10}, respectively, illustrate perfect plastic behavior. The values of I_{10}/I_5 and I_{30}/I_{10} for all the mixes given in Table 4 indicate that they are less than 2 and 3, respectively. However, the obtained higher ratios indicate that, though a perfect plastic behavior is not achieved, a good measure of ductility and post-crack plastic behavior is obtained by adding a high volume (0.5 percent and 1.0 percent) of fibrillated polypropylene fibers.

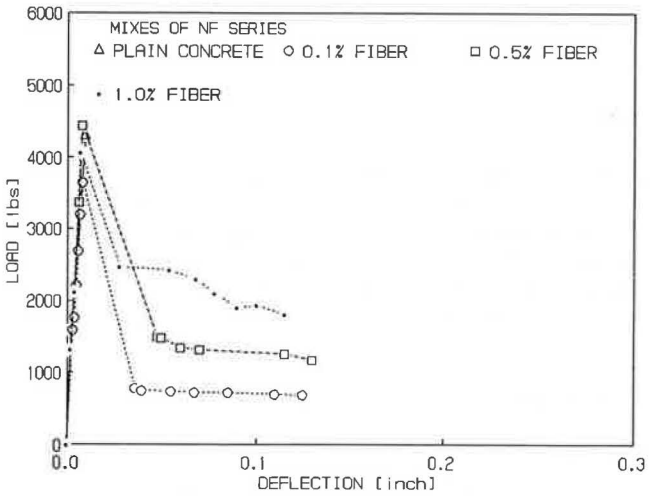

FIGURE 1 Load-deflection comparison curves for NF series.

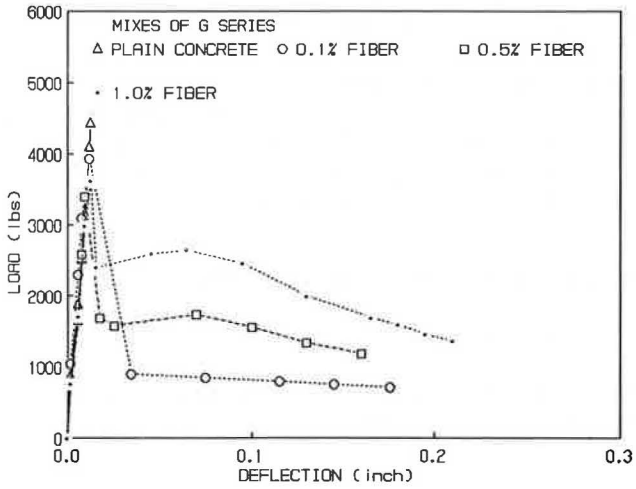

FIGURE 2 Load-deflection comparison curves for G series.

TABLE 4 TOUGHNESS INDEXES OF FIBER REINFORCED BEAMS

MIX #	FIRST CRACK TOUGHNESS (in-lbs)	I_5	I_{10}	I_{30}	I_{10}/I_5	I_{30}/I_{10}
NP4	----	1.000	1.000	1.00	1.00	1.00
NF1	17.28	3.519	5.110	9.00	1.47	1.76
NF7	----	1.000	1.000	1.00	1.00	1.00
NF3	24.65	3.330	5.320	11.99	1.60	2.30
NF5	19.22	4.650	7.330	14.37	1.58	1.96
NF2	19.79	3.510	6.530	16.49	1.87	2.53
NF6	13.57	4.810	8.360	21.98	1.75	2.62
G1	----	1.000	1.000	1.00	1.00	1.00
G2	23.39	4.120	5.590	9.13	1.35	1.64
G3B	17.08	4.020	7.690	21.12	1.91	2.73
G4	14.86	3.510	6.230	16.06	1.78	2.58
G5	----	1.000	1.000	1.00	1.00	1.00

The values in the above table are the mean values of three to four specimens tested.

Post-Crack Load Drop Phenomenon

Post-crack load drop is defined as the difference between the maximum load and the load recorded at a deflection equal to three times the deflection measured at first crack. The load drops expressed as a percentage of maximum loads are 45 percent, 27 percent, and 26 percent, respectively, for the beams of NF series with 0.1 percent, 0.5 percent, and 1.0 percent fiber contents. The load drops are 78 percent, 52 percent, and 30 percent for the beams of G series with 0.1 percent, 0.5 percent, and 1.0 percent fiber contents, respectively. The post-crack load drop generally decreases as the fiber content increases (Figures 1 and 2). Compared with polypropylene fibers, the straight steel fibers had higher post-crack load drops (*8*). The table below compares the load drops for typical load-deflection curves of two types of fibers.

Fiber Content (percent)	*Types of Fibers*	
	Polypropylene (percent)	*Straight Steel (percent)*
0.1	45	—
0.5	27	80
1.0	26	77

Impact Strength

The drop-weight test used in this investigation (*6*) is not completely scientific and is not expected to give accurate quantitative values for impact resistance. However, the test is simple and inexpensive and can be performed anywhere, including in the field.

The number of blows to failure for plain concrete specimens was very low; for specimens reinforced with polypropylene fibers the number of blows to failure increased tremendously. The comparison bar charts for first crack and full failure are shown in Figure 4. The figure shows that, for all fiber concrete mixes, the number of blows for first crack and final failure is higher than that for plain concrete. Also, the impact resistance increases with an increase in fiber content. These results prove that fiber concrete with fibrillated polypropylene fiber has excellent impact resistance.

FLEXURAL FATIGUE BEHAVIOR

Fatigue properties of fibrillated polypropylene FRC was the main objective of this investigation. Beams made with plain concrete and the concretes with 0.1 percent, 0.5 percent, and 1.0 percent fiber contents by volume were tested for flexural fatigue.

Results of fatigue tests are tabulated in Table 5, column 3, which shows maximum stress in psi. This was calculated using the actual dimensions of the beam at the failed cross section and the upper load limit used for the test. Similarly, column 6 shows the maximum fatigue stress of each specimen as a ratio of the average modulus of rupture for the same mix. Column 7 shows the number of cycles at failure. Figures 5 through 12 illustrate various relationships between the number of cycles (N), fatigue strength, and endurance limits. Based

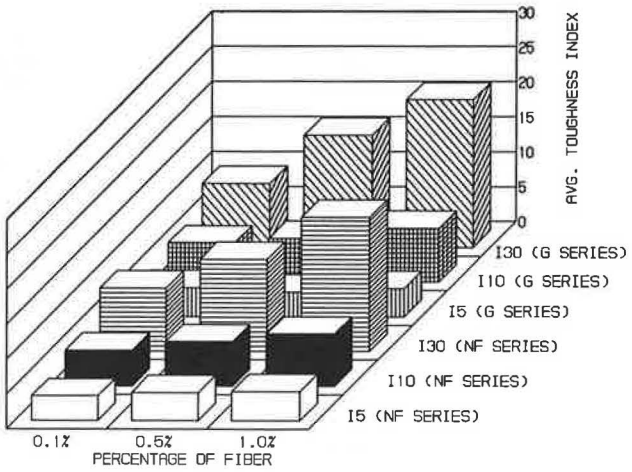

FIGURE 3 Toughness index bar chart.

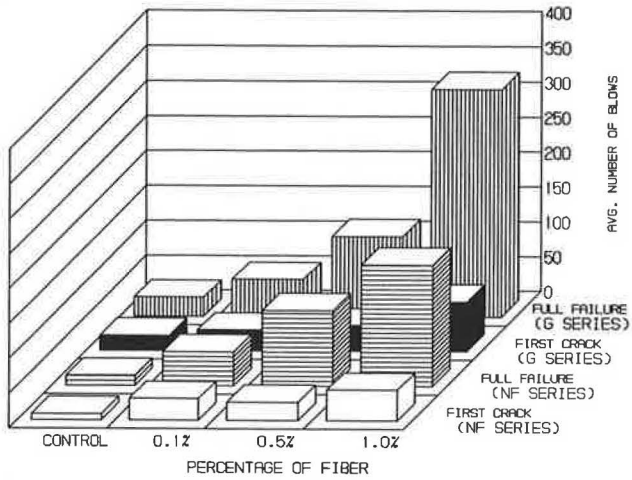

FIGURE 4 Impact test results.

on the figures and results given in the tables, fatigue strength and endurance limit were analyzed.

Fatigue Strength

Fatigue strength is defined as the maximum fatigue flexural stress at which the beam can withstand 2,000,000 cycles of nonreversed fatigue loading. Fatigue strength increased when fibrillated polypropylene fibers were added to the concrete. In the NF series, the fatigue strength was 395 psi for plain concrete; it was 386 psi, 500 psi, and 521 psi for 0.1 percent, 0.5 percent, and 1.0 percent fiber concrete mixes, respectively, showing a decrease of 2 percent for the 0.1 percent fiber concrete mix and an increase of 27 percent and 32 percent for the 0.5 and 1.0 percent fiber concrete mixes, respectively. Similarly, in the G series, there was an increase in fatigue strength of the fiber concrete mixes compared with plain concrete. Graphs were drawn for fatigue flexural stress versus the logarithm of the number of cycles for all mixes in the NF and G series. A linear relationship was found between fatigue stress and log N. As seen in Figure 13, fatigue strength increases with fiber content.

TABLE 5 FATIGUE TEST RESULTS

SP. #	AGE (DAYS)	MAX. STRESS f_{max} (psi)	MIN. STRESS (psi)	STRESS RANGE (psi)	f_{max} / f_r	CYCLES TO FAILURE
NP4-7	36	450	82	368	0.57	5660
NP4-8	34	383	77	306	0.48	2618700+
NP4-9	33	582	83	499	0.74	500
NP4-10	33	483	81	402	0.61	1860
NP4-11	33	477	80	397	0.60	75990
NP4-12	33	409	82	327	0.52	1951330
NF1-4	53	386	64	322	0.58	2190780+
NF1-5	54	521	65	456	0.79	993320
NF1-6	55	467	67	400	0.71	104380
NF1-7	55	483	69	414	0.73	2607340+
NF1-8	56	513	68	445	0.78	2580900+
NF1-9	30	330	66	264	0.50	2000150+
NF1-10	30	409	68	341	0.62	58560
NF1-11	30	481	69	412	0.73	1060
NF1-12	30	521	65	456	0.79	4280
NF7-1	119	749	88	661	0.84	23300
NF7-2	118	758	84	674	0.85	1104600
NF7-3	119	787	87	700	0.88	296000
NF7-4	117	749	88	661	0.84	2032290+
NF7-6	119	730	86	644	0.82	38500
NF7-7	119	659	88	571	0.74	2000000+
NF7-8	118	786	87	699	0.88	633100
NF7-9	119	648	86	562	0.73	2000000+
NF7-10	118	828	87	741	0.93	19200
NF7-11	118	823	87	736	0.92	1700
NF3-4	60	580	83	497	0.69	1058810
NF3-5	59	532	82	450	0.63	2390610+
NF3-6	59	614	88	526	0.73	121900
NF3-7	32	462	84	378	0.55	2818830+
NF3-8	31	405	81	324	0.48	2241100+
NF3-9	31	500	83	417	0.59	18510
NF3-10	31	514	86	428	0.61	8520
NF3-11	31	567	81	486	0.67	9940
NF5-5	79	712	79	633	0.88	23100
NF5-6	80	650	76	574	0.81	2002310+
NF5-7	81	668	79	589	0.83	2018780+
NF5-8	79	819	82	737	1.00	1170
NF5-9	80	716	80	636	0.89	24780
NF5-10	79	644	81	563	0.80	2030690+
NF5-11	79	759	80	679	0.94	2830
NF5-12	75	554	79	475	0.69	2011580+
NF5-13	78	696	77	619	0.86	2118020+
NF2-4	32	529	76	453	0.70	7830
NF2-5	30	375	75	300	0.50	2308100+
NF2-8	57	521	74	447	0.69	2001710+
NF2-9	58	580	77	503	0.77	372890
NF2-10	58	559	75	484	0.74	2032940+
NF2-11	59	590	74	516	0.78	116360
NF2-12	59	553	74	479	0.73	887210
NF6-5	84	583	65	518	0.83	859260
NF6-6	82	558	70	488	0.80	2382840+
NF6-7	85	548	69	479	0.78	2024730+
NF6-8	84	662	66	596	0.95	46550
NF6-9	84	612	70	542	0.87	11980
NF6-10	87	604	71	533	0.86	2076340+
NF6-11	86	560	66	494	0.80	2006900+
NF6-12	84	558	70	488	0.80	370240
NF6-13	88	578	68	510	0.83	2000000+

TABLE 5 (*continued on next page*)

TABLE 5 (*continued*)

SP. #	AGE (DAYS)	MAX. STRESS f_{max} (psi)	MIN. STRESS (psi)	STRESS RANGE (psi)	f_{max}/f_r	CYCLES TO FAILURE
G1-2	90	488	81	407	0.60	2029550+
G1-3	89	560	80	480	0.70	1279610
G1-4	88	653	82	571	0.82	316320
G1-5	88	709	79	630	0.89	2020
G1-6	91	545	84	641	0.69	2009760+
G1-10	134	498	77	430	0.66	2013000+
G1-11	136	462	77	394	0.62	2011970+

+ - No failure
f_r - Average Modulus of rupture of three to four specimens tested at 28 days

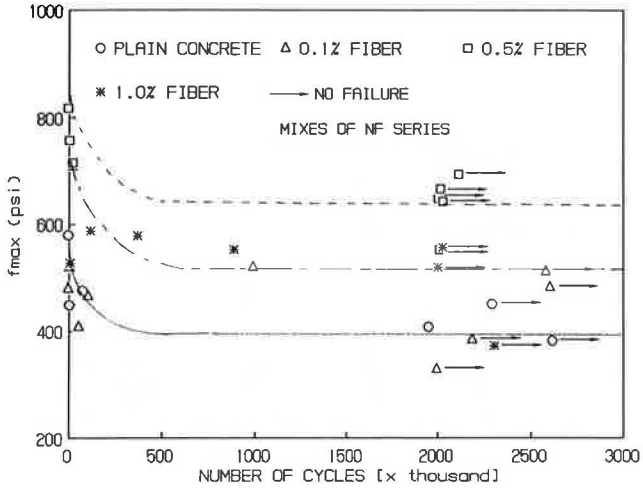

FIGURE 5 Fatigue stress versus number of cycles.

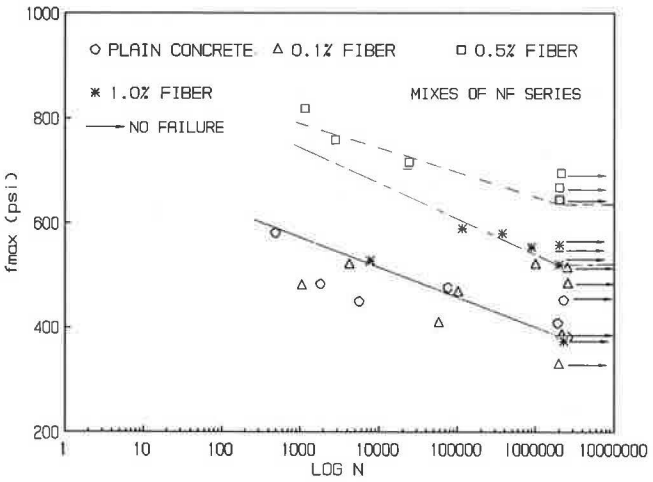

FIGURE 7 Fatigue stress versus log of number of cycles.

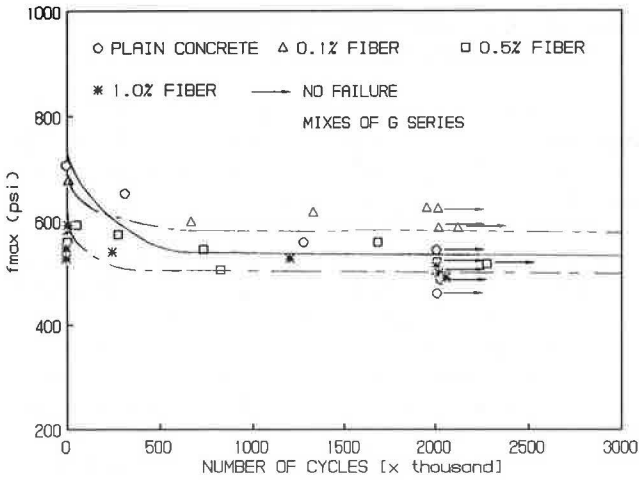

FIGURE 6 Fatigue stress versus number of cycles.

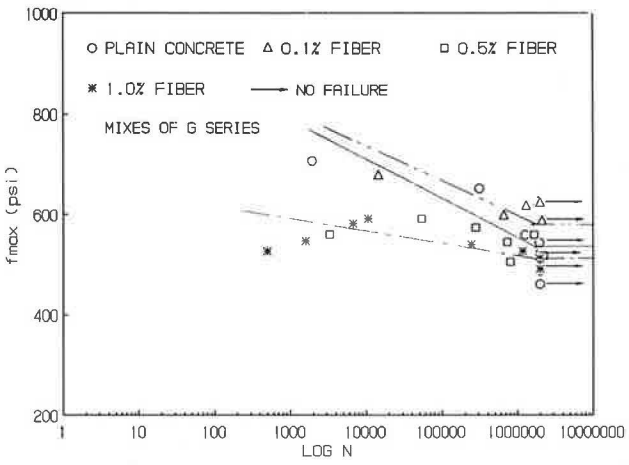

FIGURE 8 Fatigue stress versus log of number of cycles.

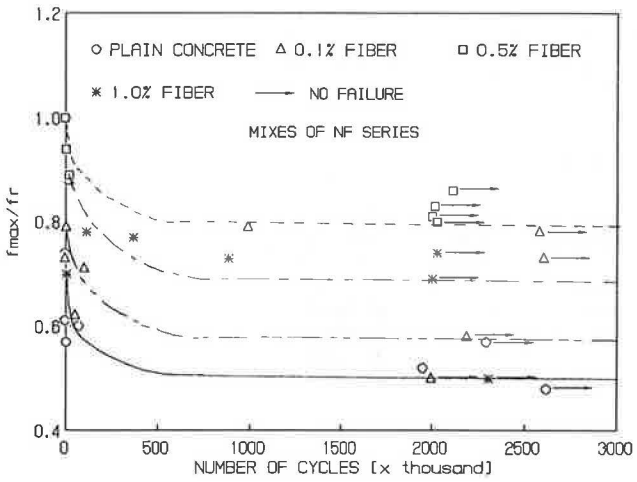

FIGURE 9 Number of cycles versus ratio of fatigue stress and flexural stress.

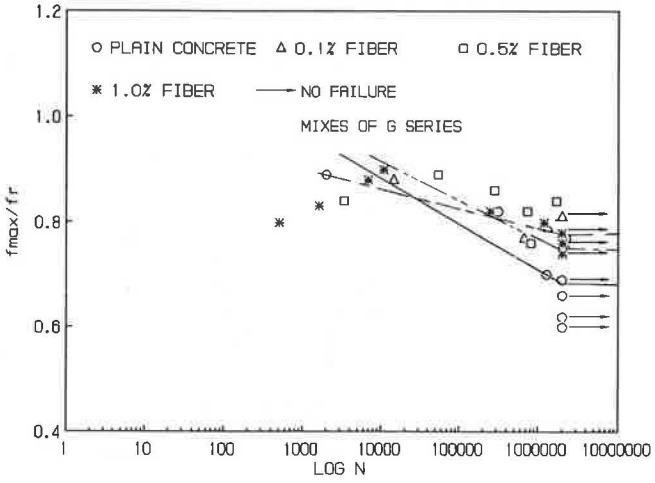

FIGURE 12 Log of number of cycles versus ratio of fatigue stress and flexural stress.

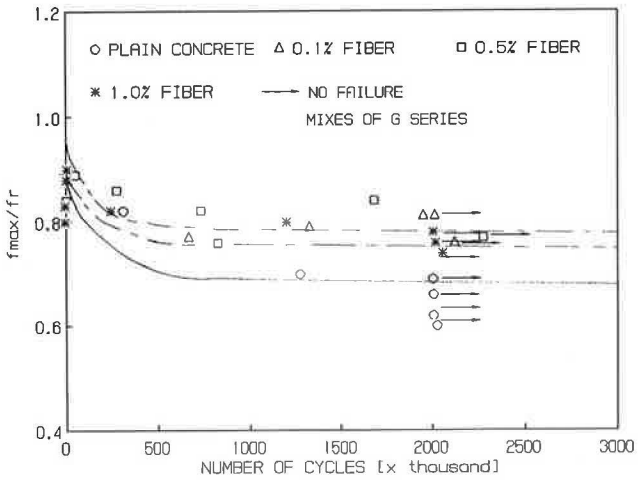

FIGURE 10 Number of cycles versus ratio of fatigue stress and flexural stress.

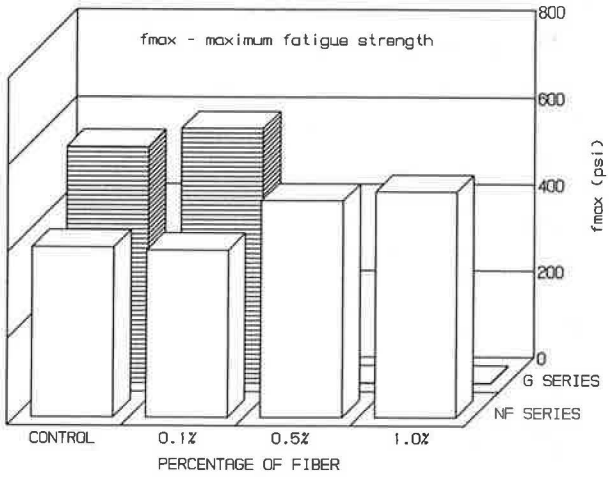

FIGURE 13 Fatigue strength bar chart.

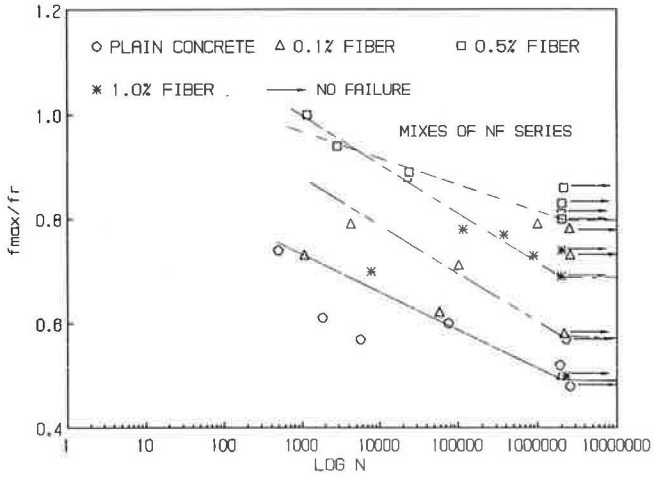

FIGURE 11 Log of number of cycles versus ratio of fatigue stress and flexural stress.

Endurance Limit Expressed as a Percentage of Modulus of Rupture of Plain Concrete

The endurance limit is defined as the maximum fatigue flexural stress at which the beam can withstand 2,000,000 cycles of nonreversed fatigue loading, expressed as a percentage of modulus of rupture of plain concrete.

Figure 14 indicates that, for the beams with 0.5 percent fiber content, the endurance limit increases when expressed as a percentage of modulus of rupture of plain concrete. In the mix with 0.5 percent fiber content in the NF series, the endurance limit was 63 percent when expressed as a percentage of modulus of rupture of plain concrete; it was 59 percent when expressed as a percentage of its modulus of rupture. However, in the NF series for the mixes with 0.1 percent fiber contents, the endurance limit expressed as a percentage of modulus of rupture of plain concrete was lower than that expressed as a percentage of its modulus of rupture.

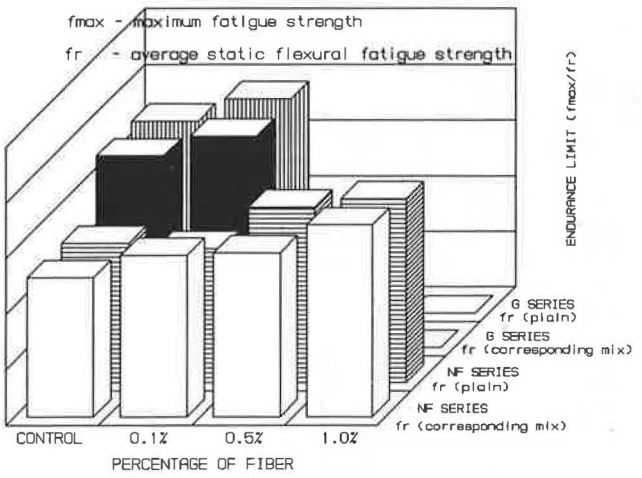

FIGURE 14 Endurance limit bar chart.

This is due to the lower compressive strength in these mixes compared with those of plain concrete. For the G series mixtures, the endurance limit expressed as a percentage of modulus of rupture of plain concrete was higher than that expressed as a percentage of its modulus of rupture.

Endurance Limit Expressed as a Percentage of Its Modulus of Rupture

The endurance limit of concrete can also be defined as the fatigue stress at which the beam can withstand 2,000,000 cycles of nonreversed fatigue loading, expressed as a percentage of its modulus of rupture.

The endurance limits for the mixes with 0.1 percent, 0.5 percent, and 1.0 percent fiber contents were 58 percent, 59 percent, and 69 percent, respectively. It was 50 percent for plain concrete, thus showing an improvement in the fatigue performance of FRC. Similarly, in the G series, the endurance limit increased with increases in fiber content. The endurance limit bar charts are shown in Figure 14.

Graphs of the ratio of fatigue flexural stress to modulus of rupture (f_{max}/f_r) versus the number of cycles are shown for all the mixes in Figures 9 and 10. The relationship is curvilinear until the fatigue strength of that particular mix is reached, then the line becomes parallel to the x-axis. Graphs were also drawn for f_{max}/f_r versus the logarithm of number of cycles for all the mixes (Figures 11 and 12). In this case, the relationship is linear.

The specimens that did not fail after more than 2,000,000 cycles in the flexural fatigue test were tested again in the static flexural test to determine if microcracks had developed or strength degradation had occurred in concrete because of the fatigue test at a fatigue loading below the endurance limit. The test results are shown in Table 6. The 2 million cycle fatigue loading below the endurance limit did not lead to a decrease in flexural strength. In most cases, the flexural strength increased slightly, especially when the fatigue stress to which the specimen was subjected earlier was lower.

The considerable amount of apparent scatter in the test results can be attributed to time factors. Fatigue tests take a long time. The ages at which different specimens of the same mix were tested vary considerably; this age difference influenced the test results. The static flexure test was performed at 28 days, while the fatigue tests were performed at much later ages. Therefore, the ratio f_{max}/f_r, and hence the endurance limit, is not consistent. The endurance limit was determined by using the above referred factors.

Based on the test results, the addition of fibrillated polypropylene fiber improved the concrete's ability to withstand dynamic and fatigue loads. A significant advantage of polypropylene fiber under dynamic loads is its relatively low elastic modulus at slow rates of loading, which increases substantially because the effect of time-dependent viscoelastic behavior is eliminated. The polypropylene fiber reinforcement contributed to the improvement of fatigue strength of concrete.

CONCLUSIONS

Conclusions from the research are as follows:

- The addition of 0.5 and 1.0 percent by volume of fibrillated polypropylene fibers significantly improved the fatigue strength.
- The endurance limit (for 2,000,000 cycles) was considerably increased with the addition of fibrillated polypropylene fibers, which, when applied to pavement slabs, would substantially extend the service life of highways.
- The static flexural strength of the fiber concrete beams increased after the beams were subjected to fatigue loading.
- The toughness index values increased with increases in fiber contents. All concrete specimens reinforced with fibrillated polypropylene fibers exhibited an improved ductile behavior when compared with plain concrete.
- The concrete incorporating fibrillated polypropylene fiber had excellent impact resistance. The impact resistance increased with an increase in fiber content.
- The fiber reinforcement had no appreciable effect on the flexural strength when the same mix proportions for different quantities of fibers were used. However, when the fiber factor adjustment is made, the flexural strength may increase with increased fiber content. More research is needed to optimize fiber performance at higher fiber volumes.
- The fiber content in the concrete mix had no appreciable effect on the pulse velocity.
- The addition of fibrillated polypropylene fibers had no significant influence on the static modulus of concrete.
- Good workability can be maintained in polypropylene FRC by adding an appropriate quantity of superplasticizer. No balling or tangling of fibers occurred during mixing and placing even for concretes with 1 percent by volume of polypropylene fibers.
- When using high volumes (0.5 percent and 1.0 percent) of fibrillated polypropylene fibers, fiber factor adjustments are necessary for the mix proportions to balance the mix for workability, placeability, appearance, and strength.

TABLE 6 STATIC FLEXURAL TEST AFTER FATIGUE

SP. #	AGE	f_{max} / f_r	MAXIMUM STRESS IN FATIGUE	FLEXURE STRESS BEFORE FATIGUE	FLEXURE STRESS AFTER FATIGUE	IN PERCENT
	(DAYS)		f_{max} (psi)	f_r (psi)	(MOR) (psi)	
(1)	(2)	(3)	(4)	(5)	(6)	(6)-(5)
NP4-6	119	0.57	453	790	925	17.08
NP4-8	46	0.48	383	790	730	-7.59
NF1-4	93	0.58	386	660	910	37.88
NF1-7	93	0.73	483	660	885	34.09
NF1-8	93	0.78	513	660	880	33.33
NF1-9	49	0.50	330	660	575	-12.88
NF7-4	174	0.84	749	890	1065	19.66
NF7-7	174	0.74	659	890	1045	17.42
NF7-9	174	0.73	648	890	995	11.80
NF3-5	91	0.63	532	845	945	11.83
NF3-7	47	0.55	462	845	680	-19.53
NF3-8	47	0.48	405	845	740	-12.43
NF5-6	89	0.81	650	810	925	14.20
NF5-7	89	0.83	668	810	910	12.35
NF5-10	89	0.80	644	810	990	22.22
NF5-12	89	0.69	554	810	895	10.49
NF5-13	89	0.86	696	810	910	12.35
NF2-5	48	0.50	375	755	815	7.95
NF2-8	92	0.69	521	755	985	30.46
NF2-10	92	0.74	559	755	905	19.87
NF6-6	89	0.80	558	700	875	25.00
NF6-7	89	0.78	548	700	885	26.43
NF6-10	89	0.86	604	700	850	21.43
NF6-11	89	0.80	560	700	835	19.29
NF6-13	181	0.83	578	700	770	10.00
G1-2	180	0.60	488	760	990	30.26
G1-6	180	0.69	545	760	715	-5.92
G1-10	180	0.66	498	760	850	11.84
G1-11	180	0.62	462	760	690	-9.21
G2-1	180	0.81	624	780	890	14.10
G2-4	180	0.76	587	780	945	21.15
G2-11	180	0.76	587	780	905	16.03
G3B-1	180	0.78	514	660	715	8.33
G3B-3	180	0.76	501	660	605	-8.33
G3B-6	180	0.74	491	660	650	-1.52
G4-5	180	0.77	518	670	750	11.94
G4-6	180	0.78	521	670	720	7.46
G5-2	174	0.82	636	775	920	18.71
G5-4	174	0.86	670	775	860	10.97
G5-5	174	0.88	686	775	840	8.39

REFERENCES

1. V. Ramakrishnan. Materials and Properties of Fiber Reinforced Concrete. *Proc., International Symposium on Fiber Reinforced Concrete*, Madras, India, 1987.
2. V. Ramakrishnan, G. Oberling, and P. Tatnall. Flexural Fatigue Strength of Steel Fiber Reinforced Concrete. In *Report SP-105: Fiber Reinforced Concrete—Properties and Applications*, American Concrete Institute, Detroit, Mich., 1987, pp. 225–245.
3. V. Ramakrishnan, W. V. Coyle, V. Kulandaisamy, and E. K. Schrader. Performance Characteristics of Fiber Reinforced Concretes With Low Fiber Contents. In *ACI Journal Proceedings*, Vol. 78, No. 5, 1981, pp. 384–394.
4. V. Ramakrishnan and C. Josifek. Performance Characteristics and Flexural Fatigue of Concrete Steel Fiber Composites. *Proc., International Symposium on Fiber Reinforced Concrete*, Madras, India, 1987, pp. 2.73–2.84.
5. V. Ramakrishnan, S. Gollapudi, and R. Zellers. Performance Characteristics and Fatigue Strength of Polypropylene Fiber Reinforced Concrete. In *Report SP-105: Fiber Reinforced Concrete—Properties and Applications*, American Concrete Institute, Detroit, Mich., 1987, pp. 159–177.
6. ACI Committee 544. *Measurement of Properties of Fiber Reinforced Concrete*. Report 544 2R-78. American Concrete Institute, Detroit, Mich., 1978.
7. *Recommended Practice for Evaluation of Strength Test Results of Concrete*. Report 214-77. American Concrete Institute, Detroit, Mich., 1977.
8. G. Hosali. Properties of Steel Fiber Reinforced Concrete and Effects of Different Fiber Volume. M.S. thesis. South Dakota School of Mines & Technology, 1988.

Field Evaluation of Steel Fiber Reinforced Concrete Overlay With Various Bonding Mechanisms

G. CHANVILLARD, P.-C. AÏTCIN, AND C. LUPIEN

An experimental rehabilitation project was conducted on the Transcanadian Highway where old concrete pavement was recovered with a thin, steel fiber reinforced concrete overlay (*1*). In this project, 18 different construction conditions were investigated. The surface of the old pavement was either sandblasted or scarified. Three different types of steel fibers were used, and all the overlay was bonded with a thin cement grout. In addition, two lanes were repaired with some mechanical bonding provided by 37.5-mm (1½-in.) steel nails. The most significant results obtained during the construction period as well as all data recorded over the succeeding two winters are reported and analyzed in this paper.

Progressive degradation of the highway system necessitates greater attention to rehabilitation techniques. One alternative for concrete pavements is to cover the old pavement with a thin concrete overlay, although this approach is not always successful. Only well-bonded concrete overlays give satisfactory results and can increase both the surface quality and bearing capacity of the pavement, which results in thicker, monolithic pavement (*2*).

This rehabilitation method has been used in many projects, but not always with the expected results (*3*). Two major problems are faced in the field when this method is used. On the one hand, a good bond between the old and new concrete must be developed to avoid any delamination at their inteface, which will cause general debonding of the overlay. The other important aspect is to use compatible concretes so they behave monolithically in spite of differential shrinkage behavior, differential thermal dilation characteristics, and cracking problems. In this context, fiber reinforced concrete, due to its improved fatigue and toughness characteristics, should be particularly suitable for the rehabilitation of old concrete pavements with thin bonded concrete overlays.

Several successful experiments with high fiber content (greater than 1 percent by volume, i.e., 80 kg/m³ or 130 lb/yd³) have previously been reported (*3–5*), so it is possible to foresee a rational use of this technique for old concrete pavement rehabilitation. However, none of these experiments was done in climatic conditions similar to those in the Montréal area, which is characterized by temperature spreads of −40°C to +40°C (−40°F to +100°F), repeated freeze-thaw cycles, and extensive use of deicing salts.

The introduction of 1 percent or more by volume of steel fiber in the concrete presents two major disadvantages. First, it doubles the cost of the concrete; second, it makes the concrete very difficult to place. Overcoming these drawbacks means decreasing the amount of fiber added to the overlay concrete. This approach was adopted in the experiment reported in this paper: the maximum fiber content was limited to 0.44 percent by volume (34 kg/m³ or 58 lb/yd³).

Department of Civil Engineering, Université de Sherbrooke, Québec J1K 2R1.

LOCATION AND FIELD CONDITIONS

The experiment took place in late October 1986 on a section of Autoroute 40 in West Montréal, where the average traffic is 30,000 vehicles per day. In that location, the actual condition of the old concrete pavement was still quite good, and a thin overlay was the only rehabilitation work required. Some damaged areas were first repaired to the full depth of the pavement, and the entire crack network was carefully recorded before the thin overlay was placed.

The originality of this experiment lies in the mechanical bonding of the old pavement and the new overlay with concrete nails partially embedded in the old pavement and in the use of less than 0.5 percent steel fiber content to enhance the mechanical properties of the overlay concrete.

The experiment took place in cold weather, with temperatures reaching freezing almost every night, in what could be considered the worst possible conditions for this kind of job.

Eighteen different field conditions were tested. They were divided into three main catagories:

1. *Surface preparation.* The existing concrete slabs were either scarified with a diamond saw or sandblasted.
2. *Mechanical bonding.* Some of the experimental slabs were bonded to the old pavement with concrete nails driven on 300 or 450 mm (1 ft or 1½ ft) centers. The nails were 37.5 mm (1½ in) long and were driven halfway into the old pavement.
3. *Steel fibers.* Three different brands of steel fibers were used at volumetric contents of 0.28 percent and 0.44 percent, i.e., 22 and 34 kg/m³ (37 and 58 lb/yd³). Some experimental slabs were made solely of plain concrete.

The part of the overlay with steel fiber reinforced concrete was 75 mm (3 in.) thick, while the part with plain concrete was 100 mm (4 in.) thick.

Figure 1 shows the locations of the different experimental conditions.

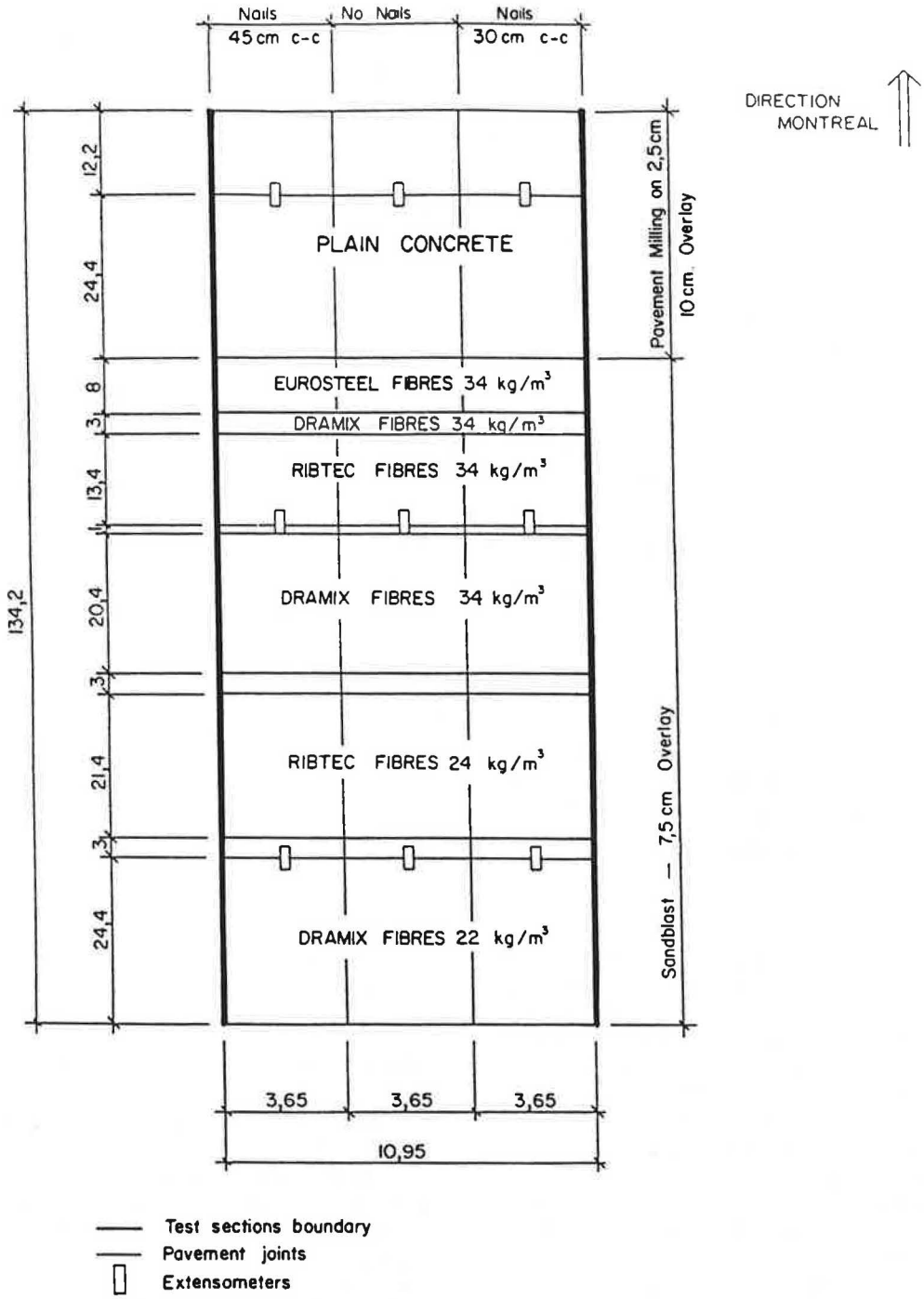

FIGURE 1 Plan view of the test sections (length in meters).

CHARACTERISTICS OF THE FRESH CONCRETE

To avoid the main drawbacks that can be encountered in making fiber reinforced concrete, basic design rules governing the formulation of such concretes were followed. These require that the cement content be higher than that of normal concrete, the maximum size of the coarse aggregate be reduced to no more than half the length of the fibers (in fact, 20 mm or ¾ in.), and the volume of the fine aggregate be increased to match that of the coarse aggregate. The plain and fiber reinforced concrete compositions are given in Table 1. The fibers were introduced manually at the concrete plant, directly on top of the aggregate on the conveyor leading to the central mixer.

In this project, the three different brands of steel fibers used were Dramix, Eurosteel, and Xorex. Their main characteristics are given in Table 2.

These fibers do not perform well in matrixes with a very low water/cement ratio because the bonding that develops is too strong (*6*). Chanvillard (*1*) has shown that the critical water/cement ratio is between 0.30 and 0.40 for the type of

TABLE 1 COMPOSITION OF CONCRETE MIXES

		Concrete composition			
		kg/m³		lb./cu.yd.	
		Fibres	No fibres	Fibres	No fibres
Cement		420		706	
Water		160		269	
Sand		850	720	1430	1210
Coarse aggregate	10 mm	650	210	1100	350
	14-20 mm	216	830	360	1400
	Total	866	1040	1460	1750
Air-entraining admixture		0.5 L/m³		1.9 oz/100 lb of cement	
Unit weight		2296	2340	3865	3935
W/C ratio		0.38		0.38	

fibers used in this project. Consequently, the selected water/cement ratio was 0.38. Moreover, in spite of the fiber content used (0.28 percent and 0.44 percent), it was hoped that the post-fissuration behavior would correspond to a fiber pull-out from the matrix and not a failure of the fibers. This pull-out should be favored by the incorporation of 6 percent air entrained in the mix, reducing the anchorage of the fiber.

To facilitate the placing of the concrete and to have a freeze-thaw resistant overlay, the selected slump was 60 mm (2½ in.) and the air content was 5 to 7 percent. If, at the job site, the delivered concrete did not have a high enough slump or entrained-air content, superplasticizer and air-entraining admixture were added until the designated values were obtained.

The concrete was transported to the job site within 30 to 45 min in transit mixer trucks.

The overlay concrete was placed by a GOMACO C650.5 finishing machine equipped with slip forms. This machine has an auger that levels the concrete and a vibrating cylinder that oscillates laterally to consolidate the concrete and finish the overlay surface.

Initially, the overlay surface was to be burlap textured, but it rapidly became evident that the burlap was partially lifting the fibers located near the surface, requiring extensive manual correction. After the second load of concrete, the surface was no longer textured. Curing compound was spread over the overlay surface 10 to 15 min after placing to prevent drying during hydration. The concrete was completely covered with insulating blankets at night for protection against the freezing temperatures.

Field Controls

The fiber content homogeneity was checked carefully in each truck at the beginning, middle, and end of unloading by washing a weighed amount (about 5 kg or 10 lb) of fresh concrete in a 5-mm sieve (No. 4 ASTM) and extracting the fibers with a magnet. This demonstrated that the selected method for adding the fibers to the mix provided fairly good results (see Table 3).

To monitor slump loss, the slump was measured at four stages for each load using an ASTM C143 standard cone (see Figure 2). An average slump loss of 40 mm (1½ in.) was observed after transport to the job site.

Field Observations

Superplasticizer was added at the job site to correct the slump. This provided unequal workability throughout the concrete load, particularly the top of the load. The more the slump deviated from the recommended level, the harder it was to correct. Increasing the slump of a full load of fiber reinforced concrete in the field presented difficulties.

When the trucks were half unloaded, concrete workability

TABLE 2 CHARACTERISTICS OF FIBERS

	unit	DRAMIX ZP 50/.50	XOREX RIBTEC 2" (50 mm)	EUROSTEEL 60/1.00
Length	mm	50	53.5	60
Diameter	mm	0.50	1.44	1.00
Section		circular	semi-circular	circular
Equiv. dia.	mm	0.50	0.96	1.00
L/d ratio		100	55.7	60
Density *	kg/m^3	7850	7850	7850
Number of fibres/kg**		12800	3300	2700
Shape		hooked ends	crimped	crimped

* 1 lb/cu.ft. = 0.624 kg/m^3

** No/lb = 0.45 No./kg

1 inch = 25.4 mm

TABLE 3 FIBER-CONTENT HOMOGENEITY

Truck Number	Fibre-Content at different Unloading period (%)			Theorical Content	
	Beginning	Half period	End	%	(kg/m^3)
1	0.28	0.25	0.29	0.28	22
2	0.33	0.23	0.27	0.28	22
3	0.25	0.35	0.29	0.30	24
4	0.42	0.43	0.45	0.44	34
5	0.40	0.41	0.46	0.44	34
6	0.38	0.45	0.44	0.44	34

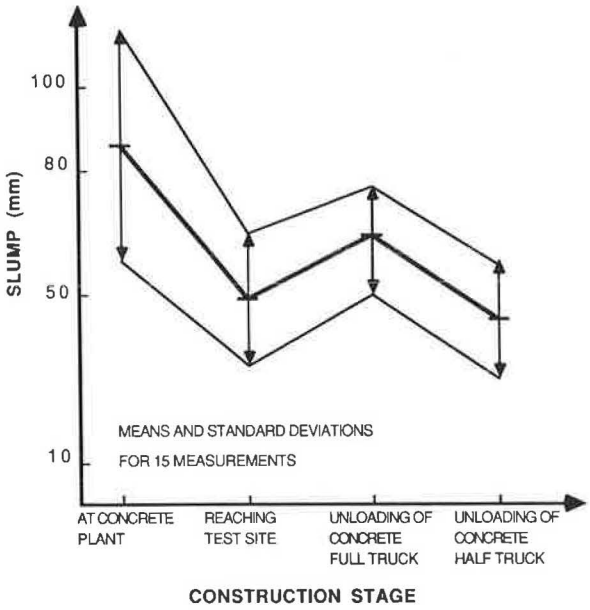

FIGURE 2 Slump versus construction stage.

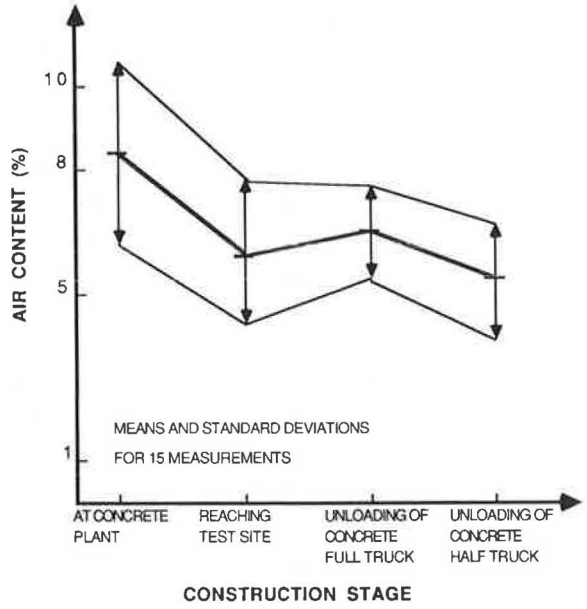

FIGURE 3 Entrained air versus construction stage.

was checked using the inverted cone slump test (ASTM C995). When the percentage of entrained air was increased, the measured flow time decreased. Thus, air content plays a key role in the workability of fiber reinforced concrete.

If workability is checked by the standard cone method, it is preferable to adjust the slump at the plant to between 100 and 150 mm (depending on the travel duration) to avoid the problems posed by field adjustment. However, if workability is checked with the inverted cone flow, this research indicates that the flow time should be about 5 sec with an air content of 5 to 7 percent.

Air content, like slump, was checked at different stages. The total air content was found to decrease by 2 to 2.5 percent during transportation (see Figure 3). When the air content was low, an air-entraining admixture was directly added to the load, followed by 3 min of mixing. It was observed that the concrete unloaded immediately after this redosing had generated an increased air content. However, the air content of the middle of the load was often lower than the first air content reading.

As with slump, correcting the air content of a full load of fiber reinforced concrete in the field proved very difficult. However, it is not difficult to entrain air at a ready-mix plant. Therefore, the air-entraining admixture dosage should be adjusted in a couple of trial batches at the plant to avoid the need for correction at the job site.

CHARACTERISTICS OF HARDENED CONCRETE

Concrete specimens were tested for compression and flexure. While a knowledge of concrete compressive strength is not fundamentally important for pavement application, it does reflect the overall quality of the concrete.

For the selected water/cement ratio of 0.38 and an average air content of 6 percent, the tested concrete had a compressive strength of approximately 60 MPa (8,700 psi), irrespective of

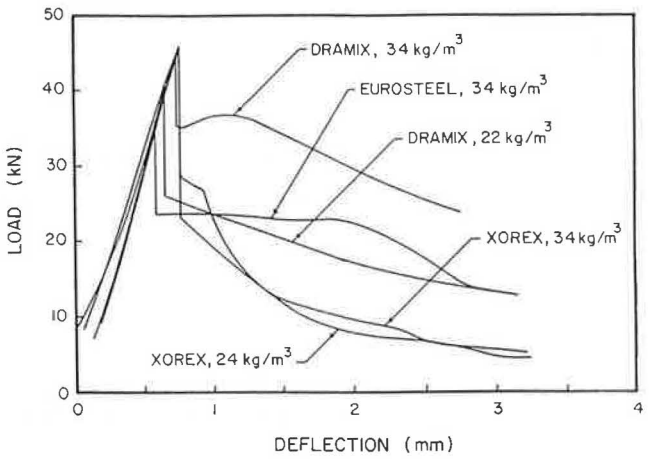

FIGURE 4 Load versus deflection for different concretes.

fiber content. These steel fibers had a more pronounced effect on the flexural strength of concrete. This effect was tested on 150 mm × 150 mm × 500 mm (6 in. × 6 in. × 20 in.) specimens submitted to flexural tests at a constant rate of strain.

As seen in Figure 4, the cracking of the matrix corresponds to the drop in the load that can be withstood by the specimen. The observed drop is mainly due to the low contents used in this field application (0.28 and 0.44 percent by volume). The cracking point corresponds to the maximum load the concrete sample can withstand (between 36 kN and 46 kN), representing its modulus of rupture. In this project, the average was 5 MPa (725 psi), with a range of about 4.6 to 5.9 MPa (674 to 862 psi).

The load curves in Figure 4 show that the presence of fibers allows a quasi-ductile failure of the concrete specimens and that additional energy is necessary to open up a crack, even at these low fiber contents. This behavior is particularly interesting for pavement applications where a dual loading mode can be observed. First, traffic along a road develops a given

load on the pavement; consequently, the modulus of rupture of concrete is an important factor in designing concrete pavements. Second, moisture and temperature variations cause volumetric changes in the concrete that create internal stresses. When a pavement is cracking, the presence of fibers produces a residual load in the concrete, which limits the crack from opening further. Volumetric changes are also less harmful.

In conclusion, concrete with a high modulus of rupture is useful because it allows high loadings but is of no use after cracking. Quasi-ductile behavior allows a continuous load transfer across the cracks and maintains the pavement integrity.

BEHAVIOR OF SLABS IN THE FIELD

The crack network was observed periodically. Fine transversal microcracks were noticed a few weeks after the construction of the overlay, some of which propagated quite rapidly. The network of cracks at different ages is presented in Figures 5 through 7. They have been characterized in terms of length of cracks by length of overlay (both in meters) as a function of the number of months after construction.

After 13 months of service, two types of cracks were observed:

1. Very fine cracks that remained nearly closed. These cracks are difficult to see when the pavement is dry and hot but are readily visible in cold, humid weather.
2. Wider, constantly visible cracks that appeared very clear and seemed to be deeper than the first type.

Influence of Mechanical Bonding

Figure 5 illustrates the cracking behavior of slabs made with plain concrete (without fibers) according to different bonding conditions. The overall performance of these slabs was very poor.

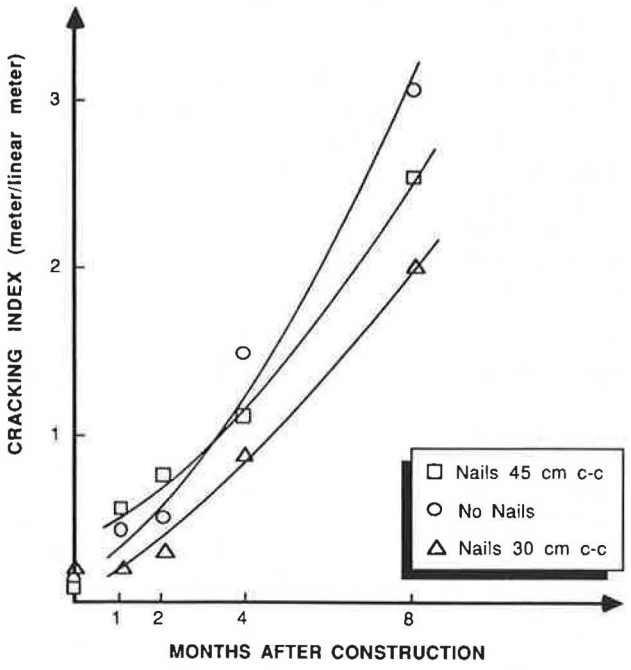

FIGURE 5 Development of cracking index for plain concrete.

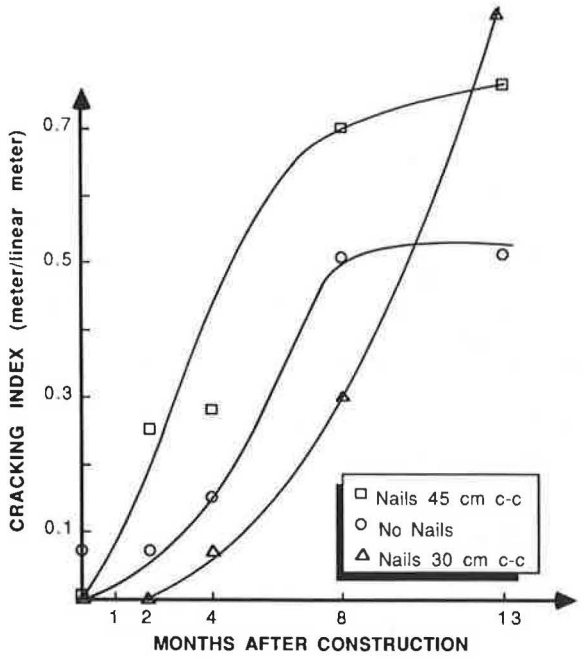

FIGURE 6 Cracking index versus time for steel fiber reinforced concrete (22 kg/m³).

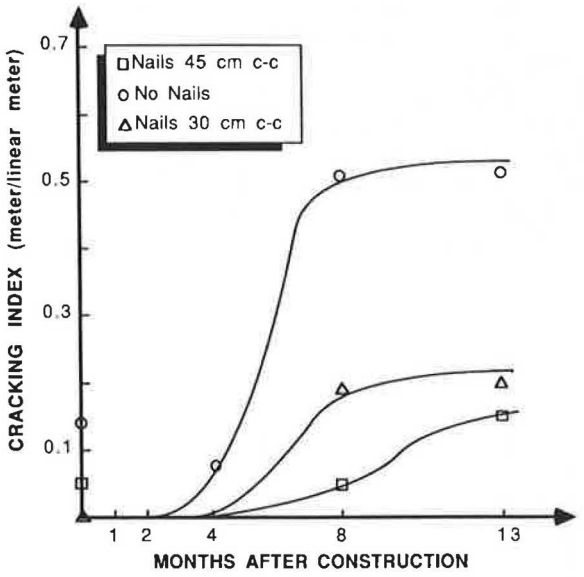

FIGURE 7 Cracking index versus time for steel fiber reinforced concrete (34 kg/m³).

In Figures 6 and 7, the cracking index of the experimental slabs built with the various fiber reinforced concrete mixes (fiber contents of 22 and 34 kg/m³) is presented. In general, the degree of cracking was much smaller than with the plain concrete, so the influence of the nails used to anchor the overlay to the old pavement is less evident. In the concrete with the higher fiber content, however, there was less cracking in the slabs with nails than in those without (see Figure 7).

Influence of Fiber Content

In Figure 8, the average level of cracking for all the experimental slabs is presented. A comparison of the three corresponding curves indicates the beneficial influence of the fibers on the control of the crack growth.

The network of cracks developed rapidly during the first few months. After 8 months, these cracks were almost stabilized in the fiber reinforced concrete but continued to develop in the conventional concrete.

The nonreinforced part of the overlay rapidly showed a number of signs of distress, which resulted in debonding. This portion had to be replaced by an asphalt patch after only 18 months of service, which confirms the difficulty in obtaining a good level of performance with a conventional concrete in severe climatic and traffic conditions.

Overlay Bonding

To check the level of bonding between the old pavement and the overlay, full-depth core samples with a diameter of 100 mm (4 in) were taken through the overlay and the pavement at different locations, particularly where cracks were observed. It was impossible to recover a complete core where the overlay was made of conventional concrete. In all cases, the core broke at the interface between the old pavement and the overlay. This behavior demonstrates that the bond was unable to resist the shear stresses resulting from the strains induced in the overlay.

In the case of the cores drilled in the fiber-reinforced part of the overlay, the bonding between the old pavement and the new overlay was so good that the cores never exhibited interface failure when they were extracted from the pavement (see Figure 9), even when a cracked area was cored. Moreover, the different cores taken after 18 months of service

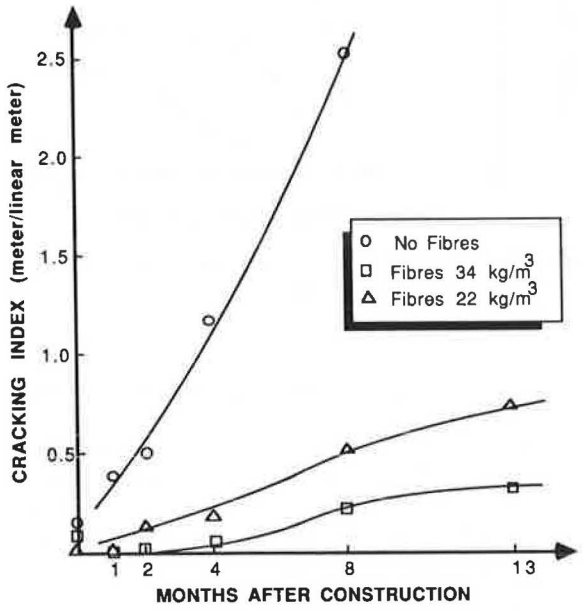

FIGURE 8 Development of cracking index versus concrete type.

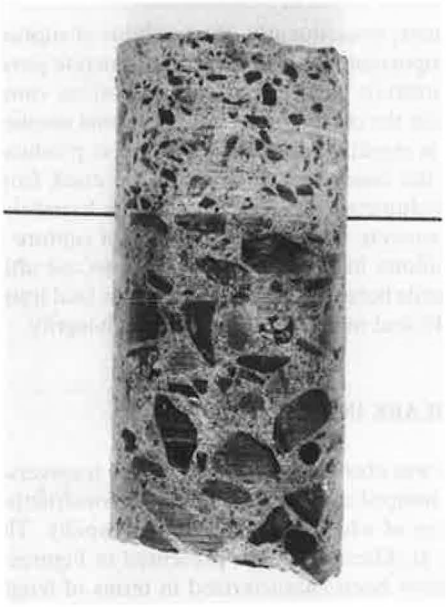

FIGURE 9 Core sample showing good bonding between concrete layers.

clearly revealed the different nature of the two types of cracks that were observed in the overlay's surface.

Cracks almost always occurred over existing cracks in the old pavement. However, these reflected cracks never resulted in interface delamination. This was apparently due to the presence of fibers in the overlay, since the fibers allow good load transfer across the cracks (see Figure 10).

The finer cracks were only superficial—no more than 40 mm (1½ in.) deep. In this case, the presence of fibers apparently inhibited crack propagation (see Figure 11). It is believed that these cracks were either due to the differential shrinkage between the new overlay and the old concrete or were of thermal origin.

The positive impact of the fibers is clearly evidenced in all core samples. The presence of the steel fibers in these overlays inhibited crack propagation and reduced the intensity of the shear stress along the interface, thereby preventing delamination.

It can be concluded that the presence of fibers in the overlay contributed significantly to the monolithic behavior of the old pavement/overlay system.

DISCUSSION OF OVERLAY BEHAVIOR

Cracks appeared quite rapidly after the construction of the overlay but were almost stabilized after 8 months of service in the fiber reinforced sections. These cracks were transversal and very fine. The development of microcracks can be explained by thermal stresses as well as by concrete shrinkage, both of which create differential movement between the old concrete pavement and the new overlay.

This early appearance of cracks has been observed in similar projects. Bagate et al. (*7*) and Betterton et al. (*8*) reported similar behavior with thin fiber reinforced concrete overlays. Domenichini (*9*) demonstrated that a temperature difference

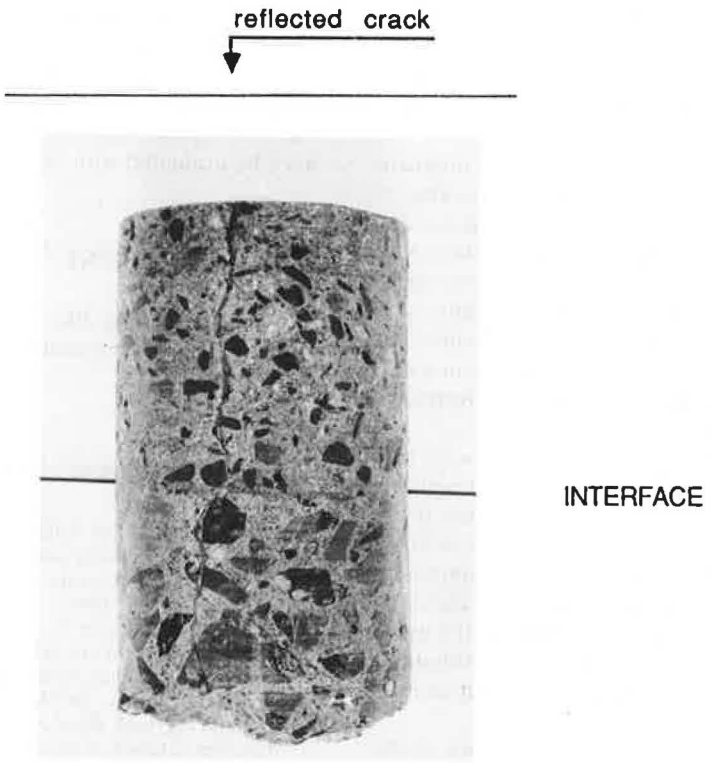

FIGURE 10 Core sample showing reflection cracking but good bonding between concrete layers.

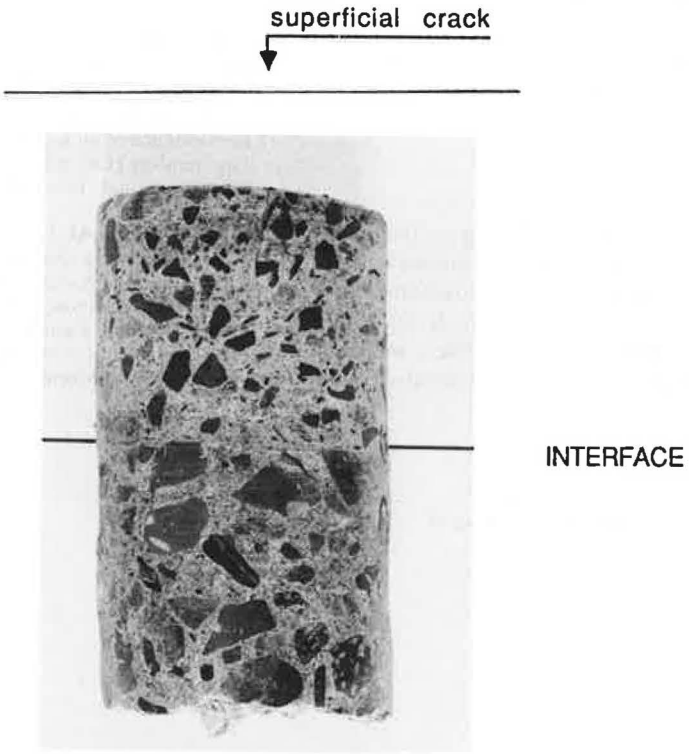

FIGURE 11 Core sample showing good bonding and a small thermal or shrinkage cracking at surface.

of 6°C (11°F) through the thickness of a 75-mm (3-in.) overlay, combined with shrinkage stress, can result in major shear stresses at the old pavement/new overlay interface. This is why a reduction in the overlay thickness can quite rapidly result in the formation of some cracks.

The cracks observed in the overlay surface can originate from the reflection of existing cracks in the old pavement. This phenomenon cannot be avoided with monolithic overlay when dealing with transversal cracks (*2, 3*). This explains why the use of thin overlays is not easy. These weaknesses appear soon after overlay costruction and propagate so rapidly, due to fatigue, that the overlay is often ruined by delamination at the interface. The experiment reported by Betterton et al. (*8*) in Iowa, however, shows that satisfactory performance after 10 years of service is possible.

In the research described in this paper, the cracks that appeared during the first 6 months stayed almost closed and did not grow. Therefore, the beneficial action of the fibers cannot be contested in this experiment. The presence of fibers that bridge the two edges of the cracks results in a continuity of the overlay, permitting some load transfer across the crack and, above all, limiting its growth. While reducing the width of the cracks, fibers provide better shear-stress distribution, resulting in a better bond between the old pavement and the new overlay.

As discussed earlier, it is believed that satisfactory results can be obtained at a fiber content of 0.5 percent by volume (40 kg/m^3).

Finally, very harsh climatic conditions such as those in Québec, where the temperature of the overlay can vary from −40°C to +40°C, the durability of the fibers needs to be established due to frequent deicing salt applications. Since the cracks are widest in winter, the bridging fibers are more extensively exposed to corrosive attack.

CONCLUSION

The use of a thin, bonded fiber reinforced concrete overlay to rehabilitate old concrete pavements yielded encouraging results. Due to the various field conditions encountered, it was possible to establish the main influence of the fibers and their content in the overlay. The presence of fibers in the overlay stabilized the development of the transversal crack network, resulting in more monolithic behavior between the old pavement and the overlay. The use of concrete nails to achieve a mechanical bond between the overlay and the old pavement did not produce conclusive results. The possible corrosion of the steel fibers bridging the crack by deicing salt must be evaluated with time.

ACKNOWLEDGMENT

The authors would like to thank the Québec Provincial Department of Transporation for financial support in this field experiment.

REFERENCES

1. G. Chanvillard. Les bétons renforcés par de faibles dosages de fibre d'acier: propriétés mécaniques, utilisation comme matériaux de resurfaçage. *Mémoire de maîtrise.* Université de Sherbrooke, Québec, Canada, 1988.
2. G. F. Voigt, M. I. Darter, and S. H. Carpenter. Field Performance of Bonded Concrete Overlays. In *Transportation Research Record 1110*, TRB, National Research Council, Washington, D.C., 1987.
3. R. L. Hutchinson. *NCHRP Synthesis of Highway Practice 99: Resurfacing with Portland Cement Concrete*. TRB, National Research Council, Washington, D.C., Dec. 1982.
4. G. C. Hoff. Steel Fibre-Reinforced Concrete Pavements and Overlays. In *Report SCM-10(85): Design With Fibre-Reinforced Concrete*, American Concrete Institute, 1985.
5. C. D. Johnston. Steel Fibre-Reinforced Concrete-Present and Future in Engineering Construction. *Composites*, April 1982, pp. 113–121.
6. R. J. Gray and D. Johnston. The Effect of Matrix Composition on Fibre/Matrix Interfacial Bond Shear Strength in Fibre-Reinforced Mortar. *Cement and Concrete Research*, Vol. 14, No. 2, March 1984, pp. 285–296.
7. M. Bagate, B. F. McCullough and D. Fowler. Construction and Performance of an Experimental Thin-Bonded Concrete Overlay Pavement in Houston. In *Transportation Research Record 1040*, TRB, National Research Council, Washington, D.C., 1985, pp. 25–33.
8. R. M. Betterton, M. J. Knutson and V. J. Marks. Fibrous Portland Cement Concrete Overlay Research in Green County, Iowa. In *Transportation Research Record 1040*, TRB, National Research Council, Washington, D.C., 1985, pp. 1–7.
9. L. Domenichini. Factors Affecting Adhesion of Bonded Concrete Overlays. *Record 1, Workshop on Theoretical Design of Concrete Pavements* (Abridgement), Epen, The Netherlands, June 1986.

Natural Fiber Reinforced Concrete

R. SETHUNARAYANAN, S. CHOCKALINGAM, AND R. RAMANATHAN

In recent years, several investigations have been reported on the strength and behavior of concrete reinforced with natural fibers. Since natural fibers are available in abundant quantities in many developing countries, more elaborate research should be directed toward the various problems associated with the use of these fibers. This paper presents a critical review of the factors that affect the properties and behavior of natural fiber reinforced concrete (NFRC). Test results for concretes obtained by using water blended with yeast granules are also reported in this paper.

During the past two decades, there has been considerable interest in the study of fiber reinforced concrete and its applications to several types of structures. Most of the studies have been concerned with concrete reinforced with steel, glass, or other synthetic fibers, and adequate literature regarding their manufacture, handling, structural applications, and performance is available.

The manufacture of synthetic fibers is quite expensive and consumes considerable energy. It is in this context that low modulus natural fibers, which are readily available in many parts of the world, could be put to their best advantage, particularly in the production of building components. Because of the acute shortage of essential building materials, coupled with low income, unemployment, and a high increase in the population growth, millions of people in many developing countries do not have proper shelter. Providing proper shelter for the masses remains a real challenge to all associated with the planning and execution of various housing schemes (*1*).

Roofs, floors, and walls form the major load-carrying structural components of a building. While concrete can be used, it makes the construction very expensive and sometimes difficult, particularly in the construction of low-cost houses for the poor. In rural areas, roofs are traditionally made from straw, palm leaves, grass, or coconut thatch. These types of roofs not only need frequent replacement but are seldom water tight. They are also easily infested and are not fire resistant. Provision of such roofs in rural areas is not safe, particularly during disputes among the people. Asbestos cement sheets and corrugated steel sheets provide a better substitute but are again expensive and also are not suitable for tropical regions. The use of burnt clay tiles where timber is scarce requires additional structures consisting of purlins and rafters, which increases the cost of roofing. Roofs with clay tiles are also not suitable for resisting earthquakes.

Natural vegetable fibers have long been used for reinforcing clay and mud, and the properties of plain concretes are improved by the introduction of these fibers at the time of making concrete. Several studies have been reported on the mechanical properties, structural behavior, and possible applications of natural fibers in buildings. To identify the various problems associated with the use of natural fibers, a joint research project was initiated by the Department of Building Frame Works at the Royal Institute of Technology in Stockholm, Sweden, in collaboration with the Government of Tanzania. A comprehensive report has been published (*2*) on the various problems associated with the use of two types of natural fibers (sisal and coconut fibers) for the manufacture of roofing sheets.

Department of Structural Engineering, Annamalai University, Annamalainagar 608 002, India.

NATURAL FIBER REINFORCED CONCRETE (NFRC)

The use of natural fibers in making concrete is recommended since several types of these fibers are available locally and are plentiful. The idea of using such fibers to improve the strength and durability of brittle materials is not new; for example, straw and horse hair are used to make bricks and plaster. Natural fibers that are suitable for reinforcing concrete and are easily available in developing countries can be broadly classified as shown in Figure 1.

Wood fibers have been attempted as reinforcement in cement concrete productions. Hast fibers include hemp, flax, and ramie. These fibers are reported to be stronger than other vegetable fibers and possess a higher modulus of elasticity. Among the leaf fibers, sisal is one of the most important and widely used and is plentiful in many tropical countries. Among the seed and fruit fibers, coconut or coir is reported to be the most suitable for concrete. Previous studies have been concerned with the use of sisal and coconut fibers in making corrugated roofing sheets and ribbed or folded plates. Fibers derived from palm trees are considered to be stronger than coconut fibers, and a detailed investigation of their use is worth pursuing. The use of bamboo fibers also needs to be investigated. Many types of bamboos are available in tropical countries, and their fibers may be suitable as reinforcement in concrete products. It is reported that the mechanism for metallic fiber reinforcements are also valid for natural fibers. Experimental investigations reported from Bangaladesh (*3*) indicate that the addition of jute and coconut fibers decreases the compressive strength and increases only slightly the tensile strength of the concrete composites.

Few studies have been reported on the long-term behavior of natural fiber reinforced concrete beams. Singh (*4*) reported that the useful life of such beams increases when subjected to cyclic loading and that the method of mix proportioning of natural fiber needs to be standardized.

After conducting several tests on slabs reinforced with coconut coir fibers, Paramasivam et al. (*5*) concluded that the strength of the slabs is comparable to that of asbestos cement sheets. They have, therefore, recommended the use of such slabs in housing.

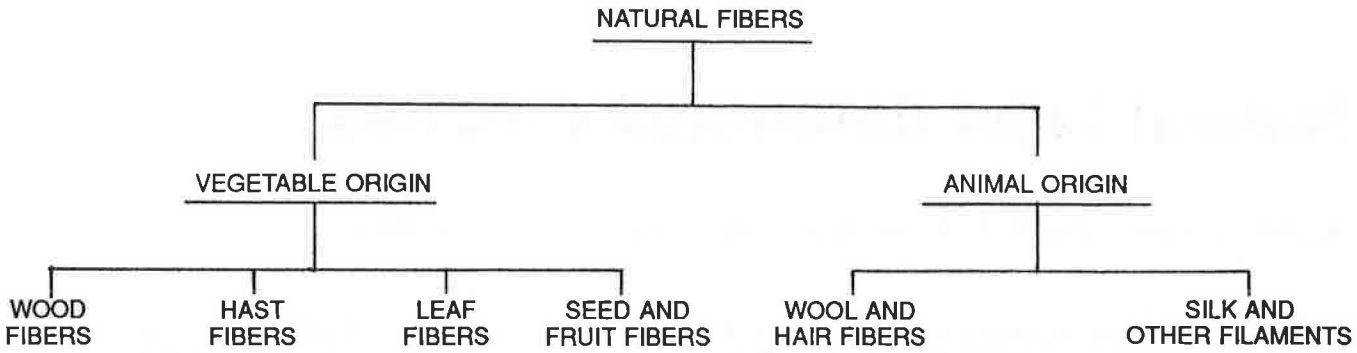

FIGURE 1 Classification of natural fibers.

BAMBOO FIBERS

Pakotiprapah et al. (*6*) studied the mechanical properties of cement composites made out of bamboo fibers, both experimentally and theoretically. The fibers used were extracted by hammering short bamboo sticks.

While most of the studies have been concerned with the mechanical properties of NFRC obtained from short-term tests, Gram et al. (*7*) conducted durability tests on several samples, which were tested after 360 days and 540 days. To prevent the decay of fibers, the partial replacement of cement with rice husk ash has been recommended. Since the strength and stiffness of natural fiber concrete reduces with time, adequate precautions should be taken when using natural fibers.

Among the various studies reported on the use of natural fibers in concrete, the results reported from Sweden (*2*) could be regarded as the first systematic study on these fibers. The factors that affect the properties of NFRC are given in Table I. A typical stress-strain curve for natural fibers is shown in Figure 2.

When used as roofing sheets, the allowable crack width is not recommended in any design guideline. Hence, suitable design guidelines have to be established.

TABLE 1 FACTORS AFFECTING PROPERTIES OF NATURAL FIBER REINFORCED CONCRETE

Factors	Variables
Fiber type	Coconut, sisal, sugarcane, bagasse, bamboo, jute, wood and vegetables, canes, skin from trunk
Fiber geometry	Length, diameter, cross section, rings, and hooked ends
Fiber form	Mono-filament, strands, crimped, and single-knotted
Fiber surface	Smoothness, presence of coatings
Matrix properties	Cement type, aggregate type and grading, additive type
Mix design	Water content, workability aids, defoaming agents, fiber content
Mixing method	Type of mixer, sequence of adding constituents, method of adding fibers, duration and speed of mixing
Placing method	Conventional vibration, vacuum dewatering, sprayed-up concrete member, extrusion, and guniting
Casting technique	Casting pressure
Curing method	Conventional, special method

OTHER FIBERS

While many investigators have studied the behavior of concrete reinforced with such fibers as coir and sisal, Ramanathan et al. (*8*) recently reported the results of their study on yeast fiber concrete. The addition of yeast was found to improve both the mechanical properties and workability of concrete.

Yeast (fungi) belongs to the Ascomycetes class of the plant kingdom. This microorganism has a peculiar property of reproduction by means of bud formation. It is a unicellular organism with a smooth, gelatinous cell membrane. A single yeast cell becomes doubled, then tripled, and all the cells thus reproduced orient along almost straight chain lines. These chain-like interlinks act as "elastic fibers" or wires, making connective bonds with every contour terminal of the concrete mass; hence the name "yeast fiber reinforced concrete."

All the tests on yeast fiber concrete were conducted at the Structures Laboratory of the Annamalai University. For a total concrete mass of 14 kg (having 2 kg of cement in a 1:2:4

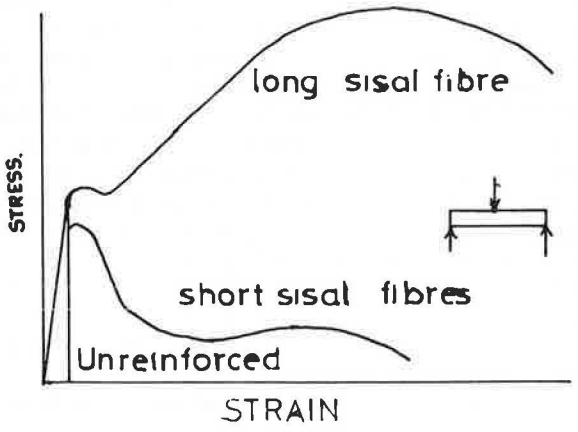

FIGURE 2 Typical stress-strain curves for natural fiber concrete.

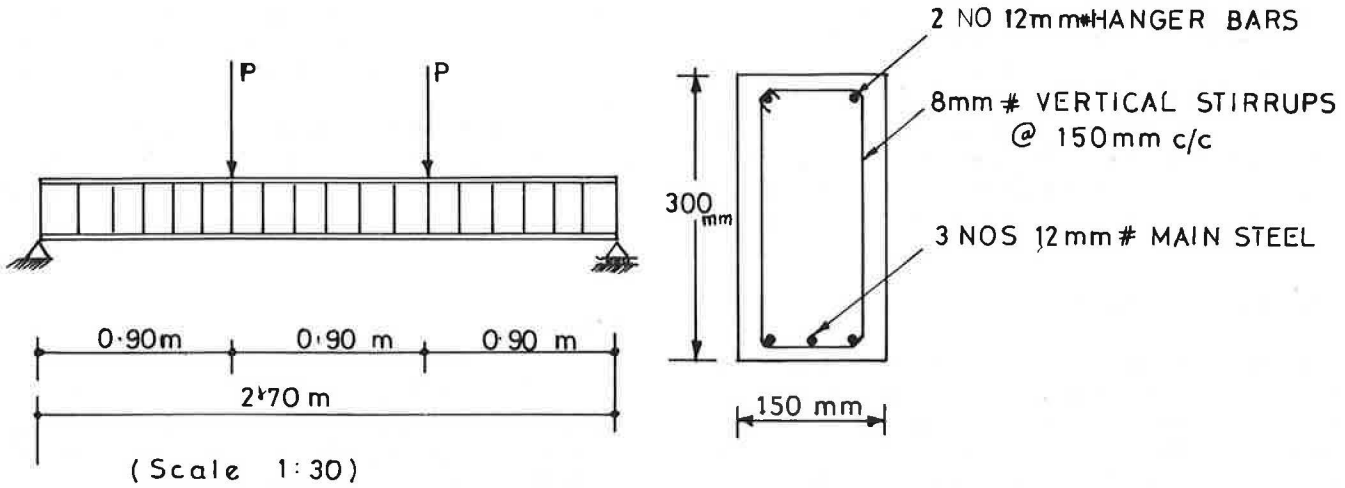

FIGURE 3 Details of cross section and loading of reinforced concrete beams.

TABLE 2 COMPARISON OF STRENGTH PROPERTIES OF PURE WATER CONCRETE WITH WBY-MADE CONCRETE (*8*)

Properties	Number of Days	Percentage Increase in Strength for WBY-Made Concrete
Tensile strength	3	16
Tensile strength	7	12
Compressive strength	7	7.5
Compressive strength	28	6.77

TABLE 3 COMPARISON OF FLEXURAL STRENGTH OF PURE WATER CONCRETE AND WBY-MADE CONCRETE (*8*)

Test Beams Number	Effective Span	Cracking Load (tons)	Ultimate Load (tons)
1[a]	2.7	0.82	3.62
2[a]	2.7	0.82	3.552
3[b]	2.7	1.43	4.03
4[b]	2.7	1.23	4.098

[a]RC beam made with pure water.
[b]RC beam made with WBY.
Percentage increase in cracking load = 62
Percentage increase in ultimate load = 13

concrete), the amount of yeast granules added was only about 10 g. The following tests were conducted to determine the various properties of yeast fiber concrete:

- Compression test,
- Tension test,
- Consistency and setting time tests,
- Slump test,
- Vee-bee degree test, and
- Flexural test.

The consistency and setting time tests were performed using a Vicats apparatus. From a total of 72 briquettes, 36 samples were made out of water blended with yeast (WBY) and another 36 samples were made with pure water. The samples were cast under identical laboratory conditions. The ratio of cement to fine aggregate was 1:3, and the water added was 8 percent of the total weight of the dry mix in both cases. Out of 36 briquettes made from WBY, 18 were tested for tension at the end of 3 days and another 18 after 7 days. Curing was done by keeping all the samples immersed in water. For the compression test, concrete cubes (10 cm size) were cast and tested after 7 days and 28 days. Yeast-blended water was also used for casting two reinforced concrete (RC) beams, and the beams were tested under two-point loading as shown in Figure 3.

The normal consistency of the cement pastes made out of WBY increased by only 1 percent, but there was not much difference in the initial setting time of these pastes.

As shown in Table 2, the tensile strength of cement mortar briquettes made with WBY had increased by 16 percent at the end of 3 days; in the 7-day test, the tensile strength of these briquettes increased by 12 percent.

Table 2 shows that the compressive strength of concrete cubes made with WBY had increased by 7.5 percent after 7 days and by 6.77 percent after 28 days. The increase in tensile strength could be attributed to the presence of yeast chain links acting as fibers.

The experiments for measuring workability also provided encouraging results. For the same water/cement ratio, the slump obtained for the concrete made with WBY was more than that made with pure water. Increased slump value and better workability can be achieved by adding yeast to the normal quantity of water used for making concrete.

In the vebe tests, the concrete made with WBY showed better flow property than that made with pure water; the other conditions remained the same. The increase in workability can be attributed to the presence of gelatinous cell membranes, which act as lubricants inside the mass of concrete.

Table 3 compares the measured values for the cracking and ultimate loads for the beams made using pure water and those made with WBY. The cracking load increased by 62 percent

and the ultimate load increased by about 13 percent in the beams made with WBY. The load-deflection behavior for yeast-blended beams also showed a definite increase in the stiffness of the beams.

It should be mentioned that the name yeast fiber reinforced concrete was chosen since the yeast cells develop in the form of a chain. This chain-like formation has been referred to as fiber even though these fibers cannot be seen by unaided eyes.

CONCLUSIONS AND RECOMMENDATIONS

- While there has been considerable research relating to steel fiber reinforced concrete elements, few attempts have been made to study the behavior of structural elements made out of natural fibers. Only limited types of fibers have been tried; hence, more investigations are needed on the behavior of structural elements made from all available types of natural fibers, including bamboo fibers, palm tree fibers, and canes.
- Most of the vegetable fibers, when dried, lose their moisture. To achieve better results, the presence of certain amounts of moisture is necessary, and this aspect needs further study.
- The effect of creep and cyclic reversal of stresses on NFRC should be investigated.
- The use of NFRC in the construction of shell-type roofs should be explored.
- The use of natural fibers should be popularized. All problems associated with the extraction of fibers, such as mix design, casting, curing, placing, and transportation, should be investigated and a code of practice formulated.
- A major disadvantage in using natural fibers is that the fibers will decay over time and the composite will lose its strength, resulting in sudden brittle failure. Hence, proper treatment of the fibers before mixing may be necessary. To increase durability, partial replacement of ordinary portland cement by rice husk ash or silica fume is recommended. Other types of admixtures, such as resins and gums, can be tested to prevent decay of natural fibers that have been embedded in concrete.
- The problem of providing proper housing should be treated as a global issue. It can be solved only through research and the transfer of technology and resources (*9*). The efforts of the Government of Sweden in this direction are applauded.

REFERENCES

1. *Proc., National Seminar on Housing for the Rural Poor in India*, Annamalai University, India, 1985.
2. H. K. Gram, H. Person and A. Skarendahl. *Natural Fibre Concrete*. Report R2:1984. Swedish Agency for Research Cooperation With Developing Countries, Sweden.
3. R. Islam and A. K. M. K. Alam. Study of Fiber Reinforced Concrete With Natural Fibres. *Proc., ISFRC*, Vol. II, Madras, India, 1987.
4. R. N. Singh. Flexural Behaviour of Notched Coir Reinforced Concrete Beam Under Cyclic Loading. *Proc., ISFRC*, Vol. II, Madras, India, 1987.
5. P. Paramasivam, G. K. Nathan and N. C. Das Gupta. Coconut Fibre Reinforced Corrugated Slab. *The International Journal of Cement Composite and Light Weight Concrete*, Vol. 6, No. 1, Feb. 1984.
6. B. Pakotiprapah, R. P. Pama and S. L. Lee. Behaviour of Bamboo Fibre Cement Paste Composite. *Journal of Ferro-cement*, Vol. 13, No. 3, July 1983.
7. H. E. Gram and P. Nimityongskul. Durability of Natural Fibre in Cement-Based Roofing Sheets. *Journal of Ferro-Cement*, Vol. 17, No. 4, Oct. 1987.
8. R. Ramanathan, S. Chockalingam and R. Sethunarayanan. Yeast Fibre Reinforced Concrete. *Proc., ISFRC*, Vol. II, Madras, India, 1987.
9. S. Chockalingam. A New Technology for Rural Development. *Proc., National Seminar on Housing for the Rural Poor in India*, Annamalainagar, India, 1985.

Properties and Design of Fiber Reinforced Roller Compacted Concrete

ANTONIO NANNI

Extensive experimentation in pavement construction has been conducted using steel fiber reinforced concrete (SFRC). Although SFRC has demonstrated outstanding mechanical properties, its commercial application has been limited because of high cost. Cost savings could be realized for paving projects constructed with the emerging roller compacted concrete (RCC) technology. In particular, pavement thickness reduction due to the inclusion of fibers in RCC can allow single-lift construction where two lifts of unreinforced concrete would be required. Alternatively, for two or more lifts, SFRC can be confined to the most stressed layer(s). This paper presents compression and split tension results of laboratory cylinders and field cores reinforced with different types of steel fiber in various percentages. The concrete matrix contained fly ash, either Class F (used as a filler) or Class C (used as a binder). Fiber inclusion disturbed the consolidation of laboratory specimens, whereas field cores did not indicate any loss of density or compressive strength. Post-cracking characteristics were greatly enhanced by fibers with ultimate strength and toughness indexes derived from stress-strain curves for split tension. Sample design calculations compare the preliminary pavement thickness of unreinforced and fiber reinforced RCC with cost estimates for each.

The inclusion of fibrous reinforcement in concrete to produce a better construction material is an important development of concrete technology. Extensive experimentation has been conducted on various types of fiber (such as steel, glass, asbestos, synthetic, and natural), and basic properties of the composite material behavior have been obtained. However, the number of applications of fibrous concrete remains limited as a consequence of side effects, which invariably accompany the use of each fiber and detract from its merits (*1*). Examples are cost (steel), durability (glass), health hazard (asbestos), low modulus (synthetic), and fire resistance (natural).

Steel fiber primarily has been used in highway and airport pavements because it improves the mechanical characteristics of the concrete matrix (*2*), for example, flexural (tensile) strength, toughness, fatigue endurance, post-cracking ductility (pseudo-ductility), and impact resistance. Flat work construction is an attractive research topic for two reasons: large amounts of materials are used with consequent economical implications; and innovative technology can be readily explored, since this type of structure can take a comparatively greater risk than others. In recent years, several publications (*3–7*) have reviewed the performance of steel fiber reinforced concrete (SFRC) pavements constructed during the 1970s and early 1980s. From these evaluations, it is apparent that the overall performance has been satisfactory, though failures have been experienced in four areas (*4*): corner curling and warping, improper jointing, load transfer between adjacent slabs, and exposed fibers.

Department of Architectural Engineering, The Pennsylvania State University, University Park, Pa. 16802.

Finally, the use of SFRC has not emerged as a viable alternative to conventional plain concrete paving for economical reasons (*1*). Predicted savings have not materialized, and this situation is not likely to change if specifications, such as those presently adopted by the Navy (*7*), do not allow pavement thickness reduction when plain concrete is substituted with SFRC.

NEW DEVELOPMENTS

Roller compacted concrete (RCC) paving (*8*) may represent a new opportunity for using concrete at a competitive cost that inherently contains its own reinforcement. It has been demonstrated that construction of steel fiber reinforced RCC (FRRCC) is feasible (*9*), because steel fibers can be included and randomly distributed in the concrete matrix by a pugmill mixer (i.e., continuous mixing). Furthermore, FRRCC can be laid by a heavy-duty paver without losing compaction efficiency.

The merging of these two technologies produces mutual benefits. A pavement thickness reduction due to the use of fibrous reinforcement is particularly advantageous in multilift RCC construction. Not only can the number of lifts be reduced, but when pavement thickness requires more than one lift, the use of fibers can be confined to the lift(s) subjected to the maximum stress (*10*). Plain RCC is currently laid without contraction joints or with saw-cut joints having no load-transfer device. FRRCC pavements without joints would exhibit different cracking behavior from plain RCC. Fewer, and therefore wider, cracks would not be desirable. The fiber micro-dowel action at the saw-cut joints can enhance the aggregate interlock load transfer between adjacent slabs. Fibers bridging the crack will experience corrosion (*11*); therefore, the use of larger diameter fibers is appropriate. Mix constituents and proportions of RCC correct the major defect (i.e., corner warping and curling) encountered in conventional SFRC pavements (*5*). In fact, low cement factor, use of fly ash, and very low mixing water substantially reduce autogenous shrinkage, heat of hydration, and, to a lower extent, dry shrinkage.

EXPERIMENTAL PROGRAM

Series A (South-Florida Limestone, Class F Fly Ash)

The matrix constituents for this series were portland cement Type I, Class F fly ash, and crushed South-Florida limestone

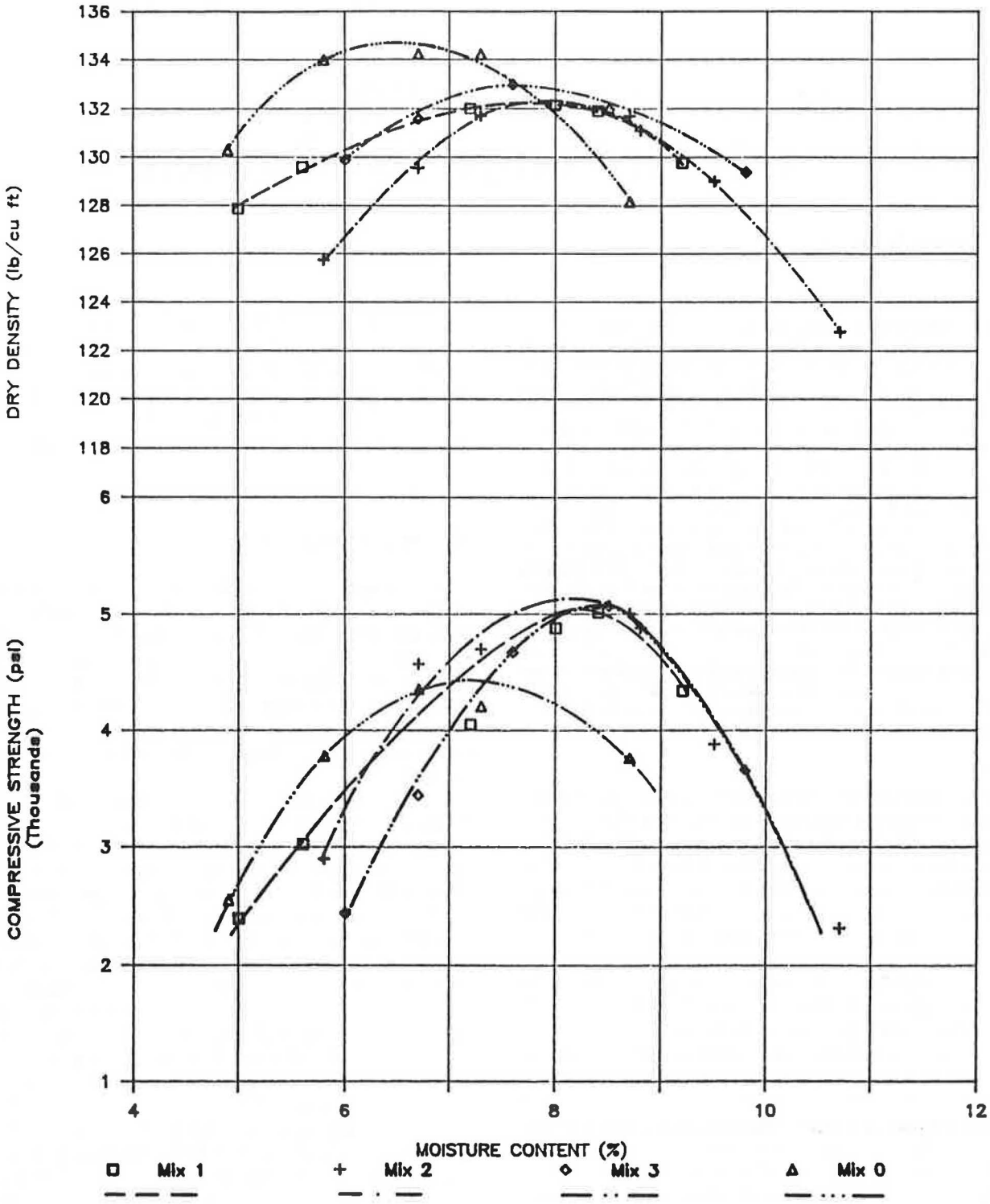

FIGURE 1 28-day compressive strength and initial dry density vs. moisture content (series A, 12 percent cement).

aggregate. The fine and coarse aggregate complied with ASTM D-448 sizes 10 and 57, respectively.

Selection of Matrix Proportions

Several combinations of mix constituents were investigated to empirically determine the proportions that would optimize density and compressive strength. In this instance, Class F fly ash was used as a filler. The objective was to improve mix compactability, since pozzolanic reaction of low calcium ash is negligible at 28 days. Each selected mix was compacted according to the modified Proctor method (ASTM D-1557, 4 in. × 4.5 in. mold) at five different moisture contents. Figure 1 shows the results obtained for some of the mixes with 12 percent by dry weight of cement. Both 28-day compressive strength and dry density at fabrication are plotted as a function of the initial water content. The properties relative to the

TABLE 1 MATRIX PROPORTIONS, DENSITY, AND STRENGTH (SERIES A)

Mix	Type I Cement (%)*	Class F Fly-ash (%)*	Fine Aggregate (%)*	Coarse Aggregate (%)*	Total Water (%)*	Initial Dry-Density (lb/cu.ft)	Cement Factor (lb/cu.yd)	W/C** Ratio	28-Day Compressive Strength (psi)
0	12	0	40	48	6.7	134.3	435	0.29	4356
1	12	6	46	36	8.4	131.9	427	0.45	5013
2	12	6	37	45	8.7	131.7	427	0.47	5005
3	12	6	32	50	8.5	132.0	428	0.46	5071
5	12	12	35	41	8.0	129.4	419	0.43	4151
8	12	18	32	38	8.9	125.3	406	0.52	3841
11	12	24	29	35	9.0	125.7	407	0.55	3572

* Percent of Total Dry Weight

** Aggregate Water Absorption: Fine=3.4%, Coarse=3.9%

mixes with the highest compressive strength are presented in Table 1 under mix denominations 0, 1, 2, and 3. From this data, it is evident that: (a) varying the coarse to fine aggregate ratio between 0.8 and 1.6 (Mixes 1, 2, and 3) does not significantly affect strength or density, and (b) including 6 percent by dry weight of Class F fly ash improves compactability, and therefore strength, despite a higher water to cement ratio.

Compressive strength results of other mixes (i.e., mixes 5, 8, and 11) reported in Table 1 indicate that addition of fines in the form of fly ash is not beneficial at a cement content of 12 percent.

Properties of Laboratory FRRCC

Mix 2 was selected as the matrix for fiber reinforced specimens. Three types of steel fibers were used: straight slit sheet (SS), hooked-end wire (HE), and mill cut bar (MC). The fiber length was limited to 1 in. because of the overall cylinder dimensions (4 in. × 4.5 in.). The aspect ratio (L/D) of the three fibers was 60, 60, and 30, respectively. The fiber content by volume (V) varied between 0 and 1.64 percent (i.e., 0 and 6 percent by weight). Test results of specimens compacted according to the modified Proctor method at an average moisture content of 7.6 percent (standard deviation = 0.3 for 90 specimens) are shown in Figure 2. The lower part of the diagram indicates that the matrix dry density at fabrication decreases with fiber dosage expressed in terms of the VL/D factor (volume percentage × aspect ratio). The 28-day compressive strength as plotted in the central part of the diagram reveals the same trend. This is a clear indication that the presence of fibers disturbs laboratory consolidation. Even though the quality of the matrix is lowered, the ultimate split tensile strength at 28 days increases with the VL/D factor, as shown in the upper part of the diagram.

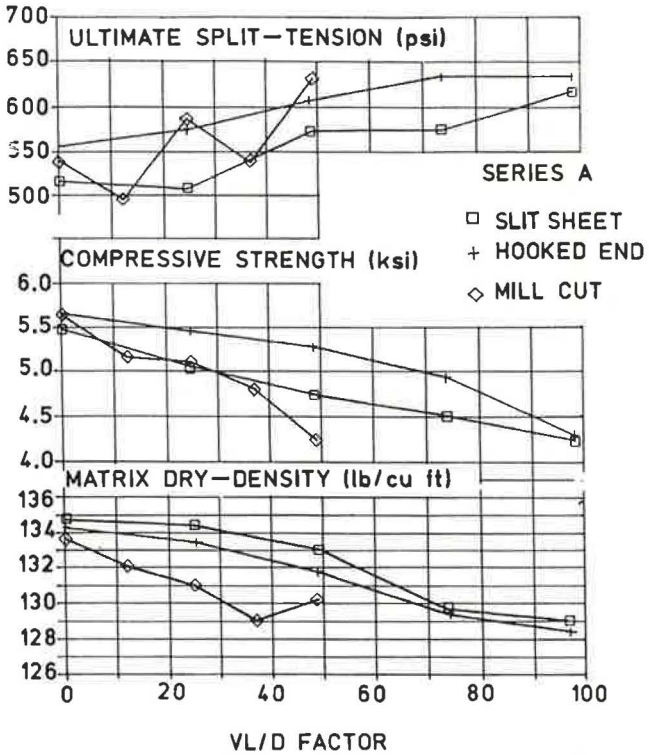

FIGURE 2 Dry density, compression strength and ultimate split tension vs. VL/D factor (series A).

The average 28-day split tension stress-strain curves for cylinders reinforced with fiber type HE are given in Figure 3. Deformation is measured along the diameter perpendicular to the load plane, and stress is computed according to ASTM C-496. The diagram illustrates the lack of improvement in first crack strength. This is due to fiber inclusion,

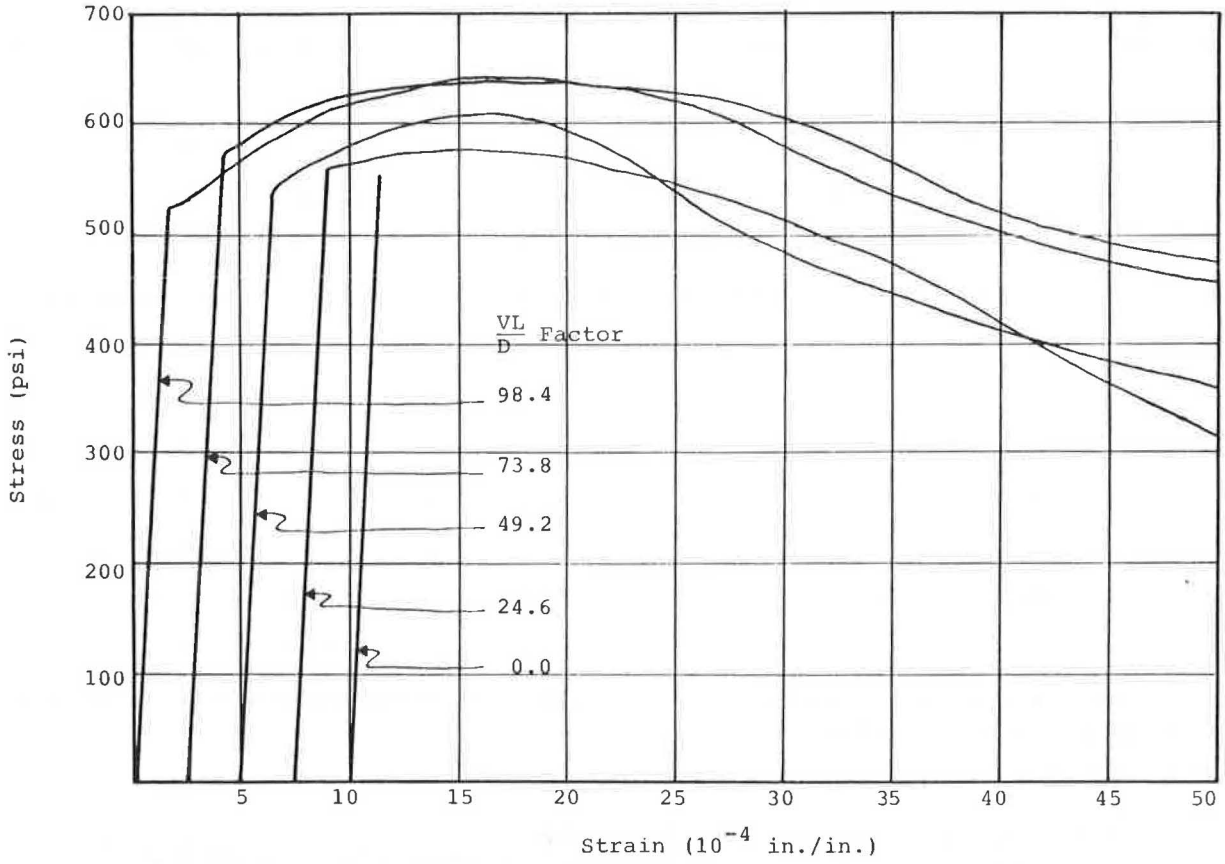

FIGURE 3 Stress-strain curves for split tension (series A, fiber HE).

since the matrix has become less dense. However, the post-cracking behavior is significantly affected by the presence of fibers in terms of ultimate strength and pseudo-ductility. The same conclusion can be reached by considering Figure 4, where the toughness indexes I_5, I_{10}, and I_{30} are computed for the flexural test (ASTM C-1018) and plotted as a function of the VL/D factor.

Series B (Texas Limestone, Class C Fly Ash)

The matrix constituents and proportions were selected based on a successful field project (*12*, p. 14). Portland cement Type I and Class C fly ash were used in equal amounts of 260 lb/yd^3 and fine and coarse aggregates in equal amounts of 1,610 lb/yd^3. The total water content was 5.9 percent by dry weight (standard deviation = 0.25 for 63 samples).

Properties of Laboratory FRRCC

Three types of steel fiber were used in this series. Two types were previously described as SS and HE, whereas the third type was a crimped slit sheet fiber (CR), 1 in. long and with an aspect ratio of 60. Test results on laboratory-fabricated specimens are given in Figure 5 as a function of fiber dosage. These data confirm what is presented in Figure 2 for Series A. In particular,

- The matrix dry density decreases as the VL/D factor increases,
- The first crack split tensile strength remains practically unchanged, and
- The ultimate split tensile strength is directly proportional to the VL/D factor.

The average 28-day split tension stress-strain curves for cylinders reinforced with fiber type SS are reported in Figure 6.

FRRCC Field Cores

Test results under split tension of field cores with identical matrixes and reinforced with 0.49 percent by volume of fiber type SS are reported in Figure 7. These results emphasize the primary difference between field cores and laboratory-fabricated specimens. Testing was conducted between 28 and 39 days from construction. Field inclusion of fibers in RCC neither disturbed consolidation nor compromised the resulting density and compressive strength (*9*). As a consequence, the first crack strength of FRRCC cores (Figure 7, curves a and c) is appreciably higher than that of corresponding unreinforced RCC (Figure 7, curve e). Also, two curves (b and d) relative to specimens cored from the bottom half of the pavement lift, which had a dry density 4 to 5 percent lower than that of the top half (*9*), are reported in the figure. This condition is common in plain RCC pavements constructed with double-screed double-tamping bar pavers (*13*). Based on these results, it was concluded that compaction of fibrous concrete obtained in the laboratory using the Proctor hammer is representative of the lower portion of the pavement lift.

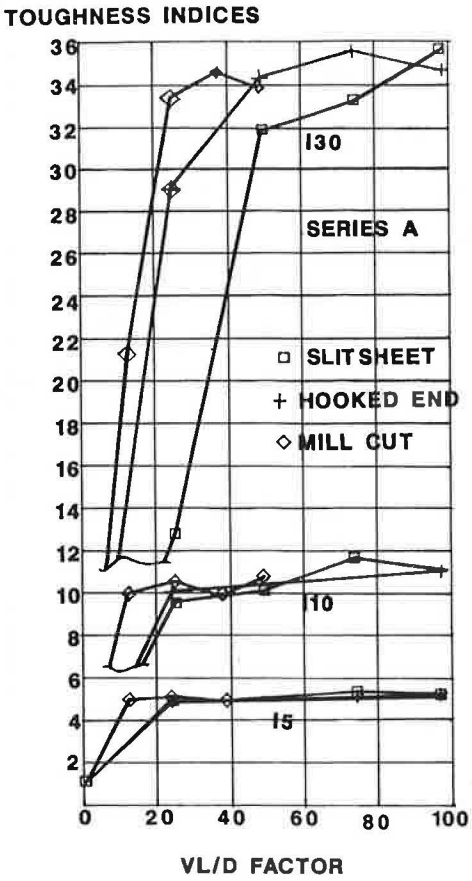

FIGURE 4 Split tension toughness indexes (series A).

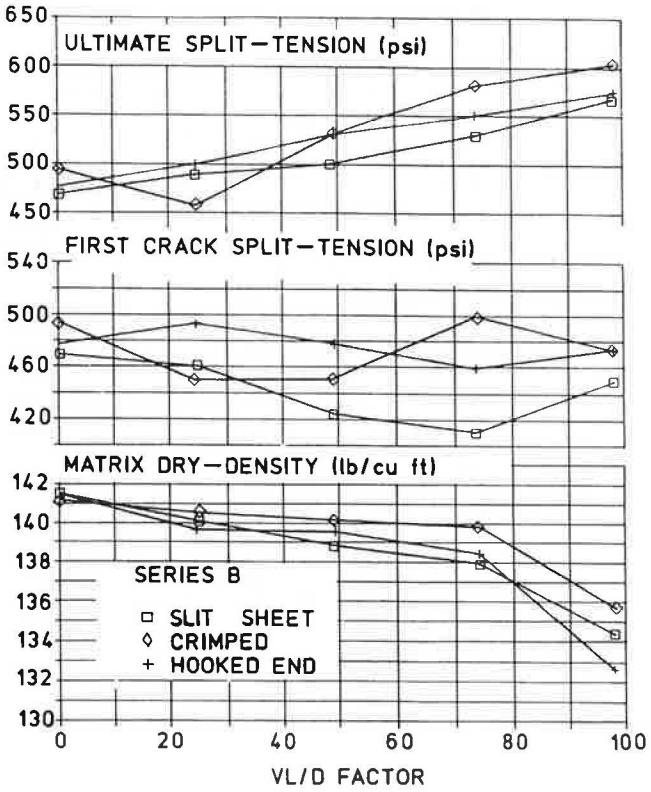

FIGURE 5 Dry density, first crack split tension, and ultimate split tension vs. VL/D factor (series B).

DESIGN EXAMPLES

Pavement Thickness

The two pavement thickness design examples reported below illustrate a comparison between conventional and FRRCC. The following assumptions are common to both examples:

	RCC	*FRRCC*
Design flexural strength (psi)	660	660
Modulus of elasticity (10^6 psi)	3.80	3.80
Steel fiber content (lb/yd^3)	—	100
Fatigue life	Figure 8	Figure 8
Modulus of subgrade reaction (Subgrade + 6 in granular base) (pci)	140	140

Both unreinforced and fiber reinforced RCC are assumed to have the same first crack strength, which is equal to 660 psi. Since the first crack strength of SFRC is higher than that of the corresponding unreinforced matrix (*9, 16, 17*), this assumption is conservative for the FRRCC alternative. A major benefit of fiber inclusion in concrete is the improved fatigue life. Design data for the two alternatives were derived from the literature as presented below. RCC flexural fatigue performance is reported to be quite similar to that of conventional concrete (*14*). This evaluation by the Portland Cement Association (PCA) was based on field beams of four different RCC mixes. Values of the stress ratio (load stress modulus of rupture) as a function of allowable load repetitions were derived according to the design procedure used by PCA for conventional airport and highway concrete pavements (see Figure 8).

Figure 8 also shows the derived design data from tests conducted at the South Australian Institute of Technology (*15*) on SFRC with 125 lb/yd^3 of fibers. This stress ratio to load repetition relationship is considered appropriate even if derived for conventionally cast SFRC; more recent research (*17*) indicates higher endurance values for smaller amounts of fibers with mechanical anchorage.

The pavement thickness is determined by stress values computed with the PCA microcomputer program (*18*), which is based on Westergaard's modified analysis for loads at the interior of a slab. Similar pavement thickness values for unreinforced RCC are determined using the modified Corps of Engineers design method for airports (*19*). For the purpose of this comparison, no consideration has been given to the problem of load transfer at construction joints and natural or saw-cut contraction joints (*20*) or to the case of vehicles traveling close to the pavement edge (*14*).

Heavy-Duty Freight Yard (20-Year Life)

For heavy-duty freight yards, the problem data are as follows:

Vehicle type	*Piggypacker loader*
Single wheel load (kip)	110
Tire inflation pressure (psi)	100
Tire contact area (in^2)	1,090
Total wheel load applications	20,000

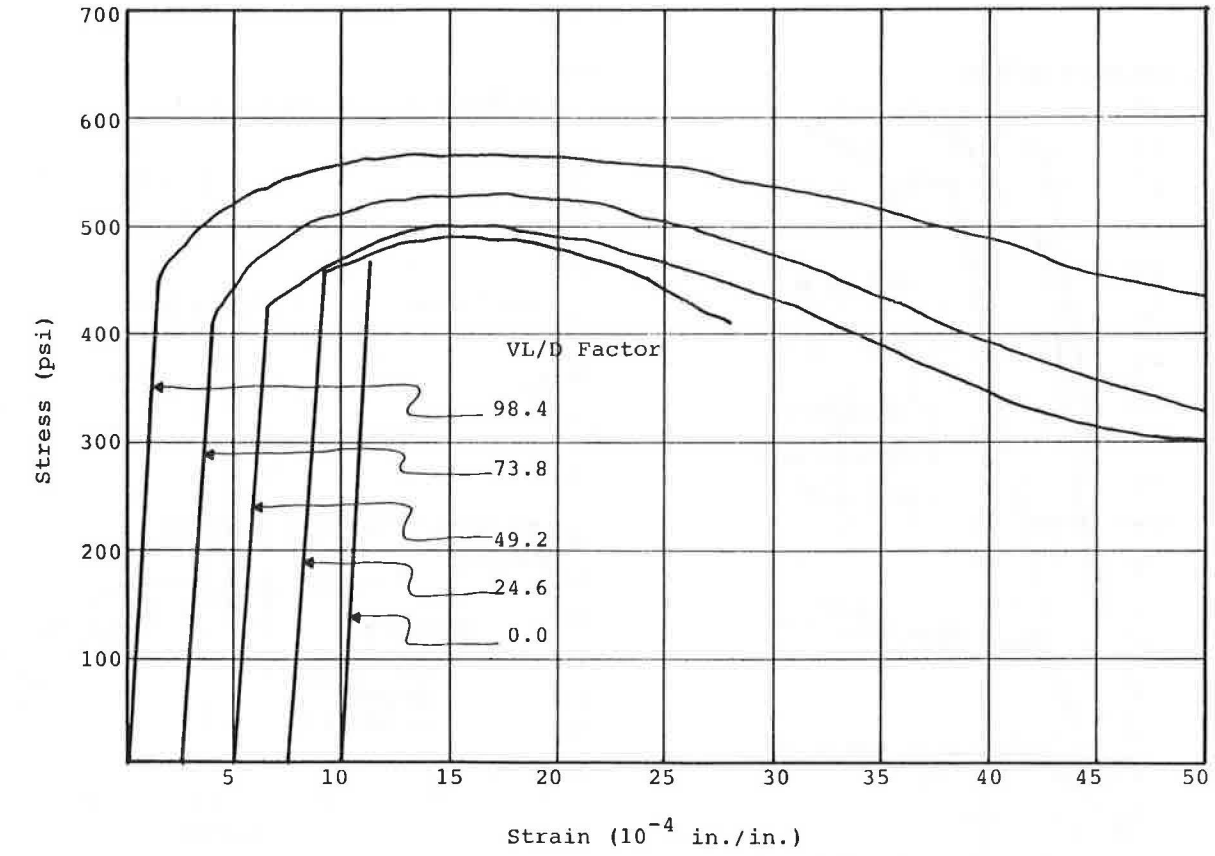

FIGURE 6 Stress-strain curves for split tension (series B, fiber SS).

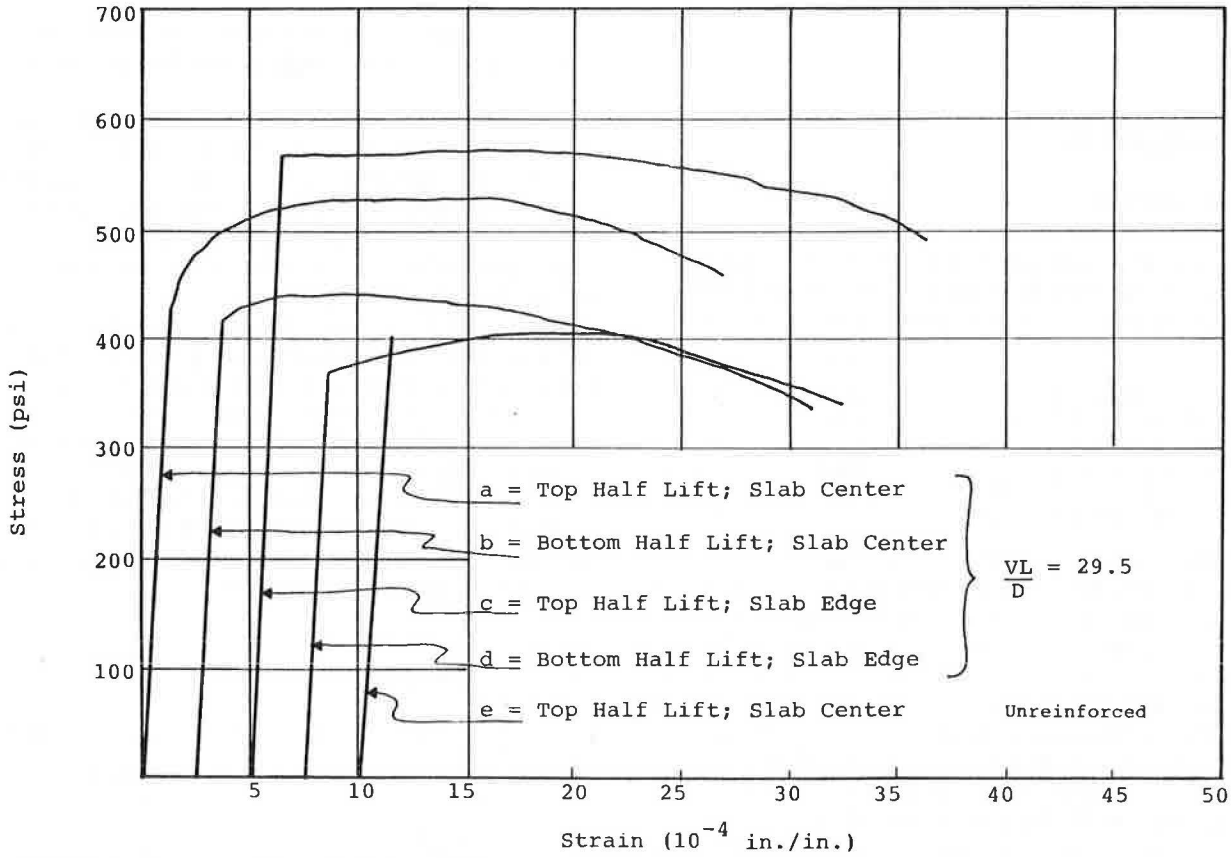

FIGURE 7 Stress-strain curves for split tension (field cores, fiber SS).

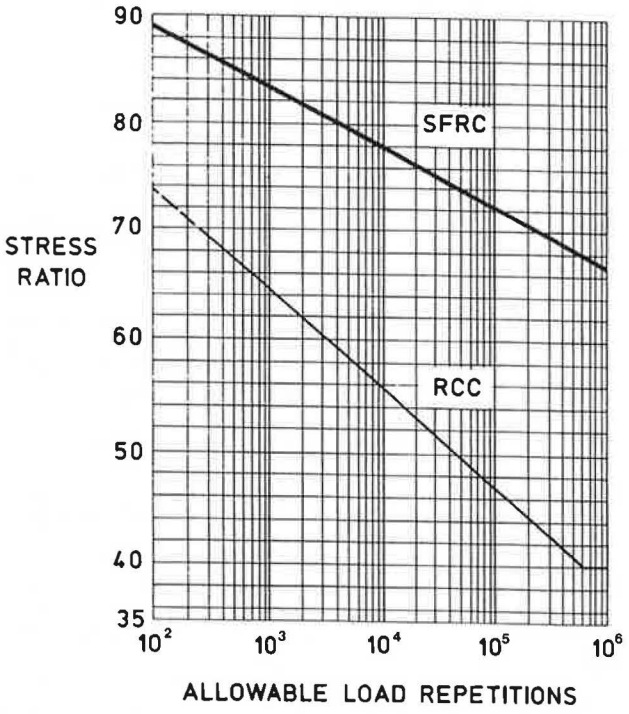

FIGURE 8 Stress ratio vs. allowable load repetitions.

The design results are:

	RCC	*FRRCC*
Pavement thickness (in.)	18.0	14.0
Maximum stress (psi)	343	511
Allowable stress (psi)	660 × 0.53 = 350	660 × 0.77 = 508

The reduction in pavement thickness due to the inclusion of fibers is 22 percent.

Industrial Pavement (20-Year Life)

For industrial pavement, the problem data are:

Vehicle type	*Straddle carrier*
Single wheel load (kip)	26
Tire inflation pressure (psi)	100
Tire contact area (in²)	260
Total wheel load applications	200,000

The design results are

	RCC	*FRRCC*
Pavement thickness (in.)	10.5	7.5
Maximum stress (psi)	281	486
Allowable stress (psi)	660 × 0.44 = 290	660 × 0.72 = 475

The reduction in pavement thickness due to the inclusion of fibers is 29 percent.

Cost Analysis

The following costs have been estimated for paving projects of approximately 20,000 yd² of surface. Based on field experience with heavy-duty pavers, the lift depth range for acceptable compaction is between 4 and 8 in (*21*). Listed below are the unit costs per square yard of paved surface:

Concrete	\$1.50/in. of lift depth
Fibers (@ 100 lb/yd³)	\$1.10/in. of lift depth
Mixing/placing/curing	\$3.00 + \$0.25/in. of lift depth

Heavy-Duty Freight Yard

Due to required pavement thickness, the unreinforced RCC pavement is constructed in three lifts (8, 5, and 5 in.) and the FRRCC in two lifts (8 and 6 in.), the top of which is plain RCC. In the latter case, the use of two types of mix in the same project is not necessarily impractical even when pugmill mixers are used. In fact, the addition of fibers does not require a modification of mix proportions or plant recalibration. Costs are as follows:

RCC

8.0 × \$1.50 + \$5.00 = \$17.00
5.0 × \$1.50 + \$4.25 = \$11.75
5.0 × \$1.50 + \$4.25 = \$11.75
\$40.50

FRRCC

8.0 × (\$1.50 + \$1.10) + \$5.00 = \$25.80
6.0 × \$1.50 + \$4.50 = \$13.50
\$39.30

The FRRCC alternative is 3 percent cheaper.

Industrial Pavement

Due to required pavement thickness, the unreinforced RCC pavement is constructed in two lifts (6 and 4.5 in.) and the FRRCC in one lift (7.5 in.). Costs are as follows:

RCC

6.0 × \$1.50 + \$4.50 = \$13.50
4.5 × \$1.50 + \$4.12 = \$10.87
\$24.37

FRRCC

7.5 × (\$1.50 + \$1.10) + \$4.87 = \$24.37
\$24.37

As shown, the two alternatives have identical costs.

CONCLUSIONS

In this paper, the existence of post-cracking strength and pseudo-ductility of RCC resulting from the inclusion of steel fiber reinforcement is shown. All fibers tested indicated that post-cracking performance is directly proportional to fiber content. This study was limited to one length of steel fiber; longer and

thicker fibers should be included for a more complete coverage of the cost-performance ratio. The performance of field cores was better than that of equivalent laboratory-fabricated samples because fiber presence does not disturb the consolidation efforts of both paver and roller.

Based on improved fatigue life, inclusion of fibers in RCC results in pavement thickness reduction. Savings in material and construction costs compensate for the additional cost of fibers. In the given examples, improvement in first crack strength due to the presence of fibers was not considered. Fiber content may be lowered depending on the type of fiber.

ACKNOWLEDGMENTS

This material is based on work supported by the National Science Foundation. Steel fibers were donated by Bekaert, Harex and Mitchell Fibercon.

REFERENCES

1. R. I. T. Williams. Cement-Treated Pavements. *Elsevier*, London, England, 1986.
2. ACI Committee 544. *State-of-the-Art Report on Fiber Reinforced Concrete*. Report 544.1R-82. American Concrete Institute, Detroit, Mich., 1982.
3. G. C. Hoff. Use of Steel Fiber Reinforced Concrete in Bridge Decks and Pavements. *U.S./Sweden Joint Seminar (NSF-STU)*, Swedish Cement and Concrete Research Institute, Stockholm, Sweden, 1985, pp. 67–108.
4. R. G. Packard and G. K. Ray. Performance of Fiber Reinforced Concrete Pavement, In *Report ACI SP-81: Fiber Reinforced Concrete* (G. C. Hoff, ed.), American Concrete Institute, Detroit, Mich., 1984, pp. 325–349.
5. R. S. Rollings. Field Performance of Fiber Reinforced Concrete Airfield Pavements. *Technical Report GL-86*, U.S. Army Engineer Waterways Experiment Station, Vicksburg, Miss., 1986.
6. E. K. Schrader. Fiber Reinforced Concrete Pavements and Slabs. *U.S./Sweden Joint Seminar (NSF-STU)*, Swedish Cement and Concrete Research Institute, Stockholm, Sweden, 1985, pp. 109–131.
7. G. Wu and M. Jones. Navy Experience with Steel Fiber Reinforced Concrete Airfield Pavement. In *Report SP-105: Fiber Reinforced Concrete Properties and Applications* (S. P. Shah and G. B. Batson, eds.), American Concrete Institute, Detroit, Mich., 1987, pp. 403–418.
8. *Roller Compacted Concrete Pavement*. Report C-8. American Concrete Institute, Detroit, Mich., 1987.
9. A. Nanni and A. Johari. RCC Pavement Reinforced With Steel Fibers. *ACI Materials Journal*, Vol. 13, No. 3, March 1989, pp. 64–60.
10. E. K. Schrader, et al., Composite Concrete Pavements with Roller-Compacted Concrete. In *Transportation Research Record 1003*, TRB, National Research Council, Washington, D.C., 1985, pp. 50–56.
11. G. C. Hoff. Durability of Fiber Reinforced Concrete. In *Report SP-100: Concrete Durability* (J. M. Scanlon ed.), Vol. 1, American Concrete Institute, Detroit, Mich., 1987, pp. 997–1041.
12. Brief News: RCC Paves Municipal Street. *Civil Engineering*, Vol. 57, No. 11, November 1987.
13. O. Keifer, Jr. Paving with RCC. *Civil Engineering*, Vol. 57, No. 10, October 1987, pp. 65–68.
14. Structural Design of Roller-Compacted Concrete for Industrial Pavements. Report IS233.01P. Portland Cement Association, Skokie, Ill., 1987.
15. *Technical Manual*. Fibresteel, Five Dock, Australia, 1981, 47 pp.
16. E. K. Schrader. Design Methods for Pavements with Special Concretes. In *Report ACI SP-81: Fiber Reinforced Concrete* (G. C. Hoff, ed.), American Concrete Institute, Detroit, Mich., 1984, pp. 197–212.
17. V. Ramakrishnan, et al. Flexural Fatigue Strength of Steel Fiber Reinforced Concrete. In *Report ACI SP-105: Fiber Reinforced Concrete Properties and Applications*. (S. P. Shah and G. B. Batson eds.), American Concrete Institute, Detroit, Mich., 1987, pp. 225–245.
18. R. G. Packard. *AIRPORT-Concrete Thickness Design for Airport and Industrial Pavements*. Concrete Design Software Library Program No. MC006X. Portland Cement Association, Skokie, Ill., 1986.
19. Thickness Design of Roller-Compacted Concrete Pavements for Airfields, Roads, Streets, and Parking Areas. Report ETL 1110-1-141. U.S. Army Corps of Engineers, Washington, D.C., 1988. 3 pp.
20. R. S. Rollings. Design of Roller Compacted Concrete Pavements. In *Proc., Roller Compacted Concrete II* (K. D. Hansen and L. K. Guice eds.), American Society of Civil Engineers, New York, N.Y., 1988, pp. 454–466.
21. D. W. Pittman and S. A. Ragan. A Guide for Design and Construction of Roller-Compacted Concrete Pavements. In *Technical Report GL-86*, U.S. Army Engineer Waterways Experiment Station, Vicksburg, Miss., 1986.

Flexural Behavior and Toughness of Fiber Reinforced Concretes

V. RAMAKRISHNAN, GEORGE Y. WU, AND GIRISH HOSALLI

This paper presents the results of an extensive investigation to determine the behavior and performance characteristics of the most commonly used fiber reinforced concretes (FRC) for potential airfield pavements and overlay applications. A comparative evaluation of static flexural strength is presented for concretes with and without four different types of fibers: hooked-end steel, straight steel, corrugated steel, and polypropylene. These fibers were tested in four different quantities (0.5, 1.0, 1.5, and 2.0 percent by volume), and the same basic mix proportions were used for all concretes. The test program included (a) fresh concrete properties, including slump, vebe time, inverted cone time, air content, unit weight and concrete temperature, and hardened concrete properties; (b) static flexural strength, including load-deflection curves, first-crack strength and toughness, toughness indexes, and post-crack load drop; and (c) pulse velocity. In general, placing and finishing concretes with less than 1 percent by volume for all fibers using laboratory-prepared test specimens was not difficult. However, the maximum quantity of hooked-end fibers that could be added without causing balling was limited to 1 percent by volume. Corrugated steel fibers (Type C) performed the best in fresh concrete; even at higher fiber contents (2 percent by volume), there was no balling, bleeding, or segregation. Higher quantities (2 percent by volume) of straight steel fibers caused balling, and higher quantities of polypropylene fibers (2 percent by volume) entrapped a considerable amount of air. Compared with plain concrete, the addition of fibers increased the first-crack strength (15 percent to 90 percent), static flexural strength (15 percent to 129 percent), toughness index, post-crack load-carrying capacity, and energy absorption capacity. Compared with an equal 1 percent by volume basis, the hooked-end steel fiber contributed to the highest increase, and the straight steel fiber provided the least (but appreciable) increase in the above-mentioned properties.

Previous research by Ramakrishnan (*1–5,9–13*) and others (*6–8*) has established that the addition of fibers to concrete considerably improves static flexural strength, impact strength, shear and torsional strength, direct tensile strength, fatigue strength, shock resistance, ductility, and failure toughness. The degree of these improvements, however, depends on the type, size, shape, and aspect ratio of the fibers.

The research cited above involved small-scale, independent pilot projects for various types of fibers. Yet an extensive scientific investigation was still needed to determine the performance characteristics of the fibers and mix proportions most commonly used in field practice. Evaluation of the comparative behavior and properties of various fiber types at different fiber contents was also necessary. Furthermore, lack of sufficient information on the toughness and static flexural behavior of concretes with different types and quantities of fibers underscores the need for more research. This information is essential for fiber reinforced concrete (FRC) in potential airfield overlay applications.

V. Ramakrishnan and G. Hosalli, South Dakota School of Mines and Technology, Rapid City, S. Dak. 57701. G. Y. Wu, Naval Civil Engineering Laboratory, Port Hueneme, Calif. 93043-5000.

OBJECTIVES

The objectives of this investigation are as follows:

- To determine the fresh concrete properties, including workability, balling characteristics, and finishability, of concretes reinforced with four types of fibers (hooked-end steel, straight steel, corrugated steel, and polypropylene) and to compare their properties with those of corresponding plain concrete;
- To study the effect on fresh and hardened concrete properties due to the addition of the four types of fibers at 0.5, 1.0, 1.5, and 2.0 percent by volume for steel fibers and 0.1, 0.5, 1.0, and 2.0 percent by volume for polypropylene fibers to a plain concrete mix; and
- To conduct a detailed investigation of the static flexural behavior, including first-crack strength, modulus of rupture, load-deflection curve, post-crack deformation characteristics, post-crack load drop, and toughness indexes.

MATERIALS, MIXES, AND TEST SPECIMENS

Materials

Fibers

The following four types of fibers were used in this investigation:

1. *Type A*. The 2-in.-long hooked-end steel fibers used were glued together side by side into bundles with a water-soluble adhesive. During the mixing process, the glue dissolved in water and the fibers separated into individual fibers, creating an aspect ratio of 100.
2. *Type B*. The straight steel fibers used were made from low carbon steel with a rectangular cross section of 0.009 in. × 0.030 in. and a length of 0.75 in. Their aspect ratio was approximately 40.
3. *Type C*. The 2-in.-long corrugated steel fibers used were produced from a mild carbon steel with an aspect ratio of 40 to 65.
4. *Type D*. The polypropylene fibers used were collated, fibrillated, and ¾ in. long.

Cement

ASTM Type I/II (dual purpose) portland cement was used.

Coarse Aggregate

The aggregates used were maximum size ⅜ in. and maximum size 1 in. They were blended in a mixture of 60 percent aggregate with a 1-in. maximum size and 40 percent aggregate with a ⅜-in. maximum size. The mixture satisfied ASTM C33.

Fine Aggregate

The fine aggregate used was natural river sand with a water absorption coefficient of 1.64 percent and a fineness modulus of 3.02.

Admixtures

A superplasticizer satisfying the requirements of ASTM C494 for chemical admixtures and an air-entraining agent satisfying the requirements of ASTM C260 were used.

Mixes

The same proportions were used for the plain (control) and FRC mixes. The mix design is as follows:

Cement	658 lb/yd³
Coarse aggregate	1,560 lb/yd³
Fine aggregate	1,560 lb/yd³
Air content	5 ± 1.5 percent

The water-to-cement ratio was maintained at 0.4 for all concretes.

For the static flexure strength test, two mixes without fibers and four mixes each for Type B and C fibers were made with 0.5, 1.0, 1.5, and 2.0 percent by volume (66, 132, 198, and 264 lb/yd³, respectively). In the case of Type A fibers (hooked end), the maximum quantity of fibers that could be added without creating balling was 132 lb/yd³ (1 percent by volume). Therefore, only three mixes with 0.5, 0.75, and 1.0 percent by volume (66, 99, and 132 lb/yd³) of hooked-end fibers were used. For Type D fibers (polypropylene), four mixes with 0.1, 0.5, 1.0, and 2.0 percent by volume (1.5, 7.5, 15, and 30 lb/yd³) were made.

Test Specimens

For static flexural testing, beams of size 6 in. × 6 in. × 21 in. (152 mm × 152 mm × 533 mm) were cast. Cylinders 6 in. × 12 in. (152 mm × 305 mm) were cast for compression and modulus of elasticity tests. Specimens were made with a mechanical table vibrator.

TESTS FOR FRESH CONCRETE

The freshly mixed concrete was tested for slump (ASTM C143), air content (ASTM C231), fresh concrete unit weight (ASTM C138), temperature, time of flow through an inverted cone (ASTM C995), and vebe time.

TESTS FOR HARDENED CONCRETE

Cylinders were tested for compressive strength (ASTM C39) and static modulus (ASTM C469) at 28 days of age.

STATIC FLEXURE TEST

Beams were tested at 28 days for static flexural strength (ASTM C1018) and pulse velocity (ASTM C597). Some of the beams were also tested at 7 days. Toughness indexes were calculated using the load-deflection data. According to ASTM C1018, third point loading was applied to the beams in the static flexural test. The span length was 18 in. (457 mm). Deflection was measured at mid span using a dial gauge accurate to 0.001 in. (0.0254 mm). This test was a deflection-controlled test, with the rate of deflection kept in the 0.002 to 0.004 in./min range as per ASTM C1018. The loads were recorded at every 0.002-in. increment in deflection until the first crack appeared. Thereafter, the loads were recorded at different intervals.

TEST RESULTS AND DISCUSSION

Aspect Ratio

It is well known that the aspect ratio of straight fibers has a considerable effect on the performance of fresh and hardened concrete. Yet it is not practical to assess the relative value of the aspect ratio with regard to deformed or modified fibers (corrugated, hooked, collated, or fibrillated). Hence, the aspect ratio was not selected as a parameter for study. In this investigation, four commercially available and commonly used fibers were selected. Each has substantially different apparent aspect ratios (Type A fiber has twice as much as that of Types B and C). The cost difference between the fibers is also substantial (one fiber costs twice as much as another fiber).

Fresh Concrete Properties

Room temperature, humidity, and concrete temperature were recorded to ensure that all the mixes were combined under similar conditions. The room temperature and humidity varied in the range of 18°–27°C and 33 percent–58 percent, respectively. The concrete temperature range was 20.4°–27.2°C.

Workability

Three tests were performed to determine the workability of the mixes: slump, inverted cone time, and vebe time. Test results indicated that, in general, satisfactory workability can be maintained even with a relatively high fiber content for corrugated steel fiber concretes. This was achieved by adjusting the amount of superplasticizer used; the water-to-cement ratio remained constant (0.40) for all mixes. For the plain concrete, about 675 cc of superplasticizer was needed. The mix with 2 percent fibers by volume required 1735 cc of super-

plasticizer, representing an increase of 157 percent. The superplasticizer dosage varied from 860 cc to 1735 cc for the fiber concrete.

For the straight steel fiber mixes, balling tendency was observed with higher fiber quantities. In the case of hooked-end steel fibers, the maximum amount of fibers that could be added without inducing balling and segregation was 1.0 percent by volume.

With higher quantities of polypropylene fibers, the concrete had poor workability and more bleeding and segregation. For mix D4 with 2.0 percent by volume of polypropylene fibers, the water-to-cement ratio was increased to 0.49, and a higher quantity of superplasticizer was added to obtain better workability. In spite of this, the concrete was difficult to place and finish, resulting in bleeding and segregation. Concretes with higher quantities of polypropylene fibers also had higher quantities of entrapped air.

Based on test results, the relationship between vebe time and slump for each type of fiber is not affected by fiber contents for the range tested in this investigation. The relationship is different, however, for other types of fibers.

The inverted cone test was specifically developed to measure the workability of FRC in the field. Since both the inverted cone test and the vebe test are based on the energy requirements for flowability and compaction, a linear correlation exists between the two tests.

Finishability

Good finishability was achieved with an appropriate dosage of superplasticizer.

Hardened Concrete Properties

Compressive Strength and Static Modulus

The average values of compressive strength (f'_c) and static modulus of elasticity (E_c) for different concretes with four types of fibers and different volumes are shown in Tables 1 through 4. Each value in the tables represents the average of four tests.

The compressive strength was 7,040 psi for plain concrete. For the fibrous concrete with 0.5 percent and 1.0 percent fiber contents, the strength decreased slightly except for Type A fiber. For higher quantities of fibers (1.5 percent and 2.0 percent by volume), there was appreciable reduction in compressive strength with Type B and Type C fibers and a tremendous decrease with Type D fibers. The low compressive strength is due to the entrapped air content (13.9 percent) and low unit weight. The lower strength in fibrous concretes may be attributed to the difficulty in controlling the air content. The decrease in strength is also due to the increase in yield with a consequent reduction in cement factor. In this investigation, a basic mix proportion was maintained, and fibers in different quantities were added without considering

TABLE 1 HARDENED CONCRETE PROPERTIES FOR 0.5 PERCENT FIBER CONTENT

Fiber Type	f'_c (psi)	E_c (10^6 psi)	Pulse Velocity (fps)	f_r (psi)
Plain concrete	7,040	3.56	14,639	620
A	7,450	3.68	14,927	1,130
B	7,030	3.53	14,671	715
C	6,830	3.54	14,520	775
D	6,070	3.38	14,598	770

NOTES:
f'_c = compressive strength at 28 days
E_c = static modulus at 28 days
f_r = modulus of rupture at 28 days

TABLE 2 HARDENED CONCRETE PROPERTIES FOR 1.0 PERCENT FIBER CONTENT

Fiber Type	f'_c (psi)	E_c (10^6 psi)	Pulse Velocity (fps)	f_r (psi)
Plain concrete	7,040	3.56	14,639	620
A	8,340	3.55	14,732	1,420
B	6,830	3.49	14,743	880
C	6,070	3.38	14,113	820
D	5,550	3.30	14,215	680

NOTES:
f'_c = compressive strength at 28 days
E_c = static modulus at 28 days
f_r = modulus of rupture at 28 days

TABLE 3 HARDENED CONCRETE PROPERTIES FOR 1.5 PERCENT FIBER CONTENT

Fiber Type	f'_c (psi)	E_c (10^6 psi)	Pulse Velocity (fps)	f_r (psi)
Plain concrete	7,040	3.56	14,639	620
B	7,010	3.57	14,618	1,010
C	5,630	2.92	13,764	1,065

NOTES:
f'_c = compressive strength at 28 days
E_c = static modulus at 28 days
f_r = modulus of rupture at 28 days

TABLE 4 HARDENED CONCRETE PROPERTIES FOR 2.0 PERCENT FIBER CONTENT

Fiber Type	f'_c (psi)	E_c (10^6 psi)	Pulse Velocity (fps)	f_r (psi)
Plain concrete	7,040	3.56	14,639	620
B	5,190	3.38	13,820	900
C	5,530	3.05	13,882	1,120
D	1,470	1.44	12,120	440

NOTES:
f'_c = compressive strength at 28 days
E_c = static modulus at 28 days
f_r = modulus of rupture at 28 days

the fiber factor. If optimum mix proportions were obtained by trail mixes and used for different fiber contents, then the same compressive strengths could have been maintained.

Pulse Velocity

The results for pulse velocity are also given in Tables 1 through 4. The average pulse velocity at 28 days was 14,184 fps with a maximum of 14,639 fps (3.21 percent) and a minimum of 13,764 fps (2.96 percent), indicating a significant degree of consistency and quality control. The results also demonstrate that fiber content has little or no effect on pulse velocity. Finally, it indicates that the addition of steel fibers does not affect the elastic wave transmitting property of concrete.

Static Flexural Strength (Modulus of Rupture)

Results of static flexural strength (f_r) are tabulated in Tables 5 and 6. The values given in the tables represent the average of four test results. Within-test standard deviation and coefficient of variation values calculated for all the mixes were found to be very low. However, the variations between the beams for a given type of mix are likely to be larger for fiber reinforced specimens than those without fibers. This is due to the difficulty of achieving the same uniform distribution of the random oriented fibers. For approximately the same first-crack deflection, there is an increase in first-crack load for the concretes with increasing fiber content. It can also be observed that the flexural strength increases by 25 percent, 32 percent, 72 percent, and 81 percent for the concretes with corrugated steel fiber contents 0.5 percent, 1.0 percent, 1.5 percent, and 2.0 percent compared with that of plain concrete.

For 2.0 percent by volume polypropylene FRC, the compressive strength was very low, and hence the flexural strength was also significantly low. Similarly, for 1.5 percent and 2.0 percent fiber volumes of Type B and C fibers, the compressive strengths were low, and hence the flexural strengths were less. As a result, the direct flexural strength comparison may be misleading. Figure 1 illustrates the true effect of adding different types of fibers and quantities to a basic plain concrete mix. The maximum increase in flexural strength occurred when Type A fibers (hooked end) were added (Table 1). The increase was higher when higher quantities of fibers were added for all four fiber types. The smallest increase occurred in the case of polypropylene and straight steel FRC. Appreciable increase in flexural strength occurred when corrugated steel fibers were added. Higher quantities caused higher increases up to 2.0 percent by volume of fibers.

The values of $f_r/\sqrt{f'_c}$ for different types of fibers with various fiber contents are shown in Figure 2. A linear relationship between the fiber quantity expressed as a volume percentage (p_f) and the normalized flexural strength ($f_r/\sqrt{f'_c}$) is indicated for each type of fiber. However, the relationship varies for different types of fibers. Therefore, four separate linear equations were obtained for four types of fibers and are used

TABLE 5 MODULUS OF RUPTURE (FLEXURAL STRENGTH)

Fiber Content (%)	Fiber Type A		B		C		D	
	f_r	$f_r/\sqrt{f'_c}$	f_r	$f_r/\sqrt{f'_c}$	f_r	$f_r/\sqrt{f'_c}$	f_r	$f_r/\sqrt{f'_c}$
0.5	1,130	13.09	715	9.08	775	9.38	770	9.88
1.0	1,420	15.55	880	10.65	820	10.41	680	9.13
1.5	—	—	1,010	12.06	1,065	14.19	—	—
2.0	—	—	900	12.49	1,120	15.06	440	11.48

NOTES:
f_r = modulus of rupture
f'_c = compressive strength

TABLE 6 FLEXURAL STRENGTH AT FIRST CRACK

Fiber Content (%)	Fiber Type A		B		C		D	
	f_{fc}	$f_{fc}/\sqrt{f'_c}$	f_{fc}	$f_{fc}/\sqrt{f'_c}$	f_{fc}	$f_{fc}/\sqrt{f'_c}$	f_{fc}	$f_{fc}/\sqrt{f'_c}$
0.5	990	11.47	715	8.53	750	9.08	770	9.88
1.0	1,180	12.92	880	10.65	745	9.56	680	9.13
1.5	—	—	1,010	12.03	880	11.73	—	—
2.0	—	—	895	12.42	930	12.51	435	11.35

NOTES:
f_{fc} = flexural strength at first crack
f'_c = compressive strength

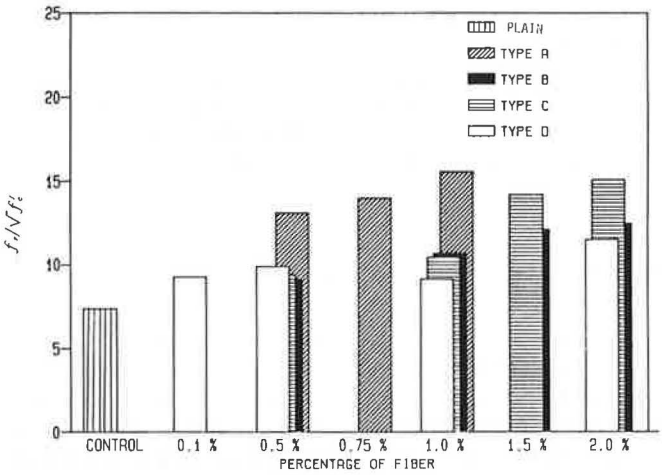

FIGURE 1 Fiber content vs. $f_r/\sqrt{f'_c}$.

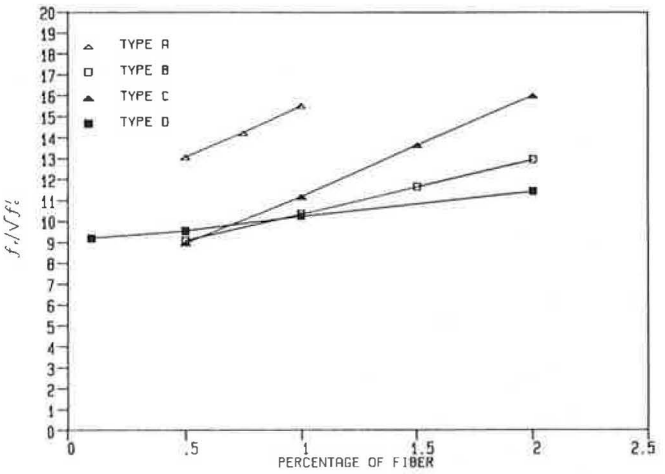

FIGURE 2 Percentage of fiber vs. $f_r/\sqrt{f'_c}$.

below. These equations are valid for fiber contents varying from 0.5 to 2.0 percent by volume except for Type A fiber (the experimental range used in this investigation). Equation 1 is only valid for fiber contents from 0.5 to 1.0 percent by volume. This range covers almost all the fiber contents currently used in the field.

$$f_{ra} = (4.82p_f + 10.68)\sqrt{f'_c} \quad (1)$$

$$f_{rb} = (2.613p_f + 7.773)\sqrt{f'_c} \quad (2)$$

$$f_{rc} = (4.667p_f + 6.667)\sqrt{f'_c} \quad (3)$$

$$f_{rd} = (1.184p_f + 9.032)\sqrt{f'_c} \quad (4)$$

where f_{ra}, f_{rb}, f_{rc}, and f_{rd} are the modulus of rupture of concretes with Type A, B, C, and D fibers, respectively, and p_f is the fiber content expressed as a volume percentage. The equations are valid only for the aspect ratios used in this investigation.

Load-Deflection Behavior

A significant performance difference of concretes with and without fibers is observed in the load-deflection curves, first-crack strengths, and toughness indexes.

Load-deflection curves are a standardized method of quantifying the energy a beam absorbs during its load-induced flexural deflection. The area under the curve represents the energy absorbed by the beam.

Load-deflection curves were drawn using the data from the static flexure test. Typical load-deflection comparison curves are given for the four fiber contents used in this investigation: 0.5 percent, 1.0 percent, 1.5 percent, and 2.0 percent by volume for Types A, B, C, and D, respectively. These curves are shown in Figures 3 through 6. Unlike plain concrete, FRC does not fail in a brittle, catastrophic manner at the formation of the first crack under a clearly identifiable maximum load. Well before signs of significant material distress are visible, the load-deflection curve becomes nonlinear; microscopic examination of the specimen revealed fine cracks. An increase in fiber content caused an increase in first-crack strength for all fiber types as shown in Figures 3 through 6. As explained

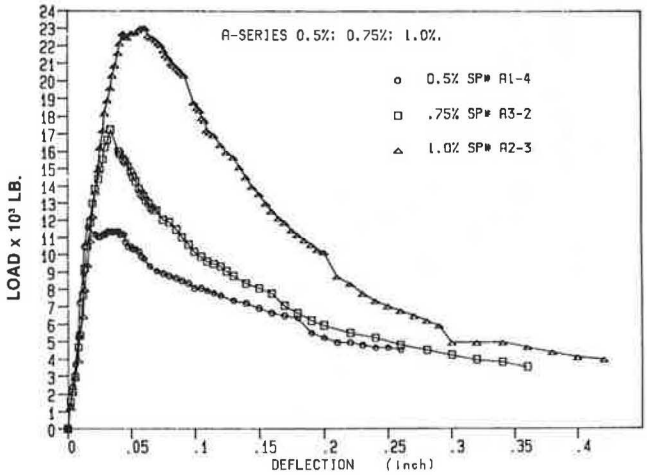

FIGURE 3 Comparison of load-deflection curves for hooked-end steel fiber.

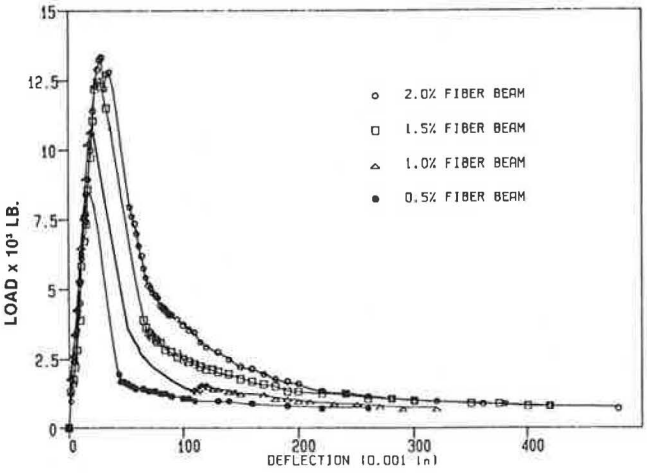

FIGURE 4 Comparison of load-deflection curves for straight steel fiber.

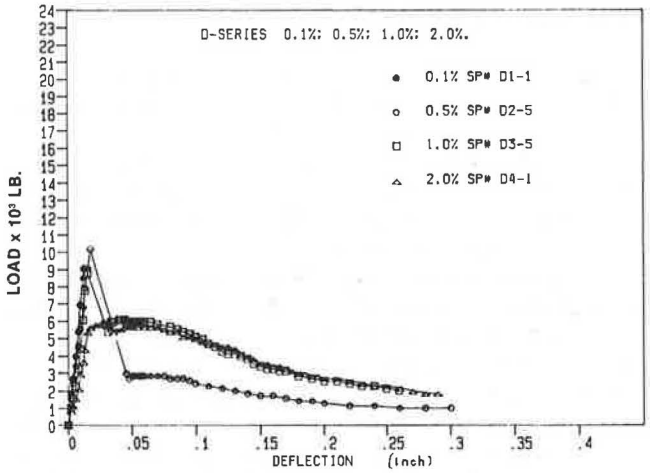

FIGURE 5 Comparison of load-deflection curves for corrugated steel fiber.

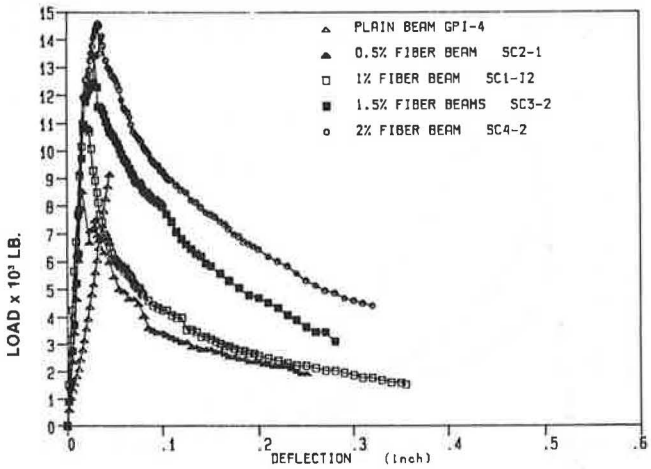

FIGURE 6 Comparison of load-deflection curves for polypropylene fiber.

previously, in the case of concretes with higher quantities of Type B and Type D fibers (2.0 percent by volume), the compressive strength (hence the flexural strength and the first-crack strength) decreased compared with the control concrete due to the balling of fibers and a considerable increase in entrapped-air content.

The load-deflection comparison curves also show an improvement in the elastic-plastic behavior of the fiber concrete composite with an increase in fiber content from 0.5 percent to 2.0 percent with plain concrete, however, the beam failed immediately after the appearance of the first crack. These curves indicate that the load-carrying capacity and the flexural rigidity of the beams rise with an increase in fiber content, resulting in a lower deflection at the corresponding load level. Compared with plain concrete, the reduction in the flexural rigidity value with increased deflection is not severe for FRC. In other words, the rate of degeneration at the moment of inertia decreases as the fibers resist the propagation of the crack growth. The observed crack widths at corresponding load levels were also smaller with increased fiber contents.

The load-deflection curves for different types of fibers are compared for 0.5 percent, 1.0 percent, 1.5 percent, and 2.0 percent by volume fiber contents in Figures 7, 8, 9, and 10, respectively. The maximum increase in first-crack strength is provided by Type A fiber (hooked-end steel), and the smallest increase is due to Type B and D fibers (straight steel and polypropylene fibers).

Post-Crack Load Drop Phenomenon

Post-crack load drop is the difference between the maximum load and the load recorded at a deflection equal to three times the deflection measured at first crack. The post-crack load drop phenomenon decreases with increasing fiber content. The load drops expressed as a percentage of maximum loads are 21 percent, 15 percent, 13 percent, and 7 percent, respectively, for the beams with 0.5 percent, 1.0 percent, 1.5 percent, and 2.0 percent corrugated steel fiber contents (Figure

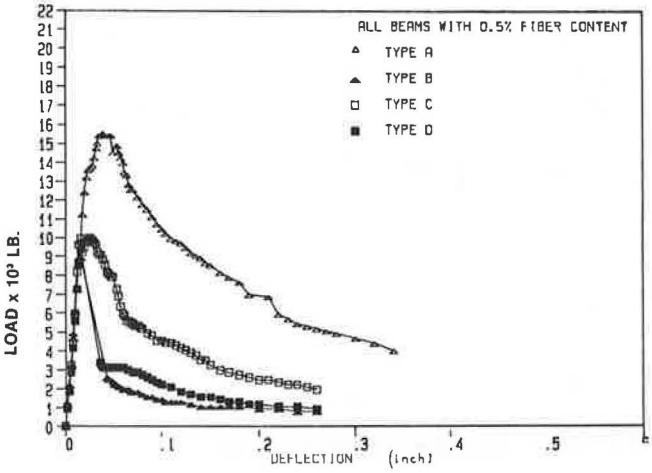

FIGURE 7 Load-deflection comparison for all fibers (0.5 percent fiber content by volume).

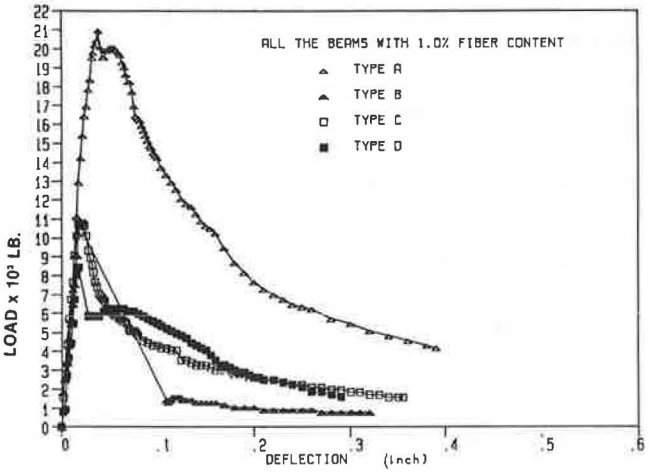

FIGURE 8 Load-deflection comparison for all fibers (1.0 percent fiber content by volume).

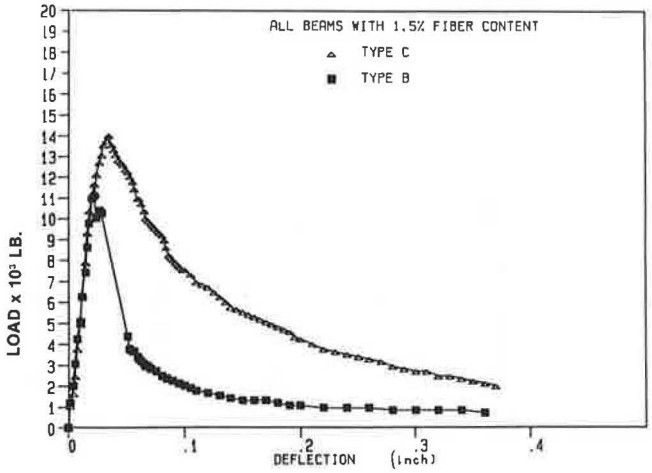

FIGURE 9 Load-deflection comparison for fibers B and C (1.5 percent fiber content by volume).

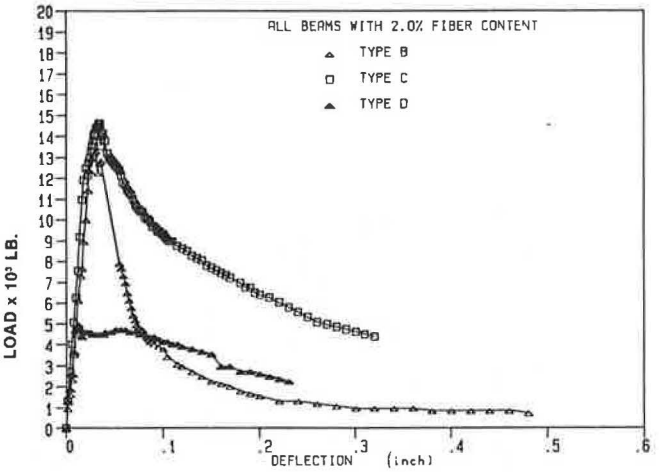

FIGURE 10 Load-deflection comparison for fibers B, C, and D (2.0 percent fiber content by volume).

5). The post-crack load drop for straight steel and polypropylene fibers is considerable as shown in Figure 4 and 6. However, in the case of hooked-end fiber, the load drop is considerably less (Figure 3). Table 7 presents a comparison of load drops calculated from the typical load-deflection curves for four types of fibers (Figures 3 through 6).

Toughness Indexes

Toughness index (ASTM C1018) is a dimensionless parameter that defines or fingerprints the shape of the load-deflection curve. By including the percentage post-crack load drop values as suggested above, the fingerprinting of the shape of the load-deflection curve can be further improved. Indexes have been defined on the basis of three service levels, identified as multiples of the first-crack deflection. The index is computed by dividing the total area under the load-deflection curve up to the given service level deflection by the area under the same curve up to the first-crack deflection. Toughness index I_5 is calculated for a deflection of three times the first-crack deflection. Likewise, I_{10} and I_{30} are the indexes up to 5.5 and 15.5 times the first-crack deflection, respectively.

TABLE 7 POST-CRACK LOAD DROP

Fiber Content (%)	Fiber Type (%)			
	A	B	C	D
0.1	—	—	—	100[a]
0.5	21	80	21	68
0.75	14	—	—	—
1.0	11	77	15	32
1.5	—	69	13	—
2.0	—	60	7	18

[a]Failed fully.

TABLE 8 TOUGHNESS INDEXES FOR 0.5 PERCENT FIBER CONTENT

Fiber Type	I_5	I_{10}	I_{30}	I_{10}/I_5	I_{30}/I_{10}
Plain concrete	1	1	1	1	1
A	5.460	10.109	21.988	1.848	2.178
B	4.379	5.862	8.823	1.331	1.716
C	4.464	8.049	15.618	1.815	1.868
D	3.606	5.675	9.295	1.568	1.653

TABLE 9 TOUGHNESS INDEXES FOR 1.0 PERCENT FIBER CONTENT

Fiber Type	I_5	I_{10}	I_{30}	I_{10}/I_5	I_{30}/I_{10}
Plain concrete	1	1	1	1	1
A	5.266	10.129	21.151	1.914	2.084
B	3.204	4.068	5.952	1.270	1.462
C	4.833	8.219	16.025	1.699	1.945
D	4.043	7.516	15.332	1.855	2.016

The toughness index for plain concrete is equal to 1 because all plain concrete beams failed immediately after first crack. The toughness indexes for fiber concretes vary greatly depending on the position of the crack, the type of fiber, the aspect ratio, the volume fraction of the fiber, and the distribution of fibers.

The calculated values of toughness indexes I_5, I_{10}, and I_{30} are tabulated in Tables 8 through 11. The I_5 values increase by 8 percent, 23 percent, and 21 percent, respectively, as the fiber content is increased from 0.5 percent to 1.0 percent, 1.5 percent, and 2.0 percent by volume for Type C fiber. Similar improvement can be observed for I_{10} and I_{30} values. The ratios of I_{10}/I_5 and I_{30}/I_{10} are good indicators of the plastic behavior of that particular specimen. The values equal to 2 and 3 for I_{10}/I_5 and I_{30}/I_{10}, respectively, indicate perfect plastic behavior.

TABLE 10 TOUGHNESS INDEXES FOR 1.5 PERCENT FIBER CONTENT

Fiber Type	I_5	I_{10}	I_{30}	I_{10}/I_5	I_{30}/I_{10}
Plain concrete	1	1	1	1	1
B	3.602	4.599	6.559	1.273	1.424
C	5.478	9.387	17.276	1.725	1.845

TABLE 11 TOUGHNESS INDEXES FOR 2.0 PERCENT FIBER CONTENT

Fiber Type	I_5	I_{10}	I_{30}	I_{10}/I_5	I_{30}/I_{10}
Plain concrete	1	1	1	1	1
B	4.275	5.987	9.077	1.401	1.517
C	5.366	9.588	21.623	1.783	2.135
D	5.341	10.653	25.542	1.993	2.392

The hooked-end and corrugated steel FRC demonstrate very close plastic behavior after first crack until 5.5 times the first-crack deflection, since the ratios I_{10}/I_5 are very close to 2. The beams with corrugated steel fiber, however, showed a decline in the load-carrying capacity after a deflection of 5.5 times the first-crack deflection, as indicated by the I_{30}/I_{10} ratios, which are considerably less than 3.0, in the region between 5.5 and 15.5 times the first-crack deflection.

Comparison of toughness indexes are shown in Figures 11, 12, and 13. For straight steel fibers (Type B), the I_{10} and I_{30} values are very low compared with those of other fibers.

CONCLUSIONS

Based on the experimental investigation, the following conclusions can be made:

- The workability of fresh FRC can be improved and maintained with the addition of an appropriate amount of superplasticizer. Generally, there was no difficulty in placing and finishing.
- There was no change in the elastic wave transmission properties of the concrete due to the addition of fibers, as indicated by the measured pulse velocities.
- Compared with plain concrete, FRC has higher first-crack strength, static flexural strength, toughness index, ductility, and post-crack energy absorption capacity. The improvement increases with increasing fiber content.
- For each fiber, there is a unique relationship between the flexural strength and the fiber content.
- The failure mode of FRC is ductile. The degree of ductility depends on the fiber type and is directly proportional to the fiber content.
- The higher the fiber content of FRC, the lower the corresponding post-crack load drop.

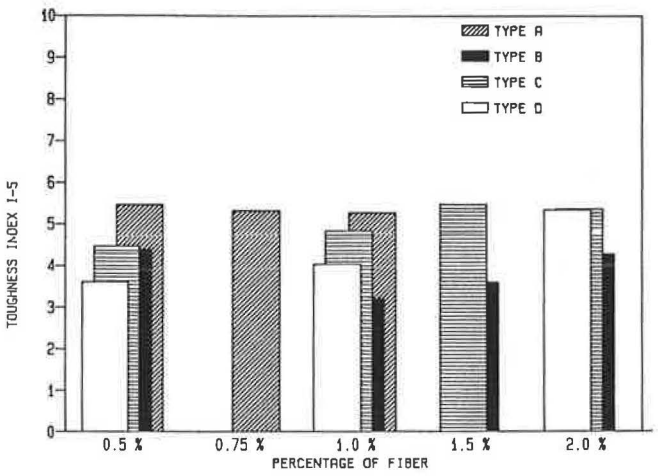

FIGURE 11 Toughness index I_5 comparison.

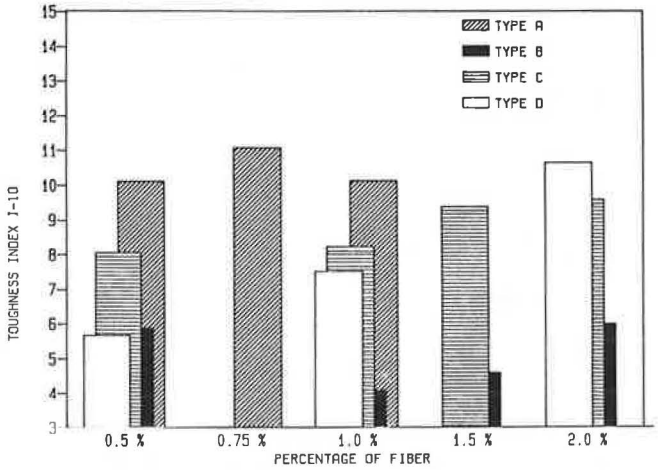

FIGURE 12 Toughness index I_{10} comparison.

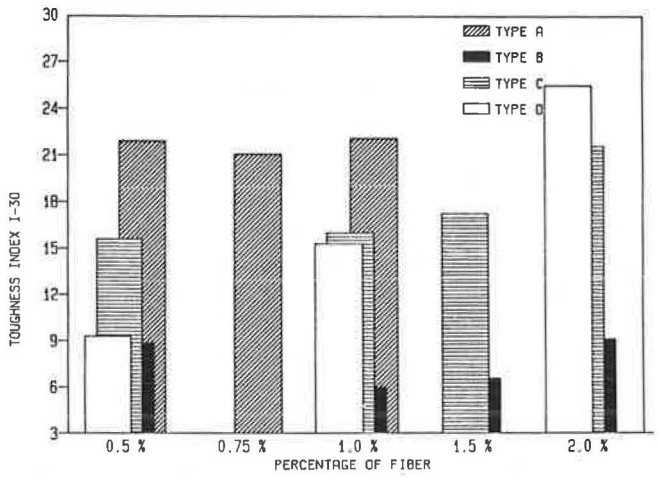

FIGURE 13 Toughness index I_{30} comparison.

ACKNOWLEDGMENT

The authors gratefully acknowledge the funding and support of the Naval Facilities Engineering Command.

REFERENCES

1. V. Ramakrishnan. *Superplasticized Fiber Reinforced Concrete for the Rehabilitation of Bridges and Pavements*, TRB, National Research Council, Washington, D.C., 1985, pp. 4–12.
2. V. Ramakrishnan, W. V. Coyle, P. A. Kopac, and T. J. Pasko. Performance Characteristics of Steel Fiber Reinforced Superplasticized Concrete. In *Report SP-68*, American Concrete Institute, Detroit, Mich., 1981, pp. 515–534.
3. V. Ramakrishnan, W. V. Coyle, V. Kulandaisamy, and E. K. Schrader. Performance Characteristics of Fiber Reinforced Concrete With Low Fiber Contents. *ACI Journal*, Vol. 78, No. 5, Sept.–Oct., 1981, pp. 384–394.
4. V. Ramakrishnan, T. Brandshaug, W. V. Coyle, and E. K. Schrader. A Comparative Evaluation of Concrete Reinforced With Straight Steel Fibers and Fibers With Deformed Ends Glued Together Into Bundles. *ACI Journal*, Vol. 77, No. 3, May–June 1980, pp. 135–143.
5. V. Ramakrishnan and W. V. Coyle. *Steel Fiber Reinforced Superplasticized Concrete for Rehabilitation of Bridge Decks and Highway Pavements*. Report DOT/RSPA/DMA-50/84-2. Office of University Research, U.S. Department of Transportation, 1983, p. 410.
6. ACI Committee 544. State-of-the-Art Report on Fiber Reinforced Concrete. In *Report 544 IR-82: Concrete International Design and Construction*, May 1982.
7. ACI Committee 544. Measurement of Properties of Fiber Reinforced Concrete. In *Report 544.2R.78: ACI Manual of Concrete Practice*, Part 5, American Concrete Institute, 1982.
8. *Report SP-81: Fiber Reinforced Concrete—International Symposium*. American Concrete Institute, Detroit, Mich., 1984.
9. V. Ramakrishnan. Performance Characteristics of Steel Fiber Reinforced Superplasticized Concrete. *Symposium L, Advances in Cement-Matrix Composites*, Materials Research Society, University Park, Pa., Nov. 1980.
10. P. Balaguru and V. Ramakrishnan. Mechanical Properties of Superplasticized Fiber Reinforced Concrete Developed for Bridge Decks and Highway Pavements. In *Report SP-93: Concrete in Transportation*, American Concrete Institute, Detroit, Mich., 1986, pp. 563–584.
11. V. Ramakrishnan. Materials and Properties of Fiber Reinforced Concrete. *Proc., International Symposium on Fiber Reinforced Concrete*, Madras, India, 1987, pp. 2.3–2.23.
12. P. Balaguru and V. Ramakrishnan. Comparison of Slump Cone and V-B Tests as Measures of Workability for Fiber Reinforced and Plain Concrete. *Cement, Concrete and Aggregates, CCAGDP*, Vol. 9, No. 1, Summer 1987.
13. P. Balaguru and V. Ramakrishnan. Properties of Fiber Reinforced Concrete: Workability, Behavior Under Long Term Loading and Air-Void Characteristics. *ACI Materials Journal*, Title No. 85-M23, May–June 1988, pp. 189–196.

The views expressed in this paper are those of the authors, who are responsible for its contents. The contents do not necessarily reflect official views or policies of the Naval Facilities Engineering Command.

A Comparative Evaluation of Plain, Polypropylene Fiber, Steel Fiber, and Wire Mesh Reinforced Shotcretes

D. R. MORGAN, N. MCASKILL, B. W. RICHARDSON, AND R. C. ZELLERS

Since the early 1970s, steel fiber reinforced shotcrete has been increasingly used for such applications as support in tunnels, mines, excavations, and rock slopes. Previous studies have shown that steel fiber reinforced shotcrete, at fiber addition rates now commonly used, can provide equivalent or even superior performance than that provided by standard wire mesh reinforcement, when properties such as residual load-carrying capacity after first crack are compared. This paper presents the results of recent studies comparing the performance of common wire mesh reinforced shotcretes with that of shotcretes reinforced with high-volume concentrations of a collated fibrillated polypropylene (CFP) fiber. The tests were conducted using wet-mix shotcrete applied to large panels, which were anchored and loaded to destruction with continuous monitoring of the crack formation and load vs. deflection characteristics of the panels. The panels were tested in the same manner as tests previously conducted on plain, wire mesh, and steel fiber reinforced shotcretes. Thus, the performance characteristics of the various shotcrete mixtures can be compared. It is shown that at certain addition rates of CFP fiber, similar residual load-carrying capacity after first crack can be obtained compared with shotcrete reinforced with wire mesh and shotcrete reinforced with steel fiber. Testing of standard flexural test beams to ASTM C1018 provided further verification of the equivalence of performance between shotcretes with these levels of addition of steel and CFP fiber with respect to parameters such as toughness index. The incorporation of high-volume concentrations of CFP fiber in wet-mix shotcrete presents opportunities for a wide range of applications where a tough, ductile, corrosion-resistant material is required.

Shotcrete has proven useful over the years for a wide variety of applications (*1*). These include

- Linings for support of underground openings in mines, tunnels, and other excavations;
- Soil and rock slope stabilization;
- Remedial works on deteriorated concrete and masonry structures;
- Construction of a wide variety of structures, including domes, culverts, canals, bulkheads, swimming pools, and water tanks; and
- Sealing surfaces of tailings and waste rock piles and toxic waste disposal sites.

Plain shotcrete has been used in some of the above applications. In most applications, however, various degrees of reinforcing are necessary to overcome the inherently low tensile strength and lack of ductility of portland cement concrete mixtures; conventional reinforcing steel or welded wire mesh fabric have long been used. More recently, steel fiber reinforcement has been found to be equivalent or even superior to traditional welded wire mesh reinforcement (*2*). Steel fiber reinforced shotcrete has enjoyed increasing use in a wide variety of shotcrete applications since the early 1970s (*3–6*).

Previous tests conducted on 1525 mm × 1525 mm × approximately 75 mm (5 ft × 5 ft × approximately 3 in) dry-mix shotcrete test panels (*2*) have established the equivalence, and even superior performance, of steel fiber reinforcement to certain wire mesh reinforcement. ASTM C1018 tests previously conducted on polypropylene fiber reinforced shotcrete (PFRS) by the authors provided a basis for the comparison of PFRS and steel fiber reinforced shotcrete. The following question, however, still arose:

> How does the performance of PFRS compare with that of mesh reinforced shotcrete in conditions of loading that might be experienced in such applications as support of rock slopes or underground openings?

This paper describes the program of testing that was undertaken to address this issue.

SHOTCRETE MIX DESIGN, PRODUCTION, AND APPLICATION

A wet-mix shotcrete mix design typical of mixes commonly used in the construction industry in the Vancouver area was selected for study. The mix proportions are given in Table 1. The shotcrete contained 400 kg/m³ (675 lb/yd³) of cement and a combined aggregate gradation that conformed to the requirements of ACI 506.2–77, Table 2.2.1. Gradation No. 2 (i.e., a 10 mm (3/8 in.) maximum size aggregate).

The shotcrete was supplied in 1.0 m³ (1.3 yd³) loads in a transit mixer. The slump, air content, and temperature were checked when the transit mixer arrived at the test site. Additional water was added to the fiber reinforced shotcrete mixes, prior to fiber addition, to produce the required slump for shooting. All shotcretes were applied at slumps in the range of 25 to 50 mm (1 to 2 in.). (If compressive strength or minimization of drying shrinkage capacity of the shotcrete are of concern, superplasticizers can be used instead of water to provide the necessary slump after fiber addition. Superplas-

D. R. Morgan and N. McAskill, Hardy BBT Limited, 4052 Graveley Street, Burnaby, B.C., Canada V5C 3T6. B. W. Richardson, Elsro Construction Products, 38 Rayborn Crescent, St. Albert, Alberta, Canada T8N 3C7. R. C. Zellers, Forta Corporation, 100 Forta Drive, Grove City, Penn. 16127.

TABLE 1 BASE SHOTCRETE MIX DESIGN

Material	lb/cu. yd.	kg/m^3
Type I Cement	674	400
10 mm Coarse Aggregate	725	430
Concrete Sand (SSD)	2166	1285
Water	320	190
Water Reducing Admixture	8 fl. oz./100 lb Cement	500 ml/100 kg Cement
Air Content	5 ± 1 %	5 ± 1 %

TABLE 2 PROPERTIES OF FRESH CFP FIBER REINFORCED WET-MIX SHOTCRETE

Mix No.	Slump	Air (%)	Mix Temperature (°C)	Comments
1	30	5.5	11	Plain
2	50	4.8	11	Plain
3	200	4.8	8	Before fibres added
	45	N/A	8	6 kg/m^3 fibres added
4	100	5.2	7	Before fibres added
	40	N/A	7	4 kg/m^3 fibres added

Notes: 1) Ambient Temperature = +4°C

2) Fibre length = 38 mm (1-1/2 in.)

3) 1 kg/m^3 = 1.6856 lb/cu. yd.

ticizers were not used in this particular study.) Results of the tests on plastic shotcrete are given in Table 2.

The plain shotcrete was brought to the point of discharge by reversing the transit mixer drum. Then, the 38 mm (1½ in.) long Forta CR CFP fiber was dumped on the shotcrete, and the mixer drum was rotated at full mixing speed for approximately 5 min. This procedure provided excellent dispersion of the fibers throughout the mix. (Note: this same procedure has been used with equal success in 10 m^3 (13 yd^3) truck loads on recent construction projects; however, longer mixing times, usually about 6 to 8 min, are required with the larger load sizes.)

On completion of mixing, the shotcrete was discharged into a wet-mix shotcrete pump. It was then applied through a 50 mm (2 in.) I.D. hose. A 5600 L^3/min (200 ft^3/min) compressor was used for a supply of compressed air at the nozzle. A standard rubber-tipped wet-mix shotcrete nozzle was used. Both the plain and fiber reinforced shotcretes were readily pumped and pneumatically placed with no excess line pressures or blockages.

MANUFACTURE OF TEST PANELS

Small Test Panels

Standard 600 mm × 600 mm × 125 mm (24 in. × 24 in. × 5 in.) test panels were fabricated for each of the following shotcretes:

- Panel No. 2—Plain shotcrete,
- Panel No. 3—Shotcrete with 6 kg/m^3 (10.1 lb/yd^3) of 38 mm (1½ in.) long collated fibrillated polypropylene (CFP) fiber, and
- Panel No. 4—Shotcrete with 4 kg/m^3 (6.7 lb/yd^3) of 38 mm (1½ in.) long CFP fiber.

The panels were oriented at an angle of about 30° from vertical at the time of the shotcrete application. Immediately after fabrication, they were covered with a plastic sheet and allowed to cure in the field for 28 days. The reason for field curing, rather than standard moist curing in the laboratory,

was to subject the shotcrete to the same curing conditions as the large, field-cured test panels.

Large Test Panels

A series of eight 1525 mm × 1525 mm × approximately 75 mm (5 ft × 5 ft × approximately 3 in.) test panels were fabricated in this test program. Two of each of the following types of panels were shot:

- Panel No. 1—Plain shotcrete reinforced with 102 × 102 MW 13.3 × MW 13.3 (4 × 4 8/8) wire mesh,
- Panel No. 2—Plain shotcrete reinforced with 152 × 152 MW 18.7 × MW 18.7 (6 × 6 6/6) wire mesh,
- Panel No. 3—Shotcrete reinforced with 6 kg/m³ (10.1 lb/yd³) of 38 mm (1½ in.) long CFP fiber, and
- Panel No. 4—Shotcrete reinforced with 4 kg/m³ (6.7 lb/yd³) of 38 mm (1½ in.) long CFP fiber.

The panel forms were placed in a horizontal orientation. Wire mesh was chaired at a nominal height of 28 mm (1.1 in.) off the base form, using metal chairs in the mesh reinforced test panels. The actual concrete cover to the mesh, measured from the bottom of the panel, is shown in Table 3. Shotcrete was applied vertically downward to a nominal thickness of 75 mm (3 in.). Screeding was performed to remove high spots and improve control of the shotcrete thickness but was kept to a minimum to prevent disturbance of the freshly placed shotcrete. Average shotcrete thicknesses for the various test panels varied between 71.0 and 87.9 mm (2.8 and 3.5 in.). Actual thickness was determined on fracture faces of the different panels after completion of testing. Detailed thickness measurements are given in Table 4.

TABLE 3 CONCRETE COVER TO WIRE MESH IN 5 ft × 5 ft PANELS

PANEL	TEST METHOD	CONCRETE COVER MEASUREMENTS (mm)	AVERAGE (mm)
1	Restrained	25, 30, 30, 30, 28, 28, 27, 28	28.3
2	Restrained	23, 25, 30, 28, 28, 30, 25, 28, 27	27.1
1	Unrestrained	25, 33, 30, 30, 30, 23, 23	27.7
2	Unrestrained	15, 28, 30, 30, 28, 23, 20	24.9

NOTES: 1) Concrete cover is the distance between the wire mesh and the bottom of the panel.

2) 1 mm = 0.03937 in.

TABLE 4 THICKNESS MEASUREMENTS IN 5 ft × 5 ft TEST PANELS

PANEL	TEST METHOD	THICKNESS MEASUREMENTS (mm)	AVERAGE (mm)
1	Restrained	78, 78, 78, 73, 70, 74, 74	75.4
2	Restrained	70, 70, 73, 75, 73, 75, 80, 76, 80	74.6
3	Restrained	77, 80, 80, 80, 78, 78, 72, 74, 72	76.7
4	Restrained	88, 85, 83, 82, 89, 90, 90, 90, 90	87.4
1	Unrestrained	75, 74, 75, 77, 77, 70, 70	74.0
2	Unrestrained	72, 70, 70, 70, 70, 71, 74	71.0
3	Unrestrained	75, 80, 79, 81, 81, 81, 83, 82, 80	80.2
4	Unrestrained	88, 85, 85, 85, 88, 90, 90, 90, 90	87.9

NOTES: 1) Measurements taken along the fractured face of test panels.

2) 1 mm = 0.03937 in.

TEST PROCEDURES AND RESULTS

Standard Tests

At age 28 days, three 75 mm (3 in.) concrete cores were extracted, by diamond core drilling, from standard test panels 2, 3, and 4. The cores were trimmed, sulphur capped, and compression tested in accordance with ASTM C42. Test results are given in Table 5. Reported core compressive strengths have been corrected to equivalent 2:1 length/diameter ratios using the correction factors prescribed in ASTM C42.

An additional three 75 mm (3 in.) diameter cores were extracted at age 28 days from these same test panels to determine absorption, after immersion and boiling, and the volume of permeable voids in accordance with ASTM C642. Test results are given in Table 5.

Three 75 mm × 75 mm × 355 mm (3 in. × 3 in. × 14 in.) prisms were diamond saw cut at age 28 days from panels 2, 3, and 4. These prisms were tested in accordance with ASTM C1018 for

- First crack and ultimate flexural strength;
- I_5, I_{10}, and I_{20} toughness index; and
- $I_{5,10}$ and $I_{10,20}$ residual strength.

Test results are given in Table 5. These ASTM C1018 tests were performed on an MTS servo-controlled universal testing machine. Load vs. deformation data was recorded on an autographic X-Y plotter for fiber reinforced test specimens from test panels 3 and 4.

Tests on Large Shotcrete Panels

These tests were undertaken to simulate different loading conditions that could be imposed on an anchored shotcrete

TABLE 5 PHYSICAL PROPERTIES OF HARDENED POLYPROPYLENE FIBER REINFORCED WET-MIX SHOTCRETE AT 28 DAYS

PANEL NO./PROPERTY	2		3		4	
Fibre Dosage, kg/m^3	0	AVG.	6	AVG.	4	AVG.
Compressive Strength, MPa	47.4 47.3	47.4	38.5 40.2 40.2	39.6	42.8 41.4 41.4	41.9
First Crack Flexural Strength, MPa	5.9 5.1 5.3	5.4	4.9 5.2 3.6	4.6	4.9 4.2 4.9	4.7
Ultimate Flexural Strength, MPa	5.9 5.1 5.3	5.4	4.9 5.2 3.6	4.6	4.9 4.2 4.9	4.7
Toughness Index, I_5	-		3.5 2.8 3.6	3.3	2.3 2.5 2.8	2.5
Toughness Index, I_{10}	-		6.8 5.3 7.4	6.5	3.9 4.6 5.2	4.6
Toughness Index, I_{20}	-		10.7 8.0 11.9	10.2	5.4 6.6 7.6	6.5
Residual Strength, 20 (I_{10} - I_5), %	-		66 50 76	64	32 42 48	41
Residual Strength, 10 (I_{20} - I_{10}), %	-		39 27 45	37	15 20 24	20
Boiled Absorption, %	6.8 6.6 7.2	6.8	8.7 8.9 8.9	8.8	7.8 7.8 8.2	7.9
Permeable Voids, %	14.7 14.4 15.5	14.9	18.4 18.7 18.7	18.6	16.6 16.6 17.4	16.9

NOTES: 1) 1 mm = 0.03937 in.

2) 1 MPa = 145 psi

lining applied to surfaces such as a rock, soil, or concrete face. Two test configurations were investigated: (a) a restrained test assemblage, and (b) an unrestrained test assemblage. Details of these two test assemblages are displayed in Figures 1 and 2, respectively.

The 1525 × 1525 mm (5 ft × 5 ft) test panels were anchored at their corners at 1220 × 1220 mm (4 ft × 4 ft) centers. The restrained test assemblage used 100 mm (4 in.) diameter steel tube sections and 100 mm (4 in.) square anchor plates, but used chain links instead of steel tubes to provide an unrestrained, pin-ended loading condition.

The large test panels were tested at 28 days using central point loading. The load was applied to a 100 mm (4 in.) diameter steel plate using a calibrated hydraulic jack. The load was applied steadily in approximately 2 kN (225 lb) increments until center point deflections of approximately 50 mm (2 in.) had been reached in the restrained tests and until complete fracture and loss of load-carrying capacity had been reached in the unrestrained tests. Complete failure in the unrestrained test panels occurred at deflections in excess of 40 mm (1½ in.). Deflections were monitored with an independently supported dial gauge mounted centrally in the test panel, which could be read to an accuracy of 0.01 mm (0.0004 in.).

Complete load vs. deflection plots are shown in Figure 3 for the four restrained test panels and in Figure 4 for the four unrestrained test panels.

A record was kept of the mode of cracking and the loads at which different cracks occured in each of the test panels. All of the panels first fractured by development of a central transverse hinge. Crack widths versus load were recorded for the first primary cracks that developed. A number of the panels developed additional secondary cracks; however, the widths were not recorded.

On completion of load testing, the test panels were removed from the testing bed and broken into two halves along the prime fracture face. Panel thickness along this fracture face was measured at between 7 and 9 points along the panel, and an average thickness was calculated (see Table 4). The depth of concrete cover from the base of the test panel to the reinforcing mesh was also recorded at between 7 and 9 locations for mesh reinforced panels 1 and 2, and an average cover thickness was calculated (see Table 3).

DISCUSSION

Standard Tests

The compressive strength test results in Table 5 show that the fiber reinforced shotcrete panels have lower 28-day compressive strengths than the plain shotcrete. This is to be expected since the fiber reinforced shotcrete mixes were retempered with water to provide the necessary slump for shooting.

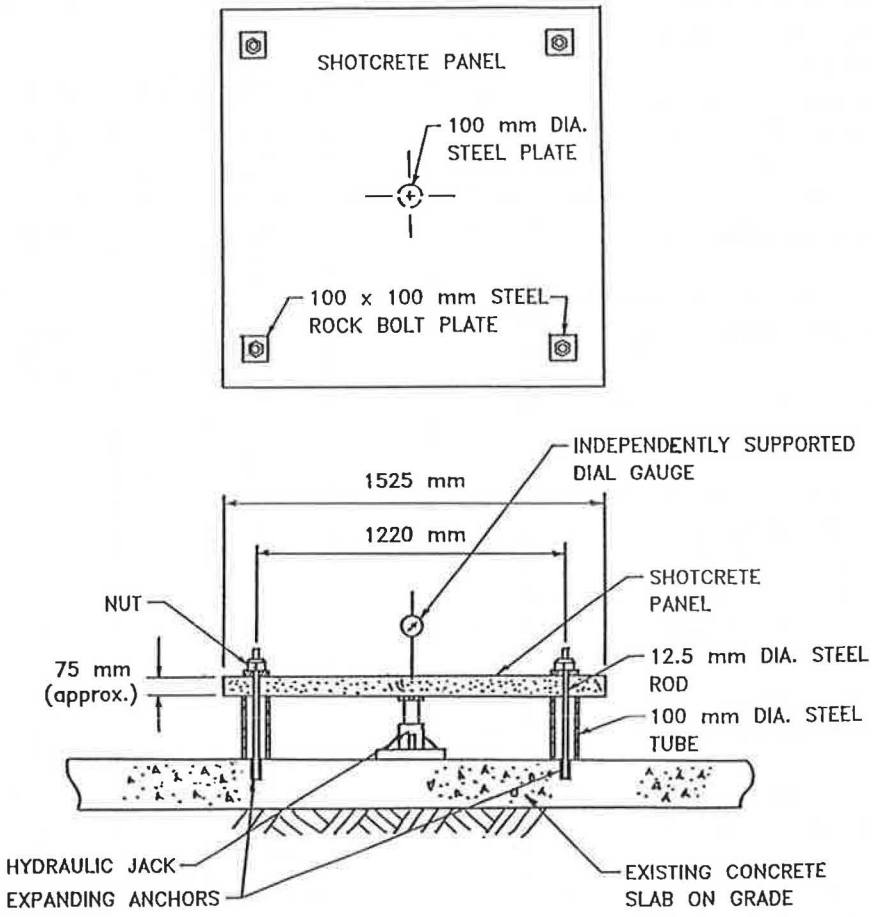

FIGURE 1 Details of restrained test assembly.

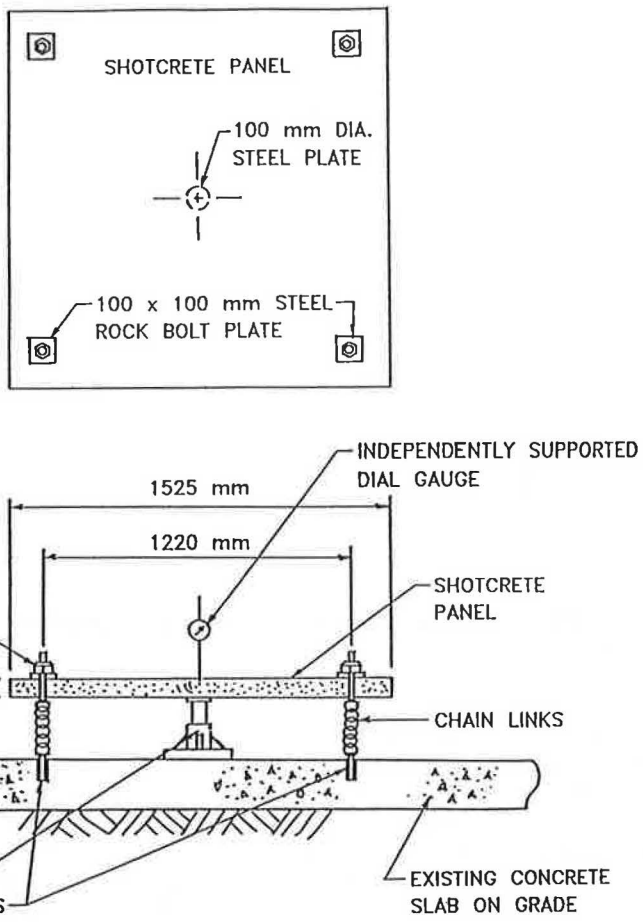

FIGURE 2 Details of unrestrained test assembly.

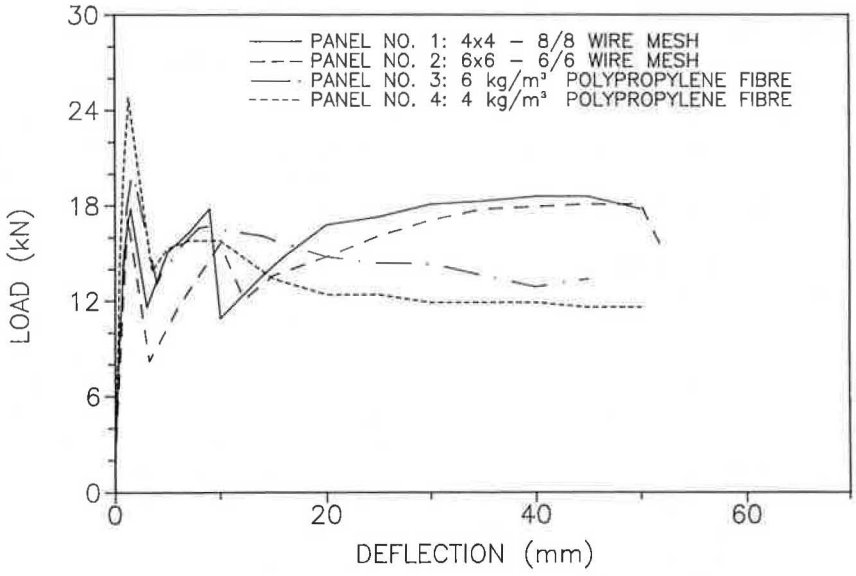

FIGURE 3 Load versus deformation (restrained) of polypropylene fiber versus wire mesh.

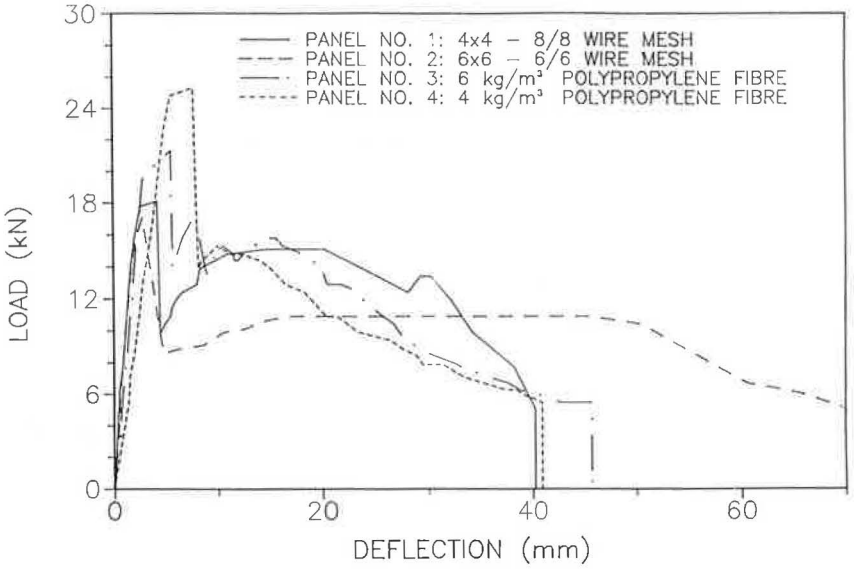

FIGURE 4 Load versus deformation (unrestrained) of polypropylene fiber versus wire mesh.

Nevertheless, the compressive strengths were quite adequate for most shotcrete applications at around 40 MPa (5,800 psi). [If concrete strength, or other factors related to increased water demand, are of concern (e.g. drying shrinkage) then the shotcrete could be retempered with superplasticizer to provide the necessary slump, without any increase in water demand.]

Similarly, the addition of water produced a reduction in flexural strength in fiber reinforced mixes (panels 3 and 4) compared with the plain shotcrete mix (panel 2), as shown in Table 5. Again, this is as expected. The recorded values of first crack and ultimate flexural strength were the same in each individual test, which reflects the fact that the load on the cracked shotcrete beams did not increase beyond the first crack load. This is as expected for the volume concentrations of fiber used in this study.

Of particular interest is the toughness index and residual strength data. The addition of 4 and 6 kg/m³ (6.7 and 10.1 lb/yd³) of 38 mm (1½ in.) long CFP fiber produced average 28-day I_5 toughness index values of 2.5 and 3.3, respectively, and I_{10} toughness index values of 4.6 and 6.5, respectively. The I_5 and I_{10} toughness index values for 4 kg/m³ (6.7 lb/yd³) of CFP fiber compare favorably with the performance of certain commercially used, lower aspect ratio steel fibers added at a rate of 60 kg/m³ (101 lb/yd³). The I_5 and I_{10} toughness index values for 6 kg/m³ (10.7 lb/yd³) of CFP fiber approach the performance of certain higher aspect ratio steel fibers commercially used at a dosage of 60 kg/m³ (101 lb/yd³) (7).

In terms of the descriptors suggested by Morgan (7) for ASTM C1018 toughness index values for steel fiber reinforced shotcretes, the mix with 6 kg/m³ (10.7 lb/yd³) CFP fiber could be given a "fair" to "good" rating. The volume concentration of 6 kg/m³ (10.7 lb/yd³) of CFP fiber in wet-mix shotcrete is 0.67 percent, and the volume concentration of 60 kg/m³ (101 lb/yd³) of steel fiber is 0.75 percent. This partially explains the good performance of the CFP fiber in shotcrete, in spite of the large difference in fiber mass compared with the mass of steel fibers used at typical dosage rates in wet-mix shotcrete. Probably of more significance, however, is the much larger number of CFP fibers, compared with steel, that span a fracture face at the above fiber addition rates. The fractured face of a PFRS specimen has an almost brush-like appearance.

The boiled absorption and volume of permeable voids in the fiber reinforced shotcrete mixes are higher than in the plain shotcrete mix, as shown in Table 5. This is attributed primarily to the effect of water addition in the fiber reinforced mixes. Retempering with superplasticizer would be expected to negate this effect. In terms of the indicators of shotcrete quality suggested by Morgan (7), the plain shotcrete mix (panel 2) and the mix with 4 kg/m³ (6.7 lb/yd³) CFP fiber (panel 4) would be rated as good and the mix with 6 kg/m³ (10.7 lb/yd³) CFP fiber (panel 3) would be rated as fair.

Tests on Large Shotcrete Panels

Two different loading configurations were evaluated: a restrained and an unrestrained test assemblage. The restrained test assemblage was designed to simulate the following conditions:

- Shotcrete has been applied to a substrate such as rock, soil, or concrete.
- The shotcrete is effectively anchored to the substrate with anchors spaced at 1.22 m (4 ft) on center.
- There is no effective bond to the substrate that can be relied on for resistance to applied loads (e.g., such conditions might exist for shotcrete applied to rock that is fractured in behind the bond interface; shotcrete applied to unconsolidated soil; or shotcrete applied to concrete that has continued to deteriorate behind the shotcrete layer, as can occur with alkali-aggregate reactivity).

The unrestrained test assemblage simulates the same conditions as the restrained test assemblage previously described, except that the restraint offered by the anchorage system has been lost. Such a condition might prevail where anchors have

TABLE 6 FIRST CRACK WIDTHS AND DEFLECTION AT TERMINATION OF LOAD TEST

PANEL NO.	TEST METHOD	AT TERMINATION OF TEST	
		CRACK WIDTH (mm)	DEFLECTION (mm)
1	Restrained	5	50
2	Restrained	10	52
3	Restrained	10	45
4	Restrained	10	50
1	Unrestrained	9	40
2	Unrestrained	17	70
3	Unrestrained	7	46
4	Unrestrained	10	41

NOTES: 1) Only first crack width at termination of test recorded.

2) For unrestrained test panels test terminated at complete failure of panel in load test.

3) 1 mm = 0.03937 in.

slipped in a weak substrate material. This presents an extremely pessimistic loading scenario, but it is useful for differentiating between the relative influences of different mesh and fiber reinforcing systems without the superimposed influences of anchor fixity.

In most loading situations, shotcrete would be subjected to uniformly distributed loading, as might be imposed by displaced soil or rock masses or hydraulic pressures. In this study, a central point load was applied for ease of load application. This presents a more severe loading condition and thus provides a lower bound statement of the load-carrying capacity of the shotcrete panels.

The results of the load vs. deflection tests on the large test panels are plotted in Figures 3 and 4 for the restrained and unrestrained tests, respectively. In comparing test results for the different panels, the variations in average panel thickness must be recognized (see Table 4). For example, restrained test panels 1, 2, and 3 are all close to 75 mm (3 in.) thick, but panel 4 is somewhat thicker. In the unrestrained tests, panel 2 is slightly thinner than 75 mm (3 in.), and panels 3 and 4 are somewhat thicker. This variation in panel thickness is reflected in the reported ultimate loads. If all panels were of identical thickness, the ultimate loads would likely be similar.

Of more interest than the ultimate load is the post-first-crack residual load-carrying capacity of the various panels. In the restrained tests, at deflections up to about 15 mm (0.6 in.), the residual load-carrying capacity of mesh reinforced panels 1 and 2 was fairly similar to fiber reinforced panels 3 and 4. At larger deflections up to the termination of the test at about 50 mm (2 in.) deflection, the mesh reinforced panels displayed a somewhat higher residual load-carrying capacity. The superior load-carrying capacity of the 6 kg/m^3 (10.7 lb/yd^3) fiber reinforced panel vs. the 4 kg/m^3 (6.7 lb/yd^3) panel with increasing deflection is well illustrated.

In the unrestrained tests, the smaller gauge mesh panel (panel 1) and fiber reinforced panels 3 and 4 displayed similar residual load-carrying capacity at deflections all the way up to failure, which occurred at deflections in excess of 40 mm (1.6 in.). The heavier gauge mesh panel (panel 2) displayed a generally lower load-carrying capacity up to 20 mm (0.75 in.) deflection and superior load-carrying capacity after about 30 mm (1.2 in.) deflection until failure at 70 mm (2.8 in.). The generally superior load-carrying capacity of the 6 kg/m^3 (10.1 lb/yd^3) fiber reinforced panel vs. the 4 kg/m^3 (6.7 lb/yd^3) with increasing deflection is also evident (particularly when the differences in panel thickness are taken into consideration).

The first crack widths increased approximately linearly with increasing deflection in most of the panels. Crack widths at termination of the load test (for restrained panels) and at ultimate failure (for the unrestrained panels) are summarized in Table 6.

The crack width at termination of the test for the restrained test panels was 10 mm (0.4 in.), except for panel 1, where multiple cracking developed and the first crack width at termination of the test was only 5 mm (0.2 in.). For the unrestrained test panels, the first crack width at failure was in the range of 7 to 10 mm (0.3 to 0.4 in), except for test panel 2, in which the first crack width was 17 mm (0.7 in.) wide when ultimate failure occurred at a deflection of 70 mm (2.8 in.).

The panels were severely deformed at deflections of 50 mm (2 in.). From a practical perspective, the portion of the load-deflection curve at deformations of up to about 15 mm (0.6 in.) is of most interest. At this deflection, first crack widths are still generally less than 3 mm (0.1 in.), and the serviceability of the shotcrete may not yet have been compromised in many applications. Figures 3 and 4 show that the CFP fiber reinforced shotcrete test panels compare favorably with the wire mesh reinforced test panels at deflections of up to 15 mm (0.6 in.), both with respect to residual load-carrying capacity and crack widths. This indicates that the addition of high-volume CFP fiber reinforcement can provide a viable alternative to traditional wire mesh or steel fiber reinforcement in wet-mix shotcrete.

COMPARISON OF STEEL AND POLYPROPYLENE FIBER REINFORCED SHOTCRETES

Previous studies (*2*) comparing plain, mesh, and steel fiber reinforced shotcrete (SFRS) were conducted on dry-mix shotcretes. Nevertheless, it is interesting to compare the performance of these shotcretes with the wet-mix, mesh, and PFRS shotcretes described previously in this paper. The shotcretes from the two different studies were tested in essentially the same way in the large test panel study. For ease of comparison, the data from the previous study (*2*) has been graphed in Figures 5 and 6, using the same scale as used in Figures 3 and 4. While direct comparisons must be made with discretion because of variations in panel thickness and shotcrete strength, certain trends are evident.

The load vs. deflection curves for restrained test panels shown in Figures 3 and 5 demonstrate that the performance of PFRS with 6 kg/m³ (10.1 lb/yd³) of CFP fiber approaches the performance of SFRS with 59 kg/m³ (100 lb/yd³) of hooked-end steel fiber. The load vs. deflection curves for the unrestrained test panels shown in Figures 4 and 6 reveal similar performance between the PFRS mix with 6 kg/m³ (10.1 lb/yd³) of CFP fiber and 59 kg/m³ (100 lb/yd³) of hooked-end steel fiber.

In short, the observations of relative performance between PFRS and SFRS in the 75 mm × 75 mm × 355 mm (3 in. × 3 in. × 14 in.) beams tested according to ASTM C1018

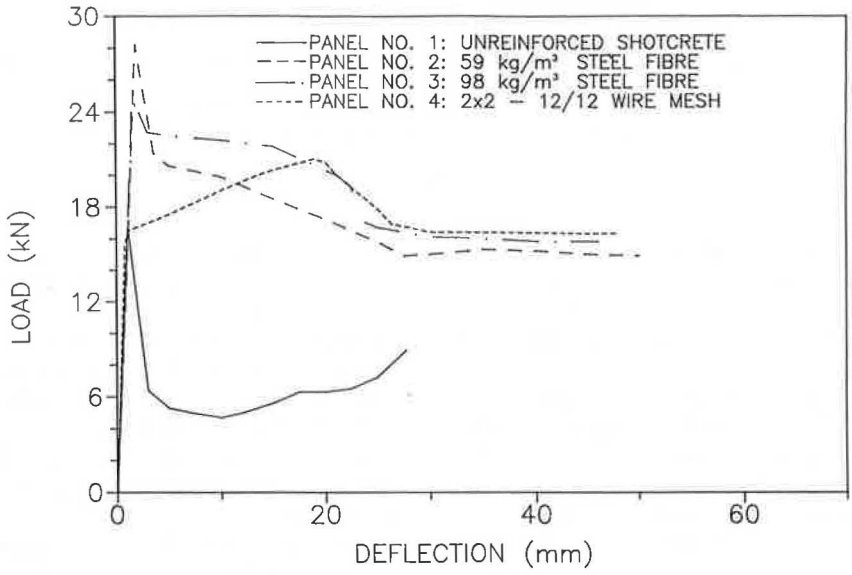

FIGURE 5 Load versus deformation (restrained) of steel fiber versus wire mesh.

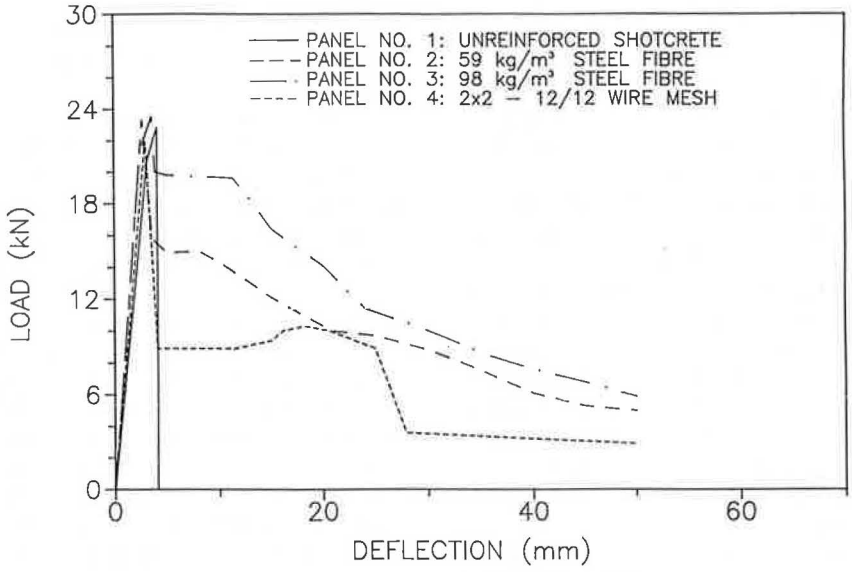

FIGURE 6 Load versus deformation (unrestrained) of steel fiber versus wire mesh.

appear to be reproduced in the large panel tests. This means designers can use the smaller scale ASTM C1018 tests and consider the statement of relative performance, as measured by toughness index values, to be representative of the behavior of shotcrete in the larger scale.

CONCLUSIONS

- The 38 mm (1½ in.) long CFP fiber evaluated in this study can be easily added to wet-mix shotcrete in a ready-mix concrete truck on site at rates of 4 and 6 kg/m³ (6.7 and 10.1 lb/yd³) and be thoroughly mixed, dispersed, and applied by the wet-mix shotcrete process, using a common shotcrete pump. No modifications to the shotcrete pump, equipment, or application procedures are required.
- The addition of CFP fiber at rates of 4 and 6 kg/m³ (6.7 and 10.1 lb/yd³) reduces the apparent workability of the mix as measured by the slump test. In this study, water was added to provide the necessary slump of 25 to 50 mm (1 to 2 in.) required for shooting. As expected, this caused some reduction in the compressive and flexural strength of the fiber reinforced shotcrete compared with the plain shotcrete. In applications where retempering with water is not desirable (for example, where high strength and minimizing the volume change potential of the shotcrete are important), then the required workability can be attained through the addition of superplasticizers in conjunction with fiber addition.
- The addition of 4 kg/m³ (6.7 lb/yd³) of CFP fiber produced ASTM C1018 I_5 and I_{10} toughness index values of 2.5 and 4.6, respectively, at 28 days. These values compare favorably with the performance of certain lower aspect ratio steel fibers added at a rate of 60 kg/m³ (101 lb/yd³) to wet-mix shotcrete.
- The addition of 6 kg/m³ (10.1 lb/yd³) of CFP fiber produced ASTM C1018 I_5 and I_{10} toughness index values of 3.3 and 6.5, respectively, at 28 days. These values are in the same range as the performance of certain higher aspect ratio steel fibers added at a rate of 60 kg/m³ (101 lb/yd³) to wet-mix shotcrete.
- The addition of CFP fiber at the rate of 4 kg/m³ (6.7 lb/yd³) and 6 kg/m³ (10.1 lb/yd³) did not result in an increase in the load-carrying capacity of either the ASTM C1018 flexural test prisms or the large test panels, after first crack. There was, however, a substantial change in post-first-crack residual load-carrying capacity. Plain shotcrete, without mesh or fiber reinforcement, would have no residual load-carrying capacity after first crack in either the ASTM C1018 toughness index test or the unrestrained large panel tests; the shotcrete would simply break into two pieces. Plain shotcrete in a restrained large test panel would continue to carry some load because of aggregate interlock and anchor restraint effects. By contrast the PFRS would continue to carry a significant portion of the ultimate load after first crack for substantial deflections.
- In the restrained large test panels, at deflections of up to about 15 mm (0.6 in.), the PFRS and the shotcrete reinforced with 102 × 102 MW 13.3 × MW 13.3 (4 × 4 8/8) and 152 × 152 MW 18.7 × MW 18.7 (6 × 6 6/6) welded wire reinforcing mesh displayed similar load-carrying capacity after cracking. At larger deflections, up to termination of the test at about 50 mm (2 in.), the mesh reinforced panels displayed somewhat higher residual load-carrying capacity. From a practical perspective, the performance of the shotcretes at deflections of about 15 mm (0.6 in.) or less is of most interest since, at deflections significantly larger than this, the width of crack opening is generally greater than 3 mm (0.1 in.); hence, the serviceability of the shotcrete would likely be compromised in most applications.
- In the unrestrained large test panels, the PFRS and the shotcrete reinforced with 102 mm × 102 MW, 13.3 mm × MW 13.3 (4 in. × 4 8/8 in.) wire mesh displayed similar residual load-carrying capacity after first crack at deflections all the way up to failure, which occurred at deflections in excess of 40 mm (1.6 in.). The panel reinforced with the heavier 152 mm × 152 MW 18.7 × MW 18.7 (6 in. × 6 6/6 in.) wire mesh displayed lower load-carrying capacity after first crack at deflections up to 20 mm (0.75 in.) and superior residual load-carrying capacity at deflections from about 30 mm (1.2 in.) to failure at 70 mm (2.8 in.).
- A comparison of load vs. deflection test results for previously tested SFRS in large restrained test panels indicated that the PFRS with 6 kg/m³ (10.1 lb/yd³) of 38 mm (1½ in.) long CFP fiber reinforcement approached the performance of SFRS with 59 kg/m³ (100 lb/yd³) of hooked-end steel fiber.
- A comparison of load vs. deflection test results for previously tested SFRS in large unrestrained test panels indicated that the PFRS with 6 kg/m³ (10.1 lb/yd³) of 38 mm (1½ in) long CFP fiber reinforcement had a similar performance to the SFRS with 59 kg/m³ (100 lb/yd³) of hooked-end steel fiber.
- The addition of high-volume concentrations of up to 6 kg/m³ (10.7 lb/yd³) of 38 mm (1½ in.) long CFP fiber can provide a viable alternative to traditional mesh or steel fiber reinforcement of wet-mix shotcretes for many applications.

ACKNOWLEDGMENTS

The studies on PFRS reported in this paper were sponsored by Elsro Construction Products Ltd. in St. Albert, Alberta, Canada, and the Forta Corporation in Grove City, Pennsylvania. All mix designs and tests were carried out by personnel from Hardy BBT Limited, Vancouver, Canada.

REFERENCES

1. *Guide to Shortcrete*. Report 506R-85. American Concrete Institute, 1985.
2. D. R. Morgan and D. N. Mowat. A Comparative Evaluation of Plain, Mesh and Steel Fibre Reinforced Shotcrete. In *Report SP-81*, American Concrete Institute, 1984, pp. 307–324.
3. *State-of-the-Art Report on Fibre Reinforced Shotcrete*. Report 506.1R-84. American Concrete Institute, 1984.
4. D. R. Morgan. Steel Fibre Reinforced Shotcrete in Western Canada. *Geotechnical News*, March 1985, pp. 24–25.
5. D. Rose. Steel Fibre Reinforced Shotcrete for Tunnel Linings: The State of the Art. *Rapid Excavation and Tunnelling Conference*, Vol. 1, Ch. 24, 1985, pp. 392–412.
6. V. Ramakrishnan. Steel Fibre Reinforced Shotcrete, A State-of-the-Art Review. *U.S./Sweden Joint Seminar (NSF-STU)*, Stockholm, Norway, 1985, pp. 7–23.
7. D. R. Morgan. Evaluation of Silica Fume Shotcrete. *CANMET/CSCE International Workshop on Silica Fume in Concrete*, Montreal, Quebec, 1987.

An Investigation of the Toughness and Compressive Toughness Index of Steel Fiber Reinforced Concrete

JINGHAI ZHAO, PENG XU, AND CHENGMOU FAN

In this paper, various methods for determining the toughness of steel fiber reinforced concrete (SFRC) are compared and evaluated using five criteria. The ASTM C1018-85 method mostly conforms to these criteria and, hence, is accepted as the foundation for China's standard test method of compressive toughness of SFRC. It is proposed that the critical-load point replace the first-crack point in defining the compressive toughness index based on an analysis of the onset and propagation of cracks in concrete under uniaxial compressive loading. The transient coefficient for load-carrying capacity (K'') is also given to indicate the variational characteristic of toughness. Experiments were carried out to verify the validity of the recommended index.

Various indexes for defining the toughness of steel fiber reinforced concrete (SFRC) have been proposed by different organizations and reseachers in the past decade. For the purpose of developing a standard test method for SFRC, especially the compressive toughness test, the optimum method must be evaluated and supplemented with new concepts when necessary.

GENERAL REVIEW OF TOUGHNESS TEST METHODS

The standard test methods for SFRC toughness were developed by various reseach groups, separately and independently. Thus, the methods for determining toughness are multifarious and can be divided into four groups:

1. Energy method,
2. Strength method,
3. Energy ratio method, and
4. Multicharacteristic point method.

In a narrow sense, toughness is defined as the energy absorption capability of material or structure under loads up to its failure. In fact, the energy method employs the idea of toughness as expressed by the area under the load-deformation curve, but this concept has not yet been available for use in design. Figure 1 shows that the toughness of a material depends largely on its load-carrying capacity, as well as on its deformation ability. Therefore, it can be induced, in a broad sense, that toughness is equivalent to viscosity and can be evaluated by the deformation at which the load-carrying capacity remains at a required constant value. As shown in Figure 2, the ductility factor, $\mu = \delta_u/\delta_y$, is used to indicate the deformation ability of material or structure, up to failure in design, for earthquake-resisting structures; where δ_y is the deformation at which the behavior of material or structure changes from elastic to elasto-plastic and δ_u is the deformation when the load-carrying capacity begins to decrease or decreases to a given value.

The strength method is based on the assumption that the average equivalent strength (flexural or compressive) of a certain amount of energy absorbed up to a specific deformation can be used to access the toughness of SFRC (*1*). The flexural and compressive toughness indexes recommended by

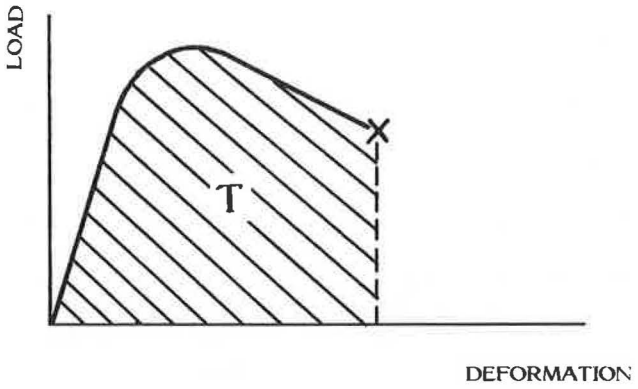

FIGURE 1 Definition of toughness.

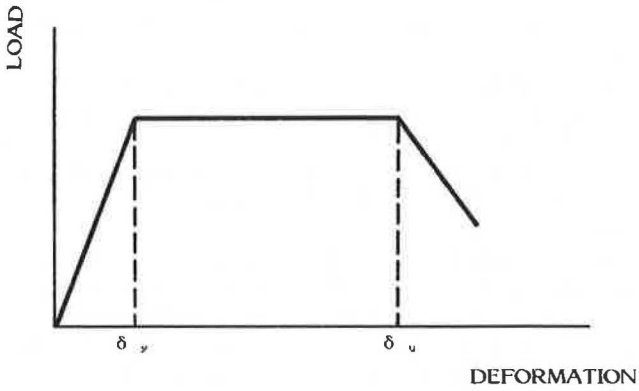

FIGURE 2 Ductility factor $\mu = \delta_u/\delta_y$.

Harbin Architectural and Civil Engineering Institute, 144 Da Zhi Street, Harbin, the People's Republic of China.

the JCI committee are illustrated in Figures 3 and 4 and expressed by

$$\bar{\sigma}_b = (T_b l)/(\delta_{tb} b h^2) \quad (1)$$

and

$$\bar{\sigma}_c = T_c/(\delta_{tc} A) \quad (2)$$

where l, b, h, and A are the span, width, depth and cross-sectional area of the specimen, respectively. T_b and T_c correspond to the energy absorbed (the toughness) by material up to a specified end-point deflection or deformation in flexure and compression. The advantage of this method lies in its general acceptance in design for adopting the fundamental property of material: the average equivalent strength. However, the optimum method for determining the standard deflection and deformation is still unclear. Neither the energy method nor the strength method can fully reflect the reinforcement of steel fiber on SFRC, nor can they avoid the effect of specimen size on toughness.

The proposal of ACI Committee 544 for measuring toughness can be cataloged as the energy ratio method, in which a prescribed total deflection is suggested (*2*). The toughness index was calculated as the ratio of the area under the load-deflection curve up to the mid-span deflection of 1.9 mm (for a 100 mm × 100 mm × 400 mm prismatic specimen with a span of 300 mm) to the area under the load-deflection curve up to the first-crack point. The formula is given as the following:

$$T.I. = (A_1 + A_2)/A_1 \quad (3)$$

where A_1 and A_2 are the shaded areas in Figure 5. Although some ratio systems with dimensionless indexes can be independent of specimen size and geometry, the ACI method is not, due to its definition in terms of a deflection that relates to a particular deflection. A major disadvantage of the energy method is that it is sensitive to the dislocation of the first-crack point; thus, the toughness index value can be substantially affected (*3–6*).

Consideration of practical serviceability requirements led to the development of the multiple characteristic point method, in which more than one end-point deflection is suggested (*7*). As shown in Figure 6, the characteristic point can be point A, the first-crack point; point B, at which the maximum load is achieved; point C, where the load-carrying capacity decreases to some extent (for instance, to that of 0.85 P_{max}); point D, at which the deformation increases to some extent (for instance, to that of three times of the first-crack deformation); point E, where crack widths are limited to some given values; or point F at which fracture of the specimen is supposed to occur.

The ASTM C1018-85 method originated from Johnston's definition of toughness index referenced to first-crack deflection (*8*), in which the ratio of total area (to any multiple of first-crack deflection) to the area up to the point of first crack

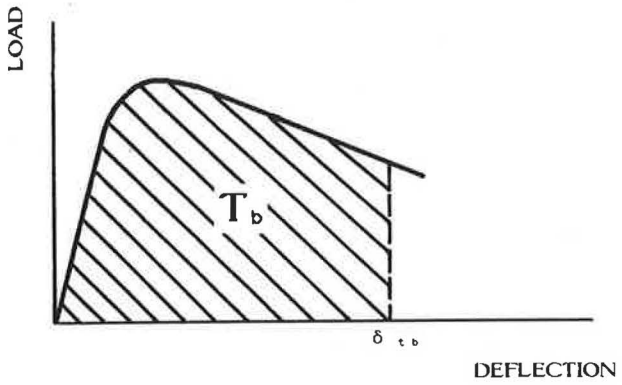

FIGURE 3 Flexural toughness coefficient σ_b.

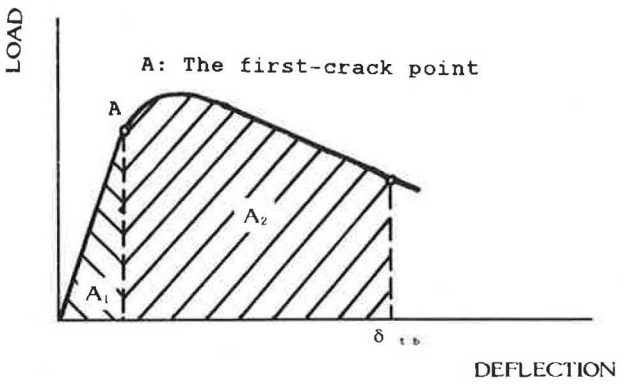

FIGURE 5 Toughness index (T.I.).

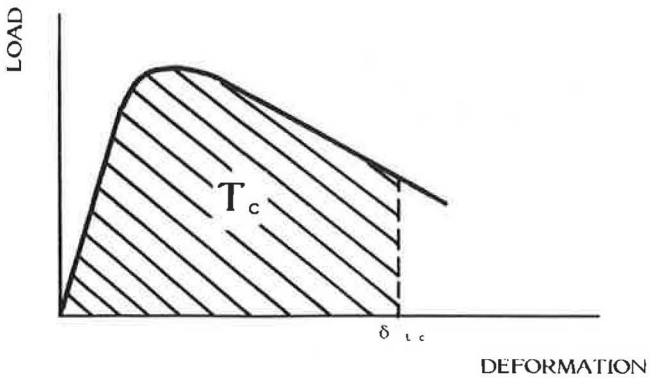

FIGURE 4 Compressive toughness coefficient σ_c.

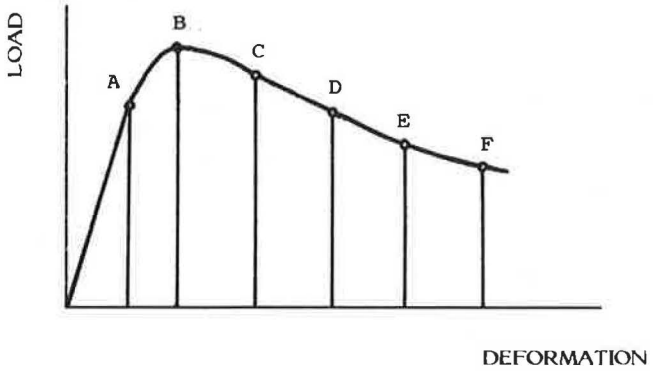

FIGURE 6 The multipoint system.

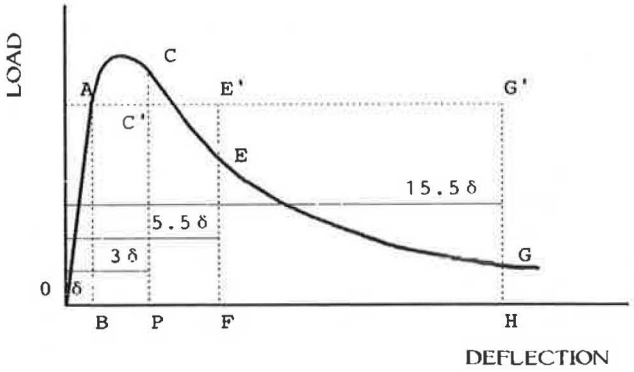

FIGURE 7 Flexural toughness indexes I_5, I_{10} and I_{30}.

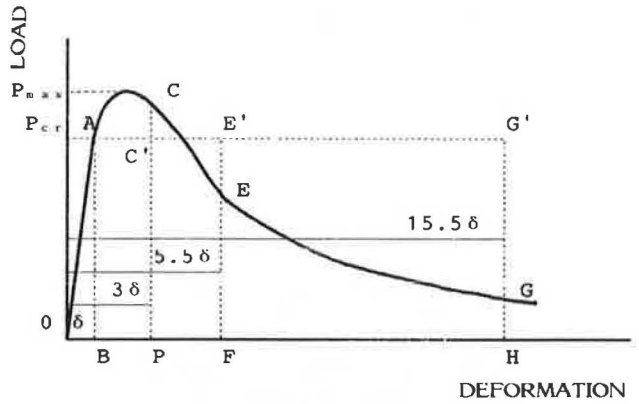

FIGURE 8 Compressive toughness indices I_5, I_{10} and I_{30}.

was given (see Figure 7). The toughness indexes (I_5 = area *OACP*/area *OAB*, I_{10} = area *OAEF*/area *OAB*, and I_{30} = area *OAGH*/area *OAB*) enable the actual performance of material to be compared with a readily understood reference level of performance, e.g., the perfect elasto-plastic material to which the values of 5, 10, and 30 for toughness index correspond. This method proved to be better with respect to various criteria, especially the precision of the toughness index. It was previously reported that the use of multiples of first-crack deflections reduced the coefficient of variation for the toughness index (*8*).

From the above discussion, the evaluating process for toughness indexes should be based on the following criteria:

- Existence of rational and physical meaning,
- Appropriateness for engineering applications,
- Ability to indicate the influences caused by the type and shape of the added steel fibers and the fiber volume,
- Ready determination with small deviation, and
- Independence of specimen size.

COMPRESSIVE TOUGHNESS INDEX

In view of the widely recognized concept of ASTM C1018-85 and the evaluation described previously in this paper, compressive toughness indexes I_5, I_{10}, and I_{30}, which are dimensionless ratios of different areas under the load-deformation curve, were recommended (see Figure 8). For uniaxial compressive concrete, the first-crack point is not easily identifiable, due to the curvilinearity of the load-deformation curve compared with the stress-strain curve of tensile and flexural concrete (*9*). Analysis of the onset and propagation of cracks in concrete under uniaxial compressive load, as well as the reinforcement of steel fiber, provided the rationale for selecting the critical-load point as the characteristic point of compressive toughness index. Liu et al. (*10*) reported the four phases of formation and propagation of microcracks in concrete:

1. Shrinkage cracks occur around the coarse aggregates even prior to loading.
2. At loads of 30 to 65 percent of ultimate strength, stable cracks occur at the interfaces.
3. The propagation of stable cracks initiates the stretching bond cracks to bridge mortar cracks into discontinuous ones, and the propagation stops right after unloading.
4. During the propagation of unstable cracks, mortar cracks increase in number and tend to form continuous cracks, which propagate automatically and lead to the collapse of concrete.

When stable crack propagation ends and unstable crack propagation begins, the load is usually 70 to 90 percent of ultimate, which is termed critical load P_{cr}. Concrete is less likely to collapse when the long-term load is smaller than P_{cr} (*11*).

As a result of the preferential distribution of steel fiber parallel to the interfaces of aggregates, steel fiber does not serve the function of arresting bond cracks in Phases 1 and 2. Apparently, the unique ability of steel fiber to bridge cracks, especially unstable cracks, is fully demonstrated in Phases 3 and 4. Thus, the critical load is less affected by the reinforcement of steel fiber. In fact, steel fiber has little influence on the increment of concrete compressive strength, and sometimes the strength even decreases in unevenly mixed concrete mixtures. It is widely accepted that the post-crack behavior of concrete after the addition of steel fiber is the most important feature (i.e., the high load-carrying capacity at large deformation).

It can be concluded from the above analysis that the critical load depends mainly on the properties of the matrix and rarely relates to the fiber content; hence, the load of 85 percent of ultimate strength was chosen as the characteristic load for specimens of various fiber content because of its easy determination from the load-deformation curve.

To indicate the trend analysis of the load-deformation curve at various deformations, as well as the difference between the post-crack behavior of a material and that of perfect elasto-plastic material, an average coefficient for load-carrying capacity (K^n) was introduced in the following formula (*3*). The formula is derived from the bi-linearized load-deformation curve shown in Figure 9:

$$K^n = (P_{cr} + \Delta P)/P_{cr} = (I_n - m)/(m - 1) \quad (4)$$

where

m = multiple of the critical-load deformation, which may be 3, 5.5, 15.5, or other multiples chosen in terms of serviceability requirements;
I_n = average toughness index of the specimens in one group (n = 5, 10, and 30);

P_{cr} = critical load, which is 85 percent of the ultimate strength; and

P = increment of load-carrying capacity at a given deformation, which is negative when the load is smaller than P_{cr}.

The transient coefficient, K^n, is at a minimum when the portion of the curve after critical load is vertical and increases from -1 through 0 to 1, and then more than one. The various values correspond to materials with behavior ranging from elastic ($K^n = -1$) to perfect elasto-plastic ($K^n = 1$) to even tougher than elasto-plastic ($K^n \geq 1$), are shown in Figure 10 and Table 1.

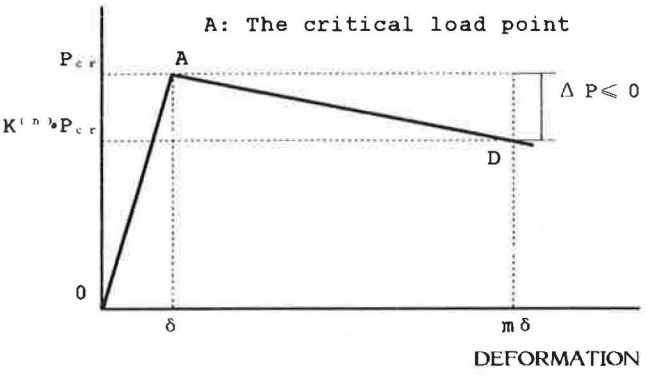

FIGURE 9 Load-deformation curve after bi-linearization.

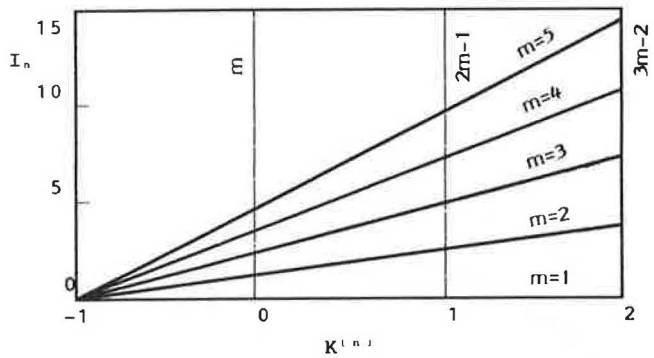

FIGURE 10 Relationship between K^n and I_n.

TABLE 1 THE VALUES OF I_n CORRESPONDING TO SOME SPECIFIC VALUES OF K^n

$K^{(n)}$	I_n
−1	1
0	m
1	2m−1
2	3m−2

EXPERIMENTAL INVESTIGATION

To verify the validity of the test method for compressive toughness index proposed in this paper, five groups of specimens were prepared with different fiber volume fractions. Ordinary portland cement with a 28-day compressive strength of 42.5 MPa was used. The coarse aggregate used was 20 mm maximum size crushed stone with a fineness of modulus of 2.63. All the specimens were 100 mm × 100 mm × 200 mm in prism. The melt-extracted carbon steel fiber (0.2 mm × 1.0 mm × 25 mm) was added into the concrete mixture with a vebe time of about 10 ± 3 sec. The mix proportions of the SFRC specimens are shown in Table 2. All uniaxial compressive tests were carried out in a universal testing machine, accompanied by two sets of oil jack as a stiffness unit. Deformation at the loading points, as well as the load were plotted by an X-Y recorder through which the load-deformation curve could be obtained automatically.

Figure 11 is the typical load-deformation curve obtained from the tests. The toughness indexes and the coefficient K^n are listed in Table 3. Figure 12 shows that the coefficient K^n can either clearly indicate the reinforcement of steel fiber on a compressive specimen or fairly describe the material behavior after cracking.

CONCLUSIONS

Based on the work presented in this paper, the following conclusions were drawn:

- The ASTM C1018-85 method has some advantages over the other existing test methods; hence, it was adopted as the basis for the standard test method of compressive toughness of SFRC.
- It was proposed that the critical-load point replace the first-crack point for measuring compressive toughness, based on the analysis of the onset and propagation of cracks in concrete.
- The toughness indexes I_5, I_{10} and I_{30}, accompanied by the coefficient K^n, can clearly reflect the post-crack behavior of SFRC.

TABLE 2 MIX PROPORTIONS OF SPECIMEN

V(%)	Contents of Materials(kg/m³)					Water-Cement Ratio	Sand Ratio
	Steel Fiber	Cement	Water	Sand	Crushed Stones		
0	0	340	170	650	1200	0.5	0.35
0.5	40	360	180	720	1080	0.5	0.40
1.0	80	380	190	790	960	0.5	0.45
1.5	120	400	200	850	850	0.5	0.50
2.0	160	420	210	910	740	0.5	0.55

TABLE 3 TOUGHNESS INDEXES I_n and K^n

		$V_f=0$	$V_f=0.5\%$	$V_f=1.0\%$	$V_f=1.5\%$	$V_f=2.0\%$
m=3	I_5	4.73	4.77	5.00	5.36	5.54
	$K^{(5)}$	0.87	0.89	1.00	1.18	1.27
m=5.5	I_{10}	7.20	8.61	9.51	10.47	11.63
	$K^{(10)}$	0.38	0.69	0.89	1.10	1.36
m=15.5	I_{30}	12.28	16.88	20.84	23,52	29.07
	$K^{(30)}$	---	0.10	0.37	0.55	0.94

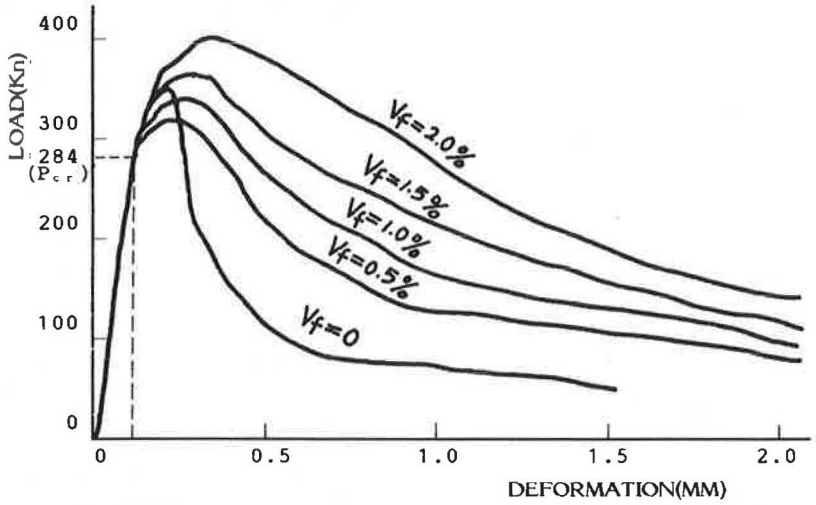

FIGURE 11 Typical compressive load-deformation curve.

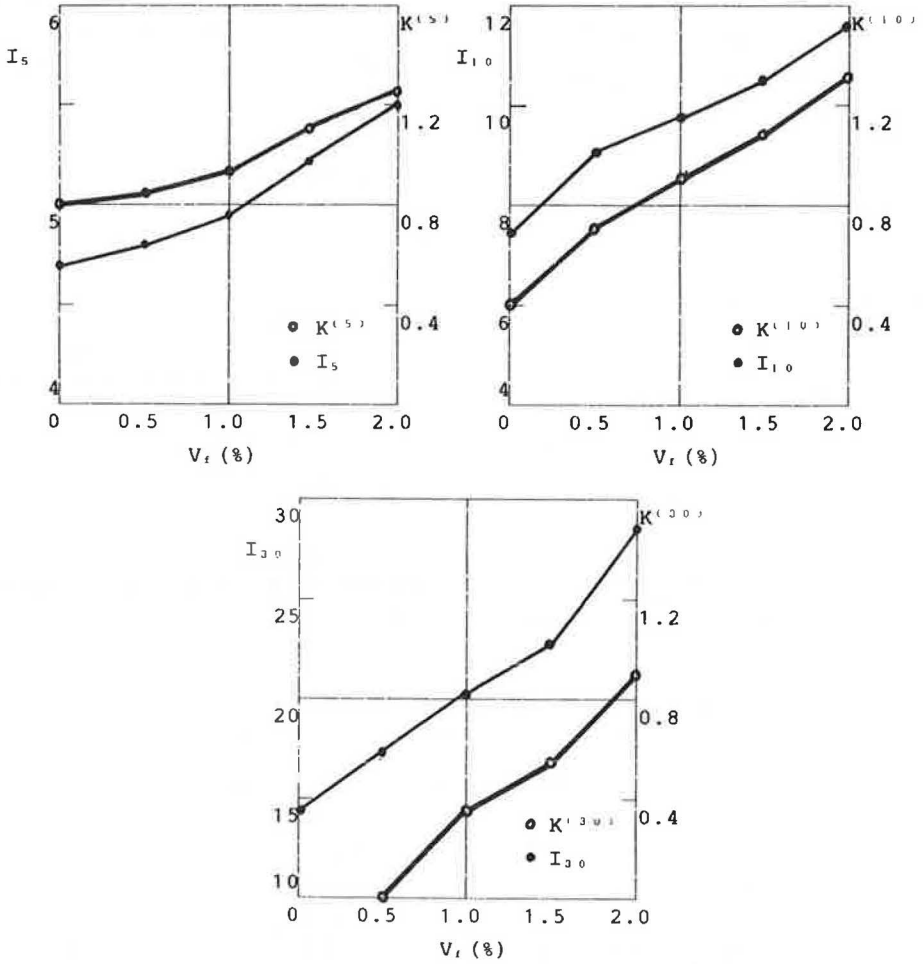

FIGURE 12 Relationship of toughness indexes, transient coefficient for load-carrying capacity, and fiber volume.

REFERENCES

1. JCI SFRC Committee. *Guide for Design and Construction of Steel Fiber Reinforced Concrete* (in Japanese), 1983.
2. ACI Committee 544. Measurement of Properties of Fiber Reinforced Concrete. *ACI Journal*, Vol. 75, No. 7, July 1978.
3. Jinghai Zhao and Peng Xu. Evaluating Method for Flexural Toughness of Steel Fiber Reinforced Concrete. *Journal of Harbin Architectural and Civil Engineering Institute* (in Chinese), Supplement 1988, pp. 65–77.
4. B. Barr and E. B. Dawood Hasso. The Precision of Toughness Indexes Based on Multiples of First-Crack Deflections. *ACI Journal*, Vol. 82, No. 6, Nov.–Dec. 1985, pp. 870–876.
5. C. D. Johnston. Precision of Flexural Strength and Toughness Parameters for Steel Fiber Reinforced Concrete. *Cement, Concrete, and Aggregates*, Vol. 4, No. 2, Winter 1982, pp. 61–67.
6. R. F. Zollo. Fibrous Concrete Flexural Testing—Developing Standardized Techniques. *ACI Journal*, Vol. 77, No. 5, Sept.–Oct. 1980, pp 363–368.
7. C. D. Johnston. Definition and Measurement of Flexural Toughness Parameters for Fiber Reinforced Concrete. *Cement, Concrete, and Aggregates*, Vol. 4, No. 2. Winter 1982, pp. 53–60.
8. C. D. Johnston and R. J. Gray. Flexural Toughness and First-Crack Strength of Fiber Reinforced Concrete Using ASTM Standard C1018. *Proc., RILEM Symposium on Development in Fiber Cement and Concrete*, Vol. 2, 1986.
9. Guofan Zhao, et al. Experiment on the Compressive Strength and Module of Elasticity of Steel Fiber Reinforced Concrete. *Proc., SFRC Standard Test Methods in China* (in Chinese), Vol. 2, 1988.
10. T. C. Y. Liu, et al. Stress-Strain Response and Fracture of Concrete in Uniaxial and Biaxial Compression. *ACI Journal*, Vol. 69, No. 5, May 1972, pp. 291–295.
11. Chuanzhi Wang, et al. *Theory of Steel Reinforced Concrete Structure* (in Chinese), Publishing House of Architecture Industry in China, Beijing, 1985.

Analysis of Fiber Reinforced Concrete Beams Under Combined Loadings

A. K. SHARMA

There is an increasing interest in the use of steel fibers to improve the properties of concrete. The higher tensile and post-cracking ductility of fiber reinforced concrete members can favorably influence their structural behavior under combined loadings. Based on the observed skew bending mechanism of torsional failure, equations were derived to analyze fiber reinforced concrete beams under axial compression, bending, and torsion. The theoretical model was compared with published test results and it gives a reasonable prediction of the ultimate torque. A design example is given to show the use of the proposed method.

The use of steel fibers to improve the properties of concrete has been a topic of many studies. Recent studies (*1–3*) indicate that the addition of steel fibers greatly increases the resistance of concrete to crack propagation. Fiber reinforced concrete can be regarded as an improved type of concrete with higher tensile strength and post-cracking ductility. Both of these characteristics favorably influence the behavior of fiber concrete beams under combined loadings (*4–7*). One such combination of loadings is axial compression, bending, and torsion. This type of loading can occur in compression members, such as columns of building frames, piers of curved and skew bridges, central columns of spiral staircases, columns supporting crane girders, and pylons of multistory car parks. These compression members may be subjected to significant torsion and bending moment, particularly if wind and seismic forces are considered.

It has been reported (*8,9*) that steel fiber reinforced concrete beams, when subjected to torsion, collapsed after the formation of cracks that spiralled around the beam. The final collapse occurred in a skew plane, similar to one described by Hsu (*10*). A method of analysis applicable to normal reinforced concrete members subjected to torsion and bending moment, with or without axial compression, was previously published (*11*). This method was an extension of the skew bending theory originally proposed by Hsu (*10*). In this paper, the method is extended to analyze fiber reinforced concrete beams subjected to combined axial compression, bending, and torsion.

ANALYSIS

The two modes assumed for the initiation of failure (*11*) are represented in Figure 1(b) and 1(c). In mode 1, it is assumed that the skew bending takes place about a centroidal axis, parallel to the wider faces and inclined at angle ϕ to the shorter faces. The fibrous concrete would be at the point of failure, due to skewed bending, when the stress at the extreme surface on the tension side becomes equal to the modulus of rupture of the fiber concrete. Figure 1(b) shows that the bending vector has no component along the bending axis, indicating that the bending moment does not influence failure in Mode 1. The component of twisting moment about the bending axis is $M_z \cos \phi$. The average intensity of compressive stress due to axial compression on the failure plane is $P_o \sin^2\phi$. Hence, equating the external moment about the bending axis to the internal resisting moment results in the following:

$$M_z \cos \phi = (1/6\ b^2h \operatorname{cosec} \phi)\ (kf_{rf} + P_o \sin^2 \phi) \quad (1)$$

where

M_z = torsional strength of fiber reinforced concrete under combined loading;
b,h = shorter and longer overall dimensions of the beam, respectively;
k = strength reduction factor, taken equal to 0.71 for fibrous concrete (*9*);
P_o = effective axial compressive stress, which equals P/bh;
P = axial force; and
f_{rf} = modulus of rupture of fibrous concrete.

Equation 1 can be rewritten in the form

$$M_z = \left[\frac{1}{3} b^2h\ kf_{rf}\right]\left[\left(1 + \frac{P_o}{kf_{rf}} \sin^2 \phi\right) \operatorname{cosec} 2\phi\right] \quad (2)$$

Equation 2 can be expressed as

$$M_z = M_{zo}\, R_\phi \quad (3)$$

where

$$M_{zo} = \frac{1}{3} b^2h\ kf_{rf} \quad (4)$$

and

$$R_\phi = \frac{(1 + r \sin^2 \phi)}{\sin 2\phi} \quad (5)$$

where

M_{zo} = torsional strength of the fiber reinforced concrete member under pure torsion,

Department of Civil Engineering, University of the West Indies, Trinidad.

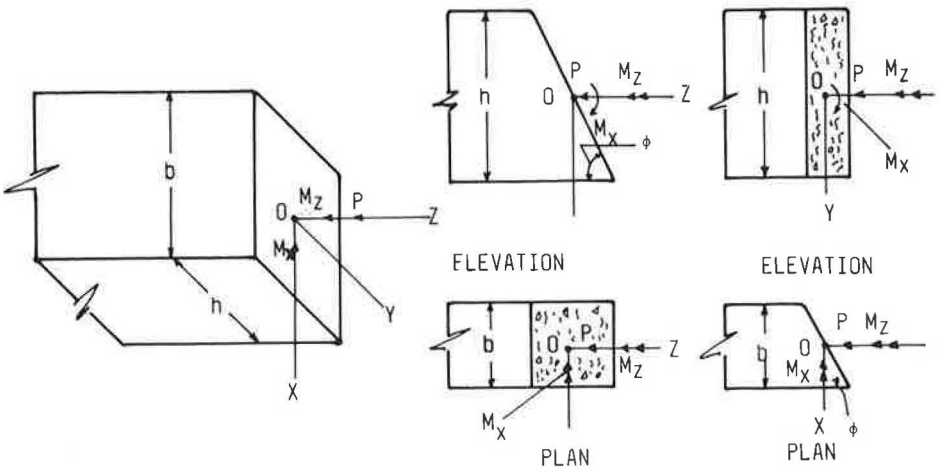

FIGURE 1 Skew bending theory.

$r = P_o/kf_{rf}$, and
R_ϕ = factor representing the effect of axial compression in Mode 1.

In Mode 2 (Figure 1(c)), the skew bending takes place about a centroidal axis, parallel to the shorter faces and inclined at angle ϕ to the wider faces. The figure shows that the component of torque and bending moment vectors along the axis of skew bending are $M_z \cos \phi$ and $M_x \sin \phi$, respectively. Hence, equating the external moment about the bending axis to the internal resisting moment gives

$$M_z \cos \phi + M_x \sin \phi = (1/6\, bh^2 \operatorname{cosec} \phi)\,(kf_{rf} + P_o \sin^2 \phi) \quad (6)$$

Equation 6 may be rewritten in the form

$$M_z = \left[\frac{1}{3} bh^2 kf_{rf}\right]\left[\frac{1 + \dfrac{P_o}{kf_{rf}} \sin^2 \phi}{2 \sin \phi(\cos \phi + \lambda \sin \phi)}\right] \quad (7)$$

where

$\lambda = M_x/M_z$, and
M_x = applied bending moment.

Equation 7 can be expressed as

$$M_z = M_{zo}\, R_\phi \quad (8)$$

where

$$M_{zo} = \frac{1}{3} bh^2 kf_{rf}, \text{ and} \quad (9)$$

$$R_\phi = (1 + r \sin^2 \phi) / [2 \sin \phi\, (\cos \phi + \lambda \sin \phi] \quad (10)$$

In Mode 2, the R_ϕ factor takes into account the effect of axial compression as well as the bending moment applied on the section.

The inclination of the axis of skew bending (ϕ) must be such as to minimize the strength.

Equations 4 and 9 show that M_{zo} is independent of ϕ. Hence, ϕ must correspond to the minimum value of R_ϕ. The minimum value of R_ϕ can be found by equating its derivative with respect to ϕ to zero; thus, the minimum strength is given by the following equation:

$$r \sin^2 \phi - \cos 2\phi - \lambda \sin 2\phi = 0 \quad (11)$$

Solving Equation 11, the inclination of the failure plane is given by

$$\sin 2\phi = (2\lambda r + 2\,[\lambda^2 r^2 + (1 + r)E]^{1/2}/E, \text{ and} \quad (12)$$

$$\cos 2\phi = [2r^2 + 4r - [(2r^2 + 4r)^2 - 4(r^2 - 4\lambda^2)E]^{1/2}/2E \quad (13)$$

where

$$E = r^2 + 4r + 4 + 4\lambda^2$$

The form of the corresponding equations for Mode 1 is identical to that of the equations for Mode 2, except that λ should be zero since there is no interaction between the bending moment (M_x) and the torsional moment (M_z). The angle 2ϕ lies between 0° and 90° if both $\sin 2\phi$ and $\cos 2\phi$ are positive and between 90° and 180° if $\sin 2\phi$ is positive and $\cos 2\phi$ is negative. Equations 12 and 13 give the value of ϕ, which reduces the value of R_ϕ to a minimum. Equation 10 is represented graphically in Figure 2, in which R_ϕ is plotted against r for different values of λ.

The addition of fiber in the concrete is reflected in the increased tensile strength of the fibrous concrete, which is expressed in the theory as equal to kf_{rf}. Thus, the ultimate torque of fiber reinforced concrete for Modes 1 and 2 can be computed using Equations 3 and 8. The lesser of the two torques governs failure.

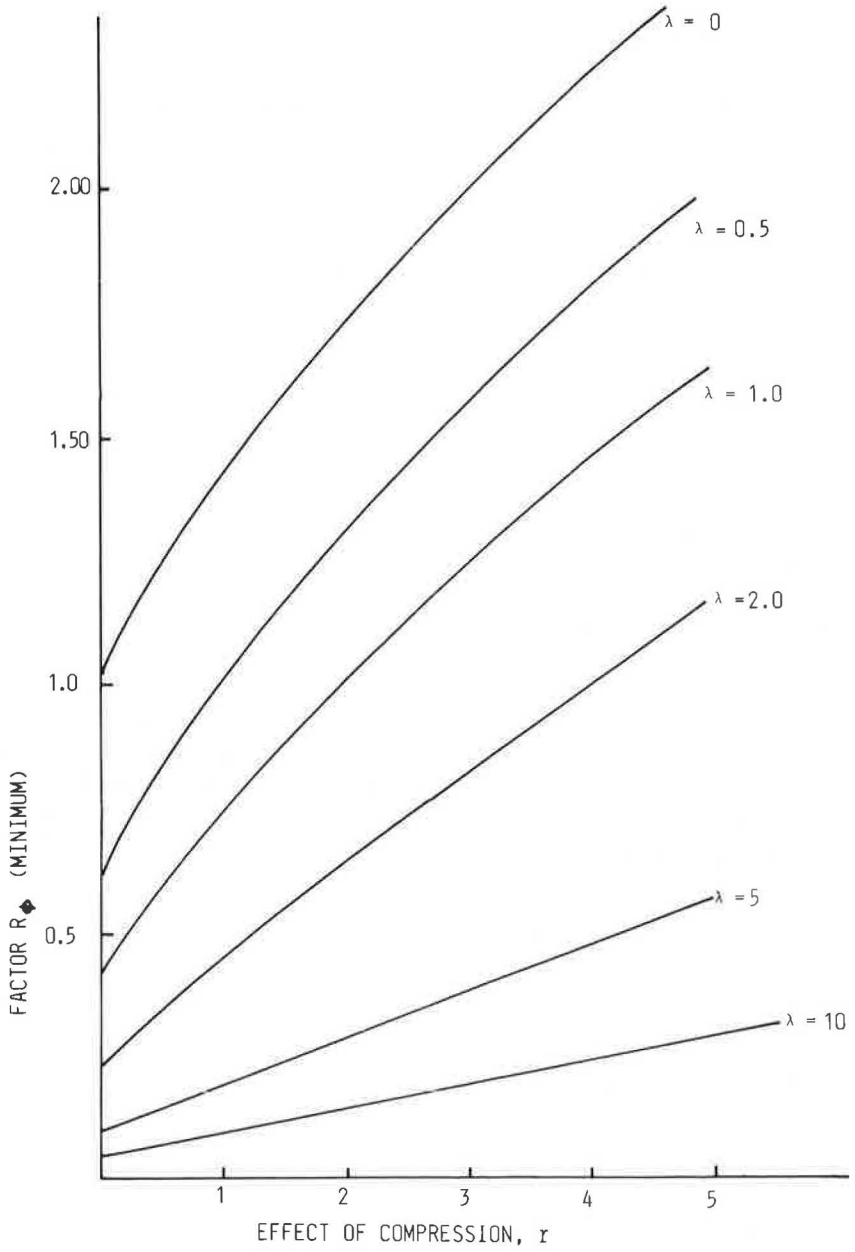

FIGURE 2 Plot of R_ϕ (minimum) versus λ and r.

CORRELATION WITH TEST RESULTS

Table 1 provides a summary of comparisons between the calculated and experimental ultimate torques for various published tests. The test results of fiber reinforced concrete beams having different aspect ratios and subjected to different combinations of loadings are compared with the proposed theory. In the computation, a factor of 0.885 was allowed for square sections as suggested by Hsu (*10*). The average value of experimental torque/calculated torque for 85 beams was estimated to be 0.989 with a standard deviation of 16.7 percent.

CONCLUSIONS

- The addition of fibers into plain concrete beams increases the tensile strength and post-cracking ductility of concrete.
- A method of analysis based on the skew bending approach is presented for analyzing fiber reinforced concrete beams subjected to combined axial compression, bending moment, and torsion. The method is used for the correlation of the published test results of 85 beams. The proposed method gives a reasonable prediction of the ultimate torque.

DESIGN EXAMPLE

The following example is included to show the use of the proposed method.

A fiber reinforced concrete column of a car park has a cross section of 300 mm × 300 mm. The member is subjected to a combined loading: axial load P = 150 kN, bending moment M_x = 23 kNm, and torsional moment M_z = 30 kNm. The column is reinforced with steel fibers so that the modulus of

TABLE 1 SUMMARY OF COMPARISONS BETWEEN THE CALCULATED AND EXPERIMENTAL VALUES OF ULTIMATE TORQUE FOR FIBER REINFORCED CONCRETE BEAMS

Group	Test Reported by	No. of Tests	Ratio of Ultimate Torques (Experimental/Calculated) Mean	Standard Deviation
Pure torsion	Mansur and Paramasivam (*8*)	18	1.069	0.088
	Craig et al (*2*)	8	1.017	0.157
	Narayanan and Kareem-Palanjian (*9*)	26	0.812	0.74
Bending and torsion	Mansur (*4*)	21	1.101	0.1036
	Mansur and Paramasivam (*6*)	6	1.223	0.128
Compression	Narayanan and Kareem-Palanjian (*7*)	6	0.918	0.079
Total		85	0.989	0.167

rupture of fibrous concrete is 6N/mm². The strength of the section is to be checked:

$$P_o = \frac{P}{bh} = \frac{150 \times 10^3}{(300)^2} = 1.666$$

and

$$r = \frac{P_o}{kf_{rf}} = \frac{1.666}{0.71 \times 6} = 0.39 \simeq 0.4$$

Mode 1

Using Equation 4

$$M_{zo} = \frac{1}{3} b^2 h\, kf_{rf}$$

$$= \frac{1}{3} \times (300)^3 \times 0.71 \times 6$$

$$= 51.12 \text{ kNm}$$

Using Figure 2, with $\lambda = 0$, $r = 0.4$ and $R_\phi = 1.23$. Therefore, torsional strength (in Mode 1) is

$$M_z = 51.12 \times 1.23 = 62.9 \text{ kNm}$$

Mode 2

Using Equation 9

$$M_{zo} = \frac{1}{3} bh^2\, kf_{rf}$$

$$= \frac{1}{3} \times (300)^3 \times 0.71 \times 6$$

$$= 51.12 \text{ kNm}$$

and

$$\lambda = \frac{M_x}{M_z} = \frac{23}{30} = 0.77$$

Using Figure 2, with $\lambda = 0.77$, $r = 0.4$ and $R_\phi = 0.65$. Therefore, torsion strength (in Mode 2) is

$$M_z = 0.65 \times 51.12 = 33.2 \text{ kNm}$$

Hence, Mode 2 governs failure. The torsional strength of the member is 33.2 kNm, against an applied torsional moment of 30 kNm. Therefore, the section provided is adequate.

REFERENCES

1. R. Narayanan and A. S. Kareem-Palanjian. Effect of Fiber Addition on Concrete Strength. *Indian Concrete Journal*, Vol. 58, No. 4, April 1984, pp. 100–103.
2. R. J. Craig, A. J. Parr, E. Germain, V. Mosquera, and S. Kamilares. Fiber Reinforced Beams in Torsion. *ACI Jorunal*, Vol. 83, No. 6, Nov.–Dec., 1986, pp. 934–942.
3. V. Ramakrishnan, G. Oberling, and P. Tatnall. Flexural Fatigue Strength of Steel Fiber Reinforced Concrete. In *Report SP-105: Fiber Reinforced Concrete—International Symposium*, American Concrete Institute, Detroit, Mich., 1987, pp. 225–246.
4. M. A. Mansur. Bending-Torsion Interaction for Concrete Beams Reinforced with Steel Fibres. *Magazine of Concrete Research*, Vol. 34, No. 121, Dec. 1982, pp. 182–190.
5. R. Narayanan and Z. Toorani-Goloosalar. Fiber Reinforced Concrete in Pure Torsion and in Combined Bending and Torsion. *Proc., Institute of Civil Engineers*, London, Part 2, Vol. 67, 1979, pp. 987–1001.
6. M. A. Mansur and P. Paramasivam. Fiber Reinforced Concrete Beams in Torsion, Bending and Shear. *ACI Journal*, Vol. 82, No. 1, Jan.–Feb. 1985, pp. 33–39.
7. R. Narayanan and A. S. Kareem-Palanjian. Torsion, Bending and Shear in Prestressed Concrete Beams Containing Steel Fibers. *ACI Journal*, Vol. 83, No. 3, May–June 1986, pp. 423–431.
8. M. A. Mansur and R. Paramasivam. Steel Fibre Reinforced Concrete Beams in Pure Torsion. *The International Journal of Cement Composites and Lightweight Concrete*, Vol. 4, No. 1, Feb. 1982, pp. 39–45.
9. R. Narayanan and A. S. Kareem-Palanjian. Steel Fibre Concrete Beams in Torsion. *The International Journal of Cement Composites and Lightweight Concrete*, Vol. 5, No. 4, Nov. 1983, pp. 235–246.
10. T. T. C. Hsu. Torsion of Structural Concrete-Plain Concrete Rectangular Sections. In *Report SP-18: Torsion of Structural Concrete*, American Concrete Institute, Detroit, Mich., 1968, pp. 203–238.
11. A. K. Sharma. Design of Reinforced Concrete Rectangular Members Under Axial Compression, Bending and Torsion. *Proc., Institute of Civil Engineers*, London, Part 2, Vol. 69, 1980, pp. 911–919.

Study of the Mix Proportion of the No Slump Concrete Melt-Extracted Carbon Steel Fiber

CHENGMOU FAN AND LIYING ZHU

This paper introduces an investigation of the mix proportion of melt-extracted carbon steel fiber reinforced no slump concrete. The optimum sand ratio, water content, and cement content, which are relevant to the fiber volume, were determined by a series of tests. Based on this investigation, a formula was derived for calculating the consistency. This formula is useful for such applications as the pavement of roads.

During the past 10 years, steel fiber reinforced concrete (SFRC) has been studied and used in China in a variety of demonstration projects. However, it has not become widely used due to the high cost of drawn wire fiber and slitting sheet fiber.

In 1986, melt-extracted carbon steel fiber was manufactured in Qing An Steel and Iron Works of the Heilongjiang Province at a cost that was about two times cheaper than that of drawn wire and slitting sheet fiber in China. The chemical composition and tensile strength of the melt-extracted carbon steel fiber are listed in Table 1, and the specifications of the fiber are listed in Table 2.

To evaluate the reinforcing effect of melt-extracted carbon steel fiber, a series of experimental investigations was conducted. Results of the compressive strength test (Figure 1) and the shear strength test (Figure 2) show that the reinforcing effect of the melt-extracted carbon steel fiber and the slitting sheet steel fiber is almost the same. The flexural strength (Figure 3) and toughness of the melt-extracted SFRC (Figure 4) also increases significantly with the increment of the fiber volume fraction. Thus, it can be concluded that melt-extracted carbon steel fiber can be used for reinforcing concrete instead of the more expensive types of steel fiber (*1–6*).

Compared with other types of fiber that have an equivalent diameter, melt-extracted steel fiber with the crescent moon shaped cross section apparently increases the concrete's bond strength because of the fiber's rough surface and larger surface area. The effect on bond strength caused by the ratio of steel fiber surface area to volume is even more significant, and the increment of internal friction of the mix leads to a gradual decrease in flowability. Therefore, the mix proportion of melt-extracted steel fiber reinforced concrete is different from that of concrete reinforced by other types of steel fiber. This study emphasized the influence of fiber volume, sand ratio, water content, and cement content on the flowability of melt-extracted steel fiber reinforced concrete. Since extensive investigations have been conducted regarding the effect of aggregate size on the distribution of steel fiber and the flowability in other types of SFRC, the maximum aggregate size was limited to 20 mm in this study (*7*). This investigation was conducted using steel fiber reinforced no slump concrete.

Harbin Architectural and Civil Engineering Institute, Harbin, the People's Republic of China.

MATERIALS

The steel fiber used in this study was of the 102–2 type, manufactured in Qing An Steel and Iron Works, with a cross-sectional property of 0.2 mm × 2.0 mm, an equivalent diameter of 0.7 mm, and a length of 35 mm. Two kinds of ordinary portland cement (with a 28-day compressive strength of 42.5 MPa and 52.5 MPa, respectively) were used. The coarse aggregates were continually graded crushed stones with a maximum size of 20 mm, a bulk volume density of 1430 kg/m^3, and an apparent gravity of 2.76. The gradation curve is shown in Figure 5.

The fine aggregates were medium size sand with a fineness modulus of 2.63. Their bulk volume density, apparent gravity, and clay content were 1590 kg/m^3, 2.50, and 1.5 percent, respectively. The screen curve is shown in Figure 6.

FIBER VOLUME

The mix proportion of SFRC is different from that of plain concrete when adding a large amount of slender fibers. Therefore, the influence of fiber volume on the flowability of concrete needed to be determined before any work could be done. A total of four groups of specimens were made with a cement content of 350 kg/m^3, a water content of 180 kg/m^3, and a sand ratio of 45 percent. The fiber volumes were 0, 0.5, 1.0, and 1.5 percent, respectively. The test results were measured by a Vebe consistency meter and are listed in Table 3.

The relationship between fiber volume (V_f) and consistency (VB) can be expressed by the following regression equation:

$$VB = e^{1.96+V_f} \quad (1)$$

It can be seen from the test data, and the curves shown in Figure 7, that the flowability decreases exponentially as the fiber volume increases. When the fiber volume is 1.5 percent, the vebe time is as much as 32 sec, which deviates greatly from 10 sec (the time considered suitable for the flowability

TABLE 1 CHEMICAL COMPOSITIONS OF MELT-EXTRACTED CARBON STEEL FIBER

Chemical Compositions					Tensile Strength (Mpa)	Approximate Type of Steel
C	Si	Mn	S	P	⩾ 380	16Mn
0.25-0.35	0.28	0.9-1.1	⩽ 0.04	⩽ 0.04		

TABLE 2 SPECIFICATIONS OF MELT-EXTRACTED STEEL FIBER

Specification	Cross Section Area (mm^2)	Equivalent Diameter (mm)	Cross Section Size (mm)	Length (mm)	Configuration and Shape	Standard Type
0.5x25	0.2	0.5	0.2x1.0	25	FS	1#
0.5x30	0.2	0.5	0.2x1.0	30	FS	
0.6x30	0.3	0.6	0.2x1.5	35	FS	2#
0.6x45	0.3	0.6	0.2x1.5	45	FS	
0.6x45T	0.3	0.6	0.2x1.5	45	EL	
0.7x45	0.4	0.7	0.2x2.0	45	FS	3#
0.7x45T	0.4	0.7	0.2x2.0	45	EL	
0.7x60	0.4	0.7	0.2x2.0	60	FS	

Note: FS---Flat-straight shape.
EL---Ends-enlarged shape.
1#---To be used for SF shotcrete.
2#, 3#---To be used for castable SF concrete.

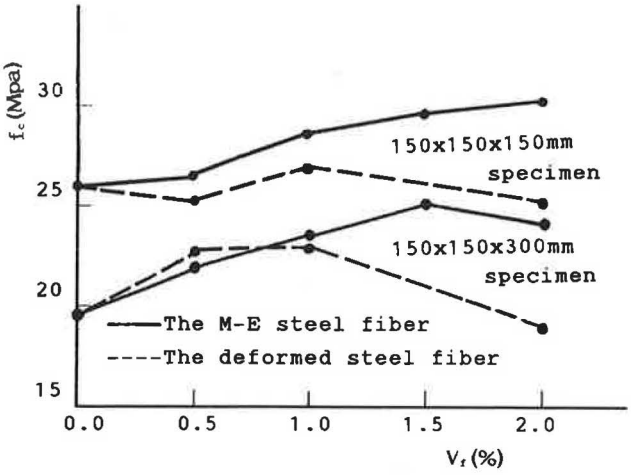

FIGURE 1 Relationship between fiber volume and the compressive strength of SFRC.

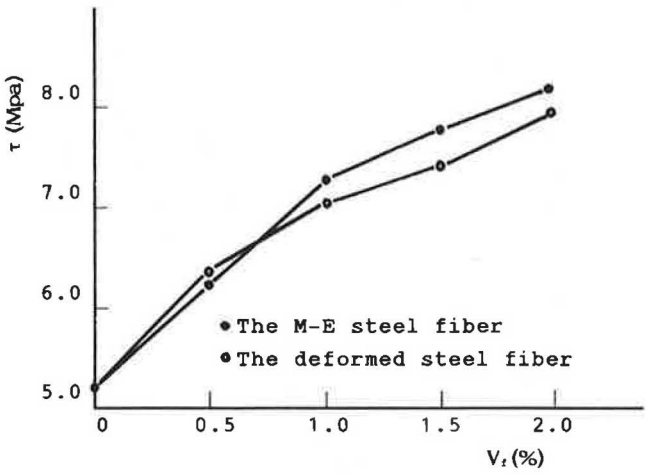

FIGURE 2 Relationship between fiber volume and the shear strength of SFRC.

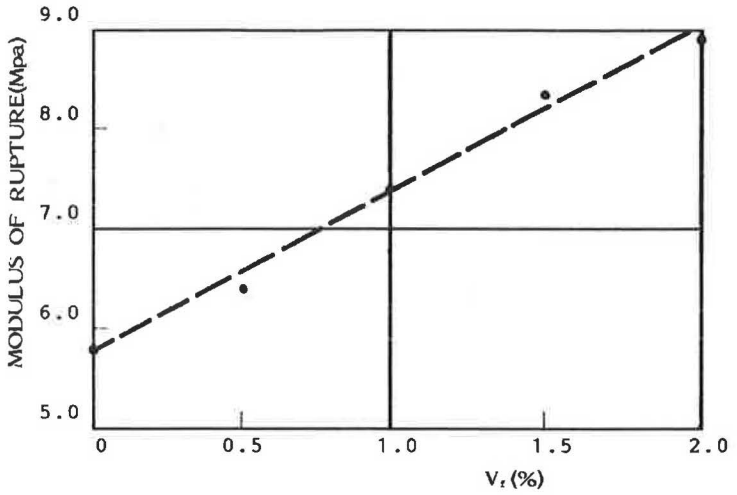

FIGURE 3 Relationship between fiber volume and the modulus of rupture of SFRC.

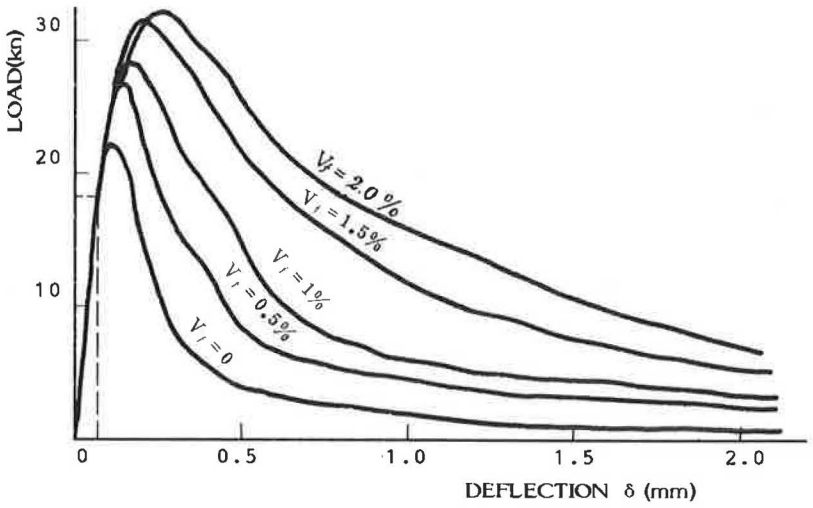

FIGURE 4 Typical load-deformation curve from the flexural test.

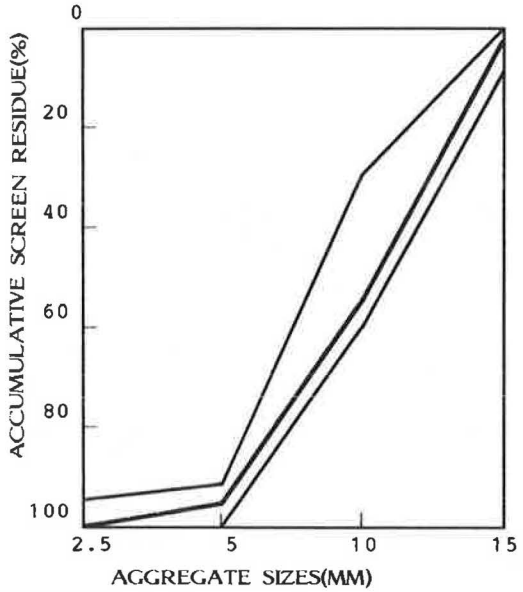

FIGURE 5 Grading curve of stones.

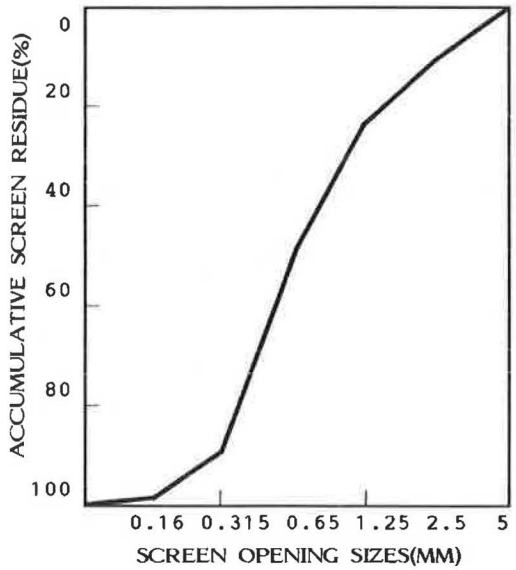

FIGURE 6 Grading curve of 1# sand.

TABLE 3 INFLUENCE OF FIBER VOLUME ON FLOWABILITY

Fiber Volume(%)	0	0.5	1.0	1.5
V-B Time(S)	10.0	11.4	16.6	32.0

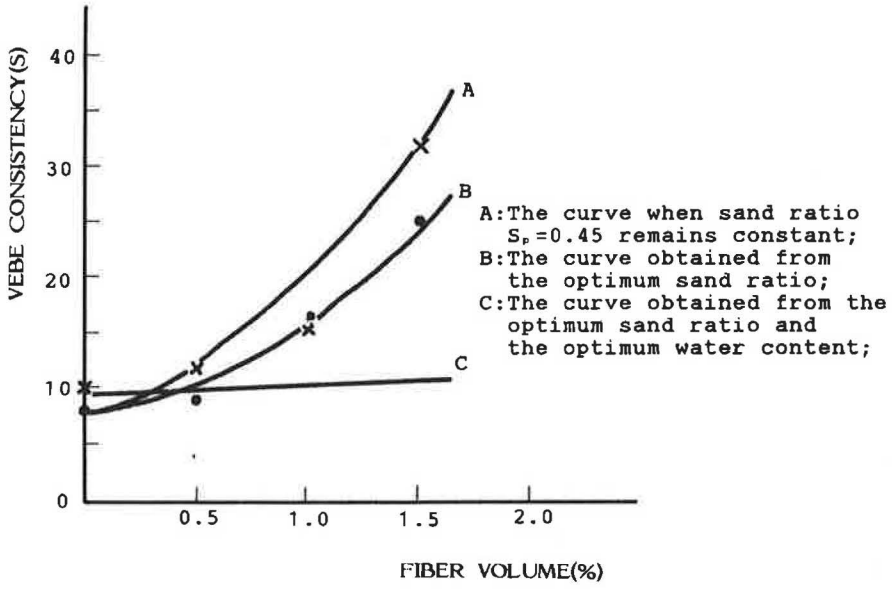

FIGURE 7 Relationship between fiber volume and consistency.

of no slump concrete). Thus, assuming the needed flexural strength, toughness, and cracking resistance are satisfied, it is critical to determine the optimum sand ratio and water content for a specific fiber volume so the flowability of SFRC will conform to that used in construction sites.

SAND RATIO

Two reasons support the data shown in Figure 8. (a) As the amount of added steel fiber increases, the cement mortar becomes insufficient to fill the space between steel fibers, and this leads to a decrease in flowability; and (b) The water content is less than the corresponding amount of steel fiber used; this problem will be discussed later.

Although steel fiber can be regarded as a type of aggregate, the sand ratio is still defined as a percentage of the amount of sand and stone. It was necessary to study whether or not an optimum sand ratio exists for SFRC with various fiber volume. Four groups of specimens were therefore prepared with different sand ratios to determine the flowability. In all SFRC specimens, the cement content remained 350 kg/m^3,

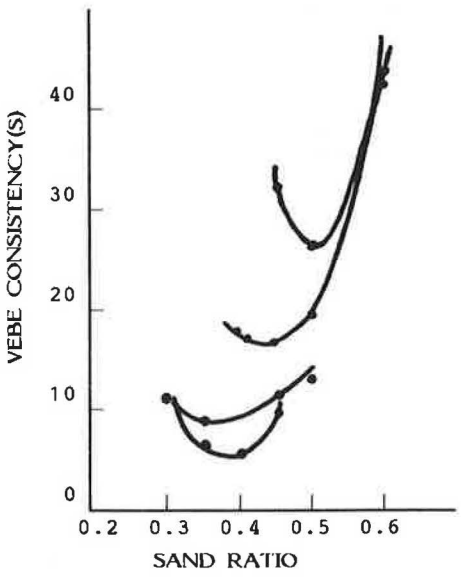

FIGURE 8 Optimum sand ratios for various fiber volumes.

while the water content remained 180 kg/m³. The test values of SFRC consistency of different mix proportions are listed in Table 4. Figure 8 illustrates the relationship between the sand ratio and the flowability for a given fiber volume. As shown in the figure, for every fiber volume where the optimum sand ratio exists, the sand ratio increases with the increment of fiber volume. This relationship can be expressed in the following optimum sand ratio formula:

$$S_p = S_p^o + 0.1\,V_f \tag{2}$$

where S_p^o refers to the sand ratio of plain concrete, which is 0.35.

The relationship between fiber volume and consistency at the optimum sand ratio is shown in the following regression equation:

$$VB = e^{2.5-1.6\,S_p+V_f} \tag{3}$$

Equations 1, 2, and 3 result in the following:

$$VB = e^{1.94+0.84\,V_f} \tag{4}$$

Substituting the fiber volume value with its corresponding optimum sand ratio in Equation 4 yields the calculated consistency, which is also listed in Table 4. The calculated values are similar to the test data, indicating that Equation 4 more accurately describes the relationship between fiber volume and consistency at the optimum sand ratio (see curve B in Figure 7.) By comparing curve A and curve B, it can be concluded that flowability increases when the sand ratio corresponds with the fiber volume. Flowability is not affected because water content is not relevant to fiber volume.

WATER CONTENT

To find the optimum water content corresponding to the fiber volume and sand ratio, four groups of specimens were prepared with different water content, which increased with the increment of fiber volume and sand ratio to determine the flowability. The cement content remained at 350 kg/m³. The test results are listed in Table 5. The optimum water content, which is relevant to the consistency index VB = 10 sec, can be expressed by the following equation:

$$W = W_o + 20V_f \tag{5}$$

where W_o is the optimum water content of the plain concrete, which is 170 kg/m³.

The relationship between the consistency, fiber volume,

TABLE 4 INFLUENCE OF SAND RATIO ON THE FLOWABILITY OF SFRC WITH DIFFERENT FIBER VOLUMES

Fiber Volume(%)	0				0.5				1.0				1.5		
Sand Ratio(%)	30	35	40	45	30	40	45	50	40	45	50	60	45	50	60
V-B Time(s)	11.1	7.1	6.4	10.0	8.6	8.5	11.4	11.8	17.0	16.6	19.2	43.0	32.0	25.6	42.2
Optimum Sand Ratio(%)	35				40				45				50		
V-B Time(s) Computed from Equation (3)	7.0				10.6				16.1				24.5		

TABLE 5 INFLUENCE OF WATER CONTENT ON FLOWABILITY

Fiber Volume(%)	0			0.5			1.0			1.5		
Sand Ratio(%)	35			40			45			50		
Water Content(kg/m³)	160	165	175	165	175	185	165	185	195	175	185	195
Water-Cement Ratio(%)	46	47	50	47	50	53	47	53	56	50	53	56
V-B Time(S)	15.4	9.4	9.2	21.0	12.6	7.4	30.4	13.6	8.6	35.4	25.0	13.0
V-B Time(S) Computed from Equation (7)	14.9	11.6	7.0	20.1	12.2	7.4	34.8	12.8	7.8	36.6	22.2	13.5
The Optimum Water Content(kg/m³)	170			180			190			200		
V-B Time(S) Computed from Equation (8)	9.0			9.5			10.0			10.5		

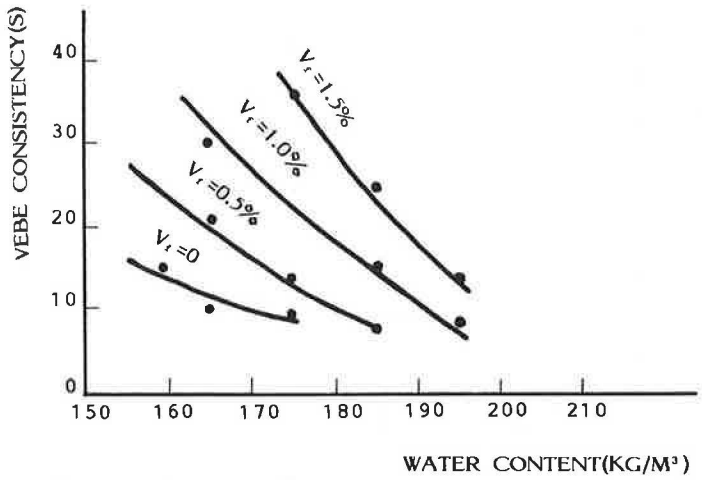

FIGURE 9 Relationship between water content and consistency.

TABLE 6 INFLUENCE OF CEMENT CONTENT ON FLOWABILITY

Cement Content (kg/m³)	317	345	380	396
V-B Time(s)	10.4	8.8	10.6	15.0

sand ratio, and water content is expressed by the following formula:

$$VB = e^{9.05 + V_f - 1.6S_p - 0.037[W - 1.35(W - W')]} \quad (6)$$

where W' is the water content actually used.

When the optimum water content is used, i.e., $W' = W$, Equation 6 becomes

$$VB = e^{9.05 + V_f - 1.6S_p - 0.037W} \quad (7)$$

Substituting Equations 2 and 5 into Equation 7 results in

$$VB = e^{2.2 + 0.1V_f} \quad (8)$$

Using Equation 6, the calculated values of the consistency were obtained and listed in Table 5. Four curves of the relationship between consistency and water content under different fiber volumes are illustrated in Figure 9. Obviously, Equation 6 accurately describes the relationship between consistency and water content.

The values of consistency corresponding to the optimum water content computed from Equation 8 are also listed in Table 5. Curve C in Figure 7 demonstrates this relationship. It can be concluded that, when both the sand ratio and water content correspond with the fiber volume used, the consistency of SFRC can be controlled at about 10 sec.

CEMENT CONTENT

In the previous discussion, the cement content was chosen as a constant value for the analysis of the sand ratio and water content. In this section, the influence of the cement content on the flowability of SFRC is explored. For the SFRC with a fiber volume of 1.0 percent, four quantities of cement were used on the basis of the optimum sand ratio and water content determined previously. The values of consistency are listed in Table 6, and Figure 10 illustrates the relationship between cement content and consistency. The figure shows that flowability is affected less when the cement content is within the range of 350 ± 30 kg/m³; however, flowability decreases slightly when the cement content approaches 400 kg/m³.

The test results show that the consistency remains constant if the cement content changes within a specific range and the water content is fixed. This special feature will be beneficial to the adjustment of cement content while satisfying the flowability requirement to meet the strength demands for SFRC.

TEST FOR INSPECTION

This paper has proposed some parameters concerning the needed flowability of SFRC used in pavement construction. To check these parameters, five groups of specimens were prepared.

Ordinary cement (with a 28-day compressive strength of 52.5 MPa) was used with a content of 350 kg/m³ and a fiber volume of 1 percent. The optimum sand ratio and water content were 0.45 and 190 kg/m³, respectively. In each group, there were three 100 mm × 100 mm × 400 mm flexural specimens and three standard compressive specimens. A flexural test was conducted with the loading on the central point of the specimen, and the results are listed in Table 7. This indicates that the vebe time of the specimen is about 10 ± 3 sec—3 sec away from the design requirement with which the engineering practical serviceability can be satisfied. The mean value of flexural strength is 8 MPa.

CONCLUSIONS

To meet the requirements of pavement and other engineering construction, the consistency of steel fiber reinforced no slump

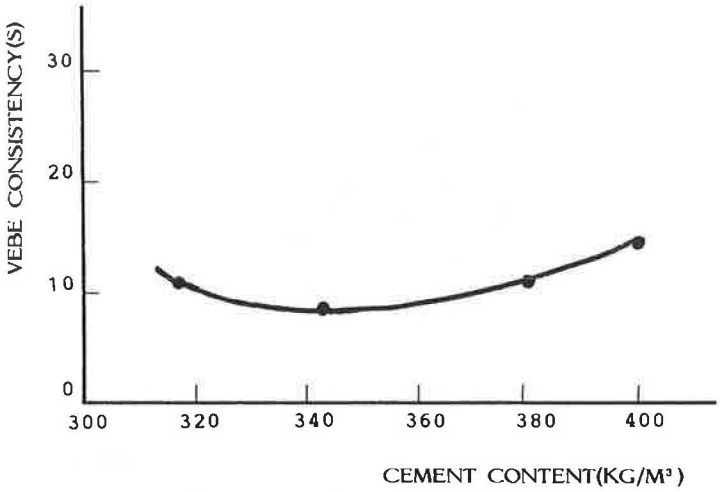

FIGURE 10 Relationship between cement content and consistency.

TABLE 7 VEBE TIME, FLEXURAL STRENGTH, AND COMPRESSIVE STRENGTH OF SFRC

Specimen Group No.	V-B Time (s)	Flexural Strength at 28 Days(MPa)	Compressive Strength at 28 Days(MPa)
1	13.5	8.0	50.8
2	8.5	8.3	53.4
3	7	8.1	53.1
4	10	7.9	56.2
5	10	7.5	57.5

concrete should be controlled at about 10 sec. The mix proportion can be obtained from the following equation:

$$VB = e^{9.05 + V_f - 1.6S_p - 0.037W}$$

This formula is based on a cement content of 350 kg/m³. The vebe time is reliable when the cement content is within the range of 350 ± 30 kg/m³.

REFERENCES

1. Gosta Odelberg. Producing and Promoting of Swedish Steel Fibers to the Market. *Steel Fiber Concrete, US-Sweden Joint Seminar (NSF-STU)*, Stockholm, 1985.
2. D. J. Hannant. *Fiber Cements and Fiber Concretes*. John Wiley & Sons Ltd., New York, 1978.
3. Guofan Zhao et. al. Experiment on the Compressive Strength and Module of Elasticity of Steel Fiber Reinforced Concrete. *Proc., SFRC Standard Test Methods in China* (in Chinese), Vol. 2, 1988.
4. Zhonggang Zhang et. al. On the Shear Strength of Steel Fiber Reinforced Concrete. *Proc., SFRC Standard Test Methods in China* (in Chinese), Vol. 2, 1988.
5. Jinghai Zhao. Experiment on the Compressive Strength and Modulus of Rupture of Steel Fiber Reinforced Concrete. *Proc., SFRC Standard Test Methods in China* (in Chinese), Vol. 1, 1986.
6. Jinghai Zhao and Peng Xu. Evaluating Method for Flexural Toughness of Steel Fiber Reinforced Concrete. *Journal of Harbin Architectural & Civil Engineering Institute* (in Chinese), Supplement 1988, pp. 65–77.
7. Chengmou Fan et al. *Application Techniques of Steel Fiber Reinforced Concrete*. Publishing House of Science and Technology, Heilongjiang, Harbin, China, 1986, pp. 122–123.